Centre Européen de Recherche et de Formation Avancée en Calcul Scientifique
European Center for Research and Advanced Training in Scientific Computing

CERFACS
Scientific Activity Report
Jan. 2017 – Dec. 2018

CERFACS
42, Avenue Gaspard Coriolis, 31057 Toulouse Cedex 1, FRANCE.
Tel. : 33 (0) 561 19 31 31 – Fax : 33 (0) 561 19 30 30
secretar@cerfacs.fr – http://www.cerfacs.fr

Contents

List of Figures

4 Scientific Software Operational Performance 141

Foreword

Welcome to the 2017-2018 CERFACS Scientific Activity Report.

CERFACS is a mutualized center of research, development, transfer and training regarding simulation and high performance computing for the benefit of its industrial and public shareholders on a set of major themes.

The mission of CERFACS was defined in the status of the company during the creation of the Civil Society in 1996. The purpose of CERFACS is as follows:

- To develop scientific and technical research to improve methods of advanced computing, including a better consideration of the physical processes involved, and the development of efficient algorithms for new computers architectures;
- To allow access, either on their own or in shared mode, to computers with new architectures which could provide a significant performance gain;
- To transfer the scientific knowledge and the technical methods for application in major industrial sectors and areas;
- To train highly qualified scientists and engineers and provide advanced training
- And, generally, all civil transactions related directly or indirectly to this object and which do not change the civilian character of the company.

In addition, CERFACS must adjust its strategy to meet three key factors of success:

- To master and develop differentiating skills and innovation
- To give priority to the mutualized needs of shareholders
- To be a key actor of national and European networks

This report reflects Cerfacs Research activity over the last two years. During this period, we defined a new Strategic Research Plan for 2018-2022, based on a core of generic activities "Strategic Axes", which provides both methods, tools and building blocks. A very fruitful interaction between science and application will be encouraged through Application Axes, developed with strong relationships with our shareholders.

CERFACS handles the following 5 themes in its core as Strategic Axes:

- Linear algebra
- Excascale
- Numerical methods for PDE

- Coupling
- Data Driven Modelling

6 Application Axes perfuse and sustain the Strategic Axes:

- Climate variability and predictability: from ocean to continental impacts
- Full Gas Turbine simulation
- Methane-Lox engine simulation
- Full Aircraft simulation
- Modelling for environment and safety
- Physics of oil reservoirs (including history matching).

The CERFACS research teams are multidisciplinary with physicists, numerical analysts, algorithm and data scientists, computer engineers,....
There were 5 research teams in CERFACS until mid-2018:

- Parallel Algorithms (ALGO): Applied mathematics, Development of advanced numerical algorithms to be used on massively parallel computing platforms
- Computational Fluid Dynamics (CFD): Aerodynamics, Combustion and Turbomachines
- Climate Modelling and Global Change (GLOBC): Climate, Data Assimilation & Couplers
- Aviation and Environment (AE): Modelling and simulation of aircraft emissions & atmospheric chemistry data assimilation
- Scientific Software Operational Performance (COOP): Technology watch & support for leadership class frontier simulations and Research codes industrialization & management of complex simulation workflows.

In July 2018, we decided to merge GLOBC and AE teams following the retirement of the AE team leader. In addition to the research teams, a transverse team named CSG is devoted to Computer Support for the research teams.

This activity report is written in independent parts so that readers interested mainly in a particular field will easily find both a detailed description of the work that has been achieved, and a complete list of references, including papers in the reviewed literature and internal reports (which can be made available upon request). I sincerely hope that through the detailed reports of the teams you will find interest to continue our collaboration or to initiate new ones.

Enjoy your reading.

Dr Catherine LAMBERT - CERFACS Director

CERFACS Structure

As a “Société Civile” CERFACS is governed by two bodies.
Firstly, the “Conseil de Gérance”, composed of 7 managers nominated by the 7 shareholders (see table i), follows quite closely the CERFACS activities and the financial aspects. It meets four times per year.
Secondly, the Board of Governors is composed of the 7 representatives of CERFACS shareholders and of 3 invited personalities, including the Chairman of the Scientific Council. It meets twice a year.

CERFACS Scientific Council met 2 times during this period 2017-2018 under the chairmanship of Dr Jean-François Minster.

CENTRE NATIONAL D’ETUDES SPATIALES (CNES)	21.3%
ELECTRICITE DE FRANCE (EDF)	21.3%
METEO-FRANCE	21.3%
AIRBUS	9 %
SAFRAN	9%
OFFICE NATIONAL D’ETUDES ET DE RECHERCHES AEROSPATIALES (ONERA)	9%
TOTAL	9%

Table i: CERFACS Shareholders

The general organization of CERFACS is depicted in the following CERFACS chart.

CERFACS chart as of Dec. 31, 2018

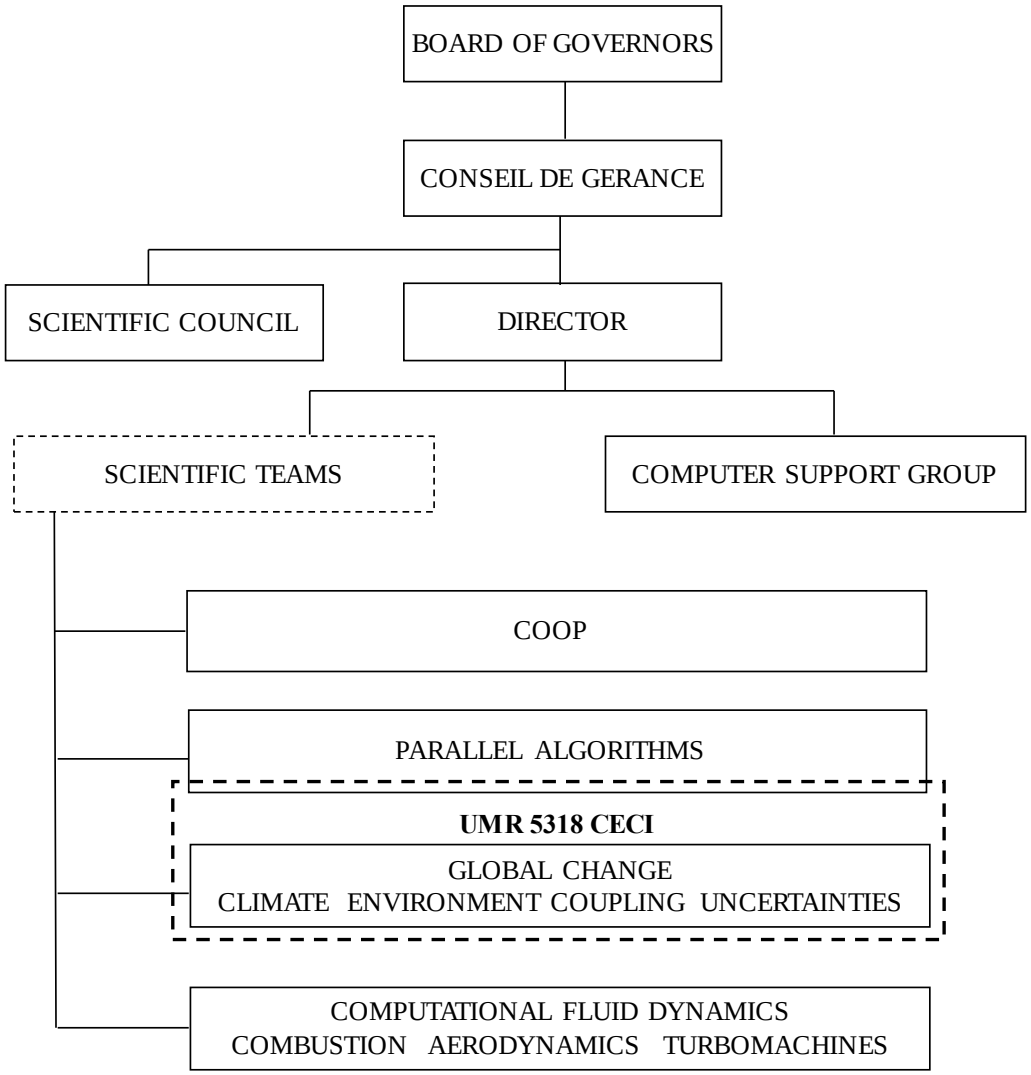

CERFACS Staff

The staff of the scientific teams and of the computing support group, consisting of, on December 31, 2018, a total of 123 scientists and technical staff is shown in Tables ii and iii.

POSITION	ALGO	CFD	CSG-COOP	GLOBC	AE	TOTAL
Team Leader	0,2	0,3	1,0	0,2	1,0	2,7
Senior	2,8	7,5	3,0	5,0	1,0	19,2
Research Engineer	0,2	4,0	3,0	10,0	1,6	18,8
Post Doc	2,8	8,5	3,3	0,8	0,7	16,2
Ph.D Student	5,7	29,3		6,2	1,0	42,2
Studies Engineer	1,5	4,2	0,3	2,0	1,3	9,4
Trainee-Teacher	0,8	5,7	0,3	3,2		10,0
Consultant	0,2	0,3		0,7	0,3	1,5
Technician			2,0			2,0

Table ii: 2017 Full time equivalent teams distribution.

POSITION	ALGO	CFD	CSG-COOP	GLOBC	AE	TOTAL
Team Leader	0,2	0,3	1,0	0,2	0,5	2,2
Senior	4,3	7,4	3,3	4,6	1,3	21,0
Research Engineer	0,2	4,2	3,0	9,0	3,0	19,4
Post Doc	1,6	7,4	4,4	0,9		14,2
Ph.D Student	4,3	31,7	0,4	1,0	7,8	45,1
Engineer	0,3	3,4	1,2	0,4	0,6	6,0
Trainee-Teacher		6,0	2,9	2,7		11,6
Consultant	0,1	0,4		0,7	0,6	1,7
Technician			2,0			2,0

Table iii: 2018 Full time equivalent teams distribution.

CERFACS Wide-Interest Seminars

Franck Nicoud (Université Montpellier II): *Challenges and opportunities in computational hemodynamics.* (2017, January 9th)

Christian Kraus (IMFT, Toulouse): *Impact of Heat Transfer on Combustion Instabilities – Progress and Challenges.* (2017, March 2nd)

Prof. William Jalby (Université de Versailles-Saint Quentin en Yvelines, Exascale Computing Research Laboratory): *Introduction to differential analysis using DECAN.* (2017, March 8th)

Prof. Elie Hachem (Computing and Fluids Research Group, MINES ParisTech, PSL – Research University, CEMEF – Centre for material forming, CNRS UMR 7635, Sophia-Antipolis): *Adaptive variational multiscale finite element method for high Reynolds number flows.* (2017, May 17th)

Dr. Mario Arioli (CERFACS): *An introduction to interpolation spaces and their applications from a numerical linear algebra perspective.* (2017, June 12nd)

Williams Exbrayat (OMP): *Comment faire efficacement de la bibliographie et de la bibliométrie quand (on n'est pas doué et) qu'on n'a pas le temps ?* (2017, June 28th)

Anne Gazaix(IRT Saint-Exupéry): *Towards the Industrialization of New MDO Technologies and Tools for Aircraft Design.* (2017, December 19th)

Lila Collet (Heriot-Watt University Edinburgh): *Villes Résilientes aux Risques Hydrologiques.* (2018, January 8th)

Jean-Michel Bruel & Benoit Combemale (IRIT – SM@RT Team): *Ingénierie Dirigée par les Modèles et Domain Specific Languages – Application à la simulation numérique haute-performance.* (2018, January 19th)

Mathieu Serrurier (IRIT): *Intelligence artificielle - Mythes et réalités.* (2018, May 29th)

Eric Petit (Intel Corporation) & **François Févotte** (EDF): *Vérification de la qualité numérique des codes en arithmétique flottantes avec Verificarlo et Verrou.* (2018, June 6th)

Andrea Saltelli (University of Bergen): *Sensitivity analysis, an introduction.* (2018, December 3rd)

1

Parallel Algorithms

Introduction

The Parallel Algorithms Project conducts research on advanced numerical algorithms to address the solution of problems in Computational Science and Engineering on massively parallel computing platforms. The Parallel Algorithms Project studies the design, the analysis and the implementation of innovative algorithms for problems that are out of reach of current standard numerical methods. Such limitations can be due to the computational cost when extremely fine resolutions are required, or innovative new methods may be needed for special nonlinear problems or when the stochastic nature of the data must be considered.
This kind of research is usually performed in collaboration with the shareholders of CERFACS, with FAU, or with other external partners. In particular, many linear-algebra- and optimization-related research activities are done in collaboration with colleagues at IRIT in the context of the joint CERFACS-IRIT Common Laboratory. Research using Lattice Boltzmann methods relies on the availability of waLBerla, a highly scalable and efficient Lattice-Boltzmann framework developed at FAU in Erlangen. Some of the work on multigrid methods is also conducted in collaboration with U. Ruede's group at FAU Erlangen-Nuremberg. Currently two PhD students of the Algo-team are expected to graduate both at French universities and at FAU Nuremberg in cotutelle-agreements. This and frequent mutual visits help to exploit the synergies between FAU Erlangen-Nuremberg and CERFACS.
The Parallel Algorithms Project builds on three decades of successful work on parallel numerical methods at the forefront of computational mathematics, constantly expanding its scope into new areas. The field is characterized by the continued progress in computer technology to ever higher degree of parallelism so that constantly new algorithms with improved scalability are needed. The trend towards using an abundance of data from sensors and measurements creates further algorithmic challenges. Finally, the rapid entry of computational methods into nontraditional application fields, the advent of new computational paradigms, such as machine learning, opens avenues of opportunity and at the same time creates new challenges for the development and use of parallel algorithms.
In many applications of computational science and engineering, classical forward simulations are now used as building blocks for more complex and challenging computational goals. These include optimizaton problems, inverse problems, model reduction techniques, and data driven computing. In the past few years, the Parallel Algorithms Project has successfully developed new research directions in these fields. This includes especially research in the context of optimization and data assimilation. Additionally, the systematic quantification of uncertainties has become a field of research that is expected to become even more important in the future as the basis of decision support systems in fields of scientific or societal relevance.
Naturally these research topics are interconnected, since e.g. large-scale inverse problems (as they arise in big data applications) or the solution of nonlinear systems eventually all require approximate solutions of linearized systems. These developments rely on the strong research expertise in mathematical modeling, numerical analysis, partial differential equation, integral equations, scientific computing, and computational science that is present within the Parallel Algorithms Project. For the research of the Parallel Algorithms Project it is essential to identify the abstract mathematical structure of a given problem and to exploit it in the design of the algorithms.
Generally, the role of the Parallel Algorithms Project within CERFACS is to bridge from the fundamental mathematical aspects to research for real-life applications. To this end, novel parallel algorithms and methods are proposed, designed, and analyzed in terms of their accuracy and their computational cost. This research includes the quantification of convergence properties, the study of the accuracy achieved, and especially also the efficiency and scalability of the methods on advanced parallel computer architectures.

The solution of sparse linear systems is considered by tackling both sparse direct methods as well as projection based iterative methods. These methods can also be combined to derive hybrid algebraic methods close to domain decomposition or multiscale and multigrid methods. In addition to graph theory, linear algebra, and functional analysis, these activities rest upon the strong expertise in scientific software development and on an up-to-date knowledge of the current parallel computing platforms.
Optimization methods occur in several applications at CERFACS. Most often the main goal is to improve the performance of a given system. The Parallel Algorithms Project works in both differentiable optimization and derivative-free optimization. The main research topics concern the convergence to local or global minima and the efficiency of the algorithms in practice.
The Parallel Algorithms Project is also deeply involved in the design and analysis of algorithms for data assimilation. Algorithms related to differentiable optimization or derivative-free optimization are considered together with filtering techniques. All these algorithms must be adapted and improved before tackling potential applications in seismic, oceanography, atmospheric chemistry or meteorology. The Parallel Algorithms Project has notably developed a specific expertise in the field of correlation error modelling based on the iterative solution of an implicitly formulated diffusion equation.
Finally the Parallel Algorithms Project takes an active part in the Training programme at CERFACS and is also regularly organizing seminars, workshops and international conferences in numerical optimization, numerical linear algebra, high performance computing, computational science and engineering, and data assimilation.

Ulrich Rüde

Numerical linear algebra

2.1 Direct methods

2.1.1 Fast synchronization-free algorithms for parallel sparse triangular solves with multiple right-hand sides

The sparse triangular solve kernels, SpTRSV and SpTRSM, are important building blocks for a number of numerical linear algebra routines. Parallelizing SpTRSV and SpTRSM on today's manycore platforms, such as GPUs, is not an easy task since computing a component of the solution may depend on previously computed components, enforcing a degree of sequential processing. As a consequence, most existing work introduces a preprocessing stage to partition the components into a group of level-sets or colourset so that components within a set are independent and can be processed simultaneously during the subsequent solution stage. However, this class of methods requires a long preprocessing time as well as significant runtime synchronization overheads between the sets. To address this, we investigate in [ALG24] novel approaches for SpTRSV and SpTRSM in which the ordering between components is naturally enforced within the solution stage. In this way, the cost for preprocessing can be greatly reduced, and the synchronizations between sets are completely eliminated. To further exploit the data-parallelism, we also develop an adaptive scheme for efficiently processing multiple right-hand sides in SpTRSM. A comparison with a state-of-the-art library supplied by the GPU vendor, using 20 sparse matrices on the latest GPU device, shows that the proposed approach obtains an average speedup of over two for SpTRSV and up to an order of magnitude speedup for SpTRSM. In addition, our method is up to two orders of magnitude faster for the preprocessing stage than existing SpTRSV and SpTRSM methods

2.2 Solution techniques for matrices with block structure

2.2.1 An iterative generalized Golub-Kahan algorithm for problems in structural mechanics

The work [ALG38] studies the Craig variant of the Golub-Kahan bidiagonalization algorithm as an iterative solver for linear systems with saddle point structure. Such symmetric indefinite systems in 2x2 block form arise in many applications, but standard iterative solvers are often found to perform poorly on them and robust preconditioners may not be available. Specifically, such systems arise in structural mechanics, when a semidefinite finite element stiffness matrix is augmented with linear multi-point constraints via Lagrange multipliers. Engineers often use such multi-point constraints to introduce boundary or coupling conditions into complex finite element models. This work is about a systematic convergence study of the Golub-Kahan algorithm for a sequence of test problems of increasing complexity, including concrete structures enforced with pretension cables and the coupled finite element model of a reactor containment building (Figure 2.1). When the systems are suitably transformed using augmented Lagrangians on the semidefinite block and when the constraint equations are properly scaled, the Golub-Kahan algorithm is found to exhibit excellent convergence that depends only weakly on the size of the model. The new algorithm is found to be robust in practical cases that are otherwise considered to be difficult for iterative solvers.

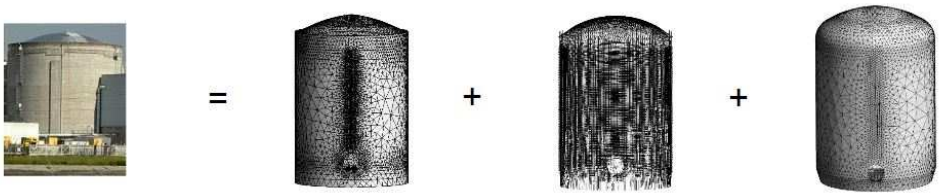

Figure 2.1: Modeling of a reactor containment building.

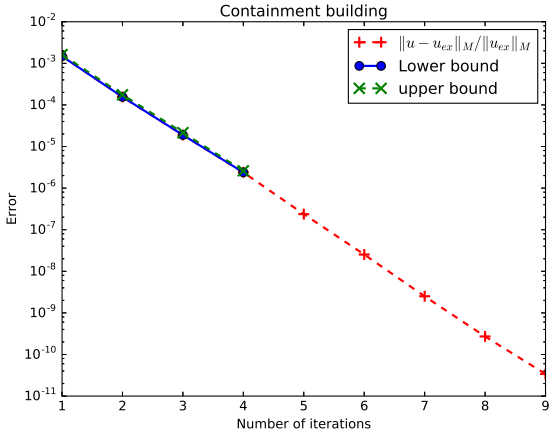

Figure 2.2: Convergence of the energy norm error and its upper and lower bound estimates.

2.2.2 A new preconditioner update strategy for the solution of sequences of linear systems in structural mechanics: application to saddle point problems in elasticity

Many applications in structural mechanics require the numerical solution of sequences of linear systems typically issued from a finite element discretization of the governing equations on fine meshes. The method of Lagrange multipliers is often used to take into account mechanical constraints. The resulting matrices then exhibit a saddle point structure and the iterative solution of such preconditioned linear systems is considered as challenging. A popular strategy is then to combine preconditioning and deflation to yield an efficient method. In [ALG28], we propose an alternative that is applicable to the general case and not only to matrices with a saddle point structure. In this approach, we consider to update an existing algebraic or application-based preconditioner, using specific available information exploiting the knowledge of an approximate invariant subspace or of matrix-vector products. The resulting preconditioner has the form of a limited memory quasi-Newton matrix and requires a small number of linearly independent vectors. Numerical experiments performed on three large-scale applications in elasticity highlight the relevance of the new approach. We show that the proposed method outperforms the deflation method when considering sequences of linear systems with varying matrices.

2.2.3 Uncovering Hidden Block Structure

In [ALG39] we develop a multistage procedure for uncovering the block structure in a matrix. Our algorithm combines standard combinatorial techniques with a novel clustering approach that merges both numerical and structural analysis. A central part of our process is to use a doubly stochastic scaling. We illustrate the use of our algorithm in partitioning sparse matrices for constructing a preconditioner for iterative methods. We also show how we can use our approach in community detection in both undirected and directed networks.

2.2.4 Low rank updates in preconditioning the saddle point systems arising from data assimilation problems

The numerical solution of saddle point systems has received a lot of attention over the past few years in a wide variety of applications such as constrained optimization, computational fluid dynamics and optimal control, to name a few. In this paper, we focus on the saddle point formulation of a large-scale variational data assimilation problem, where the computations involving the constraint blocks are supposed to be much more expensive than those related to the $(1, 1)$ block of the saddle point matrix. In [ALG17], new low-rank limited memory preconditioners exploiting the particular structure of the problem are proposed and analysed theoretically. Numerical experiments performed within the Object-Oriented Prediction System are presented to highlight the relevance of the proposed preconditioners.

2.2.5 A note on preconditioning weighted linear least squares, with consequences for weakly constrained variational data assimilation

In [ALG18] the effect of preconditioning linear weighted least-squares [ALG17] using an approximation of the model matrix is analyzed, showing the interplay of the eigenstructures of both the model and weighting matrices. A small example is given illustrating the resulting potential inefficiency of such preconditioners. Consequences of these results in the context of the weakly-constrained 4D-Var data assimilation problem are finally discussed.

2.2.6 Multigrid Smoothers for Saddle Point Problems

In [ALG14] we develop new smoothers for multigrid algorithms with saddle point structure such as they arise in Stokes flow. The smoothers are based on the Uzawa method. A convergence analysis is developed and a the performance is studies in careful numerical experiments. We discuss several classes of Uzawa smoothers for the application in multigrid methods. Beside commonly used variants, such as the inexact and block factorization version, we also introduce a new symmetric method, belonging to the class of Uzawa smoothers. For these variants we unify the analysis of the smoothing properties, which is an important part in the multigrid convergence theory. These methods are applied to the Stokes problem for which all smoothers are implemented as pointwise relaxation methods. Several numerical examples illustrate the theoretical results. The method is capable to solve finite element systems of record breaking size of more than 10^{13} degrees of freedom. These are likely the largest FE computations demonstrated to date.

Data assimilation

3.1 Parallel algorithms in data assimilation

3.1.1 "Time"-parallel diffusion-based correlation operators

Correlation operators based on the solution of an implicitly formulated diffusion equation can be implemented numerically using the Chebyshev iteration method. The attractive properties of the algorithm for modelling correlation functions on high-performance computers have been discussed in a recent paper. [ALG37] describes a straightforward variant of that algorithm that allows the matrix-vector products involved in the sequential pseudo-time diffusion process to be performed in parallel. Contrary to the original algorithm, which requires solving a sequence of linear systems involving a symmetric positive-definite (SPD) matrix, the "time"-parallel algorithm requires solving a single linear system involving a nonsymmetric positive-definite (NSPD) matrix. The key information required by the Chebyshev iteration for solving the NSPD problem is an estimate of the extreme eigenvalues of the NSPD matrix. For the problem under consideration, the extreme eigenvalues of the NSPD matrix are the same as those of the original SPD matrix, and can be pre-computed using a Lanczos algorithm applied to the latter. The convergence properties of the algorithm are studied from a theoretical perspective and using numerical experiments with a diffusion-based covariance model in a variational data assimilation system for the global ocean. Results suggest that time-parallelization can reduce the run-time of an implicit diffusion-based correlation operator by greater than a factor of two. It can be implemented practically using a hybrid parallelization approach that combines Message Passing Interface tasks in the spatial domain with Open Multi-Processing threads spanning the pseudo-time dimension. The sensitivity of the results to preconditioning, to the choice of first guess and to the stopping criterion is discussed. This work was a contribution to the ERA-CLIM2 (FP7) project [ALG10].

3.1.2 Parallelization in the time dimension of four-dimensional variational data assimilation

The current evolution of computer architectures towards increasing parallelism requires a corresponding evolution towards more parallel data assimilation algorithms. In [ALG16], we consider parallelization of weak-constraint four-dimensional variational data assimilation (4D-Var) in the time dimension. We categorize algorithms according to whether or not they admit such parallelization and introduce a new, highly parallel weak-constraint 4D-Var algorithm based on a saddle-point representation of the underlying optimization problem. The potential benefits of the new saddle-point formulation are illustrated with a simple two-level quasi-geostrophic model (Figure 3.1).

3.1.3 Block Krylov methods for accelerating ensembles of variational data assimilation

[ALG29] considers the problem of efficiently solving ensembles of variational data assimilations in the context of numerical weather prediction (NWP). Running several assimilations notably allows to initialize ensemble prediction systems and to more accurately represent background error statistics, but

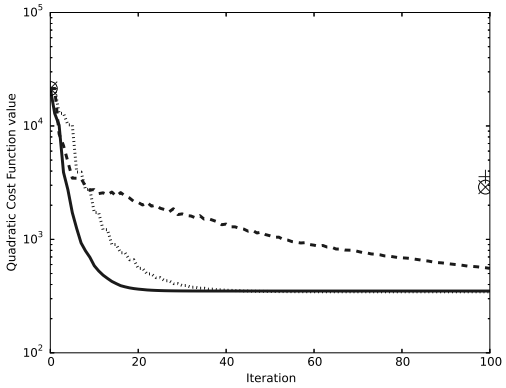

Figure 3.1: Convergence for the saddle-point and forcing formulations of 4D-Var as a function of iteration for an analysis with 12 2 h subwindows. The vertical axis shows the quadratic cost-function values. The solid curve shows the forcing formulation, the other curves are for the saddle-point formulation preconditioned by using an inexact constrained preconditioner where the model is exact, (dotted) and model is replaced by identity (dashed). The circle, cross and plus signs show the nonlinear (outer loop) cost-function values for the forcing and saddle formulation, respectively.

is computationally expensive, limiting ensemble size. We propose a new class of algorithms for speeding up the minimization of the ensemble of data assimilations. It consists in using block Krylov methods to simultaneously perform the minimization for all members of the ensemble, instead of performing each minimization separately.
We develop preconditioned block Krylov versions of the Full Orthogonal Method (FOM) and of the Lanczos algorithm in both primal and dual space. The latter works in observation space that is usually of smaller dimension than the state space, giving thus an advantage in terms of memory requirements and computational cost. We describe and compare several parallelization strategies for speeding up the minimization and limiting the communications.
These methods have been tested on a Quasi-Geostrophic system, consisting of a simplified atmospheric circulation model equipped with an ensemble of 3DVar schemes tuned to mimic some features of a limited area numerical weather prediction system. Experimentation shows that the number of iterations needed to converge is drastically reduced by the block Krylov approaches. We indicate that, while working in primal space does not allow to save significant computational time, working in the dual space may reduce the computational time by a factor 2–5 depending on ensemble size compared to standard Krylov methods, making our approach attractive for operational use.

3.1.4 Speeding up the ensemble data assimilation system of the limited area model of Météo-France using a Block Krylov algorithm

Ensembles of Data Assimilations (EDA) in Numerical Weather Prediction (NWP) are frequently used for both the initialization of ensemble prediction systems and for providing background error statistics to a deterministic variational data assimilation scheme. The EDA consists in running in parallel multiple data assimilation schemes with perturbed observations and backgrounds. This kind of ensemble is computationally expensive in particular because it requires to solve as many linear systems as there are members in the ensemble. Recently, we proposed the use of block Krylov methods [ALG29] to take advantage of the EDA structure to solve simultaneously all the linear systems, allowing to reduce the number of iterations needed to converge. This approach is further studied in [ALG30]. We develop

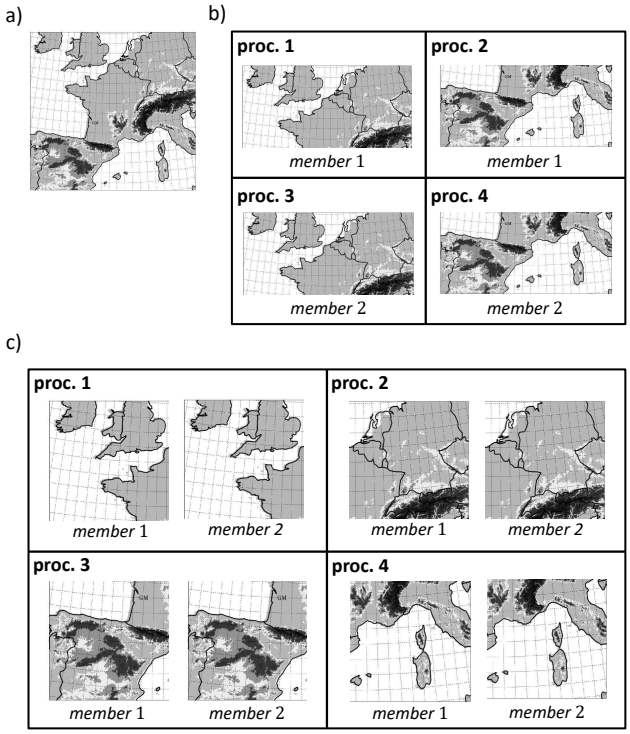

Figure 3.2: Illustration of the two workload distributions implemented in this work on the AROME-France domain for 4 MPI processes and 2 members in the ensemble. a) Geographical domain of the AROME-France NWP model. b) Workload distribution by member, combined with an underlying geographical distribution, as used in the MPI and MPIstored versions of block B-FOM, and in B-FOM. c) Workload geographical distribution (no distribution by member), as used in the SEQ version of block B-FOM.

advanced parallelization strategies for the block Krylov method formulated in observation space using the Object Oriented Prediction System (OOPS) jointly developed by the European Centre for Medium-Range Weather Forecasts, Météo-France, and their partners. The algorithm is fully tested with the EDA of the limited area model AROME of Météo-France, for different weather situations and configurations representative of the current system, namely assimilating around $10^4 - 10^5$ observations together with 25 members. This new block Krylov approach allows to gain from 13% up to 45% of the computational time of the minimizations. Experiments with extended configurations that assimilate more observations and that use more ensemble members confirm the potential of the algorithm in the future, with gains up to 65%.

3.2 Covariance modelling

3.2.1 Modelling spatially correlated observation errors in variational data assimilation using a diffusion operator on an unstructured mesh

In [1] we propose a method for representing spatially correlated observation errors in variational data assimilation. The method is based on the numerical solution of a diffusion equation, a technique commonly used for representing spatially correlated background errors. The discretization of the pseudo-time

derivative of the diffusion equation is done implicitly using a backward Euler scheme. The solution of the resulting elliptic equation can be interpreted as a correlation operator whose kernel is a correlation function from the Matérn family. In order to account for the possibly heterogeneous distribution of observations, a spatial discretization technique based on the finite element method (FEM) is chosen where the observation locations are used to define the nodes of an *unstructured* mesh on which the diffusion equation is solved. By construction, the method leads to a convenient operator for the *inverse* of the observation error correlation matrix, which is an important requirement when applying it with standard minimization algorithms in variational data assimilation. Previous studies have shown that spatially correlated observation errors can also be accounted for by assimilating the observations together with their directional derivatives up to arbitrary order. In the continuous framework, we show that the two approaches are formally equivalent for certain parameter specifications. The FEM provides an appropriate framework for evaluating the derivatives numerically, especially when the observations are heterogeneously distributed. Numerical experiments are performed using a realistic data distribution from the Spinning Enhanced Visible and InfraRed Imager (SEVIRI). Correlations obtained with the FEM-discretized diffusion operator are compared with those obtained using the analytical Matérn correlation model. The method is shown to produce an accurate representation of the target Matérn function in regions where the data are densely distributed (Figure 3.3). The presence of large gaps in the data distribution degrades the quality of the mesh and leads to numerical errors in the representation of the Matérn function. Strategies to improve the accuracy of the method in the presence of such gaps are discussed.

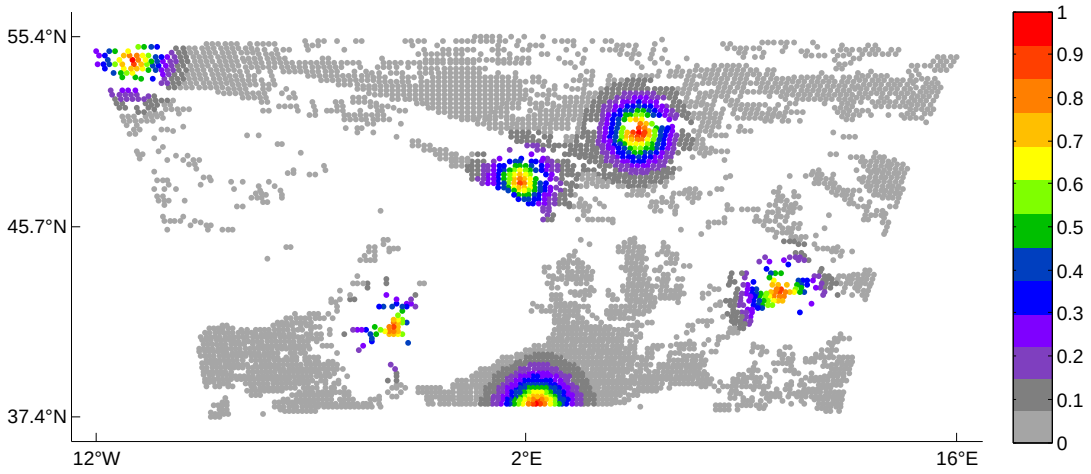

Figure 3.3: Impulse response of the FEM diffusion-based correlation operator at six points on an unstructured mesh that is built from the spatial distribution of satellite radiance observations from SEVIRI.

References

[1] O. Guillet, A. T. Weaver, X. Vasseur, M. Michel, S. Gratton, and S. Gürol, (2018), Modelling spatially correlated observation errors in variational data assimilation using a diffusion operator on an unstructured mesh, *Submitted to Quarterly Journal of the Royal Meteorological Society*.

Nonlinear Optimization

4.1 Least-Squares Problems

4.1.1 Guaranteeing the convergence of the saddle formulation for weakly constrained 4DVAR data assimilation

[ALG19] discusses convergence issues for the saddle variational formulation [ALG16] of the weakly-constrained 4D-VAR method in data assimilation, a method whose main interests are its parallelizable nature and its limited use of the inverse of the correlation matrices. It is shown that the method, in its original form, may produce erratic results or diverge because of the inherent lack of monotonicity of the produced objective function values. Convergent, variationaly coherent variants of the algorithm are then proposed which largely retain the desirable features of the original proposal, and the circumstances in which these variants may be preferable to other approaches is briefly discussed.

4.1.2 How the invasion zone can contribute to the estimation of petrophysical properties from log inversion at well scale?

In a conventional formation evaluation process, the mud filtrate invasion in the near wellbore is considered as a bias which is corrected from logs before any petrophysical evaluation. The developments presented in [ALG4] show that the invasion zone is a valuable source of information to estimate dynamical properties that generally come only from core measurements such as permeability, relative permeabilities, capillary pressure curves and formation factor. In this approach, the invasion process is not simulated in itself as it would lead to a very unstable inverse problem within the time frame of the logging. On the contrary, it considers the fluids in the invaded domain as radially equilibrated and solves the fluid distribution governed at first order by capillary pressures. Due to the multimodality of the inverse problem and the uncertainties related to the mud-filtrate parameters, the invasion zone is jointly inverted with the vertical capillary equilibrium at field scale describing the vertical water saturation profile in the reservoir for each facies. In the context of this study, we present a vertical well and consider a radial oil base mud invasion. We also assume isotropic petrophysical parameters. The final results are compared to all available sources of data such as NMR, WFT and cores for permeabilities, formation factor and capillary pressure curves.

4.1.3 Quasi-static ensemble variational data assimilation: A theoretical and numerical study with the iterative ensemble Kalman smoother

The analysis in nonlinear variational data assimilation is the solution of a non-quadratic minimization. Thus, the analysis efficiency relies on its ability to locate a global minimum of the cost function. If this minimization uses a Gauss–Newton (GN) method, it is critical for the starting point to be in the attraction basin of a global minimum. Otherwise the method may converge to a local extremum, which degrades the analysis. With chaotic models, the number of local extrema often increases with the temporal extent of the data assimilation window, making the former condition harder to satisfy. This is unfortunate because the assimilation performance also increases with this temporal extent. However, a quasi-static (QS) minimization may overcome these local extrema. It accomplishes this by gradually injecting the

observations in the cost function. In [ALG15], we generalize this approach to four-dimensional strong-constraint nonlinear ensemble variational (EnVar) methods, which are based on both a nonlinear variational analysis and the propagation of dynamical error statistics via an ensemble. This forces one to consider the cost function minimizations in the broader context of cycled data assimilation algorithms. We adapt this QS approach to the iterative ensemble Kalman smoother (IEnKS), an exemplar of nonlinear deterministic four-dimensional EnVar methods. Using low-order models, we quantify the positive impact of the QS approach on the IEnKS, especially for long data assimilation windows. We also examine the computational cost of QS implementations and suggest cheaper algorithms.

4.2 Multidisciplinary Design Optimization

4.2.1 Towards the industrialization of new Multidisciplinary Design Optimization (MDO) methodologies and tools for aircraft design

At IRT Saint Exupéry, industrial and academic partners collaborate in a single place to the development of MDO methodologies; the advantage provided by this mixed organization is to directly benefit from both advanced methods at the cutting edge of research and deep knowledge of industrial needs and constraints. [ALG3] presents the three main goals: the elaboration of innovative MDO methodologies and formulations adapted to the resolution of industrial aircraft optimization design problems, the development of a MDO platform featuring scalable MDO capabilities for transfer to industry and the achievement of a simulation-based optimization of an aircraft engine pylon with industrial Computational Fluid Dynamics (CFD) and Computational Structural Mechanics (CSM) tools.
CERFACS, as one of the partners of this project, works in developing preconditioners for subproblems of MDO, especially for bound-constrained optimization problems to accelerate the convergence.

4.3 Hybrid Methods

4.3.1 An indicator for the switch from derivative-free to derivative-based optimization

In some optimization problems found in applications, the derivatives of the objective function can be computed or approximated but at an expensive cost, and it is desirable to know when to use derivative-free methods (such as direct search, for instance) or derivative-based methods (such as gradient or quasi-Newton methods). Derivative-free methods may achieve a steady initial progress for some problems, but after some advance they may also become slower or even stagnate due to the lack of derivatives. It is thus of interest to provide a way to appropriately switch from a derivative-free method to a derivative-based one. In [ALG20], we develop a family of indicators for such a switch based on the decrease properties of both classes of methods (typically used when deriving worst case complexity bounds).

Methodological advances for uncertainty quantification

5.1 Parallel Domain Decomposition Strategies for Stochastic Elliptic Equations

5.1.1 Local KL Representations

This work [ALG12] presents a method to efficiently determine the dominant Karhunen-Loève (KL) modes of a random process with known covariance function. The truncated KL expansion is one of the most common techniques for the approximation of random processes, primarily because it is an optimal representation, in the mean squared error sense, with respect to the number of random variables in the representation. However, finding the KL expansion involves solving integral problems, which tends to be computationally demanding. This work addresses this issue by means of a work-subdivision strategy based on a domain decomposition approach, enabling the efficient computation of a possibly large number of dominant KL modes. Specifically, the computational domain is partitioned into smaller non-overlapping subdomains, over which independent local KL decompositions are performed to generate local bases which are subsequently used to discretize the global modes over the entire domain. The latter are determined by means of a Galerkin projection. The procedure leads to the resolution of a reduced Galerkin problem, whose size is not related to the dimension of the underlying discretization space, but is actually determined by the desired accuracy and the number of subdomains. It can also be easily implemented in parallel. Extensive numerical tests are used to validate the methodology and assess its serial and parallel performance. The resulting expansion is exploited in 5.1.2 to accelerate the solution of the stochastic partial differential equations using a Monte Carlo approach.

5.1.2 Accelerated Monte Carlo Sampling with Local PC Expansions

Solving Stochastic Differential Equations (SPDE) can be a computationally intensive task, particularly when the underlying parametrization of the stochastic input field involves a large number of random variables. Direct Monte Carlo (MC) sampling methods are well suited for this type of situation, since their cost is independent of the input complexity. Unfortunately, MC sampling methods suffer from slow convergence. In this manuscript [ALG13], we propose an acceleration framework for elliptic SPDEs that relies on Domain Decomposition techniques and Polynomial Chaos (PC) expansions of local operators to reduce the cost of solving a SPDE via MC sampling. The approach exploits the fact that, at the subdomain level, the number of variables required to accurately parametrize the input stochastic field can be significantly reduced, as covered in 5.1.1. This makes it feasible to construct PC expansions of the local contributions to the condensed problem (*i.e.* the Schur complement of the discretized operator). The approach basically consists of two main stages: 1) a preprocessing stage in which PC expansions of the condensed problem are computed and 2) a Monte Carlo sampling stage where random samples of the solution are computed. The proposed method its naturally parallelizable. Extensive numerical tests are used to validate the methodology and assess its serial and parallel performance.

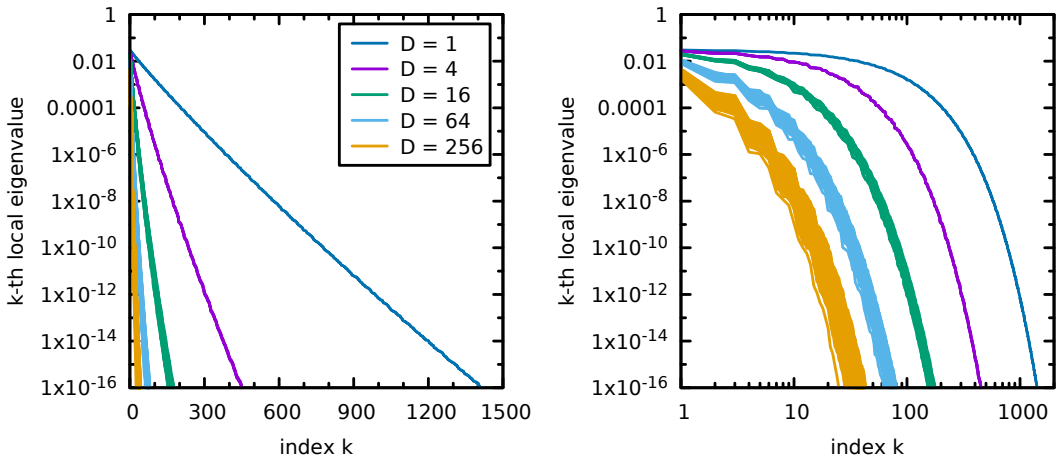

(a) (b)

Figure 5.1: Spectra of local decompositions for the squared Gaussian covariance, with $L = 0.1$, and different number of subdomains D as indicated. The plot in (a) uses a linear scale for the x-axis, while the plot in (b) uses a logarithmic scale.

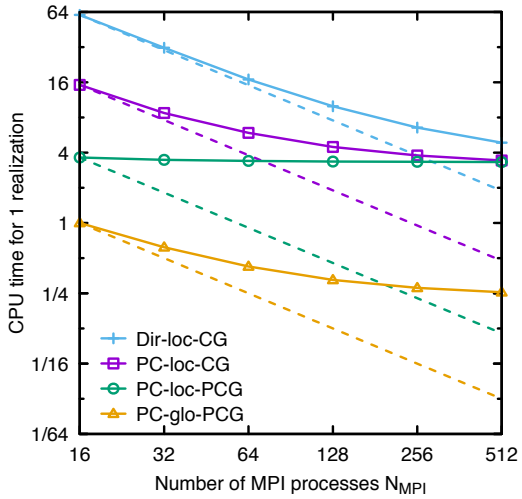

Figure 5.2: Illustration of the computational gain of the PC approach as compared to the direct sampling approach (blue line).

5.2 Multilevel Monte Carlo covariance estimation for the computation of Sobol' indices

Crude and quasi Monte Carlo (MC) sampling techniques are common tools dedicated to estimating statistics (expectation, variance, covariance) of a random quantity of interest. We focus here on the uncertainty quantification framework where the quantity of interest is the output of a numerical simulator fed with uncertain input parameters. Then, sampling the output involves running the simulator for different samples of the inputs, which may be computationally time-consuming. To reduce the cost of sampling, a first

approach consists in replacing the numerical simulator by a surrogate model that is cheaper to evaluate, thus making it possible to generate more samples of the output and therefore leading to a lower sampling error. However, this approach adds to the sampling error an unavoidable model error.
Another approach, which does not introduce any model error, is the so-called multilevel MC (MLMC) method. Given a sequence of levels corresponding to numerical simulators with increasing accuracy and computational cost, MLMC combines samples obtained at different levels to construct an estimator at a reduced cost compared to standard MC sampling. In [ALG40], we extend theorems of MLMC theory to covariance estimation, and we propose a novel version of the multilevel algorithm, driven by a target cost. These results are used in a sensitivity analysis context in order to derive a multilevel estimation of Sobol' indices, whose building blocks can be written as covariance terms in a pick-and-freeze formulation. These contributions are successfully tested on an initial value problem with random parameters; see Fig. 5.3.

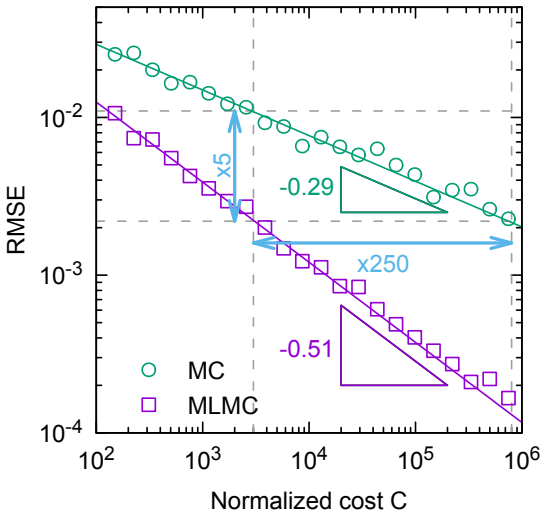

Figure 5.3: Illustration of the convergence rate of MC and MLMC for the computation of Sobol' indices on a 1d stochastic differential equation.

Numerical methods for partial differential equations

6.1 Numerical methods for mathematical biology

6.1.1 A numerical scheme for the early steps of nucleation-aggregation models

In the formation of large clusters out of small particles, the initializing step is called the nucleation, and consists in the spontaneous reaction of agents which aggregate into small and stable polymers called nuclei. After this early step, the polymers are involved in a number of reactions such as polymerization, fragmentation and coalescence. Since there may be several orders of magnitude between the size of a particle and the size of an aggregate, building efficient numerical schemes to capture accurately the kinetics of the reaction is a delicate step of key importance. In the work [ALG7], we investigate a conservative scheme, based on finite volume methods on an adaptive grid, which is capable of simulating well the early steps of the reaction as well as the later chain reactions.

6.2 Finite element methods

6.2.1 A finite element method for quantum graphs

In the work [ALG5], we study the numerical solution of boundary and initial value problems for differential equations posed on graphs or networks. The graphs of interest are quantum graphs, i.e., metric graphs endowed with a differential operator acting on functions defined on the graph's edges with suitable side conditions. We describe and analyze the use of linear finite elements to discretize the spatial derivatives for a class of linear elliptic model problems. The solution of the discrete equations is discussed in detail in the context of a (nonoverlapping) domain decomposition approach. For model elliptic problems and a wide class of graphs, we show that a combination of Schur complement reduction and diagonally preconditioned conjugate gradients results in optimal complexity. For problems of parabolic type, we consider the use of exponential integrators based on Krylov subspace methods. Numerical results are given for both simple and complex graph topologies.

6.2.2 The HyTeG finite-element software framework for scalable multigrid solvers

[ALG23] presents a new software architecture for the ultra-fast multigrid solution of FE problems on hierachically structured meshes. The new framework in under development in C++. The modular software architecture is carefully designed to exploit the resources of modern and future supercomputers. Combining an unstructured topology with structured grid refinement facilitates high geometric adaptability and matrix-free multigrid implementations with excellent performance. Different abstraction levels and fully distributed data structures additionally ensure high flexibility, extensibility, and scalability. The software concepts support sophisticated load balancing and flexibly combining finite-element spaces. Example scenarios with coupled systems of partial differential equations show the applicability of the concepts to performing geophysical simulations.

6.2.3 A New Matrix-Free Approach for Large-Scale Geodynamic Simulations and its Performance

[ALG2] studies new matrix free techniques that can be used on hierarchically structured meshes. Such techniques will become important in the upcoming age of extreme scale computing to reduce memory consumption and memory access overheads. They avoid storing a matrix and use fast techniques to re-compute the matricx entries on the fly within an iterative solution process. Here the method is integrated in a multigrid solver framework and thus enables to solve FE systems of unprecedented size. The proposed method is based on surrogate element matrices constructed by low-order polynomial approximations. It is applied to a Stokes-type PDE system with variable viscosity as is a key component in mantle convection models. We set the ground for a rigorous performance analysis inspired by the concept of parallel textbook multigrid efficiency and study the weak scaling behavior on SuperMUC, a peta-scale supercomputer system. For a complex geodynamical model, we achieve a parallel efficiency of 95% on up to 47250 compute cores. Our largest simulation uses a trillion $O(10^{12})$ degrees of freedom for a global mesh resolution of 1.7 km

6.2.4 A scalable and extensible checkpointing scheme for massively parallel simulations

[ALG22] presents and analyses resilience techniques based on checkpointing as they will become essential in the upcoming age of extreme scale computing. The probability of a failure increases both with the runtime and with the number of system components. For future exascale systems, it is therefore considered critical that strategies are developed to make software resilient against failures. The checkpoint routines developed are generic and realize a novel extensible software architecture suitable for modern coupled multiphysics applications. The full scalability and efficiency of the methods is demonstrated. We present a scalable, distributed, diskless, and resilient checkpointing scheme that can create and recover snapshots of a partitioned simulation domain. We demonstrate the efficiency and scalability of the checkpoint strategy for simulations with up to 40 billion computational cells executing on more than 400 billion floating point values. A checkpoint creation is shown to require only a few seconds and the new checkpointing scheme scales almost perfectly up to more than $2^{18} \approx 260\ 000$ processes. To recover from a diskless checkpoint during runtime, we realize the recovery algorithms using ULFM MPI. The checkpointing mechanism is fully integrated in a state-of-the-art high-performance multiphysics simulation framework. We demonstrate the efficiency and robustness of the method with a realistic phase-field simulation originating in the material sciences.

6.3 Discontinuous Galerkin and boundary element methods

6.3.1 A symmetric Trefftz-DG formulation based on a local boundary element method for the solution of the Helmholtz equation

In the work [ALG9], a general symmetric Trefftz Discontinuous Galerkin method is built for solving the Helmholtz equation with piecewise constant coefficients. The construction of the corresponding local solutions to the Helmholtz equation is based on a boundary element method. A series of numerical experiments displays an excellent stability of the method relatively to the penalty parameters, and more importantly its outstanding ability to reduce the instabilities known as the "pollution effect" in the literature on numerical simulations of long-range wave propagation.

6.4 Lattice Boltzmann methods for complex flows

The massively parallel simulation of multiphysics scenarios involving complex flows requires many levels of innovation.

6.4.1 Extreme-Scale Block-Structured Adaptive Mesh Refinement

In [ALG36] adaptive mesh refinement and load balancing for meshes with a trillion cells and on up to a million threads is demonstrated. The software infrastucture is generic but can be used to simulatate multiphysics scenarios based on lattice Boltzmann methods. More generally, we present a novel approach for block-structured adaptive mesh refinement (AMR) that is suitable for extreme-scale parallelism. All data structures are designed such that the size of the metadata in each distributed processor memory remains bounded independent of the processor number. In all stages of the AMR process, we use only distributed algorithms. No central resources such as a master process or replicated data are employed, so that an unlimited scalability can be achieved. For the dynamic load balancing in particular, we propose to exploit the hierarchical nature of the block-structured domain partitioning by creating a lightweight, temporary copy of the core data structure. This copy acts as a local and fully distributed proxy data structure. It does not contain simulation data but only provides topological information about the domain partitioning into blocks. Ultimately, this approach enables an inexpensive, local, diffusion-based dynamic load balancing scheme. We demonstrate the excellent performance and the full scalability of the new AMR implementation for two architecturally different petascale supercomputers. Benchmarks on an IBM Blue Gene/Q system with a mesh containing 3.7 trillion unknowns distributed to $458\,752$ processes confirm the applicability for future extreme-scale parallel machines. The algorithms proposed in this article operate on blocks that result from the domain partitioning. This concept and its realization support the storage of arbitrary data. In consequence, the software framework can be used for different simulation methods, including mesh-based and meshless methods. In this article, we demonstrate fluid simulations based on the lattice Boltzmann method.

6.4.2 A scalable multiphysics algorithm for massively parallel direct numerical simulations of electrophoretic motion

In article [ALG8] we present new methods to simulate a coupled system consisting of a fluid phase with an embedded particulate solid phase This requires the additional computation of electrostatic fields and modeling the charge transport in a massively parallel constellation. We introduce a novel coupled algorithm for the direct numerical simulations of electrophoresis in microfluidic flows. This multiphysics algorithm employs an Eulerian description of fluid and ions, combined with a Lagrangian representation of moving charged particles. The fixed grid facilitates efficient solvers and the employed lattice Boltzmann method can efficiently handle complex geometries. Validation experiments with more than 70000 time steps are presented, together with scaling experiments with over 4×10^6 particles and 1.96×10^{11} grid cells for both hydrodynamics and electric potential. We achieve excellent performance and scaling on up to $65\,536$ cores of a current supercomputer.

6.4.3 A comparative study of fluid-particle coupling methods for fully resolved lattice Boltzmann simulations

[ALG34] is a comparative study of fluid-particle coupling methods for fully resolved lattice Boltzmann simulations. For the lattice Boltzmann method, different variants exist to incorporate the fluid-particle interaction into the simulation. This paper provides a detailed and systematic comparison of two different methods, namely the momentum exchange method and the partially saturated cells method by Noble and Torczynski. We discuss their algorithmic parts in detail, show and propose improvements to the

commonly applied algorithms, and eventually identify three suitable subvariants of each method. These subvariants are used in the benchmark scenario of a single heavy sphere settling in ambient fluid to study their respective strengths and weaknesses in accurately reproducing characteristic physical phenomena for particle Reynolds numbers from 185 up to 365. The sphere must be resolved with at least 24 computational cells per diameter to achieve velocity errors below 5%. The momentum exchange method is found to be more accurate in predicting the streamwise velocity component whereas the partially saturated cells method is more accurate in the spanwise components. The study reveals that the resolution should be chosen with respect to the coupling dynamics, and not only based on the flow properties, to avoid large errors in the fluid-particle interaction.

6.4.4 Lattice Boltzmann simulations of the bead-spring microswimmer with a responsive stroke: from an individual to swarms

[ALG32] describes the use of massively parallel Lattice Boltzmann methods and extended particle simulation methods as tools to study active swimmers. Propulsion at low Reynolds numbers is often studied by defining artificial microswimmers which exhibit a particular stroke. The disadvantage of such an approach is that the stroke does not adjust to the environment, in particular the fluid flow, which can diminish the effect of hydrodynamic interactions. To overcome this limitation, we simulate a microswimmer consisting of three beads connected by springs and dampers, using the self-developed waLBerla and pe framework based on the lattice Boltzmann method and the discrete element method. In our approach, the swimming stroke of a swimmer emerges as a balance of the drag, the driving and the elastic internal forces. We validate the simulations by comparing the obtained swimming velocity to the velocity found analytically using a perturbative method where the bead oscillations are taken to be small. Including higher-order terms in the hydrodynamic interactions between the beads improves the agreement to the simulations in parts of the parameter space. Encouraged by the agreement between the theory and the simulations and aided by the massively parallel capabilities of the waLBerla-pe framework, we simulate more than ten thousand such swimmers together, thus presenting the first fully resolved simulations of large swarms with active responsive components.

6.5 Rigid body dynamics

6.5.1 The maximum dissipation principle in rigid-body dynamics with inelastic impacts

The article [ALG33] develops a novel mathematical model for contacts between rigid particles, as it can be used in the direct numerical simulation of fully resolved particulate flows or as a standalone tool to simulate granular systems. Formulating a consistent theory for rigid-body dynamics with impacts is an intricate problem. Twenty years ago Stewart published the first consistent theory with purely inelastic impacts and an impulsive friction model analogous to Coulomb friction. In this paper we demonstrate that the consistent impact model can exhibit multiple solutions with a varying degree of dissipation even in the single-contact case. Replacing the impulsive friction model based on Coulomb friction by a model based on the maximum dissipation principle resolves the non-uniqueness in the single-contact impact problem. The paper constructs the alternative impact model and presents integral equations describing rigid-body dynamics with a non-impulsive and non-compliant contact model and an associated purely inelastic impact model maximizing dissipation. An analytic solution is derived for the single-contact impact problem. The models are then embedded into a time-stepping scheme. The macroscopic behaviour is compared to Coulomb friction in a large-scale granular flow problem.

6.5.2 Toward Large Scale Modeling of Carbon Nanotube Systems with the Mesoscopic Distinct Element Method

[ALG31] presents new work using rigid body dynamics as simulation tool to study the physics of carbon nanotube systems. We introduce a new scalable and efficient implementation of the mesoscopic distinct element method for massively parallel numerical simulations. Carbon nanotubes are represented as chains of rigid bodies, linked by elastic bonds and dispersive van der Waals (vdW) forces. The enhanced vector model formalism of the elastic bond between rigid bodies, developed recently, is employed here to capture the elastic deformation of nanotubes. Dispersive interactions between the neighboring nanotubes are described with the coarse-grained vdW potential. Time integration is performed using a velocity Verlet integration scheme with tunable damping in order to describe the energy dissipation to the implicit degrees of freedom. Due to the scalable message passing interface (MPI) parallelization, enabled by rigid particle dynamics module (PE) of the waLBerla multiphysics framework, our method is capable of modeling large assemblies of carbon nanotubes. This advance enables us to move closer to the length and time scales required to extract representative mechanics of carbon nanotube materials. The promising scalability of the new implementation is probed in two examples of self-assembly of ultra-thin carbon nanotube films and carbon nanotube buckypapers, where formation of hierarchical networks of carbon nanotube bundles, storing both elastic and vdW adhesion energies is observed. The relaxation of one cubic micrometer of buckypaper illustrates the code scalability.

6.5.3 A coupled lattice Boltzmann method and discrete element method for discrete particle simulations of particulate flows

In article [ALG35] the authors present the coupling of rigid body dynamics with a lattice Boltzmann flow solver with novel coupling techniques that do not require the full geometric resolution of the particles and that rely on simplified models for the momentum transfer. Discrete particle simulations are widely used to study large-scale particulate flows in complex geometries where particle–particle and particle–fluid interactions require an adequate representation but the computational cost has to be kept low. In this work, we present a novel coupling approach for such simulations. A lattice Boltzmann formulation of the generalized Navier–Stokes equations is used to describe the fluid motion. This promises efficient simulations suitable for high performance computing and, since volume displacement effects by the solid phase are considered, our approach is also applicable to non-dilute particulate systems. The discrete element method is combined with an explicit evaluation of interparticle lubrication forces to simulate the motion of individual submerged particles. Drag, pressure and added mass forces determine the momentum transfer by fluid–particle interactions. A stable coupling algorithm is presented and discussed in detail. We demonstrate the validity of our approach for dilute as well as for dense systems by predicting the settling velocity of spheres over a broad range of solid volume fractions in good agreement with semi-empirical correlations. Moreover, the accuracy of particle–wall interactions in a viscous fluid is thoroughly tested and established. Finally, simulations of mono- and bi-disperse fluidized beds highlight the capability of our new approach to handle configurations with large particle numbers.

Publications

7.1 Books

[ALG1] I. Duff, A. Erisman, and J. Reid, (2017), *Direct Methods for Sparse Matrices. Second Edition.*, Numerical Mathematics and Scientific Computation, Oxford University Press, second edition ed.

7.2 Conferences Proceedings

[ALG2] S. Bauer, M. Huber, M. Mohr, U. Ruede, and B. Wohlmuth, (2018), A New Matrix-Free Approach for Large-Scale Geodynamic Simulations and its Performance, In *Lecture Notes in Computer Science*, S. Y. et al., ed., vol. 10861, International Conference on Computational Science, Springer, Cham, 17–30.

[ALG3] A. Gazaix, F. Gallard, V. Gachelin, T. Druot, S. Grihon, V. Ambert, D. Guénot, R. Lafage, C. Vanaret, B. Pauwels, N. Bartoli, T. Lefebvre, P. Sarouille, N. Desfachelles, J. Brézillon, M. Hamadi, and S. Gürol, (2017), Towards the Industrialization of New MDO Methodologies and Tools for Aircraft Design, In *18th AIAA/ISSMO Multidisciplinary Analysis and Optimization Conference, 2017, Denver, Colorado*, Denver, Colorado, USA, 1–23.

[ALG4] T. Vandamme, E. Caroli, and S. Gratton, (2017), How the Invasion Zone Can Contribute to the Estimation of Petrophysical Properties From Log Inversion at Well Scale?, In *SPWLA 58th Annual Logging Symposium*, Oklahoma City, Oklahoma, USA, SPWLA 58th Annual Logging Symposium, 17-21 June, Oklahoma City, Oklahoma, USA, Society of Petrophysicists and Well-Log Analysts.

7.3 Journal Publications

[ALG5] M. Arioli and M. Benzi, (2017), A Finite Element Method for Quantum Graphs, *IMA Journal of Numerical Analysis*, 1–45.

[ALG6] M. Bakry, S. Pernet, and F. Collino, (2017), A new accurate residual-based a posteriori error indicator for the BEM in 2D-acoustics, *Computers and Mathematics with Applications*, **73**, 2501–2514.

[ALG7] H. T. Banks, M. Doumic, and C. Kruse, (2017), A numerical scheme for the early steps of nucleation-aggregation models, *Journal of Mathematical Biology*, **74**, 259–287.

[ALG8] D. Bartuschat and U. Ruede, (2018), A scalable multiphysics algorithm for massively parallel direct numerical simulations of electrophoretic motion, *Journal of Computational Science*, **27**, 147–167.

[ALG9] H. Barucq, A. Bendali, M. Fares, V. Mattesi, and S. Tordeux, (2017), A symmetric Trefftz-DG formulation based on a local boundary element method for the solution of the Helmholtz equation, *Journal of Computational Physics*, **330**, 1069–1092.

[ALG10] R. Buizza, S. Brönnimann, L. Haimberger, P. Laloyaux, M. Martin, M. Fuentes, M. Alonso-Balmaseda, A. Becker, M. Blaschek, P. Dahlgren, E. de Boisseson, D. Dee, M. Doutriaux-Boucher, X. Feng, V. John, K. Haines, S. Jourdain, Y. Kosaka, D. Lea, F. Lemarié, M. Mayer, P. Messina, C. Perruche, P. Peylin, J. Pullainen, N. Rayner, E. Rustemeier, D. Schepers, R. Saunders, J. Schulz, A. Sterin, S. Stichelberger, A. Storto, C.-E. Testut, M.-A. Valente, A. Vidard, N. Vuichard, A. T. Weaver, J. While, and M. Ziese, (2018), The EU-FP7 ERA-CLIM2 Project Contribution to Advancing Science and Production of Earth System Climate Reanalyses, *Bulletin of the American Meteorological Society*, **99**, 1003–1014.

[ALG11] F. Chatelin and M. Rincon-Camacho, (2017), Hermitian matrices: Spectral coupling, plane geometry / trigonometry and optimisation, *Linear Algebra and its Applications*, **553**, 282–310.

[ALG12] A. A. Contreras, P. Mycek, O. P. Le Maître, F. Rizzi, B. Debusschere, and O. Knio, (2018), Parallel Domain Decomposition Strategies for Stochastic Elliptic Equations. Part A: Local Karhunen–Loève Representations, *SIAM Journal on Scientific Computing*, **40**, C520–C546.

[ALG13] A. A. Contreras, P. Mycek, O. P. Le Maître, F. Rizzi, B. Debusschere, and O. M. Knio, (2018), Parallel Domain Decomposition Strategies for Stochastic Elliptic Equations Part B: Accelerated Monte Carlo Sampling with Local PC Expansions, *SIAM Journal on Scientific Computing*, **40**, C547–C580.

[ALG14] D. Drzisga, L. John, U. Ruede, B. Wohlmuth, and W. Zulehner, (2018), On the Analysis of Block Smoothers for Saddle Point Problems, *SIAM Journal on Matrix Analysis and Applications*, **39**, 932–960.

[ALG15] A. Fillion, M. Bocquet, and S. Gratton, (2018), Quasi-static ensemble variational data assimilation: a theoretical and numerical study with the iterative ensemble Kalman smoother, *Nonlinear Processes in Geophysics*, **25**, 315–334.

[ALG16] M. Fisher and S. Gürol, (2017), Parallelization in the time dimension of four-dimensional variational data assimilation, *Quarterly Journal of the Royal Meteorological Society*, **143**, 1136–1147.

[ALG17] M. Fisher, S. Gratton, S. Gürol, Y. Trémolet, and X. Vasseur, (2018), Low rank updates in preconditioning the saddle point systems arising from data assimilation problems, *Optimization Methods and Software*, **33**, 45–69.

[ALG18] S. Gratton, S. Gürol, E. Simon, and P.-L. Toint, (2018), A note on preconditioning weighted linear least squares, with consequences for weakly-constrained variational data assimilation, *Quarterly Journal of the Royal Meteorological Society*, **144**, 934–940.

[ALG19] S. Gratton, E. Simon, P.-L. Toint, and S. Gürol, (2018), Guaranteeing the convergence of the saddle formulation for weakly-constrained 4D-VAR data assimilation, *Quarterly Journal of the Royal Meteorological Society*.

[ALG20] S. Gratton, N. Soualmi, and L.-N. Vicente, (2017), An indicator for the switch from derivative-free to derivative-based optimization, *Operations Research Letters*, **45**, 353–361.

[ALG21] O. Guillet, A. Weaver, X. Vasseur, M. Michel, S. Gratton, and S. Gürol, (2018), Modelling spatially correlated observation errors in variational data assimilation using a diffusion operator on an unstructured mesh, *Quarterly Journal of the Royal Meteorological Society*.

[ALG22] N. Kohl, J. Hötzer, F. Schornbaum, M. Bauer, C. Godenschwager, H. Köstler, B. Nestler, and U. Ruede, (2018), A scalable and extensible checkpointing scheme for massively parallel simulations, *International Journal of High Performance Computing Applications*.

[ALG23] N. Kohl, D. Thönnes, D. Drzisga, D. Bartuschat, and U. Ruede, (2018), The HyTeG finite-element software framework for scalable multigrid solvers, *International Journal of Parallel, Emergent and Distributed Systems*, 1–20.

[ALG24] W. F. Liu, A. Li, J. Hogg, I. S. Duff, and B. Vinter, (2017), Fast synchronization-free algorithms for parallel sparse triangular solves, *Concurrency and computation-Practice and Experience*, **29**, 1–21.

[ALG25] T. Lunet, J. Bodart, S. Gratton, and X. Vasseur, (2018), Time-parallel simulation of the decay of homogeneous turbulence using Parareal with spatial coarsening, *Computing and Visualization in Science*, 1–14.

[ALG26] T. Lunet, C. Lac, F. Auguste, F. Visentin, V. Masson, and J. Escobar, (2017), Combination of WENO and Explicit Runge–Kutta Methods for Wind Transport in the Meso-NH Model, *Monthly Weather Review*, **145**, 3817–3838.

[ALG27] T. Lunet, C. Lac, F. Auguste, F. Visentin, V. Masson, and J. Escobar, (2017), Combination of WENO and Explicit Runge–Kutta Methods for Wind Transport in the Meso-NH Model.

[ALG28] S. Mercier, S. Gratton, N. Tardieu, and X. Vasseur, (2017), A new preconditioner update strategy for the solution of sequences of linear systems in structural mechanics: application to saddle point problems in elasticity, *Computational Mechanics*, **60**, 969–982.

[ALG29] F. Mercier, S. Gürol, P. Jolivet, Y. Michel, and T. Montmerle, (2018), Block Krylov methods for accelerating ensembles of variational data assimilations, *Quarterly Journal of the Royal Meteorological Society*.

[ALG30] F. Mercier, Y. Michel, T. Montmerle, P. Jolivet, and S. Gürol, (2018), Speeding up the ensemble data assimilation system of the limited area model of Météo-France using a Block Krylov algorithm, *Quarterly Journal of the Royal Meteorological Society*.

[ALG31] I. Ostamin, P. Zhilyaev, V. Petrov, T. Dumitrica, S. Eibl, U. Ruede, and V. Kuzkin, (2018), Toward large scale modeling of carbon nanotube systems with the mesoscopic distinct element method, *Letters on Materials*, **8**, 240–245.

[ALG32] K. Pickl, J. Pande, H. Köstler, U. Ruede, and A. S. Smith, (2017), Lattice Boltzmann simulations of the bead-spring microswimmer with a responsive stroke—from an individual to swarms, *Journal of Physics-Condensed Matter*, **29**.

[ALG33] T. Preclik, S. Eibl, and U. Ruede, (2018), The maximum dissipation principle in rigid-body dynamics with inelastic impacts, *Computational Mechanics*, **62**, 81–96.

[ALG34] C. Rettinger and U. Ruede, (2017), A comparative study of fluid-particle coupling methods for fully resolved lattice Boltzmann simulations, *Computers and Fluids*, **154**, 74–89.

[ALG35] C. Rettinger and U. Ruede, (2018), A coupled lattice Boltzmann method and discrete element method for discrete particle simulations of particulate flows, *Computers and Fluids*, **172**, 706–719.

[ALG36] F. Schornbaum and U. Ruede, (2018), Extreme-Scale Block-Structured Adaptive Mesh Refinement, *SIAM Journal on Scientific Computing*, **40**, C358–C387.

[ALG37] A. T. Weaver, S. Gürol, J. Tshimanga, M. Chrust, and A. Piacentini, (2018), "Time"-parallel diffusion-based correlation operators, *Quarterly Journal of the Royal Meteorological Society*, **144**, 2067–2088.

7.4 Technical Reports

[ALG38] M. Arioli, C. Kruse, U. Ruede, and N. Tardieu, (2018), An iterative generalized Golub-Kahan algorithm for problems in structural mechanics, technical report, Cerfacs, Toulouse, France.

[ALG39] I. S. Duff, P. A. Knight, L. Le Gorrec, S. Mouysset, and D. Ruiz, (2018), Uncovering Hidden Block Structure, technical report, Cerfacs, Toulouse, France, 42 avenue Gaspard Coriolis.

[ALG40] P. Mycek and M. De Lozzo, (2018), Multilevel Monte Carlo covariance estimation for the computation of Sobol' indices, technical report, Cerfacs, 42 avenue Gaspard Coriolis, 31057 Toulouse cedex 1.

[ALG41] A. T. Weaver, M. Chrust, B. Ménétrier, A. Piacentini, J. Tshimanga, Y. Yang, S. Gürol, and H. Zuo, (2018), Using ensemble-estimated background error variances and correlation scales in the NEMOVAR system, technical report.

[ALG42] A. T. Weaver, S. Gürol, J. Tshimanga, M. Chrust, and A. Piacentini, (2017), "Time"-parallel diffusion-based correlation operators, tech. rep., CERFACS.

7.5 Thesis

[ALG43] T. Lunet, (2018), *Stratégies de parallèlisation espace-temps pour la simulation numérique des écoulements turbulents*, phd thesis, Université de Toulouse - Ecole Doctorale : MITT.

[ALG44] T. Vandamme, (2018), *Simulation-inversion des diagraphies*, phd thesis, Université de Toulouse - Ecole Doctorale : MITT.

2

Climate and Environment

Introduction

During the last two years, three research and development activity domains, gathered under the title "Climate and Environment", have been strongly consolidated:

- Climate Modeling
- Environment Modeling and Monitoring
- Coupling, HPC and Data for Climate

While the present report focuses on scientific achievements, it is worth relating these activities to the five strategic axes that are put forward in the CERFACS prospective. The "Linear algebra" and "Numerical methods for PDE" are not fed by the present applications axes, but the models that they are using benefit from them. The "Coupling" strategic axis is clearly addressed in the present report both through software developments and methodologies. The "Data driven modeling" strategic axis is strongly fed by the three activity domains described in this chapter, through variability analysis, data assimilation and post-processing. The "Exascale" strategic axis strongly benefits from the high performance simulations performed with climate models or data assimilation based simulations, as well as numerous technical developments on coupling, code optimization of data processing.

1.1 Climate Modeling

Research activities in climate modeling address a large variety of topics. They are all included in the framework of climate Change.

A first topic deals with the Atlantic Multidecadal Variability through an intercomparaison of climate simulations in which CERFACS has played an important role. Statistical analyses and sensitivity experiments have provided significant results: the non-stationarity of the oscillation, the main physical processes involved and the impacts on European climate.

Polar climate is a very specific topic that strongly involves sea ice extent predictability at annual scales in the framework of its projected loss at the end of the century. High potential for future improvements of regional predictions has been suggested through coupled models, and impacts on the mid latitude atmospheric circulation have been investigated.

A statistical analysis based on historical observations has been developed to separate the impacts of anthropogenic forcings from other variability drivers such as volcanic eruptions of solar variations. This approach has been used to estimate the time of emergence of anthropogenic warming, which proved to depend on the considered regions.

A new statistical downscaling method has been developed to estimate the meteorological forcing that drives the French river flows. The resulting simulations show that climate change is the main factor for the observed and predicted rivers flows variations, with increasing droughts.

Using historical and scenario simulations with a high-resolution regional climate model, the occurrence of climate extremes in France, in the framework of climate change, has been analyzed. The patterns of the

increasing mega-heatwaves events have been computed, the causes of increasing occurrence of low yieds have been determined and the statistical analysis of increasing flash floods occurrence has focused of the southeastern France.

While studying the mechanisms at the origin of the storm tracks with a multi-model approach, the need to lesser the weight of the climate models that share algorithms such as parametrization of components (e.g. ocean) has been put forward. These considerations are likely to improve the multi-model climate projections.

Ensemble simulations of a high resolution forced oceanic model have been performed to assess the intrinsic variability of the ocean dynamics, showing that it can be comparable to the atmospheric variability in specific regions. In parallel, forced atmospheric simulations have been performed at various resolution to assess the influence of small scale ocean structure on the atmosphere. A first topic was dealing with the Atlantic Multidecadal Variability through an intercomparaison of climate simulations in which CERFACS has played an important role. Statistical analyses and sensitivity experiment have provided significant results: the non-stationarity of the oscillation, main physical processes involved and impacts on European climate.

1.2 Environment Modeling and Monitoring

The "Environment Modeling and Monitoring" chapter gathers various research and development activities mixing high-fidelity numerical simulations and methodologies such as data assimilation, uncertainty quantification or high performance computing, with applications such as air quality, atmospheric chemistry, wild fire or hydraulics.

Satellite data assimilation for atmospheric chemistry combines a global model with stratospheric dynamics with various observations such as Ozone columns or radiances. Significant improvements in the accuracy of the estimated concentrations have been achieved through both modeling development and multiple data comparisons.

Large Eddy Simulations using several micro-scale models have been used to simulate the atmospheric dispersion of pollutants in various configurations: benchmarking of several models compared to a reference field-scale experiment, urban canopy strongly influenced by inflow conditions, accidental dispersion of a failing rocket propellant or dispersion of chemical species in a fictive airport. Numerical and methodological developments such as immersed boundary method or surrogate models have been achieved for these applications.

Wildfire spread modeling is a topic that has been used to apply or develop various methods addressing the CERFACS "Data driven modeling" strategic axis: assimilation of front data with metrics used in image-processing, combination of state and parameter estimations, uncertainty quantification to analyze model dependency, sensitivity analysis to reduce the control space, use of surrogate models or fire and atmosphere models coupling.

Rivers and estuaries have also strongly contributed to the "Data driven modeling" strategic axis. Ensemble simulations of 2D or 1D hydrodynamics models have been performed in the framework of state-of-the-art data analysis: uncertainty quantification, surrogate models or data reduction. These approaches strongly feed the various data assimilation applications used for flood forecast or bathymetry determination. Coupling of 1D and 2D models has also been a significant achievement of these productive activities.

At last, ensemble-variational data assimilation and covariance modeling have been successfully implemented in an ocean global model, based on advanced mathematical methods such as the use of diffusion tensors or implicit solvers on high-performance computers.

1.3 Coupling, HPC and Data for Climate

The last chapter, mixing coupling software and methods, High Performance Computing (HPC) and data processing for climate simulations, gathers high level developments in scienfic computing paving the path towards exascale computing.

Significant improvements have been achieved within the OASIS coupler, specialized in the coupling of Earth System components, including ocean and atmosphere. The inclusion of the MCT software in its core has proven to be a good decision. Models with several millions of grid points, running in parallel on thousands of cores, have their surface fields coupled on different grids with negligible time compared to the total computer time. These constant developments are at the root of the international success of this coupler.

Addressing a different HPC user community, the OpenPALM coupler has also significantly evolved, thanks to the decision to include the CWIPI software in its chain. New developments such as remote machines interface, ensemble runs launching or mixing of message passing protocols have been achieved to answer the needs of a growing number of users: urban climate, hydraulic or hydro-geologic applications, aerothermal or aeroacoustic coupling for aeronautic or automotive applications, etc.

Beyond these coupler improvements, coupling methods have been developed in the framework of various applications. The effects of nonlinearities of flux interopolations between different grids have been measured in the framework of both ocean and land coupling with the atmosphere. In the framework of data assimilation for flood forecasting, 1D/2D coupling algorithms have been developped with free surface flow models.

Several highly technical activities have been reinforced to ease the path towards exascale computing, in term of computing performance or data processing. A benchmark between several couplers has revealed that OASIS was well ahead other couplers, scaling up to 10 000 cores. Optimization of the NEMO oceanic model have produced significant results by looking at the effect of single precision computations or rewriting some key parts of the code. Using parallel input/ouput softwares and optimizing the load balancing of coupled system has led to significant improvements for the computer time performances. At last, multiple activities in the development of data processing workflows have reinforced the highly visible contribution of CERFCAS in data infrastructures: metadata standardization, resources scheduling, data locality, interoperability, etc.

Climate Modeling

2.1 Introduction

A common ground for the various topics addressed in this chapter is the use of great volumes of data coming out from climate reanalyses or climate scenarios. All these research topics lies in the framework of climate change: Atlantic multidecadal variability, polar climate, regional-scale attribution, river flows, climate extremes, multi-model representation of storm tracks and influence of oceanic variability or small scale structures.

2.2 Decadal-scale variability, predictability and associated impacts

The importance for many societal applications of improved information about near-term (from one year to a decade in advance) climate evolution at regional scale has prompted considerable research in the field of decadal climate prediction [8]. The so-called Atlantic Multidecadal Variability (AMV), characterized by basin-wide low-frequency variations of the North Atlantic sea surface temperature (SST), has been identified as one of the sources of predictability. The relatively short observational record severely limits our understanding of the physical mechanisms leading to the AMV. A model study revealed that the non-stationary behaviour of the AMV time series, suggested in observations, can be found in 7 out of 11 multi-century preindustrial climate simulations, and that sampling errors is not the main cause for this non-stationarity [CE125].
As part of the CMIP6 Decadal Climate Prediction Project, coordinated experiments to investigate the climate response to the AMV have been designed. CERFACS has been playing a leading role in this activity as both C. Cassou and R. Msadek are part of the panel that was in charge of defining the protocol and testing it before the forcing patterns were released to the community. Initial experiments made with the GFDL and NCAR climate models showed that during summer, a warm phase of the AMV yields reduced precipitation over the western United States, drier conditions over the Mediterranean Sea, and wetter conditions over Northern Europe [CE141]. The winter response to the AMV in these two models is associated with anomalies over the Pacific that project onto the interdecadal Pacific oscillation pattern. This winter response is a lagged adjustment of the Pacific Ocean to the AMV forcing in summer. Most of the simulated global-scale impacts are driven by the tropical part of the AMV, except for the winter North Atlantic Oscillation–like response over the North Atlantic–European region, which is driven by both the subpolar and tropical parts of the AMV.
Similar experiments were done with the CNRM-CM5 model as part of S. Qasmi Phd Thesis [15](to be defended in December 2018), and overall the results were comparable to those of [CE141]. The work of Qasmi et al. focused on the Euro-Atlantic climate response to the AMV, which is characterized by warmer temperatures and increased rainfall over most of the continent (Figure 2.1) during a positive AMV, compared to a negative AMV. The climate anomalies over land were found to be relatively weak in the standard experiments where the AMV pattern corresponds to 1std. The linearity of the response was investigated by scaling the forcing pattern and repeating the 1XAMV experiments with 2XAMV and 3XAMV respectively, which showed a much stronger response for temperature and precipitation over land. Further, in order to quantify the relative roles of the dynamical and non-dynamical processes in the AMV-forced response, we have employed a statistical technique based on circulation analogs [2], [11]

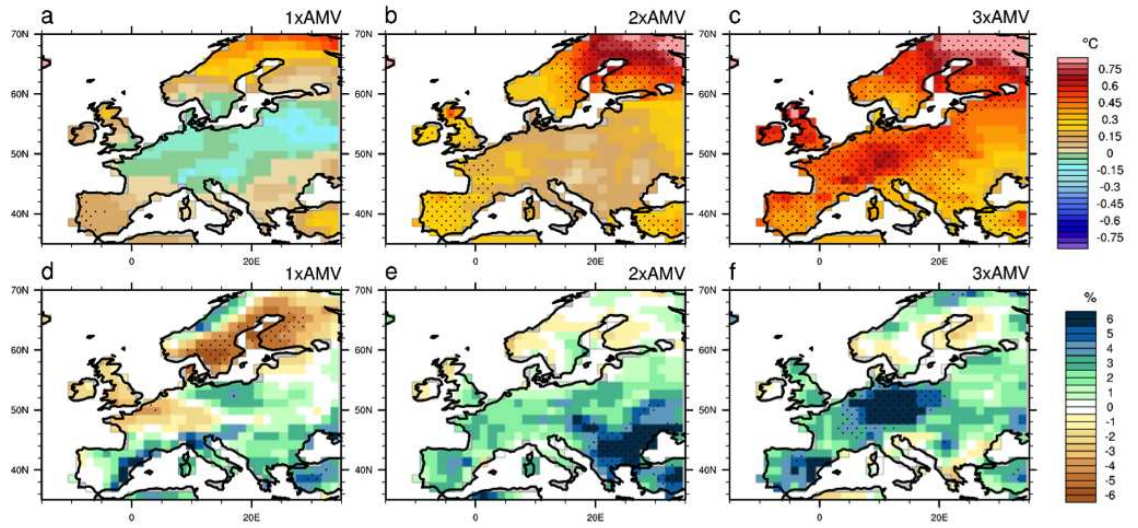

Figure 2.1: Difference between the 40-member 10-yr average ensemble mean between AMV+ and AMV- experiments for December-February seasonal mean for T2m (top panel, C), and precipitation (bottom panel, in relative percentage) for 1xAMV (left), 2xAMV (center) and 3xAMV (right). Stippling indicates regions that are above the 95% confidence level of statistical significance. Source: Qasmi et al to be submitted

that allows to decompose the response into a dynamical part and a thermodynamical part. The dynamical response can be interpreted as solely due to circulation anomalies, whereas the thermodynamical component is the residual that is mainly explained by thermal forcing. The temperature response is dominated by thermodynamical processes and is broadly linear with respect to AMV strength. The precipitation response is more complex and more regionally dependent. Both dynamical and thermodynamical parts contribute when the AMV forcing gets stronger (2XAMV and 3XAMV). We investigated the physical mechanisms associated with the AMV response and showed that in the CNRM-CM5 model, the thermodynamical response to the AMV is mainly driven by the advection of warm and moist oceanic anomalies by the western climatological flow and by changes in radiative fluxes associated with cloud cover anomalies. The dynamical response is driven by a tropically-induced diabatic heating which leads to Rossby wave propagation, cyclonic anomalies and a cooling over Europe. Interestingly, our work revealed a competing effect between the dynamical and thermodynamical response in T2m, which may partly explain the difficulty to detect the response to the AMV [14].

We also looked at how the AMV can modulate climate extremes over North America and showed that the AMV plays a role in the modulation of heat wave occurrence. We found an increased number of heat wave days by about 30% during an AMV warming compared to an AMV cooling. The physical mechanism of these impacts can be viewed a Gill-type atmospheric response to the tropical Atlantic SST anomalies that leads to a warming of the whole tropospheric column and to a decrease of relative humidity, cloud cover and precipitation. Soil moisture response to the AMV was also shown to play a role in the modulation of heat wave occurrence [CE140].

While skillful predictions of societal relevant variables like temperature and rainfall over land remain limited to few areas and few years, recent improvements in global dynamical climate prediction systems have resulted in skillful predictions of variables that are relevant for living marine resources, which can improve our understanding of ecosystem dynamics and has consequences in terms of fisheries [CE149].

2.3 Polar Climate

2.3.1 Regional predictability and predictions of Arctic sea ice extent

Seasonal predictions of Arctic sea ice on regional spatial scales are a pressing need for a broad group of stakeholders; however, most assessments of predictability and forecast skill to date have focused on pan-Arctic sea ice extent (SIE).

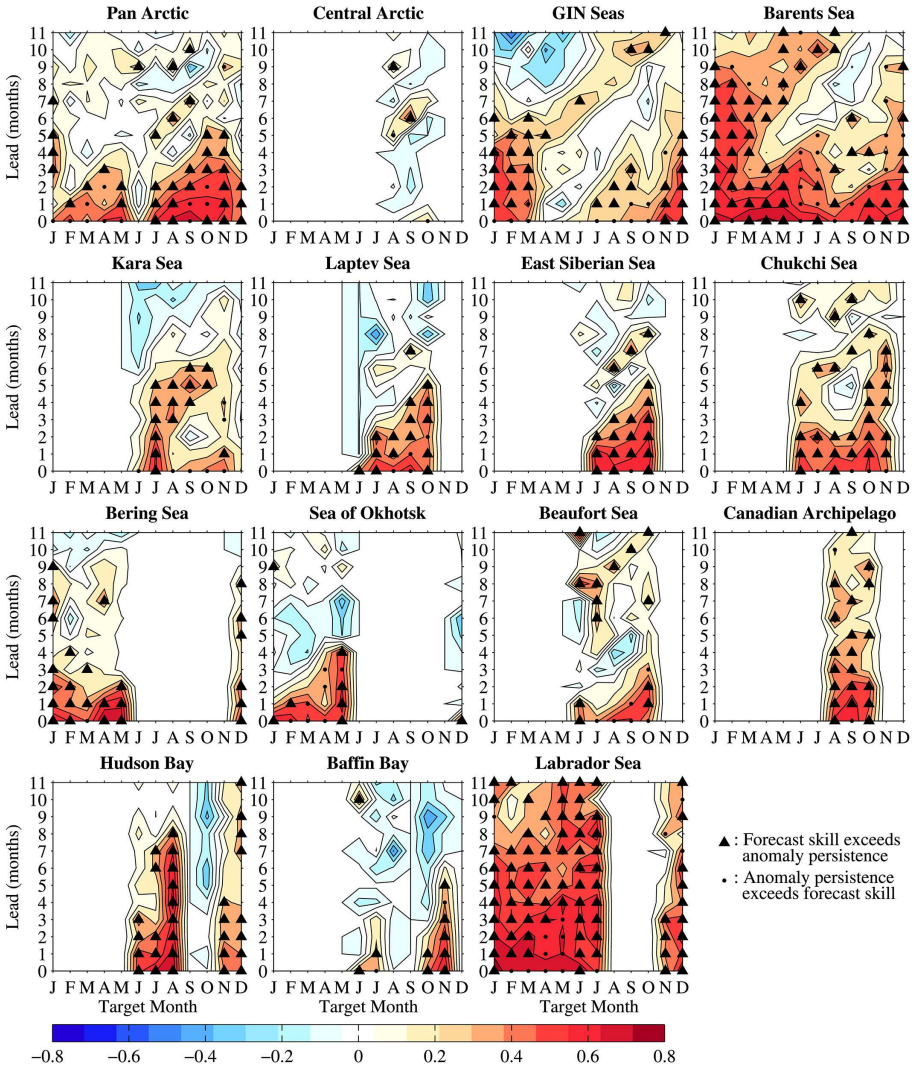

Figure 2.2: Seasonal prediction skill (ACC) for detrended regional Arctic SIE in the GFDL seasonal forecast system. The triangle and dot markers indicate months in which the ACC values are statistically significant at the 95% confidence level. Triangles indicate months in which the dynamical model's skill exceeds that of a persistence forecast, and circles indicate months in which the persistence forecast exceeds the model's skill. Correlations are only plotted for target months with SIE standard deviation greater than $0.03X10^6$ km2. Source: [CE99].

We analyzed a suite of retrospective initialized forecasts based on the GFDL global coupled model spanning 1981-2015, and found that predictions of detrended regional SIE are skillful at lead times up to 11 months (Figure 2.2). Regional prediction skill is highly region and target month dependent and generically exceeds the skill of an anomaly persistence forecast. We showed that initializing the ocean subsurface in a seasonal prediction system can yield significant regional skill for winter SIE [CE99]. In addition, consistent with previous work [4] [CE100], we found that sea ice thickness initial conditions provide a crucial source of skill for regional summer SIE. Further, using a $\ll$ perfect model $\gg$ approach that provides an estimate of the intrinsic predictability, we performed the first direct comparison of perfect model and operational seasonal prediction skill for region Arctic SIE with a common prediction system based. While their absolute skill values are different, the perfect model and operational regional predictions generally display similar correlation skill structures, indicating similar physical mechanisms at play. We found that regional winter SIE is generally more predictable than summer SIE. In nearly all Arctic regions we found a substantial skill gap between perfect model and operational predictions of regional SIE suggesting a high potential for future improvements in regional Arctic SIE predictions, in particular during winter [3].

2.3.2 Atmospheric linkages driven by Arctic sea ice decline

As shown by [6] and in the PhD thesis of T. Oudar [CE133] [9], the direct forcing of Arctic sea ice loss that is projected to occur at the end of the twenty-first century on the atmosphere can have an effect on midlatitude westerlies that is opposite to that driven by GHG increase. This stresses the need to properly separate the effect of radiative forcing from that of sea ice and to understand the mechanisms through which Arctic sea ice loss can affect the large scale atmospheric dynamics and yield to climate anomalies over land.
The linkages between sea ice concentration anomalies over the eastern arctic and the mid latitude atmospheric circulation have been investigated in a set of CMIP5 ensemble simulations under current climate conditions with historical plus RCP4.5 radiative forcings in the period 1979-2013. Using a method based on maximum covariance analysis, all the models analyzed revealed that a reduction of sea ice over the eastern Arctic was followed by a negative NAO/AO-like pattern, consistent with the relationship derived from observations [CE114]. Results suggest that a stratospheric pathway could be at play as the driving mechanism during early winter. However, this work in line with previous studies suggest that the atmospheric sensitivity to sea ice changes is likely model dependent and that coordinated experiments are needed to properly isolate the atmospheric response to sea ice decline. This is currently done as part of the PhD thesis of S. Chripko within the H2020 APPLICATE project and the CMIP6/PAMIP experiments.

2.4 Regional-scale attribution and interplay between variability drivers

Decadal-scale excursions of global and regional mean temperature away from the forced response to well-mixed greenhouse gas forcings are to be expected due to the current level of forcing and non-linear interactions in a coupled dynamical system. The origin of these excursions can be due to events related to changes in natural external forcing such as volcanic eruptions [CE128] or solar irradiance variations, variations in short-lived anthropogenic forcings such as aerosols, or internal climate variability. Decadal-scale climate attribution consists in estimating the respective contributions of the different factors, their constructive or destructive interference and the related mechanisms. The first case-study is that of the recent and strong hydro-climate trends of the Southwest United States[CE122]. The U.S. Southwest experienced strong hydro-climate trends from the 1980s to the 2010s, from cool and wet to warm and dry conditions. We have used a dynamical adjustment method purely based on observations and constructed

circulation analogues to assess the contribution of atmospheric circulation variability to the recent observed hydro-climate trend. We first show that the warming is largely due to greenhouse gas forcing. We then demonstrated that the observed precipitation trend from 1983 to 2012 is mainly due to internal atmospheric circulation variability that is driven in part by decadal-scale tropical Pacific sea surface temperature changes. Removing this internal dynamical component brings the observed precipitation trend into closer agreement with the anthropogenically forced response simulated by climate models. The second case-study is an idealized model one that studies the sensitivity of the climate response to volcanic forcing to the phase of the Atlantic Multi-decadal Variability (AMV). The protocol is based on large initial condition ensembles starting from two different AMV phases and with a Pinatubo eruption a few months after the start. In [CE126] we show that there are no significant changes in the North Atlantic Oscillation (NAO), in the first and the second winters after the eruption. Based on clustering techniques, we provide evidence for inhibition of the occurrence of negative NAO-type circulation in response to volcanic forcing during the third winter. This forced signal is amplified in cold AMV conditions and is related to sea ice/atmosphere feedbacks in the Arctic and to tropical-extratropical teleconnections. This study also suggests that small ensemble size could easily lead to misleading conclusions regarding the volcanic fingerprint on the NAO. In related studies such as [CE117] and [CE147], we have also shown the possible influence of tropical volcanic eruptions on other variability modes such as El Nino Southern Oscillation (ENSO) and other mid-latitude modes.

A similar approach has been used to assess the uncertainties associated with the estimates of the time of emergence (ToE) of anthropogenic warming. Time of emergence of anthropogenic climate change is a crucial metric in risk assessments surrounding future climate predictions. However, internal climate variability impairs the ability to make accurate statements about when climate change emerges from a background reference state. In [CE121], we use the same dynamical adjustment method as above to provide new estimates of time of emergence of anthropogenic warming over North America and Europe from both a local and spatially aggregated perspective. For observations in winter, most of Canada emerged in the 1990s whereas most of the United States has not yet emerged by 2010. In summer, large parts of North America are emerged by 2010 and as early as the 1980s over western Canada and Florida. In Europe, a considerable region has already emerged by 2010 in both seasons. In winter, we show that atmospheric circulation advanced ToE over Canada by one decade and delayed it over the United States by two decades. After removing the influence of atmospheric circulation, most of North America showed emergence between the 1990s and 2000s (dynamical adjustment does not greatly change ToE over Europe). Accounting for the effects of internal atmospheric circulation variability on ToE of anthropogenic warming leads to increasing signal-to-noise ratios for detection and attribution of forced climate change and enables assessment of the relative contributions of dynamic and thermodynamic processes.

2.5 Hydrological cycle variations and changes

Over the past two years, with R. Bonnet's doctoral thesis [CE180], we have worked on the characterization and physical understanding of the multi-decadal variability of the hydrological cycle in France over the instrumental period. We showed, based on observations, that large multi-decadal variations in French river flows exist [1]. However, long-term river flows observations on the 20th century are very scarce and may be impacted by artificial influences such as dams or pumping. Moreover, crucial variables of the continental hydrological cycle such as snow cover, soil moisture, groundwater levels are virtually not observed on long periods. To overcome these limitations, provide a robust picture of multi-decadal hydrological variations over France and describe the associated physical mechanisms, we have developed a long hydrological reconstruction for the Seine basin on the 1850-2010 period, based on hydrological modelling with the ISBA-MODCOU system [7].

We have developed a new method to obtain the necessary meteorological forcing, building on previous works [CE97]. The method is based on the statistical downscaling of the NOAA-20CR long term reanalysis [5], that starts in 1850, constrained by some scarce long-term daily and monthly precipitation and temperature observations. Thanks to data rescue efforts within the Les Enveloppes Fluides et l'Environnement VITESSE project with colleagues of UMR METIS, we have been able to better evaluate this reconstruction, on a longer period and based on a diversity of hydrological variables. Based on this reconstruction, we have demonstrated that the multi-decadal river flows variations over France are driven by climate variations rather than artificial influences such as dams, pumping etc. Multi-decadal variations in precipitation in spring are the main driver of the multi-decadal variations of the continental hydrological cycle over the Seine basin, that do not exist only on river flows and are not limited to spring. We have highlighted the role of soil moisture and groundwater dynamics in extending the impacts of spring precipitation variations to other seasons. The spring precipitation variations are themselves driven by large-scale atmospheric variations that seem in turn to be controlled by variations in oceanic temperature both in the Atlantic and Pacific ocean. For the Atlantic, we show using paleoclimatic data that this mechanism exists at least from the end of the 18th century.

Over the past two years, we have completed the analysis of the future hydrological projections over France produced during G. Dayon's Ph.D thesis [CE109]. This study characterizes the main impacts of climate change on the hydrological cycle over France and the associated uncertainties, due to climate simulations, hydrological modelling, and emission scenarios. We also have worked on the characterization in these projections of the future evolution of different types of droughts (hydrological, hydrogeological and agricultural droughts) on the Seine basin, in collaboration with local water managers [CE154]. We have shown that drought conditions may become much more frequent for business as usual scenarios (Figure 2.3). We also have put the future expected changes in the context of the great droughts of the last 150 years, thanks to the hydrological reconstructions described above.

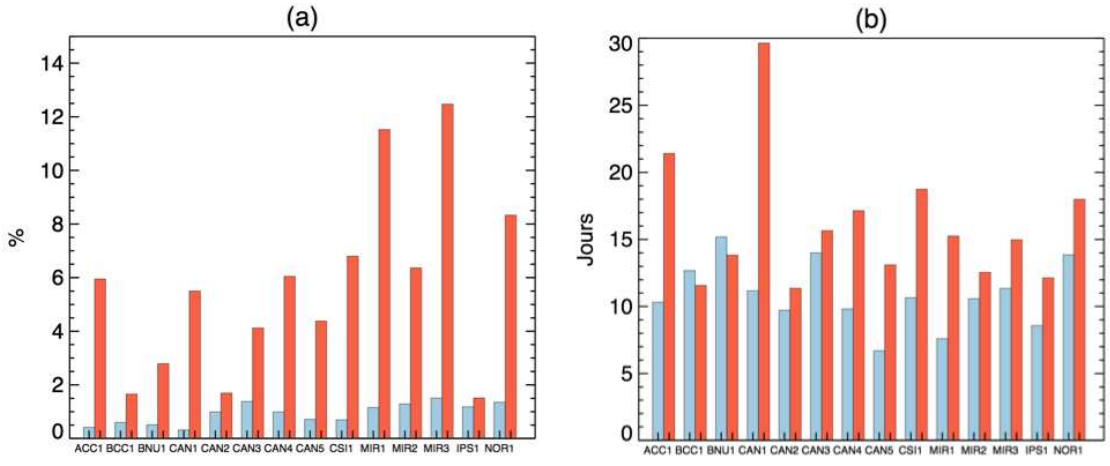

Figure 2.3: (a) Percentage of time (%) spent in hydrological droughts (b) Mean length of hydrological droughts (days). The red bars correspond to the 2031-2060 period, the blue bars correspond to the 1961-1990 period. Each couple of red and blue bars correspond to a different climate simulation. Mean on the Seine-Normandie basin. RCP8.5 scenario. Source: [CE154].

2.6 Climate extremes

We have focused on the analysis of how climate change affects the intensity and occurrence of climate extremes in France. The objectives are twofold: i) to investigate the effects of human-induced climate change of climate extremes and physical mechanisms beneath; and ii) to quantify the impact of such changes in climate extremes on society (crop yields, flash-floods).

The recent study of [CE90] about summer mega heat waves in France under a warmer climate has received particular attention in the community. The main objective was to investigate the occurrence of a mega-heatwave in a much warmer mean climate as well as the relevant physical mechanisms. The focus was on heatwaves as extreme as the 2003 event with respect to their contemporaneous mean climate. On this purpose, daily temperature observations and a pair of historical and scenario (RCP8.5) simulations conducted with the high-resolution (∼12.5 km) ALADIN regional climate model were analyzed. First, the spatial distribution of the mega-heatwaves in France and their 21st century evolution were examined. Five regions were identified with an extreme event spatial clustering algorithm applied to observed temperatures. These are used to diagnose the 21st century heatwave spatial patterns (Figure 2.4). Second, the mega heat wave of summer 2075 was selected to be as extreme as 2003 in terms of extreme temperature and downscaled using ALADIN model. A 20-member initial ensemble is performed and used to assess the sensitivity of this future heatwave to the internal variability in the regional climate model. Results show that even in a much warmer and drier climate in France, late spring dry land conditions may lead to a significant amplification of summer extreme temperatures and heatwave intensity through limitations in

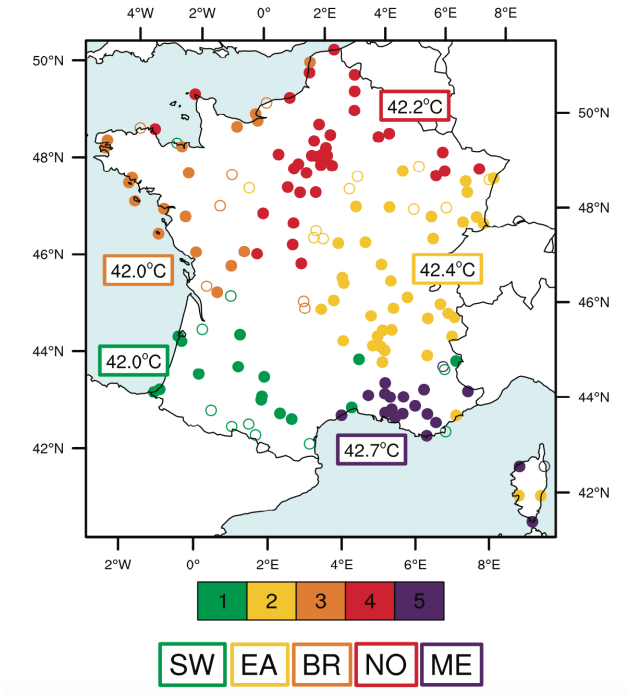

Figure 2.4: Results from the spatial clustering algorithm applied to the observations. Open circles indicate lack of significance (silhouette coefficient less than 0.5). Regions are numbered with regard to the cluster strength (average of the silhouette coefficient over significant points only), from the weakest to the strongest (1 to 5), as illustrated by the colors. For each cluster, the maximum value of observed current summer record maximum value across the stations is indicated. Source: [CE90].

evapotranspiration. By 2100, the increase in summer temperature maxima exhibits a range from 6 °C to almost 13 °C in the five regions in France, relative to historical maxima. These projections are comparable with the estimates given by a large number of global climate models.

Climate impacts on crop yields have been addressed in [CE94] We have focused on 2016 year to be exceptional in France, since the country suffered its most extreme yield loss in over half a century. The extremely low yields in 2016 combined with lower exchange prices on international markets compared to 2015 induced a substantial income loss for farmers. None of the public seasonal forecasts provided by the operational centers was able to anticipate the magnitude of this yield loss. Here we have studied the precise climatic conditions that led to it. We analyzed long-term yield and climate time series (SAFRAN analysis and CMIP5 database) to address the following questions: (i) how exceptional were climate conditions, individually and combined, in the breadbasket region during the 2015–2016 growing season? (ii) Can 2016 help us improve forecasting systems? And (iii) will such events become more frequent in the future? By using binomial logistic regression we showed that the huge wheat yield loss in 2015–2016 is a new type of compound extreme with a conjunction of abnormally warm temperatures in late autumn and abnormally wet conditions in the following spring. Finally, based on future climate warming projections, we show that the specific conditions that led to the 2016 wheat yield loss are projected to become more frequent towards the end of the century.

Flash floods in the southeastern France (“Cevennes region”) can also induce important societal and human damages. These are originated by extreme precipitation episodes regionally known as the “Cévenols” events), whose cumulative extreme precipitation can locally reach 600 mm in 24 h within some river catchments. The Mediterranean region has been identified as a hotspot of climate change in the form of possible amplification of extreme precipitation associated with a decrease in total precipitation. In [CE182] and [CE106] we have assessed the climate change impact on mean and extreme precipitation events in some river catchments located over the Gulf of Lyon region using high-resolution (12 km) EuroCORDEX and MedCORDEX simulations and SAFRAN reanalysis as reference dataset. The focus was made on three regions, Lez and Aude located in France, and Muga located in north-eastern Spain. First the model skills were evaluated in terms of annual cycle precipitation biases over the historical period. Then future changes in extreme precipitation under two emission scenarios (RCP4.5 and RCP8.5) were estimated through the computation of past/future change coefficients of quantile-ranked model precipitation outputs. Over the 1981–2010 period, the cumulative precipitation is overestimated for most models over the mountainous regions and underestimated over the coastal regions in autumn and higher-order quantiles. Extreme precipitation events are intensified over the three catchments with smallest ensemble spread under RCP8.5 scenario revealing more evident changes than the RCP4.5, especially in the later part of the 21st century.

2.7 Model evaluation and multi-model construction

Today, large ensembles of multi-model climate projections are available. These ensembles are very useful for studying climate variability and change, understanding the mechanisms involved and characterizing the robust part of the models response. However, the optimal use of these “ensembles of opportunity” with models with vastly different performances, not independent, to produce robust multi-model probabilistic climate projections remains a major challenge. We have continued to work on these questions over the past two years.

We have worked on the multi-model evaluation of the spatial pattern and intensity of the surface storm tracks in Coupled Model Intercomparison Project Phase 5 models (CMIP5[16]), with a special interest for western boundary currents, where strong ocean atmosphere interactions occur[CE98]. A robust equatorward shift

of the surface storm track in these regions is found, which illustrates the dual influence on the surface storm track of the upper atmosphere and of the ocean, with the atmosphere having the larger relative influence.

We have also worked on the best way to combine the information from multiple climate models to characterize robustly climate changes and the associated uncertainties. Current coupled climate models from the Coupled Model Intercomparison Project Phase 5 models are indeed far from independent, because they share large portions of codes, sometimes even entire components (such as the four principal components, i.e. the atmosphere, ocean, ice, land models and secondary components such as interactive chemistry etc.). The model democracy that consists to give the same weight to each climate models in the probabilistic estimations, independently of the similarity of their codes and therefore wrongly implicitly assuming their independence is still used in the majority of studies.

In [CE96], we have evaluated the relationships between the similarity of the climate models codes and the similarity of their results, based on all the CMIP5 models. We show that the more components are shared between two GCMs, the closer are their results. It is hardly unexpected, but we have quantified robustly this

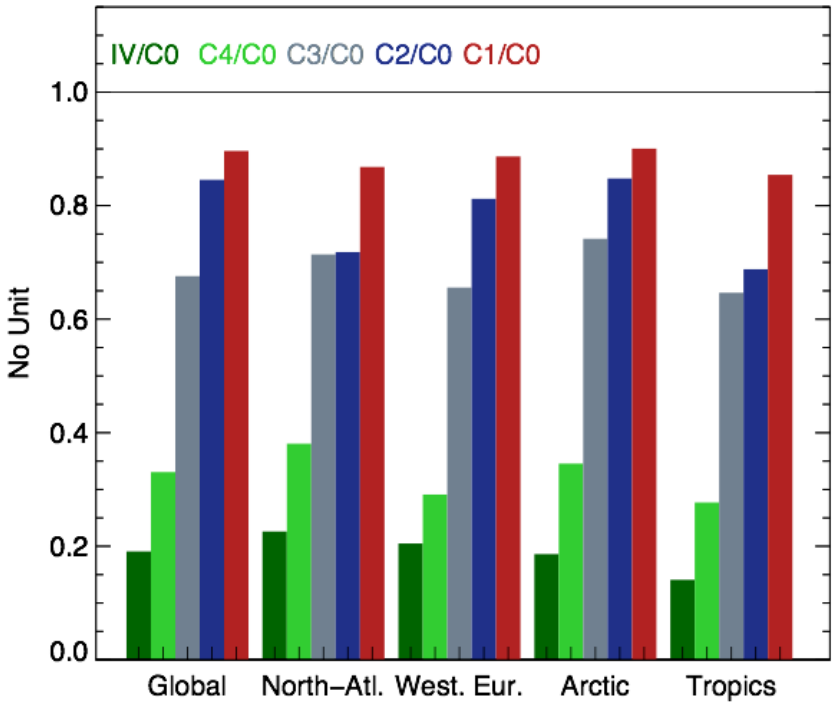

Figure 2.5: Ratio between the mean pairwise root-mean-square errors (RMSEs) of future temperature change for each category given by the colored bars on the mean pairwise RMSE of C0. The RMSEs are calculated on different regions of the world, given on the x axis. The boundaries of the North Atlantic domain are 30°N–70°N, -65°E–0°E. The boundaries of the Western Europe domain are 37°N–65°N, -10°E–20°E. Only land points are considered. The Tropics are defined as the area between -20°N and 20°N. The Arctic is defined as the zone with latitudes greater than 70 ◦ N. IV correspond to simulations from the same climate model, which only differ by the initial conditions. C4 corresponds to simulations from models that share their 4 main components. In that case, the models therefore differ either by their resolution or by the addition of secondary “components”. C3 (C2, C1, C0) corresponds to simulations from climate models that share 3 (2, 1, 0) components. IV in dark green, C4 in light green, C3 in dark gray, C2 in purple, and C1 in red. Source: [CE96].

effect for the first time. In general, even the impact of a single shared component is significant. Based on current ensembles, it is hard to show whether a component is more important than the others in that context (Figure 2.5). We therefore show that the "model democracy" is clearly problematic and that effort should be done to avoid the replication of components in multi-model ensembles, or to devise weighting schemes for the climate models to give the same weight to each components.

2.8 Small-scale oceanic variability

Global ocean models that admit mesoscale turbulence spontaneously generate a substantial interannual-to-multidecadal chaotic intrinsic variability in the absence of atmospheric forcing variability at these timescales. Improving the understanding and description of this intrinsic oceanic variability was the main objective of the OCCIPUT project led by T. Penduff from IGE [CE95]. The main product of OCCIPUT was the realization of a large initial condition ensemble of forced ocean simulations with an eddy-permitting model. This ensemble provides a robust framework to disentangle the externally forced ocean variability (due to atmospheric variability) and its internally generated (chaotic) variability. Theory suggests that nonlinear interactions between mesoscale eddies induce "inverse cascades" of kinetic energy, leading to increasing spatial and temporal scales of mesoscale structures. In the absence of other opposing processes, the chaotic character of small-scale mesoscale variability is therefore expected to propagate toward larger and slower scales [CE145]. In several mid-latitude regions, chaotic ocean processes have more impact than atmospheric variability on both the low-frequency variability and long-term trends of ocean variables. For instance, maps of 30-year trends in regional ocean heat content show many regions (western boundary currents, Indian and Southern Ocean) where changes cannot be unambiguously attributed to the atmospheric forcing [CE144]. Another example is that of the interannual and decadal Atlantic meridional overturning circulation (AMOC) variability [CE123]. The analysis of the OCCIPUT ensemble suggests that AMOC fluctuations north of 40°N are largely driven by the atmospheric variability, which forces meridionally coherent fluctuations reaching decadal time scales. The amplitude of the intrinsic interannual AMOC variability never exceeds the atmospherically forced contribution in the Atlantic basin. However,it reaches up to 100 percent of the latter around 35°S and 60 percent in the Northern Hemisphere mid-latitudes. All these results raise questions about the attribution of observed and simulated oceanic signals at regional scales over periods of a few decades. It also suggests that these intrinsic oceanic variability patterns could possibly impact the atmosphere.

The impact of small scale ocean SST structures on the atmosphere was firstly addressed in the PhD thesis of M. Piazza ([13]). We have continued to work on this topic in a PhD thesis starting in late 2017 (V. Rousseau). The goal is get further knowledge of mechanisms explaining if/how small scale SST structures over the Gulf Stream can impact the atmosphere not only in the MABL but also in the free underlying atmosphere and downstream. On this purpose we have used the atmosphere stand-alone simulations performed with the new version of ARPEGE (v6) at low (LR, T127L91) at high (HR, T359L91) resolution within the H2020-PRIMAVERA project framework. ARPEGE was forced here by HadiSST2 dataset over the period 1950-2014. Firstly, we have performed a comparison LR versus HR by using different diagnostics to characterise small scale air-sea interactions over the Gulf Stream. Results show that HR model simulates stronger winds, latent heat release and precipitation over the Gulf Stream. A recent study [10] has suggested that the Gulf Stream Convergence Zone is linked to the SST but mainly through the influence of strong storms, highlighting the importance of accounting for the whole distribution of wind divergence rather than just the mean. In order to verify this mechanism in our models, we use the approach introduced by [12], which consists of selecting extreme air-sea coupling events based on the deciles of the distribution of latent heat release over the Gulf Stream. We show that in wintertime, the air-sea coupling in our model is modulated by a continuous series of synoptic systems acting as "baroclinic waveguides". We further look at the relationship between low level wind divergence and mesoscale SST anomalies and show

that the influence of the latter on the former can be masked by synoptic atmospheric activity.

References

[1] J. Boé and F. Habets, (2014), Multi-decadal river flow variations in France, *Hydrology and Earth System Sciences*, **18**, 691–708.

[2] L. Boé, J.and Terray, E. Martin, and F. Habets, (2009), Projected changes in components of the hydrological cycle in French river basins during the 21st century, *Water Resour. Res.*, W08426.

[3] M. Bushuk, R. Msadek, M. Winton, G. Vecchi, X. Yang, A. Rosati, and R. Gudgel, (2018), Regional Arctic sea–ice prediction: potential versus operational seasonal forecast skill, *Climate Dynamics*, 1–23.

[4] M. Chevallier and D. Salas-Mélia, (2012), The Role of Sea Ice Thickness Distribution in the Arctic Sea Ice Potential Predictability: A Diagnostic Approach with a Coupled GCM, *Journal of Climate*, **25**, 3025–3038.

[5] G. P. Compo, J. S. Whitaker, P. D. Sardeshmukh, N. Matsui, R. J. Allan, X. Yin, B. E. Gleason, R. S. Vose, G. Rutledge, P. Bessemoulin, S. Brönnimann, M. Brunet, R. I. Crouthamel, a. N. Grant, P. Y. Groisman, P. D. Jones, M. C. Kruk, a. C. Kruger, G. J. Marshall, M. Maugeri, H. Y. Mok, Ø. Nordli, T. F. Ross, R. M. Trigo, X. L. Wang, S. D. Woodruff, and S. J. Worley, (2011), The Twentieth Century Reanalysis Project, *Quarterly Journal of the Royal Meteorological Society*, **137**, 1–28.

[6] C. Deser, R. A. Tomas, and L. Sun, (2015), The Role of Ocean Atmosphere Coupling in the Zonal-Mean Atmospheric Response to Arctic Sea Ice Loss, *Journal of Climate*, **28**, 2168–2186.

[7] F. Habets, A. Boone, J. L. Champeaux, P. Etchevers, L. Franchistéguy, E. Leblois, E. Ledoux, P. Le Moigne, E. Martin, S. Morel, J. Noilhan, P. Quintana Seguí, F. Rousset-Regimbeau, and P. Viennot, (2008), The SAFRAN-ISBA-MODCOU hydrometeorological model applied over France, *Journal of Geophysical Research: Atmospheres*, **113**.

[8] G. A. Meehl, L. Goddard, G. Boer, R. Burgman, G. Branstator, C. Cassou, S. Corti, G. Danabasoglu, F. Doblas-Reyes, E. Hawkins, A. Karspeck, M. Kimoto, A. Kumar, D. Matei, J. Mignot, R. Msadek, A. Navarra, H. Pohlmann, M. Rienecker, T. Rosati, E. Schneider, D. Smith, R. Sutton, H. Teng, G. J. van Oldenborgh, G. Vecchi, and S. Yeager, (2014), Decadal Climate Prediction: An Update from the Trenches, *Bulletin of the American Meteorological Society*, **95**, 243–267.

[9] T. Oudar, (2016), *Réponse de la circulation atmosphérique aux forçages anthropiques : des modes annulaires aux dépressions synoptiques*, phd thesis, Université Toulouse 3 Paul Sabatier.

[10] L. W. O'Neill, T. Haack, D. B. Chelton, and E. Skyllingstad, (2017), The Gulf Stream Convergence Zone in the Time-Mean Winds, *Journal of the Atmospheric Sciences*, **74**, 2383–2412.

[11] C. H. O'Reilly, T. Woollings, and L. Zanna, (2017), The Dynamical Influence of the Atlantic Multidecadal Oscillation on Continental Climate, *Journal of Climate*, **30**, 7213–7230.

[12] R. Parfitt and A. Czaja, (2016), On the contribution of synoptic transients to the mean atmospheric state in the Gulf Stream region, *QUARTERLY JOURNAL OF THE ROYAL METEOROLOGICAL SOCIETY*, **142**, 1554–1561.

[13] M. Piazza, L. Terray, J. Boé, E. Maisonnave, and E. Sanchez-Gomez, (2016), Influence of small-scale North Atlantic sea surface temperature patterns on the marine boundary layer and free troposphere: a study using the atmospheric ARPEGE model, *Climate Dynamics*, **46**, 1699–1717.

[14] S. Qasmi, C. Cassou, and J. Boé, (2018), Mechanisms of teleconnection between Atlantic Multidecadal Variability and European climate in CNRM-CM5. to be submitted.

[15] S. Qasmi, (2018), *Sensibilité du climat européen à la variabilité Atlantique multidécennale*, phd thesis, Université Toulouse 3 Paul Sabatier.

[16] K. E. Taylor, R. J. Stouffer, and G. A. Meehl, (2012), An Overview of CMIP5 and the Experiment Design, *Bulletin of the American Meteorological Society*, **93**, 485–498.

Environment Modeling and Monitoring

3.1 Introduction

The topic of "environment modeling and monitoring" relates to the prediction of industrial or environmental risks that could be induced by natural disasters, human activities and/or industrial accidents. These issues are of great importance for public safety, industrial plant safety as well as environmental protection. Research dedicated to environment modeling and monitoring at CERFACS focuses on the following topics: natural hazards monitoring (floods/inundations, wildfire); anthropogenic impacts on the environment (aviation, rocket launch); and environment surveillance (regional-/global-scale air quality, global-scale oceanography). This research is multidisciplinary and addresses a wide variety of objectives (surveillance, early warning system, monitoring, reanalysis, scenarios, forecasting), spatio-temporal scales (from flame scale, meso-scale to regional and global scales), simulation tools and algorithms (data assimilation and optimization, uncertainty quantification, machine learning, code coupling, high performance computing). CERFACS, in synergy with the research activities conducted among its shareholders, is an ideal place to address these research activities since the expertise is already present across the different teams. In particular, the activities related to industrial risk is in line with the activities related to explosions and safety in the "Computational Fluid Dynamics" chapter. The data assimilation applications presented here are also in line with the methodological developments linked to data-driven modeling in the "Parallel Algorithms" chapter. There is indeed strong synergy between applications and methods for the environment topic at CERFACS.

3.2 Regional-to-Global-Scale Atmospheric Chemistry

CERFACS' activities on atmospheric composition continue regularly since 2003 and are based on a strong collaboration with Météo-France and external funding from Europe (Copernicus program), CNES (Tosca program), CNRS (INSU/LEFE program) and Midi-Pyrénées region. During the 2017-2018 period, the main efforts were dedicated to: i) the finalization of a PhD thesis on global ozone assimilation; ii) the development of radiance assimilation capabilities in the UV-IR region; iii) the development of a new numerical solver for atmospheric chemistry equations; and iv) the optimization of both the forecast and the assimilation codes for the MOCAGE chemistry-transport model (Météo-France).

3.2.1 Assimilation of Satellite Products for Decadal Ozone Monitoring

Tropospheric ozone is a major pollutant and the third most important greenhouse gas, but its global and decadal variability is not yet well quantified. Thanks to the current generation of infrared sounders like IASI, daily estimates of tropospheric ozone with global coverage and at very high spatial resolution are now possible. The high frequency of these observations allows to characterize the ozone variability from the intra-daily to the decadal scales. In Ref. [CE135], we investigated the accuracy of a global ozone reanalysis obtained through the assimilation of both limb (MLS) and nadir (IASI) observations in MOCAGE. This reanalysis permitted to characterize the monthly variability of tropical ozone due to ENSO; this represents a unique long-term dataset for atmospheric composition studies.

3.2.2 Assimilation of Satellite Radiances for Ozone Monitoring

Satellite radiances (Level 1) are assimilated routinely since the early nineties to improve meteorological forecasts in operational centers. Nowadays, chemical forecasts are also provided by an increasing number of operational centers, but rely mostly on the assimilation of satellite retrievals (Level 2). Assimilating directly the Level 1 data should in principle improve the quality of the results, especially for measurements affected by a small information content (e.g. nadir sounding satellites), and simplify the modeling and estimation of measurement errors. Following the encouraging results of Ref. [CE184] obtained for IASI ozone retrievals, we recently included full radiative transfer capabilities in the MOCAGE assimilation system to assimilate IASI thermal infrared and GOME-2 UV spectra.

Concerning IASI assimilation, we demonstrated with a one-month-long simulation that the Level 1 assimilation improves the results against Level 2 assimilation, especially at tropical latitudes and in the Southern Hemisphere (Fig. 3.1). The radiative transfer code used for both Level 1 assimilation and Level 2 processing is RTTOV, developed and maintained by Météo-France, UK Met Office and ECMWF. In this regard, the configuration of RTTOV used for the Level 1 assimilation and the Level 2 retrievals has been kept identical. These results have been presented at the 2018 EUMETSAT conference and a manuscript has been

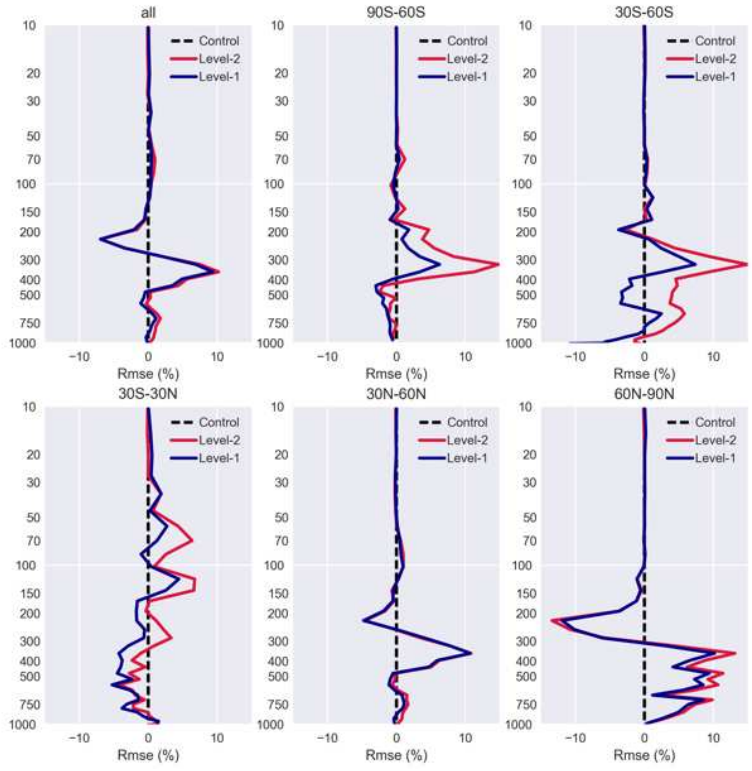

Figure 3.1: Change of Root Mean Square Error (RMSE) for simulated ozone against ozonesondes (in percent of the average ozonesonde values) over the global domain (top left plot) and for five latitude bands. The black dashed line is for the MLS reference reanalysis (Control), the red line is when assimilating IASI Level 2 retrievals on top of MLS, the blue line is when assimilating IASI Level 1 radiances. Negative values mean that the assimilation decreased the RMSE with respect to the Control, i.e. improved the accuracy of the simulated ozone field.

submitted to Atmospheric Measurements Techniques. The next step is to understand and correct residual biases that might be related to inaccurate radiative transfer (e.g. due to aerosols or surface properties) or measurements errors, which affect both Level 1 assimilation and Level 2 retrievals.
The assimilation of GOME-2 UV measurements is part of an ongoing Copernicus project and is based on the radiative transfer code DOME, developed by the German Aerospace Agency (DLR). The assimilation of UV spectra (270-330 nm) is more challenging than in the IR region, due to instrumental noise, numerical cost and non-linearities of the radiative transfer. We first tackled these issues with extensive testing in a synthetic observation framework, where we highlighted the necessity of using multiple outer-loops and including the surface albedo within the control vector. Second, the comparison of radiances simulated from the global reanalysis of Sec. 3.2.1 with real GOME-2 measurements showed good consistency [CE158]. This constitutes an important step before proceeding with further assimilation of real data.

3.2.3 Development of Numerical Solvers for Atmospheric Chemistry Models

To solve the ordinary differential equation systems associated with the time evolution of the species concentrations, the solver ASIS [CE102] adopts a one-step linearized implicit scheme with specific treatments of the Jacobian of the chemical fluxes. It conserves mass and has a time stepping module to control the accuracy of the numerical solution. In idealized box-model simulations, ASIS gives results similar to the higher order implicit schemes derived from the Rosenbrock's and Gear's methods but requires less computation and run time at the moderate precision required for atmospheric applications. When implemented in MOCAGE (Météo-France) and Mars (LMD/GCM), the ASIS solver performs well and reveals weaknesses and limitations of the original semi-implicit solvers used by these two models. Within the CAMS European project, the ASIS solver has been introduced in the ECMWF C-IFS model; we obtained consistent results with those obtained with MOCAGE. The solver implementation in C-IFS still needs to be improved to reduce computational time.

3.2.4 Developments and Evolution of the Assimilation for MOCAGE

During 2017-2018, CERFACS continued the activity of development and optimization of MOCAGE and its assimilation suite (DAIMON project). The main accomplishment concerning the forward model was the implementation of a new MPI parallelization: a complete overhaul of MOCAGE provides now an efficient memory distribution among MPI tasks and will permit to run chemistry simulations at much higher resolutions than it was previously possible. Significant upgrades were also performed on the assimilation code, among which we can list: i) multi-species and multi-scale (global plus nested domains) assimilation is now possible thanks to a complete refactoring of the background error covariance (B) and of the observation operator (H); ii) the B and H codes have both been parallelized using a hybrid OpenMP-MPI approach; iii) input/output for the assimilation code switched to modern json and HDF5 formats; and iv) the control of single families or mixtures of aerosols has been implemented. The most up-to-date version of the DAIMON suite is a much more capable and optimized system than before, which can fully serve current and future needs in chemical forecasts at CERFACS and Météo-France.

3.3 Micro-Scale Atmospheric Pollutant Dispersion Simulation

Accurately predicting the unsteady short-to-medium range plume dynamics and dispersion induced by emission source(s) remains a challenge for air quality prediction and health impact assessment. Large eddy simulations (LES) have been identified as a promising tool to tackle this challenge. At the scale of micro-meteorology, simulating the near field is a multi-physics multi-scale problem since pollutant concentrations can vary by orders of magnitude in time and space due to the complex flow dynamics induced by the

presence of obstacles (e.g. buildings, mountains) in a urban district or an industrial site as well as time-transient meteorological conditions. We address this problem through several projects, among whom the 2017-2019 MOSIQAA-CORAC project (*MOdélisation et SImulation de Qualité de l'Air Aéroportuaire*) aiming at designing accurate air quality simulations on airport site in collaborating with ONERA and INERIS; the 2018-2020 RTRA-STAE PPM project (*Prévision d'ensemble de la dispersion atmosphérique de Polluants pour des applications Micro-météorologiques à l'échelle d'un site*) following the 2016-2018 MIRAP chantier (*Modélisation et Incertitudes pour l'évaluation du Risque de dispersion Atmosphérique de Polluants*) in collaboration with CNRM, ONERA and CEREA; and the 2018-2019 CNES project dedicated to simulating the toxic cloud after a rocket crash and to establishing safety perimeters. This part was partly supported by GENCI HPC computational resources.

3.3.1 Benchmark Case of Micro-Scale Large Eddy Simulations

We carried out an extensive comparison of LES for micro-scale atmospheric dispersion of air pollutants in the framework of the MUST experiment in near-neutral boundary layer conditions, including MNH-IBM, YALES2-AE and AVBP (YALES2-AE and AVBP are usually dedicated to LES in combustion applications). The first objective was to investigate the capability of LES to capture the unsteady short-to-medium-range plume dynamics and dispersion within the urban canopy. The second objective was to analyze the sensitivity of the LES results to different physical and numerical choices (e.g. model equations, computational grids, numerical schemes, physical assumptions) using the multi-model simulations. Detailed analysis of the simulation-observation discrepancies was carried for both the dynamic variables and the gas concentration in terms of the standard statistical metrics commonly used in dispersion model evaluation but also in terms of concentration fluctuations that are directly provided by the LES. The LES results were found in very good agreement with the experimental measurements, especially for tracer concentrations above 1 ppm. The different solutions provided by AVBP, MNH-IBM and YALES2-AE did not feature significant discrepancies highlighting their consistency. In particular, AVBP and YALES2-AE capture a deviation of the plume centerline that was observed during the MUST trial. This deviation modifies the structure of the lateral and vertical pollutant dispersion within the idealized canopy, which is important to predict the location of tracer concentration peak values. We thereby obtained an estimate of the epistemic uncertainty in the tracer concentration LES predictions [CE162].

3.3.2 Sensitivity of Micro-Scale Simulations to Inflow Boundary Conditions

LES predictions are highly dependent on the inflow boundary conditions that are influenced by meso-scale meteorological conditions. It is thus of great interest to study how these inflow boundary conditions affect the pollutant concentration within the urban canopy. Since LES are computationally expensive, we have access to a limited number of simulations to carry out aleatory uncertainty quantification and global sensitivity analysis. To overcome this issue, we performed a preliminary work based exclusively on the YALES2-AE model for the MUST experiment. We investigated the use of an emulator or "surrogate". Two types of surrogate models were trained and compared, generalized Polynomial Chaos and Gaussian Process. The training step consisted in building a dataset of LES (30 YALES2-AE simulations, each simulation corresponding to a different inlet wind scenario) using a suitable design of experiment to adequately sample the range of the uncertain wind parameters. The comparison consisted in analyzing errors, statistical moments, Sobol' sensitivity indices to make sure the results were not emulator-dependent. Preliminary results [CE161] provided a proof-of-concept; this analysis will continue within the PPM project to extend this ensemble approach to more models and more realistic configurations.

3.3.3 Multi-Scale Toxic Gas Dispersion from Rocket Launch Failure Scenario

Following the benchmark simulations of micro-scale pollutant dispersion, the CNES project ("dispersion de nuage toxique en cas d'accident lanceur") aims to predict safety perimeters resulting from the accidental release of propellant after a rocket launch failure. In this frame, preliminary LES computations of the toxic compound evaporation and dispersion were performed. A multi-scale strategy was adopted by coupling two instances of AVBP with the CWIPI[1] library from ONERA. The strategy was initially developed for turbo-machinery computations in the Computational Fluid Dynamics team. This allows to capture both the evaporation process occurring at the meter scale and the dispersion in the gaseous phase occurring at the kilometer scale, with significant reduction in computational cost thanks to local time-stepping.

3.3.4 Micro-Scale Large Eddy Simulation at Airport Scale using Meso-NH

Within MOSIQAA, we study the emission dispersion for a fictive airport with LES using the Meso-NH (MNH) model jointly developed by CNRM and LA. To be in capability to explicitly represent the airport topography, MNH includes an immersed boundary method (IBM) that was validated using canonic test cases and the MUST (Mock Urban Setting Test) field-scale experiment corresponding to an idealized urban environment [18]. We successfully applied the IBM method to the 2001 AZF plant explosion to model and studies the NO_2 dispersion over Toulouse districts [17]. We analyzed the sensitivity of the LES

[1] Coupling With Interpolation Parallel Interface

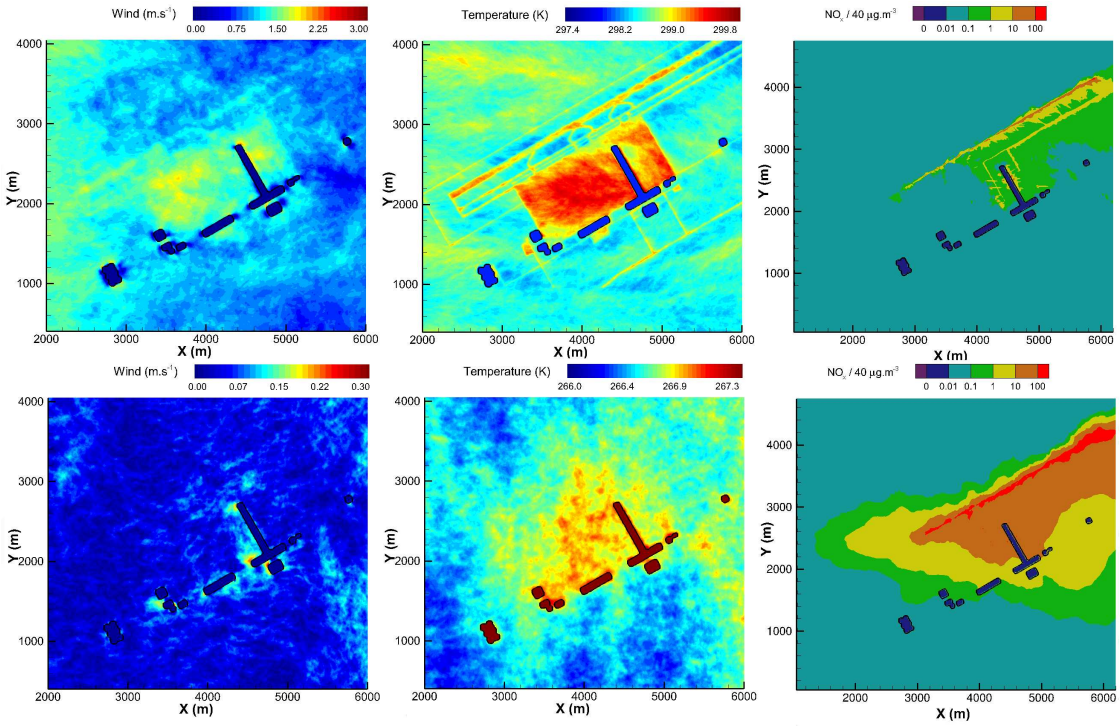

Figure 3.2: Wind, temperature, ratio of NO_x concentration and quality threshold for two atmospheric stability conditions (mean value integrated during 1 h and at 2 m above the ground): (top panels) unstable case; and (bottom panels) stable case.

predictions to the meteorological situation, i.e. stable, neutral and unstable conditions. For this purpose, several numerical developments were required in MNH: representation of the airport environment (unsteady large-scale forcing and emissions); recycling method to generate an incoming turbulent flow; immersed wall models in presence of thermal effects; adequacy between IBM and the ECMWF radiation scheme; adequacy between IBM and the SURFEX externalized scheme, etc. The studied passive or chemical species are: CO, CO_2, SO_2, SO_4, PM2.5, PM10, HC, NO_x. The atmospheric pollution (large scale contribution) is given by INERIS: NO_x, CO, CO_2, O_3. Figure 3.2 presents MNH-IBM results simulating unstable and stable meteorological situations. In the long term, MNH-IBM could be applied to a real airport (french airport implication and experimental investigations). More generally, MNH-IBM could be valuable for studies dedicated to urban climate and air quality.

3.4 Front-scale Data-Driven Wildfire Spread Modeling

Data assimilation offers a mathematical framework to take advantage of the recent advances in infrared remote sensing technology to improve predictions of wildland fires (Rochoux et al., "Designing the future of wildfire modeling", Wildfire Magazine, March-April 2017). While the application of classical data assimilation techniques to wildland fire spread modeling clearly benefits from past developments made for numerical weather predictions, it is important to recognize that there are yet a number of application-specific technical barriers that need to be overcome. This work was part of C. Zhang's PhD thesis (University of Maryland, 2018) [31] funded by the National Science Foundation (NSF-1331615, WIFIRE) and is mainly supported by "Agence Nationale de la Recherche" (ANR-16-CE04-0006, FIRECASTER) in complement to CNES/TOSCA, SMAI, CNRS INSU/LEFE and LabEx AMIES fundings at CERFACS.

3.4.1 Object-oriented Data Assimilation

The application of data assimilation to wildfire problems requires the formulation of an adequate measure of the discrepancies between model predictions and observations. Regional-scale wildland fires are commonly described as propagating fronts. The fire front may be subject to strong shape deformation, its motion may be unsteady and present irregularities due to highly heterogeneous land surface conditions (e.g. terrain topography). Topological changes can even occur due to fire spotting. Errors in wildland fire spread models therefore correspond to position errors rather than amplitude errors. Using standard data assimilation algorithms to this front problem could produce spurious fronts and thereby nonphysical solutions. To overcome this issue, we investigated an object-oriented data assimilation approach derived from the Chan-Vese contour fitting functional used in image processing [CE137]. The burning area is then treated as a moving object that can undergo shape deformations and topological changes. We demonstrated that object-oriented data assimilation is suitable for both Eulerian and Lagrangian-type front-tracking solvers [29].

3.4.2 Merits of Hybrid State-Parameter Estimation

The application of data assimilation to wildland fire problems also requires a suitable choice of the control variables to reduce the sources of uncertainties and provide a better forecast of the wildland fire spread. It is not enough to correct the position of the fire perimeter for model restart at a given time, the correction of the model state being not persistent over time [29]. This is due to the presence of large bias in the input parameters such as the near-surface wind field, the biomass properties (moisture, thickness, fuel surface load, etc.). We demonstrated the merits of a hybrid state-parameter estimation approach to improve forecast performance [30]. This hybrid approach simultaneously estimates the fire front position and some of the input parameters of the model. For state estimation, we adopted a cost-effective Luenberger observer formulation borrowed from control theory to reconstruct a complete view of the burning state at a given time. For parameter estimation, we used an ensemble transform Kalman filter to solve the inverse modeling

problem consisting of inferring more realistic parameters given observation of the actual burning state. Both state estimation and parameter estimation rely on the front shape similarity measure presented in Sec. 3.4.1. Note that parameter estimation was adapted to treat spatially-distributed inputs by introducing localization to dynamically select in which areas the input parameters of the wildfire spread model are corrected [CE153].

3.4.3 Comparison of Emulators for Global Sensitivity Analysis

Parameter estimation was found to be a key component of the data-driven wildfire spread model in Sec. 3.4.2. However, the computational cost of the ensemble Kalman filter increases with the number of control parameters. We then computed Sobol' sensitivity indices to identify which uncertain parameters contribute the most to the spread in the fire perimeter position and then select which parameters to control (see Fig. 3.3). To limit the number of model simulations, fast emulators based on generalized Polynomial Chaos (gPC) and Gaussian Process (GP) were trained and used to perform predictions of fire front shape and topology for a wide range of input parameters [CE137, 26]. The performances of the surrogates for varying size and type of training sets as well as for varying parameterization and choice of algorithms were compared [CE138, 26]. The best performance was achieved using a gPC strategy based on a sparse least-angle regression (LAR). Still, the LAR-based gPC surrogate tended to filter out the information coming from parameters with large length-scale [26]. In any case, sparsity ensures an emulator can be built using an affordable number of model simulations, even if the model response is highly multi-scale and nonlinear.

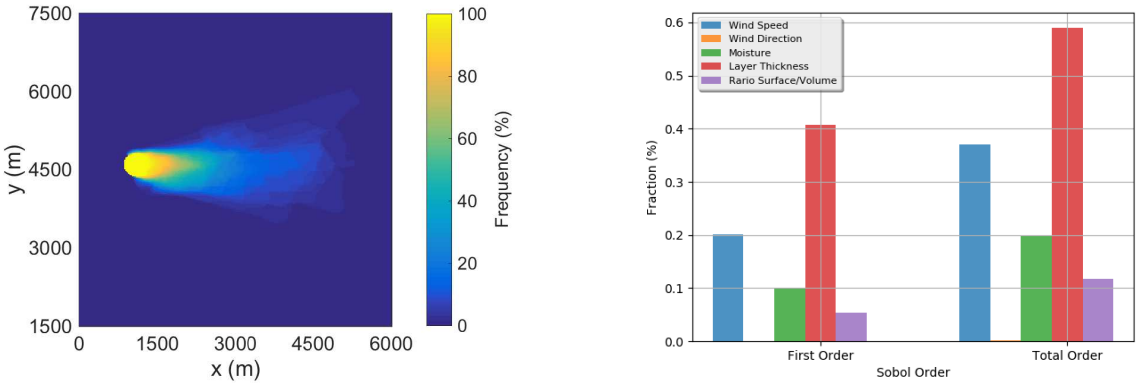

Figure 3.3: Global sensitivity analysis illustrated for a synthetic case in Corsica (France). Left panel: Probability map of the burnt area using an ensemble of wildfire spread simulations obtained by perturbing near-surface wind and biomass fuel properties. Right panel: Sobol' sensitivity indices to evaluate the contribution of each input parameter to the burnt area size. Source: [CE159].

3.4.4 Validation against Field-Scale Experimental Data

The merits of the methodological developments presented in Sec. 3.4.1–3.4.2–3.4.3 were evaluated on synthetic cases (see Fig. 3.3) and on the three-hectare 2012 RxCADRE S5 field-scale experiment [29, 30]. We demonstrated that data-driven wildfire spread modeling provides more accurate forecast of fireline propagation than if either the wildfire spread model or the observations were taken separately. Results showed that when the observation frequency becomes lower than 1/60 s^{-1}, the forecast performance of the data-driven model is improved compared to simply extrapolating observation data. This is inline

with the emerging physics-guided data-driven modeling as highlighted by the 2017 Earth Observation summit [CE63] gathering research scientists, forest agencies and space agencies.

3.4.5 Bi-Directional Fire-Atmosphere Coupling in Compressible Mode

Within the framework of the ANR-FIRECASTER project [CE2] and A. Costes' PhD thesis (CNRM/CERFACS), we implemented a compressible version of the 3-D Meso-NH meso-scale atmosphere code (Météo-France/Laboratoire d'Aérologie); the standard version of Meso-NH relying on an anelastic assumption and prevents horizontal density variations. The objective is to investigate the impact of this assumption on the fire propagation and on the air quality degradation induced by the wildland fire. To make Meso-NH compressible, we developed a new upper boundary condition relying on characteristic-based boundary conditions, known as NSCBC, proposed in Ref. [22]. These boundary conditions are known to be non-reflecting and also local in space and time to limit memory storage and preserve scalability. However, the NSCBC formulation comes out as partially non-reflecting as it can be considered as a low pass filter. We therefore adapted to the NSCBC to environmental flows by adding a plane wave masking. Preliminary fire-atmosphere coupled simulations showed significant differences in the fire propagation due to the changed micro-meteorological conditions nearby the fire between the anelastic and compressible versions of Meso-NH [CE1]. This quantitative analysis of the benefits of compressible Meso-NH is ongoing.

3.5 Hydrodynamics

Two main axes are investigated in hydrodynamics for rivers and estuaries. The first one concerns uncertainty quantification and reduction. Building from previous works in data assimilation for real-time flood forecasting, the challenge of going beyond deterministic simulation was tackled. In an ensemble framework, the question of identifying predominant sources of uncertainties and building surrogates to replace the direct solver was addressed. Still aiming at lowering the computational cost and meeting with operational constraint, the second axis focusses on multi-dimensional coupling with various coupling strategies. This work was supported by CERFACS shareholders (EDF-LNHE, EDF-PRISMES, CNES, Météo-France), with complementary funding from CNES/TOSCA, national and European projects (INSU/LEFE, H2020 EoCoE), PhD funding from SCHAPI, CEREMA and Région Occitanie as well as strong collaboration effort with various institutes among which LHSV, INRIA, LIMSI, IRSTEA and ARTELIA.

3.5.1 Sensitivity Analysis for Estuaries with 2-D Hydrodynamics Model

High tide coefficients combined with high meteorological surge levels and high discharges over the Garonne and Dordogne rivers in the Gironde estuary, in South-West France, may lead to high water levels and floods near the Blayais nuclear plant and the city of Bordeaux, with important economic and social impacts. A global sensitivity analysis was performed with TELEMAC-2D, already used for operational water level forecast in the framework of V. Laborie's PhD thesis (Cerema/LHSV - Cerema-EDF R&D-ENPC – direction : N.Goutal, EDF R&D – co-direction : S. Ricci, CERFACS). The generation of the simulation ensemble stands in sampling scalar and functional aleatory variables: constant and uniform friction coefficients as well as time varying hydrological and maritime forcing. The temporal perturbation of time-dependent upstream hydrological and downstream maritime forcing is assumed to be represented by a Gaussian Process (GP) derived from observed chronicles. A Karhunen-Loève decomposition was then applied to retain a limited number of eigenmodes. Global sensitivity analysis is being performed for 20 random variables thanks to GENCI HPC computational resources; it implies the integration of 250,000 members for an elapsed simulation time of 101 days on 32,768 cores. For a 2003 storm-event, the maritime boundary conditions and the Strickler coefficients were found to have a predominant role all along the

estuary with an influence driven by the tide cycle (see Fig. 3.4). In the upstream fluvial areas, the friction coefficient and hydrological inputs are predominant. These results are under review in Ref. [21].

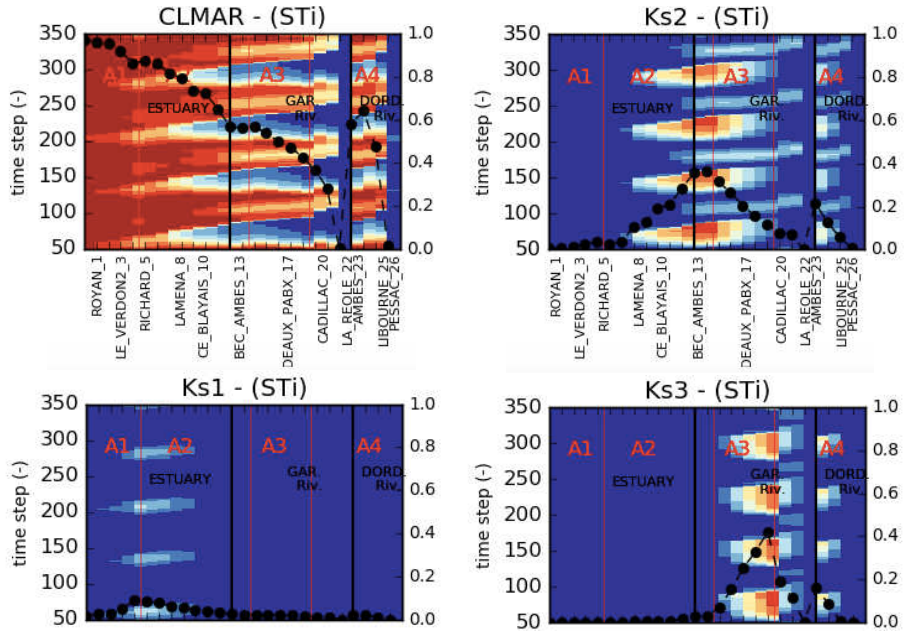

Figure 3.4: Total Sobol' indices along the Gironde estuary during Feb. 2003 storm for maritime boundary conditions and friction coefficients for estuarine, confluence and fluvial areas (Ks1, Ks2, Ks3). Source [CE28].

3.5.2 Surrogate Modeling: Application and Tools

The prediction of free surface flow characteristics requires the description of initial conditions, river geometry, boundary conditions and hydraulic physical parameters such as friction coefficients. Works from [CE111, CE138, CE183] showed that GP and generalized Polynomial Chaos Expansion (gPC) methods can be successfully implemented to build a surrogate for 1-D hydraulic modeling of subcritical steady flows with respect to the upstream hydrological forcing and the river bed spatially distributed friction coefficient. The water level probability density function (PDF), Sobol' sensitivity indices and the covariance matrix (in the perspective of ensemble-based data assimilation) are better estimated with the gPC-surrogate than with a Monte Carlo random sampling approach given a limited budget of forward model evaluations. This work was carried on a 50-km reach of the Garonne River with complex bathymetry; a budget of 50 forward model simulations was sufficient to build a reliable surrogate. The gPC- and GP-surrogates are used for sensitivity analysis with respect to the upstream hydrological forcing and the river bed spatially distributed friction coefficient. This work was achieved using the BATMAN-OT Python library. BATMAN-OT stands for Bayesian Analysis Tool for Modelling and uncertAinty quaNtification, using OpenTURNS (OT). It is a Python module distributed by CERFACS under the open-source CECILL-B license (MIT/BSD compatible) and available on Git (https://gitlab.com/cerfacs/batman). It relies greatly on the OpenTURNS library (http://www.openturns.org/, developed by EDF, Airbus, Phimeca and IMACS), scikit-learn (http://scikit-learn.org/) as well as in-house complementary developments. The main features of BATMAN-OT, described in the on-line documentation, are experimental design, parameter space resampling, surrogate modeling (GP, gPC), optimization (expected improvement), uncertainty

quantification, sensitivity analysis, multi-dimensional visualization (HDR, Kiviat), data reduction (POD) and automatic managing of code computations in parallel, see Ref. [25]. Ongoing discussion aims at merging capabilities from BATMAN-OT directly in OpenTURNS.

3.5.3 Ensemble-based Data Assimilation for Model Parameter Correction

In line with previous sensitivity analysis and uncertainty quantification studies, an ensemble-based data assimilation algorithm was favored as an improvement to the existing extended Kalman filter algorithm implemented in DAMP (Data Assimilation with MASCARET Prototype) for data-driven flood forecasting [20, 23]. Great efforts were made on the generation of realistic ensemble members with perturbations on scalar and functional inputs such as temporal and spatially varying boundary conditions (hydrologic, maritime, bathymetry). For the latter, the temporal and spatial correlations are represented as a GP characterized by a correlation function and hyperparameters. The error covariance matrices are stochastically estimated from this ensemble to have flow-dependent information; ensemble reliability and consistency diagnostics are computed. These developments are ongoing and applied to MASCARET-1D and TELEMAC-2D. Ensemble generation and subsequent integration of the hydraulic solver in a non-intrusive way are largely eased by the use of APIs (Application Programming Interface). Both elementary and user-oriented API were developed to infer inputs, manage simulation runs and outputs in a time-evolving and multi-instance context. The key steps of data assimilation such as computing error covariances and sinnovations with respect to observations are achieved. A modular framework is developed to account for various types of observations (in-situ, remote sensing from wide swath interferometry/SWOT) such as those provided by the SWOT-simulator that provides reached averaged water level.

3.5.4 Visualization of Uncertainties

The challenge for state-of-the-art visualization solutions stands in data dimension, for instance when dealing with large input space, functional output fields discretized in both space and time and/or ensemble simulations. A visualization method for multi-dimensional data was proposed in Ref. [24] based on: i) animated functional hypothetical outcome plots (f-HOPs); ii) 3-D Kiviat plot; and iii) data sonification. Dynamic visualization augmented with data sonification offers an alternative way to infer the characteristics of a data set. For functional output, principal component analysis allows for data classification in the reduced space. The functional highest density region (HDR) metric synthesizes the data set statistics with respect to a reference. Combining dynamic and sounding f-HOPS with HDR metric allows to infer the dynamics of the physics and to detect functional correlations in the output data. We also proposed a 3-D version of the Kiviat plot to encode both input parameters and response variable features. This dual visualization takes advantage of information from f-HOPs through data sonification, coloring and stacking strategies of the response surface information.

3.5.5 Multi-Dimensional Coupling

In the context of hydrodynamics, the use of 2-D models is well adapted in areas where the flow is no longer 1-D such as in confluence zones or flood plains. Nonetheless, the lack of bathymetry/topography data and the computational cost constraints limit the extensive use of 2-D models for operational flood forecasting. Multi-dimensional 1-D/2-D coupling offers an appropriate solution: this solution makes the most of the benefits of 1D models and allows locally for the representation of complex processes in 2D models. The computational cost of the 1-D/2-D coupling solution is significantly smaller than that of the full 2-D model, while the simulated hydraulic state is significantly better than that of the full 1-D model. This was investigated in collaboration with EDF-LNHE, LHSV, ARTELIA, SCHAPI and INRIA (lateral strategy). More details are given in Sect. 4.4.2 and main references are given here : [CE92] present the 1-D/2-D longitudinal coupling with MASCARET and TELEMAC on the Adour river. The lateral coupling

between 1D and 2D models was successfully implemented for academic test cases in the framework of the EoCoE H2020 project [CE174].

3.6 Global-Scale oceanography

We have developed two complementary methods for using ensemble perturbations to define the background-error covariance matrix in the variational ocean data assimilation system NEMOVAR. These developments contributed to the ERA-CLIM2 project (EU-FP7) [19] on coupled global atmosphere-ocean reanalysis, to the AVENUE projet (RTRA-STAE) on ensemble-variational data assimilation, and the MADCOP project (CNRS/LEFE-MANU) on covariance modeling. The first method uses ensembles to estimate the variances and correlation length scales (diffusion tensor) of the diffusion-based background-error covariance model. To account for sampling error, the parameters are filtered using an objective method that depends on the ensemble size. The second method uses ensembles to construct a low-rank sample covariance matrix and includes an objective procedure to localize this matrix to eliminate remote correlations associated with sampling error. Hybrid variants of both methods have also been developed. For the first method, the hybrid formulation involves linearly combining the ensemble estimates of the covariance parameters with modeled representations of those parameters. For the second method, the hybrid formulation involves linearly combining the localized sample covariance matrix with the full-rank matrix described by the parameterized covariance model. The correlation model, localization operator and parameter filter are all based on an algorithm that involves solving an implicitly formulated diffusion equation. We have completely revised the diffusion model to make it more general and to improve the computational efficiency of the implict solver on high-performance computers [28]. All methods have been fully integrated into the NEMOVAR source code maintained at ECMWF. The developments have been validated technically and scientifically, mainly using single cycle assimilation experiments with global ocean configurations at 1° and $1/4^\circ$ horizontal resolution. Results from validation experiments are described in Ref. [27]. This work is being further developed within the framework of the ERGO project (C3S), which aims at improving ocean data assimilation capabilities at ECMWF, used in both initialization of seasonal forecasts and generation of coupled Earth System reanalyses.

References

[17] F. Auguste, C. Lac, V. Masson, and D. Cariolle, (2018), Large eddy simulations devoted to the dispersion of a pollutant and its health impacts: The 2001 Toulouse AZF chemical plant explosion, *Submitted to Atmospheric Environment*.

[18] F. Auguste, G. Réa, R. Paoli, C. Lac, V. Masson, and D. Cariolle, (2018), Implementation of an Immersed Boundary Method in the Meso-NH model: Applications to an idealized urban-like environment, *Submitted to Geoscientific Model Development*.

[19] R. Buizza, S. Brönnimann, L. Haimberger, P. Laloyaux, M. J. Martin, M. Fuentes, M. Alonso-Balmaseda, A. Becker, M. Blaschek, P. Dahlgren, E. de Boisseson, D. Dee, F. Xiangbo, K. Haines, S. Jourdain, Y. Kosaka, D. Lea, M. Mayer, P. Messina, C. Perruche, P. Peylin, J. Pullainen, N. Rayner, E. Rustemeier, D. Schepers, J. Schulz, A. Sterin, S. Stichelberger, A. Storto, C.-E. Testut, M.-A. Valente, A. Vidard, N. Vuichard, A. T. Weaver, J. While, and M. Ziese, (2018), The EU-FP7 ERA-CLIM2 project contribution to advancing science and production of Earth-system climate reanalyses, *Bulletin of the American Meteorological Society*, **99**, 1003–1014.

[20] J. Habert, S. Ricci, E. Le Pape, O. Thual, A. Piacentini, N. Goutal, G. Jonville, and M. Rochoux, (2016), Reduction of the uncertainties in the water level-discharge relation of a 1D hydraulic model in the context of operational flood forecasting, *Journal of Hydrology*, **532**, 52–64.

[21] V. Laborie, S. Ricci, M. De Lozzo, N. Goutal, Y. Audouin, and P. Sergent, (2018), Quantifying forcings uncertainties in the Gironde estuary hydrodynamics., *Submitted to Computational Geosciences*.

[22] T. J. Poinsot and S. K. Lele, (1992), Boundary conditions for direct simulations of compressible viscous flows, *Journal of Computational Physics*, **101**, 104–129.

[23] S. Ricci, A. Piacentini, O. Thual, E. Le Pape, and G. Jonville, (2011), Correction of upstream flow and hydraulics state with data assimilation in the context of flood forecasting, *Hydrology and Earth System Sciences*, **15**, 1–21.

[24] P. Roy, S. Ricci, B. Cuenot, and J.-C. Jouhaud, (2018), Sounding spider: an efficient way for representing uncertainties in high dimensions, *Submitted to Journal of Computational and Graphical Statistics*.

[25] P. Roy, S. Ricci, R. Dupuis, R. Campet, J.-C. Jouhaud, and C. Fournier, (2018), BATMAN: Statistical analysis for expensive computer codes made easy, *Journal of Open Source Software*, **3**, 00493.

[26] A. Trucchia, V. Egorova, G. Pagnini, and M. Rochoux, (2018), On the merits of sparse surrogates for global sensitivity analysis of multi-scale nonlinear problems: application to turbulence and fire-spotting model, *Submitted to Communications in Nonlinear Science and Numerical Simulation*.

[27] A. T. Weaver, M. Chrust, B. Ménétrier, A. Piacentini, J. Tshimanga, Y. Yang, S. Gürol, and H. Zuo, (2018), Using ensemble-estimated background error variances and correlation scales in the NEMOVAR system, CERFACS Technical report TR-PA-18-15. Prepared for the ERA-CLIM2 project.

[28] A. T. Weaver, S. Gürol, J. Tshimanga, M. Chrust, and A. Piacentini, (2018), "Time"-parallel diffusion-based correlation operators, *Quarterly Journal of the Royal Meteorological Society*. In press.

[29] C. Zhang, A. Collin, P. Moireau, A. Trouvé, and M. Rochoux, (2018), Front shape similarity measure for data-driven simulations of wildland fire spread based on state estimation: Application to the RxCADRE field-scale experiment, *Proceedings of the Combustion Institute*. In press.

[30] C. Zhang, A. Collin, P. Moireau, A. Trouvé, and M. Rochoux, (2018), A New Hybrid State-Parameter Estimation Approach for Data-Driven Wildland Fire Spread Modeling: Application to the 2012 RxCADRE S5 Field-Scale Experiment, *Submitted to Combustion and Flame*.

[31] C. Zhang, (2018), *Data-driven simulations of wildfire spread at regional scales*, phd thesis, University of Maryland, USA.

Coupling, HPC and Data for climate

4.1 Introduction

This last chapter, mixing coupling softwares or methods, High Performance Computing (HPC) and data processing for climate simulations, gathers high level developments in scienfic computing paving the path towards exascale computing.

4.2 The OASIS coupler

The OASIS coupler is an open source software developed at CERFACS to couple numerical codes modelling the different components of the Earth System (ocean, atmosphere, sea-ice, land, atmospheric chemistry, etc.) and developed independently by different research groups. Today, OASIS3-MCT, the last member of the OASIS family, is used by about 45 climate modelling groups in France and in Europe but also in many other countries around the world.
The main functions of OASIS3-MCT are to interpolate and to exchange the coupling fields between the components of a coupled system. OASIS3-MCT forms a library linked to the component codes. It supports coupling of 2D logically-rectangular fields but 3D or 1D fields expressed on unstructured grids are also supported using a one-dimensional degeneration of the structures. In OASIS3-MCT, the Model Coupling Toolkit (MCT), developed by the Argonne National Laboratory (USA), is used as a lower layer to implement fully parallel coupling including parallel matrix vector multiplication for the remapping and parallel exchanges of coupling fields.
The last version of the coupler, OASIS3-MCT_4.0, was released in June 2018 [CE177]. All developments included in OASIS3-MCT_4.0 to improve its performance are described in detail in [CE176].
First, the hybrid MPI+OpenMP parallelisation of the (previously fully sequential) SCRIP library leads to an important reduction in the calculation time of the remapping weights. The performance of the weight calculation was tested on Météo-France Bullx beaufix (Intel 5.1.2.150 compiler and MPI library) for 4 interpolations (4 distance-weighted nearest-neighbour, bilinear, bicubic and first order conservative) in both directions for a typical ultra-high-resolution (UHR) coupled system using the NEMO ORCA12 grid (4322x3147 grid points) and the T799 Gaussian-reduced grid (843490 grid points). Reproducibility of the results at the machine precision (due to a different order in the operations) was validated. Figure 4.1 presents the results for 1,2,4,8,20 and 40 OpenMP threads and 1,2,4,8,16,32,64,128 and 256 MPI tasks, i.e. a total of 1,2,4,8,20,40,80,160,320,640,1280,2560, 5120 and 10240 OpenMP threads (40 threads corresponding to the number of physical cores per node on beaufix). These results show a reduction in the weight calculation time of 2 to 3 orders of magnitude with the new parallel SCRIP library for these high-resolution grids. This important improvement let us envisage dynamical coupling, implying runtime weight computation, with OASIS3-MCT.
Second, new methods introduced for the global CONSERV operation reduce its calculation costs by one order of magnitude while still ensuring an appropriate level of reproducibility. This removes the bottleneck foreseen at high resolution with this important global operation, which, in few cases, is still unavoidable.
Third, a new communication method, *decomp_wghtfile*, using the remapping weights to define the intermediate mapping decomposition, offers a significant gain, especially for high-resolution cases running on a high number of tasks, thanks to a much simpler rearrangement in the sparse matrix multiplication at run

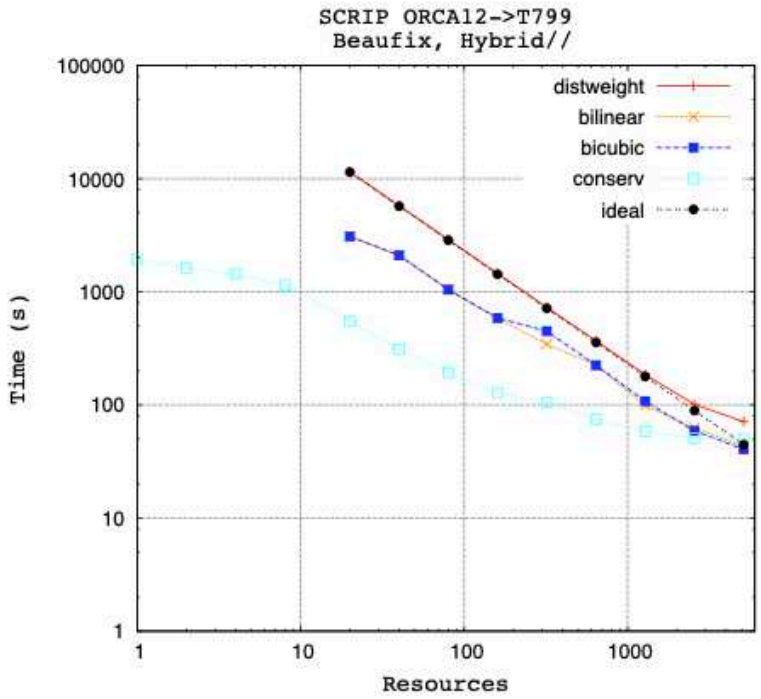

Figure 4.1: Time for the interpolation weight calculation as a function of the total number of OpenMP tasks for different interpolations with the new parallel version of the SCRIP library for the VHR case: NEMO ORCA12 (4322x3147 grid points) to Gaussian Reduced T799 (843490 grid points) coupling.

time. However, the new *decomp_wghtfile* method takes longer to initialize, as expected, partly due to the fact that the mapping weight file has to be read twice but also because of extra cost for the initialization of the mapping decomposition and sparse matrix multiplication, and for the initialization of the router between the mapping decomposition and the target decomposition. However, those increased costs are largely mitigated by an upgrade from MCT 2.8 to MCT 2.10.beta1, which reduces the absolute cost to few seconds. In general, those costs should be small enough so that for production runs, it will be worth spending extra time during initialization (which by definition happens only once at the beginning of the run) to speed up the run time. Of course, the balance between the increased cost of the initialisation and the gain obtained at runtime in the coupling exchanges has to be evaluated for each real coupled system, as it strongly depends on the specific coupled configuration (grids, decompositions, number of coupling fields, etc.) and on the length of the run.

While working on the initialisation, the explanation of a severe slow down of the initialisation phase at high number of cores observed in the IS-ENES2 coupling technology benchmarks, see section 4.5.1 below, was found. The problem was caused by some concurrent writing to the OASIS3-MCT debug file by all tasks even for the lower level of debugging.

Figure 4.2 shows the time for the coupling initialisation (on the left) and for a ping-pong exchange (on the right) with respect to the number of tasks/cores used for each component for a case coupling the ORCA025 grid (1021x1442 grid points) to a Gaussian Reduced T799 grid (843 000 grid points), for the previous OASIS3-MCT_3.0 version (dark blue) and for OASIS-MCT_4.0 activating either the old (*decomp_1d*, light blue) or new (*decomp_wghtfile*, red) communication method.

We see that the *decomp_wghtfile* method offers an important gain, especially for a number of cores of O(1000) and higher. For 10240 tasks/cores per component, the ping-pong time with *decomp_wghtfile*

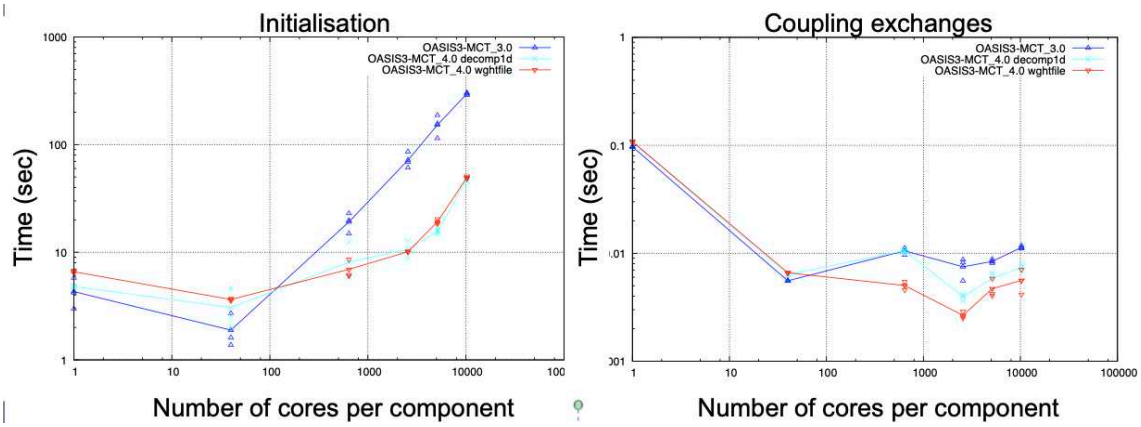

Figure 4.2: Time for the coupling initialisation (on the left) and for a ping-pong exchange (on the right) with respect to the number of tasks/cores used for each component for a case coupling the NEMO ORCA025 grid (1021x1442 grid points) to a Gaussian Reduced T799 grid (843 000 grid points), for the previous OASIS3-MCT_3.0 version (dark blue) and for OASIS-MCT_4.0 activating the old (*decomp_1d*, light blue) or new (*decomp_wghtfile*, red) communication method.

(0.0055) is 24% better than with *decomp_1d* (0.0073), which is already 35% better than the ping-pong time obtained with the previous OASIS3-MCT_3.0 version (0.0112). Regarding the initialisation, we conclude that the bug fix and the upgrade from MCT 2.8 to MCT 2.10.beta1 reduces significantly the initialisation cost, with a reduction of 82% from OASIS3-MCT_3.0 to OASIS3-MCT_4.0, while the difference between the *decomp_wghtfile* and *decomp_1D* method seems to be not significant.
These tests show the good behaviour of OASIS3-MCT_4.0 at high number of cores. Indeed it can be infered from these tests that the coupling overhead for one-year long simulation with one coupling exchange every 3 hours in each direction between codes with O(1 M) grid points running on O(10K) cores/component would take $\sim$1 minutes for the coupling initialisation and $\sim$20 secs for the data exchanges, which is very small compared to the time needed by a real coupled model at that resolution to run one simulated year.
Over the 2017-2018 period, 308 OASIS3-MCT downloads were registered from groups in Europe but also from around the world i.e. USA, Cuba, Russia, Turkey, Iran, China, Korea, Vietnam, Singapore, Thailand, Japan, India, South Africa, Nigeria, Saudi Arabia, Chile, Brazil, Colombia, Mexico, etc.
In particular, OASIS3-MCT is used at the Centre National de Recherches Météorologiques (CNRM) of Météo-France, benefiting from the coupling expertise and user support of our team, to assemble different climate models in the framework of various national, European or international projects.
The last climate coupled model developed at CNRM, with help and support from CERFACS, CNRM-CM6-1, is based on the atmospheric model ARPEGE-Climat V6.3.2 including the surface module SURFEX V8, the hydrology model TRIP routing the water to the ocean, and the ocean model NEMO 3.6 integrating CNRM GELATO sea-ice model. The high-resolution version, CNRM-CM6-1-HR uses in the atmosphere a linear triangular truncation T359 with a corresponding reduced Gaussian grid at $\sim$50 km resolution with 91 vertical levels. The ocean component uses the extended eORCA025 tripolar grid with 1442x1050 grid points horizontally, resulting in a resolution of about 25 km at the equator and 75 vertical levels.
CNRM-CM6-1-HR has been technically developed and scientifically validated in 2017-2018. Both the low and high-resolution versions of CNRM-CM6-1 are currently being used by CNRM and/or CERFACSs in the 6^{th} international Coupled Model Intercomparison Project (CMIP6), and in the PRIMAVERA and CRESCENDO European projects.
Besides the permanent manpower ensured by CERFACS and CNRS, the main sources of external funding for the development and maintenance of the OASIS3-MCT coupler in 2017-2018 were the IS-ENES2

(InfraStructure for the European Netwok of Earth System modeling, phase 2) with 27 PMs and the Centre of Excellence (CoE) in Simulation of Weather and Climate in Europe (ESiWACE) with 18 PMs. Both projects will be funded for a further phase starting in January 2019 with specific funding devoted to OASIS3-MCT (35 PMs in IS-ENES3 and 16 PMs in ESiWACE2).

4.3 OpenPALM

OpenPALM is a general tool allowing to easily integrate high performance computing applications in a flexible and evolutive way while complying with performance, software reuse and numerical accuracy criteria. OpenPALM is mainly composed of 3 complementary components, (1) the PALM[1] library developed by CERFACS, (2) the CWIPI[2] library developed by ONERA and (3) the graphical interface PrePALM developed by CERFACS. As the application programming interface is available in Fortran, C/C++ and Python, OpenPALM can couple codes written in different languages. In the context of the CERFACS/ONERA collaboration, the coupler has become open source since January 2011.

PALM has originally been designed for oceanographic data assimilation algorithms, but its application domain may extend to every kind of scientific applications [32]. In the framework of PALM, applications are split into elementary components that can exchange data though MPI communications. The main features of PALM are the dynamic launching of the coupled components, the full independence of the components from the application algorithm, the parallel data exchanges and redistribution, and the possible combination of physical modules with algebraic operations offered by the PALM algebra toolbox. It can be defined as a dynamic coupler for its ability to deal with situations where the component execution scheduling and the data exchange patterns cannot be entirely defined before execution.

Based on FVM (EDF's "Finite Volume Mesh" library under LGPL licence), CWIPI [33] provides a fully parallel communication layer for mesh based coupling between several parallel codes with MPI communications. The library takes into account all types of geometrical elements (polygon, polyhedral) with an unstructured description. CWIPI ensures the construction of the communication graph between distributed geometric interfaces through geometrical localization, the interpolation on non coincident meshes, the exchange of coupling fields for massively parallel applications and the generation of visualisation files to be used for a verification of the coupling interface.

The Graphic User Interface, called PrePALM, is a portable Tcl/Tk application. The relevant coupling features are described in the component source codes in identity cards that are loaded by PrePALM to construct the coupled applications. The user describes the execution scheduling, the parallel sections, the data exchange patterns and the algebraic treatments, entirely through the user interface. PrePALM then provides the input file for the coupler executable and the source code for the wrappers of the coupled component. These input file and wrappers take entirely care of the set-up of the communication context with no need of change in the component source code. The same graphic tool can be used at run-time to monitor the simulation status and to provide post-mortem some statistics on the memory and CPU time resources used by the different components.

The main points investigated during the period 2017-2018 are:

- Development of the IP interface (client/server mode of OpenPALM) for Python codes. These developments were made necessary to couple ONERA's elsA code in a context of remote and heterogeneous machines.

- Integration of an interface for Python codes for the PARASOL functionality. Development of accessors to PARASOL input and output variables for more flexibility for the user.

[1] Projet d'Assimilation par Logiciel Multiméthodes
[2] Coupling With Interpolation Parallel Interface

- Addition of many test cases that can be taken over by OpenPALM users. For example, transition from 2D and 3D structured meshes to unstructured meshes for CWIPI, examples available in C, Fortran and Python.
- Many improvements to the PrePALM graphical user interface; for example, the IP mirror generation directly from identity cards, or the possibility to follow progress of a coupled code in real time.
- Improvement of the CWIPI training session to make it accessible to an audience unfamiliar with unstructured meshes.
- Addition of a callable passive waiting primitive in the user code to manage resource recovery in a mixed MPI and OpenMP parallelization context.

Many OpenPALM applications were developed or maintained at CERFACS for its own use or for its partners during the last two years :

- The ACCLIMAT platform co-developed by Météo-France and CERFACS to model the urban climate; further developments of this platform are currently carried out within the framework of a thesis co-supervised by CERFACS.
- In the context of atmospheric chemistry, the variational DA suite for the Météo France chemistry transport model MOCAGE (DAIMON) is currently based on OpenPALM, which is used to schedule the DA tasks and monitor their execution.
- OpenPALM is used for multidimensional coupling between 1D and 2D hydraulic solvers. When the flow is 1D, MASCARET is used and coupled with TELEMAC 2D in areas where the flow is more complex (confluence, flood plains); this work is being carried out in collaboration with EDF and SCHAPI. More details in section 4.4.2 of this report.
- AquiFR (http://www.metis.upmc.fr/ aqui-fr/), which aims to monitor and forecast groundwater resources in France as well as to facilitate climate change impact assessments. OpenPALM makes it possible to manage the various hydro-geological applications of the 3 models (computing codes) integrated to date (Eros, Marthe and Eau-dyssée). CERFACS provided PALM support to the laboratories in charge of the development of Aqui-FR (BRGM, Meteo-France, UPMC,...);
- OpenPALM is intensively used in many multi-physic and multi-component studies in the Computational Fluid Dynamic team of CERFACS. Firstly, an important axis deals with aerothermal simulations for aeronautic (combustion chambers, turbine blades, ...) and automotive applications. In this context, a coupled model based on three codes (AVBP for the convection, AVTP for the conduction is solids and PRISSMA for the radiation) was developed with OpenPALM.
- TurboAVBP system that couples several instances of the AVBP code with OpenPALM is intensively used for compressor, turbine and integrated combustion chamber/turbine simulations in CFD team. Recent developments have concerned the interpolation order as detail in the CFD Team section 2.5.1 of the report.
- OpenPALM is used for deep learning around the AVBP code in the CSG/COOP team, it allows to send directly from memory to memory the unstructured AVBP meshes by interpolating them on structured meshes necessary for the deep learning code.
- An aeroacoustics application is developed with AIRBUS in the CFD team to simulate by coupling the interactions between an aircraft and its engines. The purpose of this application is to model the aircraft and engines separately between AIRBUS and SAFRAN and to perform the simulation

on two different sites without having to exchange meshes, which remain confidential for both companies. The solver is ONERA elsA code and data exchanges at the interface between the aircraft and engines are performed by OpenPALM client/server mode with TCP/IP protocol, which allows communications between heterogeneous computers. More details in the CFD Team section 2.5.2 of this report.

Having proved its efficiency, OpenPALM is now spreading in the scientific and engineering community. Among its users, we find 6 of the 7 CERFACS shareholders: SAFRAN, Airbus-Group, ONERA, CNES, CNRM (Météo France), EDF and about 70 other institutions.
Over 2017-2018, two 3-day training sessions on OpenPALM coupler were held at CERFACS for a total of 13 trainees.

4.4 Coupling Methods

4.4.1 COCOA

Quantities exchanged between atmosphere and ocean models in a climate simulation include ocean surface variables (temperatures, albedo, currents ...) and atmospheric fluxes (wind stress, heat, water). Usually, the grids of the ocean and atmosphere models are different (position, resolution). For example, CNRM-CM6-1 coupled model show large differences in the ocean and atmosphere resolution, particularly in the equatorial band (ratio of $\sim$1/5). These differences lead to errors in the flux calculation due to their non-linearities: one single mean ocean surface value is used, instead of separate values for each ocean grid cells.
The study started in the framework of the ANR COA project proposes to investigate the "exchange grid" solution implemented at GFDL: fluxes are calculated for each atmosphere/ocean grid intersection and a resulting flux is aggregated for the atmospheric or oceanic cells. In a preliminary study [CE164], the surface module SURFEX is forced with atmospheric variables and the coupling is implemented between SURFEX and the NEMO ocean model. This study allows to evaluate the impact of the exchange grid on the flux calculation and on the ocean but not on the atmosphere.
A first simulation (STD) was realised using the "standard" fluxes, i.e. calculated for each SURFEX mesh with the average of the temperatures of the underlying ocean meshes. These fluxes are compared to the fluxes calculated on the exchange grid. The analysis show that the impact of the exchange grid is relatively small over the open ocean but can be more important for non-solar heat fluxes in autumn in ice-forming zones.
A second simulation was realised into which fluxes calculated on the exchange grid and aggregated over SURFEX meshes are applied to the ocean with a conservative remapping. In this second simulation, the ice production increases slightly.
Given these results, we are now carefully defining the next steps, as studying the impact of the exchange grid on the atmosphere would require substantial technical work.

4.4.2 Hydro multi-dimensional

Multi-dimensional 1-D/2-D coupling in hydrodynamics makes the most of the benefits of 1D models and allows locally for the representation of complex processes in 2D models. This axis was investigated in collaboration with EDF-LNHE, LHSV, ARTELIA, SCHAPI and INRIA (lateral strategy). [CE92] present the 1-D/2-D longitudinal coupling with MASCARET and TELEMAC on the Adour river. The 1-D and 2-D models are coupled at their longitudinal boundaries with an iterative Schwarz algorithm applied at each interface. A Kalman filter algorithm is also applied in the 1-D models so that in-situ water level observations are assimilated to correct the simulated water level and discharge. This is implemented with the OpenPALM dynamical coupling software that allows for efficient task and data parallelism. This is also compatible with

operational computational cost constraints. The strategy was applied to simulate a set of seven flood events in the Adour catchment. The coupling algorithm converges with at most five iterations; the water level and velocity continuity is guaranteed at the model interfaces. The 1-D/2-D coupled model is approximately eight times faster than a full 2-D model. The coupling with the local 2-D solution significantly improves the simulation in the 1-D and 2-D areas. Data assimilation also leads to significant improvement for simulations and for short-term forecasts since only the model state is corrected. When the flow in the river overflows into the surrounding plains or vice versa, when the plains empty into the river; a lateral exchange between the river and its plains occurs. This situation can be modeled either by the complete 2-D model or by a lateral coupling between the 1-D model which simulates the flow in the river and the 2-D model for the flow in the flood plain. This strategy is computationally efficient. This also avoids the discretization of strong bathymetric gradients in the 2-D mesh; for instance dikes are included within the 1-D domain. When there is no overflow from 1-D to 2-D, lateral flows are zero and the 1-D model remains unchanged. In case of overflows, the lateral flows correspond to the source terms used in the overlapping strategy. This was successfully implemented for academic test cases in the framework of the EoCoE H2020 project [CE174].

4.5 HPC and Data for Climate

4.5.1 Coupling benchmarks

A first version of a community coupling technology benchmark was developed in the framework of the IS-ENES2 project, in a task lead by CERFACS. Today, stand-alone components running on 4 different grids are available: 1) a self-generated regular latitude-longitude grid, 2) an irregular, stretched and rotated latitude-longitude mesh, following the ORCA configuration of the NEMO ocean model, 3) a quasi-uniform icosahedral mesh, following the atmospheric DYNAMICO model, and 4) a quasi-uniform cubed sphere mesh. The stand-alone component using the self-generated regular latitude-longitude grid was used to assemble toy coupled models using five different coupling technologies, OASIS3-MCT, OpenPALM, ESMF (see https://www.earthsystemcog.org/projects/esmf/), MCT (see http://www.mcs.anl.gov/research/projects/mct/) and YAC (see https://doc.redmine.dkrz.de/YAC/html/). As a proof of concept, these coupled test cases were run in different configurations on three different platforms: Bullx at CINES in France, Cray XC40 at the UK MetOffice, and the Broadwell partition of Marconi at CINECA in Italy. The coupled components exchange coupling fields defined on grids of different sizes decomposed in parallel partitions with different aspect ratios and different orientations.

As an example, figure 4.3 shows the average time for one ping-pong exchange for components running on the same regular latitude-longitude 3000x3000 (VHR) grid with same decomposition on both sides. Tests were run on Bullx Occigen (Intel compiler 15.0.3.187, and bullxmpi 1.2.9.2) with YAC (black), OpenPALM (dark blue), ESMF (red) and OASIS3-MCT with forced remapping (green), and on Bullx beaufix (Intel 16.1.150 compiler and the Intelmpi 5.1.2.150 MPI library) with OASIS3-MCT with (pink) and without (light blue) forced remapping[3].

We see that all couplers scale very well up to about 2000 cores. For higher number of cores, the curves flatten for all couplers except for OASIS3-MCT without forced remapping (light blue), which continues to scale for up to 10 000 cores.

Other timings obtained for the coupling initialisation and coupling exchanges for different tests are detailed in [CE178], primarily to demonstrate the versatility of this benchmarking environment.

[3] In the IS-ENES2 benchmarks, the grids of the coupled component models are the same and therefore no remapping is needed. However, for the test cases implemented with OASIS3-MCT_3.0, we forced the activation of the sparse matrix multiplication, the weight matrix being in this case the identity matrix, so to be representative of real coupling exchanges usually involving a remapping. In the additional tests performed with the VHR test case on Bullx beaufix, we removed this unnecessary step for comparison.

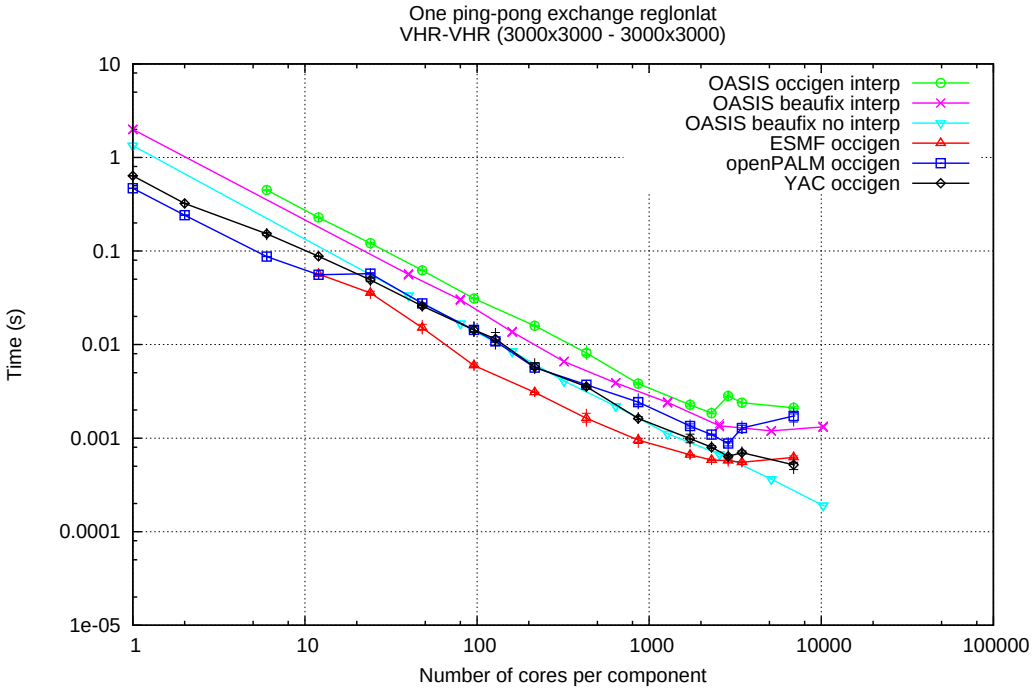

Figure 4.3: Time for a ping-pong exchange with respect to the number of tasks/cores used for each component for the VHR test case run on Bullx Occigen with YAC (black), OpenPALM (dark blue), ESMF (red) and OASIS3-MCT with forced remapping (green), and on Bullx beaufix with OASIS3-MCT with (pink - interp) and without (light blue - no interp) forced remapping.

4.5.2 NEMO optimization

In the last year, thanks to a E. Maisonnave's visit to IPSL, CERFACS has participated in significant developments in the NEMO ocean model:

- definition of a benchmarking configuration (i) reproducing performances of operational configurations (ii) but removing the need of input files, therefore simplifying porting on different architectures, and (iii) benefiting from a greater numerical stability, thereby allowing a wide range of parameter tests
- code internal instrumentation to separate calculation from communication time in order to evaluate load imbalance
- running and analysis of this instrumented benchmarking configuration to identify bottlenecks and evaluate the gain brought by different solutions proposed
- algorithmic rewriting of certain parts of the code aiming at suppressing or reducing useless communications

- feedback of these improvements in the official code version

This work has allowed us to understand how the NEMO code uses its costly communication routines but also to evaluate its bandwidth needs and to propose solutions on how to reduce them. In particular, we estimate that the throughput of the code could be doubled by reducing the real precision from double to single precision as illustrated on figure 4.4. This type of modifications has already been tested in different codes in the climate modelling community and is sometimes considered as essential for exascale computing. For NEMO this work had been prepared by people from BSC (Barcelona Supercomputing Center) associated to NEMO System Team. Complementary work is of course needed before implementing the same modifications in the official version of the code:

- evaluation of the impact and significance of the precision reduction
- identification of calculations for which double precision would be mandatory
- sustainable implementation of the tool and procedure to evaluate the minimal precision needed, in order to be able to routinely use them for new developments

This additional work has started and E. Maisonnave's visit has been extented until end of February 2019.

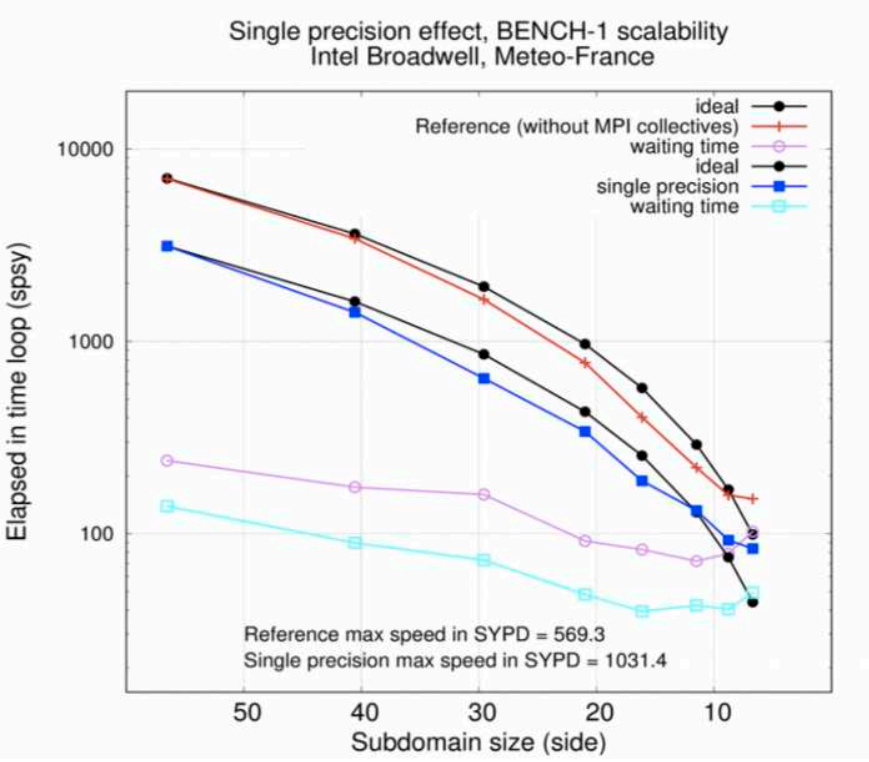

Figure 4.4: Elapse time as a function of the subdomain size for a 1-degree NEMO configuration (without ice model) for the whole model with double precision reals (in red) or with single precision reals (in dark blue) and for its communication part with double precision reals (in pink) or single precision reals (in light blue)

4.5.3 Data for CMIP6

The past two years have seen a rapid increase in climate data management and processing needs. This increase is linked to the recent development and use of higher-resolution models and to the high requirements of the on-going 6th phase of the international Coupled Model Intercomparison Project (CMIP6), in terms of number of numerical experiments to perform and number of outputs required, the so-called Data Request (DR). In the framework of CMIP6, CERFACS and CNRM, forming the CNRM-CERFACS modelling group, participate in different MIPs with the CNRM-CM6-1 model. CERFACS is responsible for the contribution of CNRM-CERFACS to CMIP6 in three MIPs: HighResMIP (High-Resolution Model Intercomparison Project), PAMIP (Polar Amplification Model Intercomparison Project) and part C of DCPP (Decadal Climate Prediction Project). CERFACS is also involved in different H2020 European project, in particular PRIMAVERA and APPLICATE which covers HighResMIP and PAMIP respectively. For PRIMAVERA, 10 types of numerical experiments were performed, each twice, at low and high resolution. This represents a total of more than 4000 simulated years, for with 40 millions of core-hours (Mh) were consumed and 1 PB of data was generated. This was permitted thanks to Météo-France special computational and storage resources attributed to CERFACS and dedicated to the CMIP6 exercise.
Given this data inflation (comparatively, CERFACS produced 20 TB for CMIP5) and the complexification of the experimental CMIP design (248 experiments, 1274 geophysical variables in CMIP6) the conceptual view and technical implementation of data workflow in the model had to be revised. One important objective of this restructuring was to avoid the use of CMOR library to produce CMIP6-compliant (standardised) data, since it requires heavy data handling and is very time consuming. To reach this objective, XIOS was implemented by CNRM in each component of CNRM-CM6-1 (ARPEGE, SURFEX, TRIP - NEMO being since a long time XIOS-enabled). XIOS, developed by IPSL, is a parallel Input/Output server allowing for a declarative description of output file content and realisation of online field operations, thereby reducing, or even completely removing, the need of post-processing. XIOS operations include time sampling and averaging, spatial remapping and reduction, vertical interpolation and simple arithmetic. These operations are configured at run time using an XML syntax. To exploit XIOS functionalities in the CMIP6 framework, an additional tool, called dr2xml (https://github.com/senesis/dr2pub), translates the CMIP6 DR for each year of each experiment in a set of XIOS conformant XML definitions. These definitions then activate the outputs in CNRM-CM6-1 components thanks to an alias table describing the correspondence between model variable names and CMIP6 DR variable names. The operations on the data is then performed online by the client part of XIOS on the model MPI tasks and sent to XIOS additional MPI tasks, called servers. Two levels of servers are used to aggregate and redistribute the parallel output fields so that any given field is gathered into one file written to disk by one single MPI task (thus avoiding parallel writing). Thanks to these tools and environment, CNRM-CM6-1 generates NetCDF output files which are directly conformant with CMIP6 requirements and ready to publish on the Earth System Federated Grid (ESGF).
CERFACS actively participated in the implementation, testing and to some developments of this environment for CNRM-CM6-1-HR, the high-resolution version of CNRM-CM6-1 (see 4.2).
One of the key aspect to have reasonable performances when running our simulations resides in the load balancing of the coupled system, which we observed to be strongly dependent on the output data load. Different trial-and-error tests were performed to determine the optimal number of processes for each component so to have a load balanced system using the lucia tool, provided with the OASIS3-MCT coupler. Without I/O, a configuration over 48 nodes with 768, 1094, 1 and 48 cores for ARPEGE, NEMO, TRIP and XIOS respectively is relatively well load-balanced. In that case, the coupled model takes 2374 sec to run one month, which leads to $\sim$3.0 SYPD (Simulated Years Per Day). But the performance and the load balance of the coupled model drastically drops when the I/O volume is increased. With an extremely heavy load of 996 GO per year (corresponding in fact to the requirements of both CMIP6 HiResMIP and the PRIMAVERA EU project), the throughput of the coupled model drastically falls down to $\sim$1 SYPD, with both ARPEGE and NEMO waiting significantly. It was observed separately that this increase in waiting time is in part due to the initial generation by XIOS of a file containing NetCDF metadata; improvement

of this aspect in XIOS is currently going on. In an effort to diminish the elapse time, we started to reduce the volume of I/O eliminating all variables that we did not consider essential for CMIP6 and PRIMAVERA and were able to get to 300 GO per year. Reducing the number of cores for NEMO to 530 while still keeping 768, 1 and 48 cores for ARPEGE, TRIP and XIOS respectively, we were again able to reach a relatively well load-balanced coupled system even if we still observe some incompressible waiting time in the initialisation phase. In that case, one month of simulation now requires 4759 sec, corresponding to $\sim$1.5 SYPD. We run now on 34 nodes (with 40 cores/node) leading to 21760 cores.hrs/SY.
In conclusion, we can state that even some non-negligible work was done regarding the load balancing of CNRM-CM6-1-HR, additional gain can certainly still be achieved, especially in XIOS initialisation phase. Another important improvement would be to be able to run CNRM-CM6-1-HR with chunks of 1 year instead of one month (as is obligatory today): the whole initialisation phase would be done 12 times less often and this would necessarily significantly reduce the overall simulation time. Work is currently going on in this direction at CNRM, based on preliminary work done at CERFACS.

4.5.4 European and International Data Infrastructures

Nowadays scientific researchers have to deal with much larger data volumes to be analyzed, as shown above for CMIP6. It is no longer possible to download all data locally for analysis. Because solutions are involving large national, European and international research infrastructures and e-infrastructures, developing a network of partners and developing the required expertise in this domain is a long term commitment. Actions and projects related to this thematic have been going on since 2009, and CERFACS has now gained a very good reputation and position to be actively involved, at National, European and International levels. Consequently, CERFACS is solicited to participate in several consortium leading project proposals on this thematic, funded by H2020 and CEF, as well as being invited to events and to give invited presentations on the subject. CERFACS shareholders collaboration is also taking place, currently with Météo-France and just beginning with CNES, also potentially with EDF.
The main objective is to ease access to climate data for several categories of users, from the researchers to the end-users in other scientific domains, going away from the download-locally and analyze workflow. This general objective enables CERFACS to gain expertise and to lead on several aspects at the European and International levels: workflow, containerization, tailored interfaces, orchestration, metadata, reproducibility, provenance/lineage, interoperability, generic APIs.
One of the main achievement has been the design and implementation of a prototype workflow interfacing several infrastructures and e-infrastructures, designed and developed within the H2020-EUDAT2020 project. The schematic of this prototype is shown in figure. 4.5. The innovative idea is to develop a data processing workflow using the generic EUDAT2020 GEF workflow prototype service (lead by CERFACS) as a generic layer to deploy calculations on the EGI-FedCloud using a container technology (docker). The GEF backend running on the EGI-FedCloud has been interfaced to the ESGF-CWT prototype future computing node to retrieve and pre-process data, leading to further computations on the EGI-FedCloud. Computations of the GEF backend are performed using CERFACS icclim python package. The whole workflow is initiated transparently by a user on the IS-ENES CDI climate4impact platform, and the user get back the results on the same platform. This prototype and work has been possible because CERFACS has been leading the metadata standardization of climate indices/indicators (FP7-CLIPC and FP7-IS-ENES2) and has been active in the EUDAT-EGI Interoperability Working Group initiated by the H2020-EUDAT2020 project.
During the last year, H2020-funded projects that sustained those activities for CERFACS were EUDAT2020 and DARE. Several project proposals were also submitted or are in preparation to further develop this activity: H2020-CCX (refused), H2020-INDIGO-Next (in preparation), CEF-PHIDIA (submitted, in collaboration with the CNES). In addition, CERFACS has been approved as a new member of the EUDAT CDI (Common Data Infrastructure), as a leader of the future workflow service (GEF: Generic Execution Framework). The upcoming IS-ENES3 will also sustain those activities, especially on the user

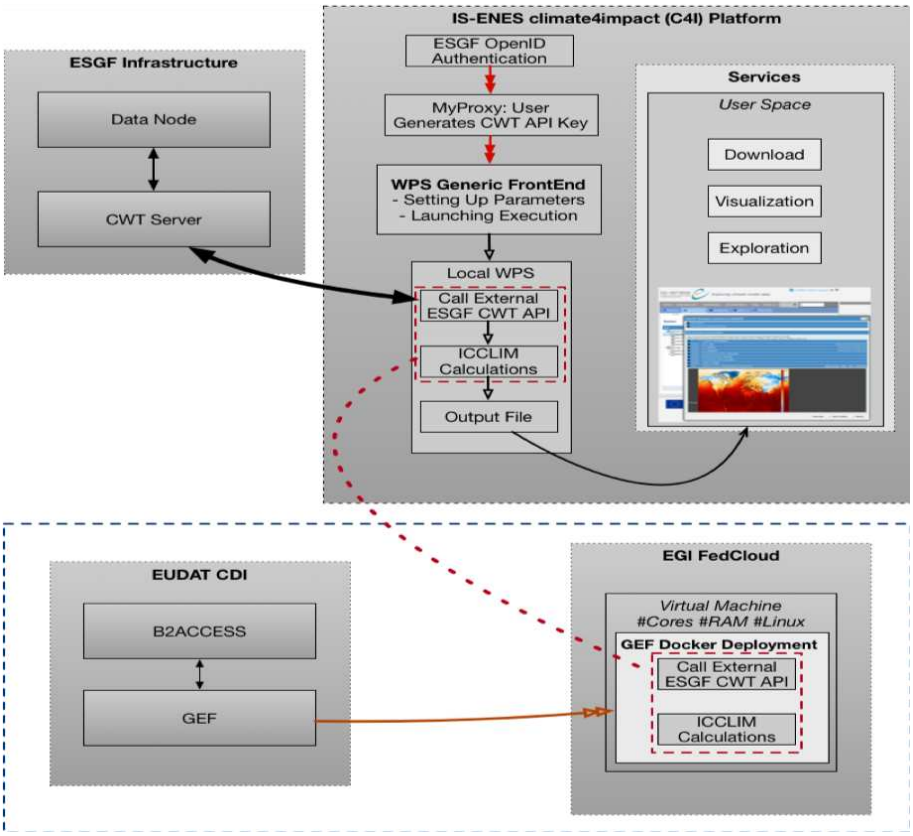

Figure 4.5: Schematics of the whole EUDAT2020 climate workflow prototype

interface (IS-ENES CDI C4I: climate4impact.eu), the processing backends as well as the interfaces to other infrastructures and e-infrastructures. Those projects also enable CERFACS to engage actively in the ESGF Compute Working Team (CWT), lead by PCMDI (US), supporting CMIP exercices as well as IPCC reports. Main results for this year are:

- Further developments and significant optimization of the open-source climate indices workflow backend created and developed by CERFACS: icclim. This python package has seen a rapid increase of interest internationally, associated with active interests from many groups. Significant achievements: used for CMIP6 official products/indices calculation, and chosen as the main processing package for Ouranos/CRIM Canadian climate research infrastructure;
- CERFACS incorporated as a new member of the EUDAT CDI;
- Development of a data processing workflow interfacing the IS-ENES climate4impact.eu platform to processing done using the EUDAT workflow prototype GEF Service;
- Acting as a facilitator of several EUDAT2020 Data Pilots;
- Significant increase in CERFACS visibility and reputation for research infrastructure developments;
- New approaches and innovative ideas to optimize data access to large data volumes (H2020-CCX and H2020-Indigo-Next);

- New collaboration with shareholders IT (Météo-France DSI and CNRM, CNES, EDF) and close collaborators (Mercator-Océan).

In conclusion, CERFACS can now provide a significant contribution to initiatives related to data processing workflows at the National, European and International levels, thanks to a long-term vision, to innovative ideas and efficient work, associated to significant efforts in networking, dissemination and adoption. This work is now beginning to be disseminated and shared with CERFACS' shareholders through active collaborations. There is still a lot of work to be done in the next few years to go from the prototype level (TRL-6) to operational (TRL-8), notably with data locality, resources scheduling, orchestration, metadata, authentication/authorization interfaces (AAI), reproducibility, interoperability and generic approaches, provenance/lineage, tailored user interfaces, building blocks standard and generic services, among others. Even if, currently, those activities are on the shoulder of only 1 FTE (Permanent Position) but with help of Temporary Engineers funded by H2020 projects, CERFACS will continue and strengthen those activities in this domain and continue to be a contributor and leader of innovative ideas and actions.

References

[32] A. Piacentini, T. Morel, A. Thévenin, and F. Duchaine, (2011), Open-palm: an open source dynamic parallel coupler., In *In iv international conference on computational methods for coupled problems in science and engineering*.

[33] A. Refloch, B. Courbet, A. Murrone, P. Villedieu, C. Laurent, P. Gilbank, J. Troyes, L. Tessé, G. Chaineray, J. Dargaud, E. Quémerais, and F. Vuillot, (2011), CFD Platforms and Coupling - CEDRE Software, *The Onera Journal Aerospace Lab*.

[34] G. Samson, S. Masson, M. Lengaigne, M. Keerthi, J. Vialard, S. Pous, G. Madec, N. C. Jourdain, S. Jullien, C. Menkès, et al., (2014), The NOW regional coupled model: Application to the tropical Indian Ocean climate and tropical cyclone activity, *Journal of Advances in Modeling Earth Systems*, **6**, 700–722.

Publications

5.1 Books

[CE1] A. Costes, C. Lac, V. Masson, and M. Rochoux, (2018), *Advances in forest fire research 2018*, Imprensa da Universidade de Coimbra, Coimbra.

[CE2] J.-B. Filippi, Y. Perez, F. Allaire, A. Costes, M. Rochoux, V. Mallet, and C. Lac, (2018), *Advances in forest fire research 2018*, Imprensa da Universidade de Coimbra, Coimbra.

5.2 Conferences Proceedings

[CE3] S. Barthélémy, S. Ricci, T. Morel, N. Goutal, and E. Le Pape, (2017), Joint1D/2D hydraulic model coupling, 2D domain decomposition and 1D data asimilation for operational flood forecasting, SimHydro 2017, 14-16 June, Sophia Antipolis.

[CE4] M. Bushuk, R. Msadek, and M. Winton, (2018), Regional Arctic sea ice prediction : potential vs operational forecast, In *POLAR2018, 18-24 June 2018, Davos, Switzerland.*

[CE5] M. Bushuk, R. Msadek, and M. Winton, (2018), Regional Arctic sea ice prediction : potential vs operational seasonal forecast skill, In *Polar Prediction Workshop, 7-9 May 2018, Montreal, Canada*.

[CE6] M. Bushuk, R. Msadek, M. Winton, and G. Vecchi, (2017), Assessing skill of Arctic regional sea ice extent in the GFDL model, In *CanSISE workshop, Toronto, June*.

[CE7] M. Bushuk, R. Msadek, M. Winton, and G. Vecchi, (2017), Regional Arctic sea ice predictions : a direct comparison of potential versus operational seasonal forecast skill, In *AGU Fall meeting, New Orleans, December*.

[CE8] M. Bushuk, R. Msadek, M. Winton, and G. Vecchi, (2017), Regional Arctic sea ice predictions : mechanisms, forecast skill and future outlook, In *Arctic Modeling Workshop, NASA, Washington, DC, June*.

[CE9] M. Bushuk, R. Msadek, M. Winton, and G. Vecchi, (2017), Regional predictions of Arctic sea ice, In *Sea ice Workshop, University of Washington, Seattle, July*.

[CE10] M. Bushuk, R. Msadek, M. Winton, and G. Vecchi, (2017), Skillful regional prediction of Arctic sea ice on seasonal timescales, In *Polar predictability workshop, Alfred Wegener Institute, Germany, March*.

[CE11] M. Bushuk, R. Msadek, M. Winton, G. Vecchi, and X. Yang, (2018), Regional Arctic sea ice prediction: potential versus operational seasonal forecast skill, In *International conference on sub seasonal to decadal predictions. NCAR, 17-21 September, Boulder, Colorado, USA*.

[CE12] S. Chripko, R. Msadek, E. Sanchez-Gomez, and L. Terray, (2018), Winter atmospheric response to summer sea ice loss in the CNRM-CM6 climate model, In *POLAR2018, 18-24 June 2018, Davos, Switzerland*.

[CE13] A. Colmet-Daage, S. Ricci, E. Sanchez-Gomez, V. Borrell Estupina, and C. Llovel, (2017), Climate change impacts on extremes rainfalls, flows and floods in Mediterraneans mesoscales catchments, In *Intenationnal Association of Hydrogeologists (IAH)*, Montpellier, France.

[CE14] A. Colmet-Daage, S. Ricci, E. Sanchez-Gomez, V. Borrell Estupina, and W. Llovel, (2017), Climate change impacts on extremes rainfalls, flows and floods in Mediterraneans mesoscales catchments, In *Internationnal Association of Hydrogeologists (IAH). Montpellier, France*.

[CE15] A. Colmet-Daage, S. Ricci, E. Sanchez-Gomez, V. Borrell Estupina, E. Servat, and C. Llovel, (2017), Climate change impacts on extremes rainfalls, flows and floods in Mediterraneans mesoscales catchments, International Association of Hydrological Science (IAHS). Port Elisabeth, South Africa.

[CE16] A. Colmet-Daage, E. Sanchez-Gomez, S. Ricci, V. Borrell Estupina, W. Llovel, P. Quintana-Segui, and C. Llasat, (2017), Evaluation of uncertainties in mean and extreme precipitation under climate change for northwestern Mediterranean watersheds from high-resolution Med and Euro-CORDEX ensembles, In *10th Hymex workshop, 4-7 July, Barcelona, Spain, Juillet*.

[CE17] A. Costes, C. Lac, V. Masson, and M. Rochoux, (2018), An upper non-reflecting boundary condition for atmospheric compressible flow, In *VIII International Conference on Forest Fire Research, Coimbra, Portugal, 12-16 November*.

[CE18] M. De Lozzo, P. Mycek, S. Ricci, M. Rochoux, P. Roy, N. Goutal, and U. Ruede, (2017), Méthodes de Monte-Carlo multi-niveaux pour la quantification d'incertitudes et l'assimilation de données - Application'a la modélisation fluviale, In *49th Days of Statistics*, Avignon, France.

[CE19] S. Denvil, M. Lautenschlager, S. Fiore, F. Guglielmo, M. Juckes, S. Kindermann, M. Kolax, C. Pagé, and W. Som de Cerff, (2017), The ENES Data Task Force — Copernicus and H2020 Program: Machine Learning and Big Data Needs and Overview, In *7th Annual ESGF Face-to-Face Conference, 5-8 December, San Francisco, CA, USA*.

[CE20] S. Denvil, M. Lautenshlager, S. Fiore, F. Guglielmo, S. Kindermann, M. Kolax, C. Pagé, and W. Som de Cerff, (2017), The ENES Data Task Force — Copernicus and H2020 Programme: Science Drive Overview, In *7th Annual ESGF Face-to-Face Conference, 5-8 December 2017, San Francisco, CA, USA*.

[CE21] J.-B. Filippi, Y. Perez, F. Allaire, A. Costes, M. Rochoux, V. Mallet, and C. Lac, (2018), High resolution weather forecasting tool chain for forest fire behaviour, In *VIII International Conference on Forest Fire Research, Coimbra, Portugal, 12-16 November*.

[CE22] M. Gollner, C. Zhang, A. Trouvé, and M. Rochoux, (2017), Data-driven fire modeling, In *Conference on Fire Prediction Across Scales*, Columbia University, USA.

[CE23] K. Goubanova, E. Sanchez-Gomez, C. Frauen, and A. Voldoire, (2017), Role of the remote and local wind stress forcing in the development of the warm SST errors in the South-Eastern Tropical Atlantic in a coupled high-resolution seasonal hindcast, In *5th WGNE on Model systematic errors,19-23 Juin, Montreal, Canada*.

[CE24] S. Joussaume, F. Guglielmo, M. Lautenschlager, S. Denvil, M. Juckes, and C. Pagé, (2018), IS-ENES data : present and future of the data infrastructure for climate modeling, In *Geophysical Research Abstracts, Vol. 20, EGU2018-15930, EGU General Assembly, 8-13 April, Vienna, Austria*.

[CE25] S. Joussaume, B. Lawrence, C. Pagé, and J. Biercamp, (2017), The Data Deluge in High-Resolution Climate and Weather Simulation, In *European Big Data Value Forum, 22 November 2017, Versailles, France*.

[CE26] M. Kerdoncuff, J. Soubeyroux, R. Vautard, C. Pagé, B. Cassaigne, F. Tocquer, P. Jardin, and G. Baillon, (2018), DRIAS portal as a national climate service, In *EMS Annual Meeting, European Conference for Applied Meteorology and Climatology, 3-7 septembre 2018, Budapest, Hungary*.

[CE27] S. Kotlarski, P. Szabo, S. Herrera, O. Räty, K. Keuler, P. Soares, R. Cardoso, T. Bosshard, C. Pagé, F. Boberg, J. Gutiérrez, A. Jaczewski, F. Kreienkamp, M. Liniger, C. Lussana, and G. Szepszo, (2017), Observational uncertainty and regional climate model evaluation: A pan-European perspective, In *EGU General Assembly 2017, 23-28 April, Vienna, Austria*, vol. 19.

[CE28] V. Laborie, N. Goutal, S. Ricci, M. De Lozzo, and P. Sergent, (2017), Global Sensitivity Analysis applied to the Telemac2D numerical forecast model of high water levels in the Gironde estuary, 24th Telemac User Conference, Graz, Austria.

[CE29] V. Laborie, N. Goutal, S. Ricci, M. De Lozzo, and P. Sergent, (2017), Uncertainty quantification applied to Gironde Estuary Telemac2D numerical model, SimHydro 2017, 14-16 June, Sophia Antipolis.

[CE30] V. Laborie, N. Goutal, S. Ricci, M. De Lozzo, and P. Sergent, (2017), Uncertainty quantification in hydrodynamics bidimensional models : the case of Gironde estuary forecast model, no. EGU2017-312 / NH1.3/HS11.25, Vienne.

[CE31] E. Maisonnave and S. Valcke, (2017), OASIS3-MCT, a coupling software for climate modeling, In *International Fall School on Terrestrial Modeling and High-Performance Scientific Computing, 25-29 September, Bonn, Germany*, Meteorological Institute, Bonn University.

[CE32] E. Maisonnave and A. Will, (2017), The quality of vertical interpolation in one- and two-way atmospheric couplings: analysis and new developments, In *CLM-Community Assembly, 19-22 September*, Austria, Wegener Center, Graz University.

[CE33] E. Maisonnave, (2017), Beneficial effects of OASIS modularity, In *4th Workshop on Coupling Technologies for Earth System Models, Princeton, New Jersey, USA*.

[CE34] M. Martin, C. Cassou, and E. Sanchez-Gomez, (2018), Role of the ocean dynamics in ENSO-tropical Atlantic teleconnection under warmer climate, In *PREFACE-TAV-PIRATA Conférence, 17-20 April, Lanzarote, Spain*.

[CE35] M. Martin, C. Cassou, and E. Sanchez-Gomez, (2018), Role of the ocean dynamics in ENSO-tropical Atlantic teleconnection under warmer climate, In *European Geosciences Union General Assembly (EGU) 8-13 April, Vienna, Austria*.

[CE36] P. Monerie, B. Pohl, and E. Sanchez-Gomez, (2017), Role of the internal variability on Sahel precipitation change, In *EGU General Assembly, 23-28 April, Viena, Avril 2017*.

[CE37] R. Msadek and C. Cassou, (2018), Modulation of Arctic climate change by Atlantic Multidecadal Variability, In *POLAR2018, 18-24 June 2018, Davos, Switzerland*.

[CE38] R. Msadek and CNRM, (2017), Evaluation of the PRE−CMIP6 CNRM−CM runs. Issues encountered for the North Atlantic and the Arctic, In *Workshop on the use of NEMO in CMIP6 climate model simulations, January 2017, Grenoble, France*.

[CE39] R. Msadek, A. Voldoire, M. Chevallier, E. Sanchez-Gomez, and C.-C. Group, (2018), Selected oceanic features of the CNRM-CM6 models, In *Nero Users Meeting, 11-12 October, Toulouse, France*.

[CE40] P. Mycek, M. De Lozzo, S. Ricci, M. Rochoux, P. Roy, and N. Goutal, (2017), Multilevel Monte Carlo estimation of covariances in the context of open-cahenne flow simulation, CEMRACS 17/07-25/08/2017, CIRM, Marseille.

[CE41] T. Oudar, E. Sanchez-Gomez, F. Chauvin, J. Cattiaux, C. Cassou, and L. Terray, (2017), Impact of Arctic Sea Ice loss on large scale atmospheric circula,on based on fully-coupled sensitivity experiments, In *AMA 2017, 30 Janvier-3 Février 2017, CIC-Météo-France, Toulouse*.

[CE42] C. Pagé, I. Klampanos, R. Filgueira, and S. Gesing, (2018), Innovative Data-Driven Platforms and VREs for Complex Earth, Space and Environmental Sciences Applications, In *AGU Fall Meeting 2018, 10-14 December, Washington DC, USA*.

[CE43] C. Pagé, I. Klampanos, W. Som de Cerff, M. Atkinson, A. Spinuso, V. Karkaletsis, and M. Plieger, (2018), DARE as a platform to support Climate Data Analytics using Cloud Infrastructures, In *Digital Infrastructures for Research, 9-11 octobre 2018, Lisbonne, Portugal*.

[CE44] C. Pagé, A. Pagani, M. Plieger, W. Som de Cerff, A. Mihajlovski, E. de Vreede, A. Spinuso, R. Hutjes, F. de Jong, L. Bärring, M. Vega, A. Cofino, A. d anca, S. Fiore, and M. Kolax, (2017), The climate4impact platform, In *The climate4impact platform: Providing, tailoring and facilitating climate model data access, Geophysical Research Abstracts, 23-28 April, Vienna Austria, EGU General Assembly*, vol. 19.

[CE45] C. Pagé, X. Pivan, A. Rajapakse, W. Som de Cerff, M. Plieger, E. de Vreede, A. Spinuso, L. Barring, A. Cofino, A. Anca, and S. Fiore, (2017), Using the ESGF CWT-API in the context of the EUDAT-EGI e-infrastructure and the ENES climate4impact platform, In *7th Annual ESGF Face-to-Face Conference, 5-8 December 2017, San Francisco, CA, USA*.

[CE46] C. Pagé, X. Pivan, A. Rajapakse, W. Som de Cerff, M. Plieger, E. de Vreede, A. Spinuso, L. Bärring, A. Cofino, A. d ' Anca, and S. Fiore, (2018), Using the EGI FedCloud and the ESGF CWT-API in a WPS workflow to provide data analysis computations for the IS-ENES climate4impact platform, In *Geophysical Research Abstracts, Vol. 20, EGU2018-12280, EGU General Assembly, 8-13 April, Vienna, Austria*.

[CE47] C. Pagé, X. Pivan, W. Som de Cerff, A. Spinuso, and M. Plieger, (2018), Improving Climate Data Access through integration of the DARE Platform, the ENES CDI and EUDAT B2 Services, In *10th International Workshop on Science Gateways (IWSG 2018), 13-15 June 2018, Edinburgh, Scotland, United Kingdom*.

[CE48] C. Pagé, W. Som de Cerff, A. Spinuso, M. Plieger, I. Klampanos, M. Atkinson, and V. Karkaletsis, (2018), Leveraging and Easing End Users' Climate Data Access by Interfacing Infrastructures, In *AGU Fall Meeting, 10-14 December 2018, Washington D.C, USA*.

[CE49] C. Pagé, (2017), Les défis de l'analyse de données en sciences du climat, In *Journées scientifiques Equip-Meso, 30-31 janvier 2017, Grenoble, France*.

[CE50] C. Pagé, (2017), Les nouveaux défis de l'analyse de données climatiques, In *Forum TERATEC 2017, 27-28 juin 2017, Palaiseau, France*.

[CE51] C. Pagé, (2018), Interfacing e-infrastructures to cope with large data volumes for end-users of climate data, In *3rd ENES Workshop on Workflows, 13-14 septembre 2018, Bruxelles, Belgique*.

[CE52] M. Plieger, W. Som de Cerff, A. Spinuso, E. de Vreede, N. Drost, and C. Pagé, (2018), Climate4impact : Provenance in processing and new ADAGUC-services analytics, In *Geophysical Research Abstracts, Vol. 20, EGU2018-17344, EGU General Assembly , 8–13 April, Vienna, Austria*.

[CE53] S. Qasmi, C. Cassou, J. Boé, and R. Msadek, (2018), Dynamical and thermodynamical impacts of the AMV on Climate, In *International conference on sub seasonal to decadal predictions. NCAR, 17-21 September, Boulder, Colorado, USA*.

[CE54] S. Ricci, S. Biancamaria, A. Boone, N. Elmocayd, C. Emery, J.-F. Creteaux, P.-A. Garambois, N. Goutal, V. Halfiger, P. Le Moigne, P.-O. Malaterre, J. Monnier, and V. Pedinotti, (2017), Combining SWOT data and numerical models with Data Assimilation methods for better simulation and forecast of water level and discharge, In *SWOT Applications User Workshop, 5-6 April, Reston VA, USA*.

[CE55] S. Ricci, N. Elmocayd, N. Goutal, M. Rochoux, C. Goeury, R. Ata, H. Oubanas, P.-O. Malaterre, and I. Gejadze, (2017), Uncertainty quantification for river flow simulation applied to a real test case: the Garonne valley, In *SimHydro 2017 conference*, Nice, France.

[CE56] S. Ricci, N. Elmocayd, N. Goutal, M. Rochoux, C. Goeury, R. Ata, H. Oubanas, P.-O. Malaterre, and I. Gejadze, (2017), Uncertainty quantification for river flow simulation applied to a real test case: the Garonne valley, SimHydro 2017, 14-16 June, Sophia Antipolis.

[CE57] S. Ricci, N. Goutal, N. Elmocayd, and F. Moussu, (2017), Ensemble-based Data assimilation with surrogate models – Garonne test case study, SWOT Science Team meeting, June 28th.

[CE58] S. Ricci, (2017), Data assimilation and flood forecasting . Data science for high impact weather and flood prediction, In *DARE, 20-22/11/2017, Henley, UK. Invited Speaker*.

[CE59] M. Rochoux, A. Collin, D. Lucor, and P. Moireau, (2017), Quantifying and reducing shape and topological uncertainties in front-tracking problems, In *Workshop Traitement des Données Massives en Mécanique des Fluides, Université Paris-Saclay (France), 29 November-1 December*.

[CE60] M. Rochoux, G. Rea, M. De Lozzo, and O. Vermorel, (2017), Quantifying uncertainties in large eddy simulations of pollutant dispersion using surrogate models, In *Workshop Traitement des Données Massives en Mécanique des Fluides, Université Paris-Saclay, 29 November-1 December.*

[CE61] M. Rochoux, S. Ricci, N. Goutal, S. Boyaval, and D. Lucor, (2017), Environmental risk prediction using reduced-cost Ensemble Kalman Filter based on Polynomial Chaos surrogate, In *Workshop Data Science and Environment*, Brest, France.

[CE62] M. Rochoux, C. Zhang, N. Frebourg, D. Lucor, A. Trouvé, P. Moireau, and A. Collin, (2018), Recent advances in data-driven wildland fire spread modeling: Treatment of position errors and joint state-parameter estimation, In *7th French National Symposium on Data Assimilation (LEFE), 26-28 September, Rennes, France*.

[CE63] M. Rochoux, C. Zhang, M. Gollner, and A. Trouvé, (2017), Designing data-driven modeling strategies for real-time wildfire spread forecasting, In *Earth Observation Summit 2017 – Workshop on Wildfire Remote Sensing*, Montreal, Canada.

[CE64] M. Rochoux, C. Zhang, R. Paugam, and A. Trouvé, (2018), Overview and challenges of data-driven wildland fire spread modeling, In *Workshop on Mathematics and Wildfires – International Center for Mathematics (CIM), 8-9 November, Coimbra, Portugal*.

[CE65] P. Rogel, (2017), Modèles et projections climatiques : du global au local et application aux risques cotiers, In *Conseil Scientifique du Comité Français de Géophysique de l'Ingénieur et de l'Environnement, 21 Septembre, CNAM, Paris*.

[CE66] O. Rössler, A. Fischer, N. Addor, S. Kotlarski, C. Pagé, and R. Wilcke, (2018), Linking climate and impact models: Challenges, approaches, solutions, In *EGU General Assembly 2018, 8–13 April, Vienna, Austria*.

[CE67] V. Rousseau, E. Sanchez-Gomez, R. Msadek, and L. Terray, (2018), Representation of air-sea coupling in the Gulf Stream region in high resolution observations and model simulations, In *European Geosciences Union General Assembly, 8-13 April, Vienna, Austria*.

[CE68] P. Roy, M. De Lozzo, S. Ricci, M. Rochoux, V. Laborie, and N. Elmocayd, (2017), Improving surrogate model-based uncertainty quantification in a costly numerical environment, 10th OpenTurns Users 06/06/2017, Chatou.

[CE69] Y. Ruprich-Robert, R. Msadek, T. Delworth, F. Castruccio, S. Yeager, and G. Danabasoglu, (2018), Impacts of the Atlantic Multidecadal Cariability on the tropical climate and tropical cyclone activity, In *International conference on sub seasonal to decadal predictions. NCAR, 17-21 September, Boulder, Colorado*.

[CE70] E. Sanchez-Gomez and S. Somot, (2018), Impact of the Internal Variability of a regional model on the Mediterranean Cyclones, In *MedClivar Conference, 17-21 september, Belgrade, Serbia*.

[CE71] E. Sanchez-Gomez, M. Martin, G. Ruggiero, and R. Msadek, (2018), Impact of the ocean stochastic parameterization on the simulated mean state and variability of a coupled model, In *PREFACE-TAV-PIRATA Conference, 17-20 April, Lanzarote, Spain*.

[CE72] E. Sanchez-Gomez, S. Qasmi, C. Cassou, and J. Boé, (2018), Assessing the climate Impacts of the Atlantic Multidecadal Variability on the Mediterranean basin, In *MedCordex-BalticEarth Conference, 14-16 March, Majorque, Spain*.

[CE73] E. Sanchez-Gomez, S. Qasmi, C. Cassou, and J. Boé, (2018), Assessing the climate Impacts of the Atlantic Multidecadal Variability on the Mediterranean basin, In *MedClivar Conference, 17-21 september, Belgrade, Serbia*.

[CE74] E. Sanchez-Gomez, G. Ruggiero, R. Msadek, R. Waldman, A. Voldoire, M. Chevallier, and L. Bessières, (2018), Impact of the NEMOv3.6 stochastic parametrisation on the CNRM-CM6.1 coupled model, In *Impact of the NEMOv3.6 stochastic parametrization on the CNRM-CM6.1 coupled model, NEMO users Meeting, 11-12 October, Toulouse, France*.

[CE75] E. Sanchez-Gomez, A. Voldoire, K. Goubanova, T. Toniazzo, S. Koseki, T. Losada, B. Rodriguez de Fonseca, and N. Keenlyside, (2017), Le couplage en anomalie dans les modèles de climat : lien entre le biais climatologique et la représentation de la variabilité interannuelle, In *AMA 2017, 30 Janvier-3 Février 2017, CIC-Météo-France, Toulouse*.

[CE76] E. Sanchez-Gomez, (2017), Model drift analysis to understand the causes of systematic errors in climate prediction systems, In *16th CTWF Symposium on seasonal and decadal forecasts, 18-20 September, Beijing, China, September*.

[CE77] E. Sanchez-Gomez, (2017), Model drift analysis to understand the causes of systematic errors in climate prediction systems, In *5th WGNE on Model systematic errors, 19-23 June, Montreal, Canada, Juin*.

[CE78] G. Sgubin, D. Swingedouw, G. Dayon, I. Garcia de Cortazar Atauri, N. Ollat, C. Pagé, and C. van Leeuwen, (2018), Late frost risk for grapevine in France, In *Geophysical Research Abstracts, Vol. 20, EGU2018-17817-3, EGU General Assembly, 8–13 April, Vienna, Austria*, G. R. Abstracts, ed., vol. 20.

[CE79] L. Terray and C. Deser, (2017), Multiple drivers of Arctic amplification, In *Understanding the Causes and Consequences of Polar Amplification, Workshop, The Aspen Global Change Institute, Aspen, Colorado, USA, June 11-16*.

[CE80] L. Terray, (2017), Towards attribution of decadal scale climate events, In *Canadian Sea Ice and Snow Evolution (CanSISE) Network project final meeting, Victoria, Canada, November 1-3*.

[CE81] S. Turquety, L. Menut, and M. Rochoux, (2017), Forecasting wildfires' impact on air quality, In *18th GEIA (Global Emissions InitiAtive) conference - Emissions Science for a Healthy Environment*, Hamburg, Germany.

[CE82] S. Valcke, L. Coquart, A. Craig, G. Jonville, E. Maisonnave, and A. Piacentini, (2018), Latest developments of the OASIS3-MCT coupler for improved performance, In *5th ENES Workshop on High Performance Computing for Climate and Weather, 17-18 May 2018 Lecce*.

[CE83] S. Valcke, R. Ford, M. Hobson, G. Jonville, A. Porter, and G. Riley, (2017), IS-ENES Coupling Technology Benchmarks, In *Platform for Advanced Scientific Computing (PASC) 2017, Mini symposium Earth System Modeling: HPC Bringing Together Weather and Climate Prediction, June 26-28, Lugano (Switzerland)*.

[CE84] S. Valcke, M. Hanke, R. Ford, M. Hobson, G. Jonville, A. Porter, and G. Riley, (2017), First results from IS-ENES Coupling Technology Benchmarks, In *Fourth Workshop on Coupling Technologies for Earth System Models, March 20-22, Princeton (USA)*.

[CE85] A. Voldoire, T. Demissie, A. Deppenmeier, E. Exarchou, C. Frauen, K. Goubanova, N. Keenlyside, S. Koseki, C. Prodhomme, E. Sanchez-Gomez, M. Shen, J. Shonk, T. Toniazzo, and A. Traore, (2017), SST bias development in the Tropical Atlantic in PREFACE coordinated experiments, In *5th WGNE on Model systematic errors, 19-23 Juin, Montreal, Canada.*

[CE86] M. Widmann, J. Bedia, J. Gutierrez, T. Bosshard, E. Hertig, D. Maraun, M. Casado, P. Ramos, R. Cardoso, P. Soares, J. Ribalaygua, C. Pagé, A. Fischer, S. Herrera, and R. Huth, (2018), Validation of spatial variability in downscaling results from the VALUE perfect predictor experiment, In *Geophysical Research Abstracts, Vol. 20, EGU2018-9284, EGU General Assembly, 8-13 April, Vienna, Austria*.

[CE87] C. Zhang, A. Collin, P. Moireau, A. Trouvé, and M. Rochoux, (2018), Front shape similarity measure for data-driven simulations of wild land fire spread based on state estimation : Application to the RxCADRE field-scale experiment, In *37th International Symposium on Combustion, Dublin, Ireland, 29 July-3 August*.

[CE88] C. Zhang, M. Rochoux, A. Collin, P. Moireau, W. Tang, M. Gollner, E. Ellicott, and A. Trouvé, (2017), Front shape comparison in data-driven wildland fire spread simulations, In *10th US National Combustion Meeting*, College Park, Maryland, USA.

[CE89] C. Zhang, M. Rochoux, W. Tang, M. Gollner, J.-B. Filippi, and A. Trouvé, (2017), Evaluation of a data-driven wildland fire spread forecast model with spatially-distributed parameter estimation in simulations of the FireFlux I field-scale experiment, In *12th International Symposium of the International Association for Fire Safety Science*, Lund, Sweden.

5.3 Journal Publications

[CE90] M. Bador, L. Terray, J. Boé, S. Somot, A. Alias, A.-L. Gibelin, and B. Dubuisson, (2017), Future summer mega-heatwave and record-breaking temperatures in a warmer France climate, *Environmental Research Letters*, **12**, 1–12.

[CE91] V. Balaji, E. Maisonnave, E. Zadeh, B. Lawrence, J. Biercamp, U. Fladrich, G. Aloisio, R. Benson, A. Caubel, J. Durachta, M.-A. Foujols, G. Lister, S. Mocavero, S. Underwood, and G. Wright, (2017), CPMIP : Measurements of Real Computational Performance of Earth System Models in CMIP6, *Geoscientific Model Development*, **46**, 19–34.

[CE92] S. Barthélémy, S. Ricci, T. Morel, N. Goutal, E. Le Pape, and F. Zaoui, (2018), On operational flood forecasting system involving 1D/2D coupled hydraulic model and data assimilation, *Journal of Hydrology*, **562**, 623–634.

[CE93] S. Barthélémy, S. Ricci, M. Rochoux, E. Le Pape, and O. Thual, (2017), Ensemble-based data assimilation for operational flood forecasting – On the merits of state estimation for 1D hydrodynamic forecasting through the example of the Adour Maritime river, *Journal of Hydrology*, **552**, 210–224.

[CE94] T. Ben-Ari, J. Boé, P. Ciais, R. Lecerf, M. Van der Velde, and D. Makowski, (2018), Causes and implications of the unforeseen 2016 extreme yield loss in the breadbasket of France, *Nature Communications*, **9**, 1627.

[CE95] L. Bessières, S. Leroux, J.-M. Brankart, J. Molines, M.-P. Moine, P.-A. Bouttier, T. Penduff, L. Terray, B. Barnier, and G. Serazin, (2017), Development of a probabilistic ocean modelling system based on NEMO 3.5: application at eddying resolution, *Geoscientific Model Development*, 1091–1106.

[CE96] J. Boé, (2018), Interdependency in Multimodel Climate Projections: Component Replication and Result Similarity, *Geophysical Research Letters*, **45**, 2771–2779.

[CE97] R. Bonnet, J. Boé, G. Dayon, and M. Martin, (2017), Twentieth-century hydrometeorological reconstructions to study the multidecadal variations of the water cycle over France, *Water Resources Research*, **53**, 8366–8382.

[CE98] J.-F. Booth, Y.-O. Kwon, S. KO, R. Small, and R. Msadek, (2017), Spatial pattern and intensity of the surface storm tracks in CMIP5 models, **30**, 4965–4981.

[CE99] M. Bushuk, R. Msadek, M. Winton, G. Vecchi, R. Gudgel, A. Rosati, and X. Yang, (2017), Skillful regional prediction of Arctic sea ice on seasonal timescales, *Geophysical Research Letters*, **44**, 4953−4964.

[CE100] M. Bushuk, R. Msadek, M. Winton, G. Vecchi, R. Gudgel, A. Rosati, and X. Yang, (2017), Summer Enhancement of Arctic Sea Ice Volume Anomalies in the September-Ice Zone, *Journal of Climate*, **30**, 2341–2362.

[CE101] M. Bushuk, R. Msadek, M. Winton, G. Vecchi, X. Yang, A. Rosati, and R. Gudgel, (2018), Regional Arctic sea-ice prediction : Potential versus operational seasonal forecast skill, *Climate Dynamics*, 1–23.

[CE102] D. Cariolle, P. Moinat, H. Teyssèdre, L. Giraud, G. Giraud, B. Josse, and D. Lefevre, (2017), ASIS v1.0: an adaptive solver for the simulation of atmospheric chemistry, *Geoscientific Model Development*, **10**, 1467–1485.

[CE103] C. Cassou, Y. Kushnir, E. Hawkins, A. Pirani, F. Kucharski, I.-S. Kang, and N. Caltabiano, (2018), Decadal climate variability and predictability : challenges and opportunity, *Bulletin of the American Meteorological Society*, 479–490.

[CE104] D. Chambers, A. Cazenave, N. Champollion, H. Dieng, W. Llovel, R. Forsberg, K. Von Schuckmann, and Y. Wada, (2017), Evaluation of the Global Mean Sea Level Budget between 1993 and 2014, *Surveys in Geophysics*, **38**, 309–327.

[CE105] M. Chevallier, G. Smith, F. Dupont, J.-F. Lemieux, G. Forget, Y. Fujii, F. Hernandez, R. Msadek, K. Peterson, A. Storto, T. Toyoda, M. Valdivieso, G. Vernieres, H. Zuo, M. Balmaseda, Y.-S. Chang, N. Ferry, G. Garric, K. Haines, S. Keeley, R. Kovach, T. Kuragano, S. Masina, Y. Tang, H. Tsujino, and X. Wang, (2017), Intercomparison of the Arctic sea ice cover in global ocean-sea ice reanalyses from the ORA-IP project, *Climate Dynamics Special Issue*, **49**, 1107–1136.

[CE106] A. Colmet-Daage, E. Sanchez-Gomez, S. Ricci, C. Llovel, V. Borrell Estupina, P. Quintana-Segui, M. Llasat, and E. Servat, (2018), Evaluation of uncertainties in mean and extreme precipitation under climate change for northwestern Mediterranean watersheds from high-resolution Med and Euro-CORDEX ensembles, *Hydrology and Earth System Sciences*, **22**, 673–687.

[CE107] L. Costantino, J. Cuesta, E. Emili, and et al., (2017), Potential of multispectral synergism for observing ozone pollution by combining IASI-NG and UVNS measurements from the EPS-SG satellite, *Atmospheric Measurement Techniques*, **10**, 1281–1298.

[CE108] A. Craig, S. Valcke, and L. Coquart, (2017), Development and performance of a new version of the OASIS coupler, OASIS3-MCT 3.0, *Geoscientific Model Development*, **10**, 3297–3308.

[CE109] G. Dayon, J. Boé, E. Martin, and J. Gailhard, (2018), Impacts of climate change on the hydrological cycle over France and associated uncertainties, *Comptes Rendus Geoscience*, **350**, 141–153.

[CE110] M. Durand, C. Gleason, P.-A. Garambois, D. Bjerklie, L. Smith, H. Roux, E. Rodriguez, P. Bates, T. Pavelsky, J. Monnier, X. Chen, G. Di Baldassarre, J.-M. Fiset, N. Flipo, R. Frasson, J. Fulton, N. Goutal, F. Hossain, E. Humphries, J. MInear, S. Ricci, B. Sanders, G. Schumann, J. Schubert, and L. Vilmin, (2017), An intercomparison of remote sensing river discharge estimation algorithms from measurements of river height, width, and slope, *Water Resources Research*, **52**, 4527–4549.

[CE111] N. Elmocayd, S. Ricci, N. Goutal, M. Rochoux, S. Boyaval, C. Goeury, D. Lucor, and O. Thual, (2018), Polynomial Surrogates for Open-Channel Flows in Random Steady State, *Environmental Modeling and Assessment*, **23**, 309–331.

[CE112] E. Flaounas, F. Kelemen, H. Wernli, M. Gaertner, M. Reale, E. Sanchez-Gomez, P. Lionello, S. Calmanti, Z. Podrascanin, S. Somot, N. Akhtar, R. Romera, and D. Conte, (2018), Assessment of an ensemble of ocean–atmosphere coupled and uncoupled regional climate models to reproduce the climatology of Mediterranean cyclones, *Climate Dynamics*, **51**, 1023–1040.

[CE113] J. Garcia-Serrano, C. Cassou, H. Douville, A. Giannini, and F.-J. Doblas-Reyes, (2017), Revisiting the ENSO teleconnection to the tropical North Atlantic., *Journal of Climate*, **30**, 6945–6957.

[CE114] J. Garcia-Serrano, C. Frankignoul, M. King, A. Arribas, Y. Gao, V. Guemas, D. Matei, R. Msadek, W. Park, and E. Sanchez-Gomez, (2017), Multi-model assessment of linkages between eastern Arctic sea-ice variability and the Euro-Atlantic atmospheric circulation in current climate, *Climate Dynamics*, **49**, 2407–2429.

[CE115] T. Houet, C. Marchadier, G. Bretagne, M.-P. Moine, R. Aguejdad, V. Viguié, M. Bonhomme, A. Lemonsu, P. Avner, J. Hidalgo, and V. Masson, (2017), Combining narratives and modelling approaches to simulate fine scale and long-term urban growth scenarios for climate adaptation, **86**, 1–13.

[CE116] J. Jouanno, O. Hernandez, and E. Sanchez-Gomez, (2017), Equatorial Atlantic interannual variability and its relation to dynamic and thermodynamic processes, **8**, 1061–1069.

[CE117] M. Khodri, T. Izumo, J. Vialard, S. Janicot, C. Cassou, M. Lengaigne, J. Mignot, G. Gastineau, E. Guilyardi, N. Lebas, A. Robock, and M. McPhaden, (2017), Tropical explosive volcanic eruptions can trigger El Nino by cooling tropical Africa, *Nature Communications*, **8**, 1–13.

[CE118] Y. Kushnir, C. Cassou, and S. St George, (2017), Decadal Climate Variability, *CLIVAR Exchanges*, **25**, 25.1.1.

[CE119] C. Lac, J. Chaboureau, V. Masson, J.-P. Pinty, P. Tulet, J. Escobar, M. Leriche, C. Barthe, B. Aouizerats, C. Augros, P. Aumond, F. Auguste, P. Bechtold, S. Berthet, S. Bielli, F. Bosseur, O. Caumont, J.-M. Cohard, J. Colin, F. Couvreux, J. Cuxart, G. Delautier, T. Dauhut, V. Ducrocq, J.-B. Filippi, D. Gazen, O. Geoffroy, F. Gheusi, R. Honnert, J. Lafore, C. Lebeaupin Brossier, Q. Libois, T. Lunet, C. Mari, T. Maric, P. Mascart, M. Mogé, G. Molinié, O. Nuissier, F. Pantillon, P. Peyrillé, J. Pergaud, E. Perraud, J. Pianezze, J.-L. Redelsperger, D. Ricard, E. Richard, S. Riette, Q. Rodier, R. Schoetter, L. Seyfried, J. Stein, K. Suhre, M. Taufour, O. Thouron, S. Turner, A. Verrelle, B. Vié, F. Visentin, V. Vionnet, and P. Wautelet, (2018), Overview of the Meso-NH model version 5.4 and its applications, *Geoscientific Model Development*, **11**, 1929–1969.

[CE120] B. Lawrence, M. Rezny, R. Budich, P. Bauer, J. Behrens, M. Carter, W. Deconinck, R. Ford, C. Maynard, S. Mullerworth, C. Osuna, A. Porter, K. Serradell, S. Valcke, N. Wedi, and S. Wilson, (2018), Crossing the chasm: how to develop weather and climate models for next generation computers, *Geoscientific Model Development*, **11**, 1799–1821.

[CE121] F. Lehner, C. Deser, and L. Terray, (2017), Toward a New Estimate of Time of Emergence of Anthropogenic Warming: Insights from Dynamical Adjustment and a Large Initial-Condition Model Ensemble, *Journal of Climate*, **30**, 7739–7756.

[CE122] F. Lehner, C. Deser, I. Simpson, and L. Terray, (2018), Attributing the U.S. Southwest's Recent Shift Into Drier Conditions, *Geophysical Research Letters*, **45**, 6251–6261.

[CE123] S. Leroux, T. Penduff, L. Bessières, J. Molines, J.-M. Brankart, G. Serazin, B. Barnier, and L. Terray, (2018), Intrinsic and Atmospherically Forced Variability of the AMOC: Insights from a Large-Ensemble Ocean Hindcast, *Journal of Climate*, **31**, 1183–1203.

[CE124] W. Llovel and L. Terray, (2017), Observed southern upper-ocean warming over 2005–2014 and associated mechanisms, *Environmental Research Letters*, **11**, 4023–4037.

[CE125] I. Mavilia, A. Bellucci, P. Athanasiadis, S. Gualdi, R. Msadek, and Y. Ruprich-Robert, (2018), On the spectral characteristics of the Atlantic multidecadal variability in an ensemble of multi-century simulations, *Climate Dynamics*, **51**, 3507–3520.

[CE126] M. Menegoz, C. Cassou, D. Swingedouw, P. Bretonnière, and F. Doblas-Reyes, (2018), Role of the Atlantic Multidecadal Variability in modulating the climate response to a Pinatubo-like volcanic eruption, *Climate Dynamics*, **51**, 1863–1883.

[CE127] P. Monerie, L. Coquart, E. Maisonnave, M.-P. Moine, L. Terray, and S. Valcke, (2017), Decadal prediction skill using high-resolution climate model, *Climate Dynamics*, **49**, 3527–3550.

[CE128] P. Monerie, M.-P. Moine, L. Terray, and S. Valcke, (2017), Quantifying the impact of early 21st century volcanic eruptions on global-mean surface temperature, *Environmental Research Letters*, **12**.

[CE129] P. Monerie, E. Sanchez-Gomez, and J. Boé, (2017), On the range of future Sahel precipitation projections and the selection of a sub-sample of CMIP5 models for impact studies, *Climate Dynamics*, **48**, 2751–2770.

[CE130] P. Monerie, E. Sanchez-Gomez, B. Pohl, J. Robson, and B. Dong, (2017), Impact of internal variability on projections of Sahel precipitation change, *Environmental Research Letters*, **12**, 114003.

[CE131] V. Ng, A. Fazil, P. Gachon, G. Deuymes, M. Radojevic, M. Mascarenhas, S. Garasia, M. Johansson, and N. Ogden, (2017), Assessment of the probability of autochthonous transmission of Chikungunya virus in Canada under recent and projected climate change, *Environmental Health Perspectives*, **125**.

[CE132] A. Nidheesh, M. Lengaigne, J. Vialard, T. Izumo, A. Unnikrishnan, and C. Cassou, (2017), Influence of ENSO on the Pacific decadal oscillation in CMIP models, *Climate Dynamics*, **49**, 3309–3326.

[CE133] T. Oudar, E. Sanchez-Gomez, F. Chauvin, J. Cattiaux, L. Terray, and C. Cassou, (2017), Respective roles of direct GHG radiative forcing and induced Arctic sea ice loss on the Northern Hemisphere atmospheric circulation, *Climate Dynamics*, **49**, 3693–3713.

[CE134] R. Paoli, O. Thouron, D. Cariolle, M. Garcia, and J. Escobar, (2017), Three-dimensional large-eddy simulations of the early phase of contrail-to-cirrus transition: effects of atmospheric turbulence and radiative transfer, *Meteorologische Zeitschrift*, **26**, 597–620.

[CE135] H. Peiro, E. Emili, D. Cariolle, B. Barret, and E. Le Flochmoën, (2018), Multi-year assimilation of IASI and MLS ozone retrievals: variability of tropospheric ozone over the tropics in response to ENSO, *Atmospheric Chemistry and Physics*, **18**, 6939–6958.

[CE136] S. Qasmi, C. Cassou, and J. Boé, (2017), Teleconnection between Atlantic Multidecadal Variability and European temperature: diversity and evaluation of the Coupled Model Intercomparison Project phase 5 models, *Geophysical Research Letters*, **44**, 11,140–11,149.

[CE137] M. Rochoux, A. Collin, C. Zhang, A. Trouvé, D. Lucor, and P. Moireau, (2018), Front shape similarity measure for front position sensitivity analysis and data assimilation for Eikonal equation, *ESAIM: Proceedings and Survey*, **63**, 215–236.

[CE138] P. Roy, N. Elmocayd, S. Ricci, J.-C. Jouhaud, N. Goutal, M. De Lozzo, and M. Rochoux, (2018), Comparison of Polynomial Chaos and Gaussian Process surrogates for uncertainty quantification and correlation estimation of spatially distributed open-channel steady flows, *Stochastic Environmental Research and Risk Assessment*, **32**, 1723–1741.

[CE139] Y. Ruprich-Robert and R. Msadek, (2017), Global impacts of the Atlantic Multidecadal Variability during the boreal winter, *CLIVAR Exchanges*, **25**.

[CE140] Y. Ruprich-Robert, T. Delworth, R. Msadek, F. Castruccio, S. Yeager, and G. Danabasoglu, (2018), Impacts of the Atlantic Multidecadal Variability on North American Summer Climate and Heat Waves, *Journal of Climate*, **31**, 3679–3700.

[CE141] Y. Ruprich-Robert, R. Msadek, F. Castruccio, S. Yeager, T. Delworth, and G. Danabasoglu, (2017), Assessing the Climate Impacts of the Observed Atlantic Multidecadal Variability Using the GFDL CM2.1 and NCAR CESM1 Global Coupled Models, *Journal of Climate*, **30**, 2785–2810.

[CE142] S. Samuel, Houpert, F. Sevault, P. Testor, A. Bosse, I. Taupier-Letage, M. Bouin, R. Waldman, C. Cassou, E. Sanchez-Gomez, X. Durrieu de Madro, F. Adloff, P. Nabat, and M. Herrmann, (2018), Characterizing, modelling and understanding the climate variability of the deep water formation in the North-Western Mediterranean Sea, *Climate Dynamics*, **51**, 1179–1210.

[CE143] E. Sanchez-Gomez and S. Somot, (2018), Impact of the internal variability on the cyclone tracks simulated by a regional climate model over the Med-CORDEX domain, *Climate Dynamics*, **51**, 1005–1021.

[CE144] G. Serazin, A. Jaymond, S. Leroux, T. Penduff, L. Bessières, W. Llovel, B. Barnier, J. Molines, and L. Terray, (2017), A global probabilistic study of the ocean heat content low-frequency variability : Atmospheric forcing versus oceanic chaos, *Geophysical Research Letters*, **44**, 5580–5589.

[CE145] G. Serazin, T. Penduff, B. Barnier, J. Molines, B. Arbic, M. Muller, and L. Terray, (2018), Inverse Cascades of Kinetic Energy as a Source of Intrinsic Variability : A Global OGCM Study, *Journal of Physical Oceanography*, **48**, 1385–1408.

[CE146] G. Sgubin, D. Swingedouw, G. Dayon, I. Garcia de Cortazar-Atauri, N. Ollat, C. Pagé, and C. van Leeuwen, (2018), The risk of tardive frost damage in French vineyards in a changing climate, *Agricultural and Forest Meteorology*, **250-251**, 226–242.

[CE147] D. Swingedouw, J. Mignot, P. Ortega, M. Khodri, M. Menegoz, C. Cassou, and V. Hanquiez, (2017), Impact of explosive volcanic eruptions on the main climate variability modes, *Global and Planetary Change*, **150**, 24–45.

[CE148] Y. Thomas, C. Cassou, P. Gernez, and S. Pouvreau, (2018), Oysters as sentinels of climate variability and climate change in coastal ecosystems, *Environmental Research Letters*, **13**, 104009.

[CE149] D. Tommasi, C. Stock, A. Hobday, R. Methot, I. Kaplan, J. Eveson, K. Holsman, T. Miller, S. Gaichas, M. Gehlen, A. Pershing, G. Vecchi, R. Msadek, T. Delworth, C. Eakin, M. Haltuch, R. Séférian, C. Spillman, J. Hartog, S. Siedlecki, J. Samhouri, B. Muhling, R. Asch, M. Pinsky, V. Saba, S. Kapnick, C. Gaitan,

R. Rykaczewski, M. Alexander, Y. Xue, K. Pegion, P. Lynch, M. Payne, T. Kristiansen, P. Lehodey, and F. Werner, (2017), Managing living marine resources in a dynamic environment : The role of seasonal to decadal climate forecasts, *Progress in Oceanography*, 15–49.

[CE150] J. Vial, C. Cassou, F. Codron, S. Bony, and Y. Ruprich-Robert, (2018), Influence of the Atlantic Meridional Overturning Circulation on the Tropical Climate Response to CO2 Forcing, *Geophysical Research Letters*, **45**, 8519–8528.

[CE151] A. Voldoire, B. Decharme, J. Pianezze, C. Lebeaupin Brossier, F. Sevault, L. Seyfried, V. Garnier, S. Bielli, S. Valcke, A. Alias, M. Accensi, F. Ardhuin, M. Bouin, V. Ducrocq, S. Faroux, H. Giordani, F. Léger, P. Marsaleix, R. Rainaud, J.-L. Redelsperger, E. Richard, and S. Riette, (2017), SURFEX v8.0 interface with OASIS3-MCT to couple atmosphere with hydrology, ocean, waves and sea-ice models, from coastal to global scales, *Geoscientific Model Development*, **10**, 4207–4227.

[CE152] A. Will, N. Akhtar, J. Brauch, M. Breil, E. Davin, H. Ho-Hagemann, E. Maisonnave, M. Thîrkow, and S. Weiher, (2017), The COSMO-CLM 4.8 regional climate model coupled to regional ocean, land surface and global earth system models using OASIS3-MCT: description and performance, *Geoscientific Model Development*, **10**, 1549–1586.

[CE153] C. Zhang, M. Rochoux, W. Tang, M. Gollner, J.-B. Filippi, and A. Trouvé, (2017), Evaluation of a data-driven wildland fire spread forecast model with spatially-distributed parameter estimation in simulations of the FireFlux I field-scale experiment, *Fire Safety Journal*, **91**, 758–767.

5.4 Technical Reports

[CE154] J. Boé, M. Radojevic, R. Bonnet, and G. Dayon, (2018), Scénarios de sécheresse sur le bassin Seine-Normandie, technical report, CECI, Université de Toulouse, CNRS, CERFACS, TR-CMGC-18-60, Toulouse, France.

[CE155] L. Coquart, I. d'Ast, and S. Valcke, (2017), Buildbot : Le logiciel utilisé pour compiler et tester automatiquement les développements réalisés dans le coupleur OASIS3-MCT, technical report, UMR 5318 CECI, CERFACS/CNRS, TR-CMGC-17-85, Toulouse, France.

[CE156] L. Coquart, E. Maisonnave, and S. Valcke, (2018), Using Open MP in OASIS3-MCT for the N-nearest-neighbor remapping, technical report, CECI, Université de Toulouse, CNRS, CERFACS, Toulouse, France - TR-CMGC-18-19.

[CE157] A. Craig and S. Valcke, (2018), OASIS3-MCT4.0 Timing Study with MCT 2.10.beta1, technical report, CECI, Université de Toulouse, CNRS, CERFACS -TR-CMGC-18-38, Toulouse, France.

[CE158] E. Emili, G. Jonville, A. Piacentini, P. Valks, O. Tuinder, and D. Efremenko, (2018), CAMS42D42.3.2.1: Implementation of UV radiance observation operator in the MOCAGE suite, contract report, CERFACS.

[CE159] N. Frebourg, A. Collin, M. Rochoux, and C. Diot, (2018), Apport de la modélisation à l'échelle du feu pour la cartographie d'urgence des incendies de forêt., technical report, CECI, Université de Toulouse, CNRS, CERFACS, Toulouse, France - TR-CMGC-18-169.

[CE160] G. Jonville, S. Valcke, L. Coquart, E. Maisonnave, and A. Piacentini, (2018), Specific analyses of the SCRIP interpolation library for OASIS coupler, working note, CECI, Université de Toulouse, CNRS, CERFACS - WN-CMGC-18-93, Toulouse, France.

[CE161] C. Lamotte, N. Frebourg, and M. Rochoux, (2018), Simuler la qualité de l'air á micro-échelle – Vers la quantification d'incertitudes et l'analyse de sensibilité par métamodèle, technical report, CECI, Université de Toulouse, CNRS, CERFACS - TR-CMGC-18-21, Toulouse, France.

[CE162] A. Lopez, G. Rea, F. Auguste, M. Rochoux, O. Vermorel, and D. Cariolle, (2017), Expérience MUST - Simulation avec YALES2 v1-0-0 et comparaison avec AVBP et MesoNH, working note, CERFACS, WN-CMGC-17-116, Toulouse, France.

[CE163] A. Lopez, G. Rea, F. Auguste, M. Rochoux, O. Vermorel, and D. Cariolle, (2017), Simulation d'un cas académique de bulle chaude avec YALES2 v1-0-0 et comparaison avec AVBP et MesoNH, working note, CERFACS, WN-CMGC-17-111, Toulouse, France.

[CE164] E. Maisonnave and A. Voldoire, (2018), Exchange grid: implementation of a test configuration to evaluate fluxes modification, working note, CECI, Université de Toulouse, CNRS, CERFACS, WN-CMGC-18-47, Toulouse, France.

[CE165] E. Maisonnave, I. Fast, T. Jahns, J. Biercamp, S. Sénési, Y. Meurdesoif, and U. Fladrich, (2017), CDI-pio and XIOS I/O servers compatibility with HR climate models, technical report, UMR5318 CECI, CERFACS-CNRS TR-CMGC-17-52, Toulouse, France.

[CE166] E. Maisonnave, D. Manubens, U. Fladrich, and O. Seland, (2017), Multi-model multi-member integrated simulation: Computing performances of a demonstrator and other single high-resolution climate models, technical report, UMR5318 CECI, CERFACS-CNRS TR-CMGC-17-62, Toulouse, France.

[CE167] E. Maisonnave, (2017), ARPEGE-Climat V6 simulation in yearly chunks, working note, UMR 5318 CECI, CERFACS-CNRS, WN-CMGC-17-38, Toulouse, France.

[CE168] E. Maisonnave, (2017), IS-ENES2 HighRes ESM performance resulting from OASIS updates, technical report, UMR 5318 CECI, CERFACS-CNRS, TR-CMGC-17-24, Toulouse, France.

[CE169] E. Maisonnave, (2018), TerrSysMP coupled model: load balancing and further improvements, working note, CECI, Université de Toulouse, CNRS, CERFACS - WN-CMGC-18-33, Toulouse, France.

[CE170] M.-P. Moine and S. Valcke, (2018), D2.3 Fully optimised and scientifically validated version of CNRM-CM-HR model (T359, 1/4 deg) implemented using a subset of the platform (XIOS, OASIS3-MCT, ...) and D2.5 CNRM-CM version at high resolution (T359 1/4 deg) using (at least large part) of the platform, technical report, CECI, Université de Toulouse, CNRS, CERFACS - TR-CMGC-18-210, Toulouse, France.

[CE171] C. Pagé, C. Jack, and R. Hutjes, (2017), Assessment of impact communities' requirements. IS-ENES2 WP5 NA4 D5.2, technical report, CECI, Université de Toulouse, CNRS, CERFACS, Toulouse, France - TR-CMGC-17-233.

[CE172] C. Pagé, M. Plieger, W. Som de Cerff, C. Jack, A. Cofino, M. Vega, M. Kolax, L. Bärring, O. Christensen, and M. Matreata, (2017), Report on derived products in CLIMATE4IMPACT. IS-ENES2 WP11 JRA3 D11.6, technical report, CECI, Université de Toulouse, CNRS, CERFACS, Toulouse, France - TR-CMGC-17-232.

[CE173] A. Piacentini, E. Maisonnave, G. Jonville, L. Coquart, and S. Valcke, (2018), A parallel SCRIP interpolation library for OASIS, working note, CECI, Université de Toulouse, CNRS, CERFACS - WN-CMGC-18-34, Toulouse, France.

[CE174] S. Ricci, N. Goutal, M. Parisot, S. Barthélémy, P. Roy, and M. De Lozzo, (2018), Estimates of hydraulic variables and uncertainty estimates for major rivers in France used for hydropower production, Deliverable EoCoE, technical report, CECI, Université de Toulouse, CNRS, CERFACS, Toulouse, France - TR-CMGC-18-204.

[CE175] S. Valcke, L. Coquart, and G. Jonville, (2018), MS2.4 : High quality interpolation weight and parallel coupling available to IPSL-CM and CNRM-CM, technical report, CECI, Université de Toulouse, CNRS, CERFACS - TR-CMGC-18-91, Toulouse, France.

[CE176] S. Valcke, L. Coquart, A. Craig, G. Jonville, E. Maisonnave, and A. Piacentini, (2018), Multithreaded or thread safe OASIS version including performance optimizations to adapt to many-core architectures, Deliverable D2.3, ESiWACE project, technical report, CECI, Université de Toulouse, CNRS, CERFACS - TR-CMGC-18-74, Toulouse, France.

[CE177] S. Valcke, A. Craig, and L. Coquart, (2018), OASIS3-MCT User Guide, OASIS3-MCT4.0, technical report, CECI, Université de Toulouse, CNRS, CERFACS - TR-CMGC-18-77, Toulouse, France.

[CE178] S. Valcke, G. Jonville, R. Ford, M. Hobson, A. Porter, and G. Riley, (2017), Report on benchmark suite for evaluation of coupling strategies, technical report, UMR 5318 CECI, CERFACS/CNRS, TR-CMGC-17-87, Toulouse, France.

[CE179] S. Valcke, Y. Meurdesoif, and M.-P. Moine, (2018), White paper on a strategy for full convergence of I/O and coupling tools, ESiWACE Deliverable D2.5, technical report, CECI, Université de Toulouse, CNRS, CERFACS - TR-CMGC-18-92, Toulouse, France.

5.5 Thesis

[CE180] R. Bonnet, (2018), *Variations du cycle hydrologique continental en France des années 1850 à aujourd'hui*, phd thesis, Université de Toulouse 3 Paul Sabatier.

[CE181] C. Cassou, (2018), *Un jour, une saison, des décennies, un siècle : Un carnet de voyage sur la région Nord Atlantique-Europe*, hdr, CNRS-CERFACS, Université de Toulouse.

[CE182] A. Colmet-Daage, (2018), *Les impacts du changement climatique sur les pluies et les inondations extrêmes de bassins versants méso-échelles méditérranéens*, phd thesis, Université de Montpellier.

[CE183] N. El Moçayd, (2017), *La décomposition en polynôme du chaos pour l'amélioration de l'assimilation de données ensembliste en hydraulique fluviale*, phd thesis, Institut National Polytechnique de Toulouse.

[CE184] H. Peiro, (2018), *Assimilation des observations satellitaires de l´interféromètre Atmosphérique de Sondage Infrarouge (IASI) dans un modèle de chimie-transport pour des réanalyses d´ozone à l'échelle globale.*, phd thesis, Université de Toulouse 3 Paul Sabatier.

[CE185] S. Qasmi, (2018), *Sensibilité du climat européen à la variabilité multidécennale de l'Atlantique Nord*, phd thesis, Université de Toulouse 3 Paul Sabatier.

3

Computational Fluid Dynamics

Introduction

The 2017-2018 period has been an important transition period for CERFACS and for the Computational Fluid Dynamics (CFD) team: an intense interaction with CERFACS shareholders has lead to a re-orientation of our research activities towards more fundamental research and less applications. This decision has started shaping our activities in 2018, leading also to the creation of the new COOP team at CERFACS in which many topics initially started in the CFD team (deep learning, HPC, interfaces...) are developed now. The CFD team remains the largest team at CERFACS and is still growing. In September 2018, twenty new PhDs have started which is the largest number ever seen in the CFD team. More than 70 researchers work in the CFD team at the end of 2018. The team's activity can still be split in three main parts:

- Numerical methods (Section 2)
- Physical models (Section 3)
- Applications (Section 4)

The development of physical models and the application of CFD codes to real systems remain an important part of the team's activity. Efficient solvers require specialists of numerical methods to address real applications and therefore to deal with models which represent the physics to simulate. Validations are still needed to address the real problems, at the right scale and to avoid limiting our research to academic, simple cases. This application field addressed by the CFD team has grown in 2017 and 2018: in addition to the classical domains of expertise of the team (aircraft aerodynamics, combustion), the CFD team is now developing new fields of application in turbomachinery (compressor and turbines), kinetics (pollutant formation such as CO, NO and soot), aeroacoustics (of aircraft and helicopter), plasma physics (for ignition or for plasma satellite engines).
The following sections describe results obtained by the CFD team in 2017 and 2018. A few important points are mentioned here:

Academic excellence
The CFD team continues to publish in the best journals and to produce PhDs. Table 1.1 provides the number of papers published per year in A journals as well as the number of PhDs defended. With an average of 12

Year	Papers in A journals	PhD defended
2017	24	13
2018	28	6

Table 1.1: Number of papers in A journals and PhD defended in the CFD team in 2017 and 2018.

permanent researchers present in the team over this period, the number of papers published per year and permanent researcher is more than 2.

The ERC advanced grant INTECOCIS on combustion instabilities
The ERC (European Research Council) advanced grant INTECOCIS in the field of thermoacoustics (intecocis.inp-toulouse.fr) has run successfully until February 2018 and has finished with more than 25

papers in A journals and 12 post doc and PhD students co supervised by IMF Toulouse and CERFACS. This group was probably the largest thermoacoustics team worldwide and the results obtained during these five years have fostered other research topics such as combustion noise or instabilities in annular chambers. In 2018, two new European ITN projects have been won: ANNULIGHT (coordinated by NTNU) and MAGISTER (coordinated by Un. Twente). These two projects focus on annular chambers typical of gas turbines and will directly benefit from the experience gained in INTECOCIS.

LES for turbomachinery, coupling and LES and for full engines
The challenge identified by CERFACS 10 years ago (computing a full gas turbine) is coming to life. LES of combustion chambers is now a well established approach and LES for turbomachinery is rapidly gaining momentum. The AVBP LES solver of CERFACS, used for combustion chambers, is also used today for turbomachinery and fully coupled simulations (compressor + combustion chamber or chamber + turbine) are now possible. This is a fundamental computer science challenge which opens new paths for engine research: many phenomena require to perform LES in the whole engine (instabilities, noise, ignition, quenching, stall) and the LES machinery developed by CERFACS is reaching a point where this is becoming a capacity and not a dream any more. This evolution corresponds to a simultaneous paradigm change for CFD where stand-alone CFD methods are losing ground, compared to coupling techniques which allow multi physics to be taken into account. The CFD team continues to collaborate with the GlobC team and with ONERA to develop the OpenPalm coupling software (cerfacs.fr/globc/PALM_WEB/). Coupling is not only a field of research in terms of physics: it rapidly becomes a computer science question where CERFACS has chosen to couple individual solvers using OpenPalm rather than merge all in a single solver.

Explosions and safety CFD
The simulation of explosions in buildings has been a success story of the CFD team where the combustion tools coming from our aerospace research have been applied to the problem of combustion in buildings containing a combustible mixture of air and gas. This project was supported by TOTAL, leading to an INCITE project in 2013 and 2014 and renewed projects in the field of safety. In 2018, EDF and TOTAL have expressed interest in developing an upscaled version of the AVBP code for explosions, both in the subsonic (deflagration) and supersonic (detonation) regimes. The objective is to develop truly predictive simulation methods for explosions in a field where heuristic methods and low quality CFD software are still used too often to analyse the safety of industrial installations. Interestingly, the tools developed for this application have also found new applications in the field of aerospace where engines using detonation are studied today to replace present, constant pressure chambers in aircraft and missiles.

Deep Learning (DL) and CFD
The use of DL tools in CFD has grown exponentially in 2018 within CFD and COOP. The most successful example came from the field of subgrid scale models for turbulent combustion, through a collaboration with Stanford during the 2018 CTR summer program. Obviously, this topic will continue to grow rapidly at CERFACS.

Elearning and training
Today, CERFACS offers two types of formations: (1) face to face sessions in Toulouse and (2) SPOC sessions based on Internet assistance. The Elearning web site of CERFACS continues to work quite well in the field of CFD (elearning.cerfacs.fr) and the SPOC sessions dedicated to CFD are developed at high speed (LBM, thermoacoustics, combustion).

Numerics

2.1 Introduction

The CFD Team develops multiple CFD softwares where the quality of the numerical methods is critical to address all the multi-physics problems encountered in complex industrial geometries but also in academic configurations. The diversity of CFD solvers used by the Team (elsA-ONERA, AVBP, ProLB, JAGUAR) requires to use different numerical formulations: finite volumes, finite elements, Lattice Boltzmann Method and discontinuous spectral methods. This section presents some of the work done on these numerical methods. In addition to this purely numerical work, enhancing the use of high-fidelity CFD in an industrial environment requires to work on all parts of the CFD workflow. For this reason, CERFACS has developed tools to control errors (Uncertainty Quantification), to couple several solvers and to post-process the data generated by these simulations.

2.2 Numerical Treatment

This subsection describes the classical CFD solvers used at CERFACS (finite elements and finite volumes). First of all, research on adaptive mesh refinement and efficient boundary conditions are carried out to reduce both the simulations pre-processing and CPU time. Moreover, with respect to realistic flow configurations, turbulence injection methods and wall modelling are also studied. Finally research on numerical spatial and temporal scheme is a permanent research activity.

2.2.1 Adaptive Mesh Refinement

To reduce the computational cost and improve the accuracy of the turbulent flows predictions, mesh refinement algorithms for Large-Eddy Simulations have been studied since 2016. Up to now, the work has focused on the compressible LES code (AVBP) and the tetrahedral fully automatic MMG3D library of INRIA [4] where metrics-based sensors are used to produce the desired local mesh refinement to match the flows physics. The research leading to these results comes from an ERC advanced grant of CERFACS (numerics) and IMFT (experiment) [CFD69], and has received funding from the European Research Council under the European Union Seventh Framework Program (FP/2007-2013) / ERC Grant Agreement ERC-AdG 319067-INTECOCIS (http://intecocis.inp-toulouse.fr).

2.2.2 Generalization of the Navier-Stokes Characteristics Boundary Conditions

The choice of boundary conditions for compressible flows, reactive or not, is crucial to increase accuracy but also to save CPU time. Current research focuses on new boundary conditions for subsonic compressible flows. The method uses characteristic analysis based on wave decomposition and describes how to specify the amplitude of incoming waves to inject simultaneously three-dimensional turbulence and one-dimensional acoustic waves while still being non-reflecting for outgoing acoustic waves. Analysis and tests show that these new boundary conditions perform much better than standard NSCBC approaches and allow to use very large values of relaxation coefficient and to obtain non drifting mean values and non reflective capacities simultaneously.

2.2.3 Turbulence Injection

Turbulence injection is essential for many applications (in turbomachinery or aeroacoustics). Two main strategies are used at CERFACS: injecting synthetic turbulence (originating from analytical approximation of homogeneous isotropic turbulence), or generating inflow turbulence using a recycling method (from a precursor simulation for example). In the past years, deep learning has generated significant interest and hype thanks to the revolution it brought to the field of artificial intelligence. In 2018, V. Xing [CFD166] investigated deep learning models that can learn efficient representations of the physics of turbulent flows for turbulence generation. A pre-existing HIT DNS [9] was compressed and decompressed using a neural network, and successfully injected in a bi-periodic channel to mimic spatially evolving turbulence. The result demonstrates the potential of learning methods to accurately reproduce turbulent flow physics.

2.2.4 Shock-Capturing Schemes

Following the work initiated during the Marie-Curie European project Aerotranet-2, research to develop new shock capturing schemes adapted to aeracoustics problems has continued by testing a new adaptive nonlinear filtering technique to capture sharp discontinuities in the ***elsA*** solver of ONERA. First, the discontinuity is detected using a shock sensor [1]. Then, a reconstruction algorithm based on irregularity measurement is used to provide the required dissipation. The procedure to measure irregularity is based on the WENO regularity measurement parameter used in the fifth-order WENO scheme [8]. This methodology was successfully applied first on a single supersonic jet in order to identify the temporal and spatial signature of broadband shock-associated noise [CFD94] and finally to predict the noise radiated in an airplane cabin by a realistic under-expanded dual-stream jet.

2.2.5 Implicit Time Integration

In an industrial environment, it may be useful to perform LES far from the wall and RANS near the wall to account easily for turbulence effects, while keeping an acceptable mesh size. Standard time integration schemes for LES and RANS equations do not follow the same constraints. For LES, an explicit time integration is generally chosen in order to obtain good spectral properties (dissipation and dispersion) whereas in RANS, it is of paramount importance to reach steady state as fast as possible, using an implicit time integration procedure. In this context, a time integrator (AION) that allows spatial coupling of explicit and implicit time integrators was designed. Two standard time integration schemes (Heun [6] and second-order implicit Runge-Kutta scheme [3]) were hybridized / blended using a transition function ω, while keeping the standard expected properties (spectral behaviour). This new hybrid temporal scheme was shown to be numerically stable, having a better quality than the standard basic schemes and reducing the CPU cost. Figures 2.1 shows the results obtained from 1D shock tube simulation. This hybrid adaptive time-step procedure was also applied successfully on DES of an axisymmetric backward facing step.

2.3 Spectral Difference Method

The next generation of CFD solvers will have to perform high-fidelity simulations (Large Eddy Simulation in most cases) in complex geometries. This requires accurate and fast simulations on unstructured grids. One promising way to acquire this feature is to use spectral discontinuous methods. Cerfacs is working on one of them called Spectral Difference (SD) in a solver named JAGUAR. Navier-Stokes equations are solved in their strong form as it is done for the finite difference method hence the name of the approach. The principle of SD is to represent the solution inside each mesh cell with a high-order polynomial. The solution is not continuous between two cells but this discontinuity is taken into account through the use of a Riemann solver. Thus, this approach is locally continuous (inside a cell) and globally discontinuous

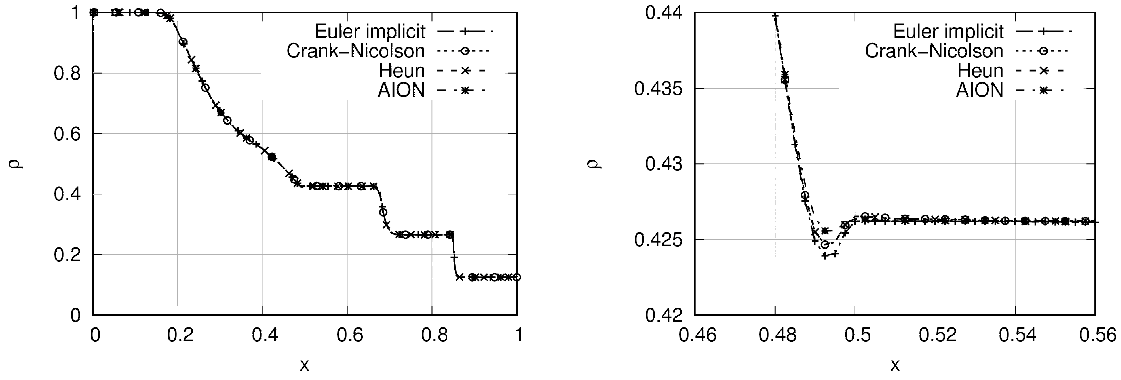

(a) Global view of the density profile at $t = 2s$.

(b) Close-up view near the rarefaction wave.

Figure 2.1: 1D shock tube.

(from cell to cell). The stencil is very limited and thus the SD are very efficient in a parallel framework. The development of JAGUAR has been initiated during the Safran CN2020 program in 2013. JAGUAR is a high-order (the maximum achievable accuracy is ten) DNS/LES solver. A good scaling (up to 95%) was measured for computations up to 131 072 cores. Moreover, the spectral behavior of the Spectral Difference approach was investigated theoretically, showing that the SD are as accurate as the most accurate method traditionally used in aeroacoustic (sixth-order compact scheme of Lele or the DRP scheme of Bogey and Bailly [CFD104]). But the Spectral Difference method enables the treatment of complex geometry by the means of unstructured grids, which is a strong point of this approach. Since 2017, through the European project TILDA, Cerfacs has developed the capability to use a different polynomial order in each mesh cell: p refinement [CFD111, CFD112]. Moreover, based on spectral analysis [CFD104], a new explicit time integration scheme increasing the stability range by 60% was developed [CFD55]. During the TILDA project, a jet noise simulation has been performed and compared with the high-order elsA-Onera software. The JAGUAR results were in perfect agreement but ten times faster. In 2017, F. Hermet [CFD145] continued the work of V. Joncquieres on the extension of the method to combustion. The use of SD for combustion is becoming important and a strong collaboration has started with Onera on this topic. Since 2018, it has been decided that JAGUAR would become a joint solver between Cerfacs and ONERA.

2.4 Lattice-Boltzmann Methods

Due to its low dissipative nature, modest CPU cost and fast mesh generation, the Lattice Boltzmann Method (LBM) is an attractive alternative to standard Navier-Stokes solvers for the simulation of isothermal and weakly-compressible flows around very complex geometries. However standard LBM (isothermal and weakly-compressible) is known to have limitations: the extension of the standard model to highly compressible flows presents accuracy and stability problems. Similarly, the use of mesh refinement levels results in spurious acoustic waves that spoil aeroacoustic simulations. Cerfacs is working with its partners to remove these limitations.

2.4.1 Compressible extension

Due to their lack of symmetry, standard lattices do not allow to recover the full set of Navier Stokes equations. Instead a "Navier Stokes like" set of equations is computed with an error proportional to M_a^3 in the viscous stress tensor and no notions of fluid temperature leading to barotropic equation of state

$p = p(\rho)$. These errors are directly linked with the velocity lattice (D1Q3, D2Q9, D3Q19/27) which do not contain enough discrete velocities to compute the third and fourth order moments of the equilibrium distribution function f_i^{eq}. It worth noting that the space and time discretization are not responsible of these defects which restrain the validity range to isothermal and weakly compressible cases.
A natural remedy is to increase the number of velocities (multi-speed) (D1Q5/Q7, D2Q37/Q49, D3Q103/Q343) following the thesis of C. Coreixas [CFD171] which allows to recover the fully compressible Navier Stokes Fourier equations. However, major problems arise such as the loss of locality of the algorithm (velocities are on multi-layers) or the increasing number of operations both leading to a higher CPU cost which becomes unaffordable for industrial computations. Above all, through several test cases and linear stability analysis [17], it turns out that increasing the number of velocities increases the number of possible modal interactions which are the cause of instabilities. Although the development of a new collision model based on recursive regularization by C. Coreixas [CFD67] has increased the stability range of this model, it still is restricted to flows with Mach number lower than $M_a < 0.5$ or, with the use of a Jameson sensor, 1D shock waves.
Finally, studies have been oriented toward the Hybrid LBM (HLBM) where a regular velocity lattice is employed solving the density ρ and the momentum ρu while an energy equation is computed using finite difference schemes. To ensure the coupling between the two systems, the equilibrium distribution function is developed in terms of temperature leading to the perfect gas equation of states (EOS) and an appropriated recursive regularized collision operator is employed ensuring the numerical stability [7]. The Mach error terms present in the viscous stress tensor are computed using finite differences and replaced directly in the momentum equation to restore the Galilean invariance of the LBM scheme. Using a total variation diminishing scheme for the energy equation and a Jameson shock sensor, this model is robust enough to handle shocks, as seen on 2.2(b), and is able to capture the correct velocity sound speed $c = \sqrt{\gamma r T}$ induced by the perfect gas thermodynamic closure, shown on 2.2(a).

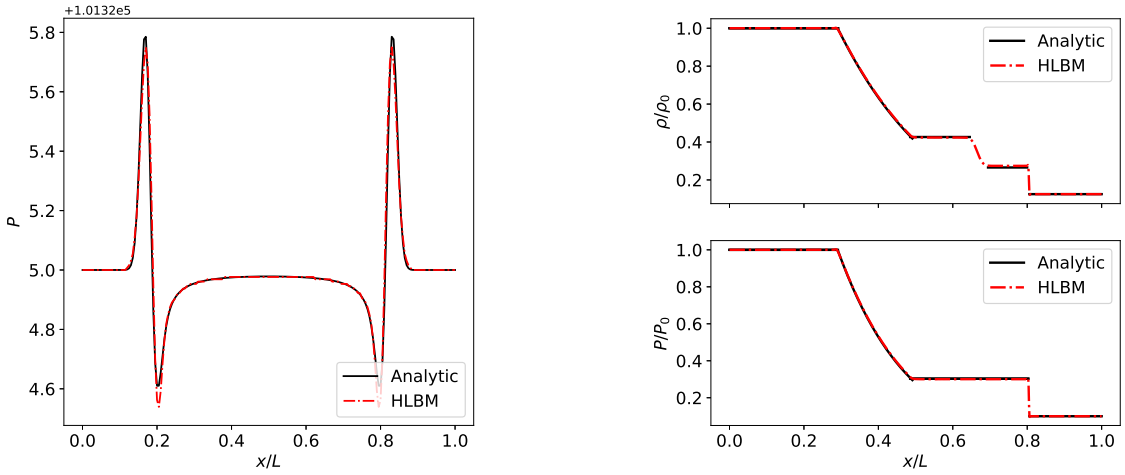

(a) Acoustic pulse for $\gamma = 1.4$ and a fluid temperature of $T_{fluid} = 300K$

(b) Sod shock tube solution for $\gamma = 1.4$

Figure 2.2: Compressible test cases using HLBM on D2Q9 lattice.

2.4.2 Grid Refinement

The Lattice Boltzmann Method (LBM) has proven to be very efficient for low Mach number applications. Furthermore, the low dissipation properties of the method make it powerful for aero-acoustic simulations.

In such simulations, the spurious noise emitted by numerical artefacts at boundary conditions or at grid refinement is of major importance. In LBM, during the propagation step, probability distribution functions (PDF) are missing and have to be reconstructed at the interface. Many algorithms exist in the literature, but in commercial solvers, the two most famous are based on works from Chen et *al.* [2] for a cell-based formulation and from Dupuis et *al.* [5] for a node-based one.

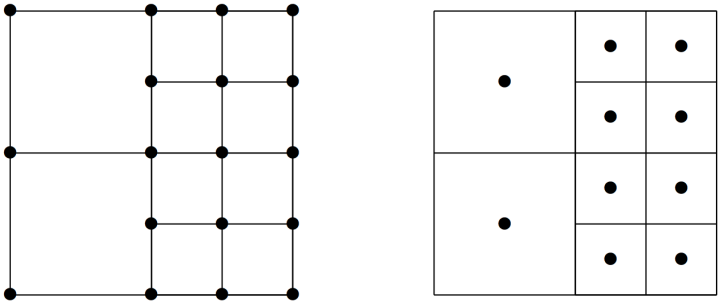

Figure 2.3: Node-based formulation (left-hand side) and cell-based formulation (right-hand side).

These two algorithms suffer from the same spurious artefacts in the presence of shear flows. This is inherent to the LBM and does not exist in the Navier-Stokes framework. Linear stability analysis allows to understand what is happening at a grid interface and more precisely, the exchange of energy between modes which are at the core of the spurious emission. The main difference between the Navier-Stokes framework where only four physical waves exist in 2D (one shear, two acoustics and one entropic) is the presence of non-hydrodynamic modes which can interact and exchange energy with the physical ones. It is possible to act on these non-physical waves by modifying the collision operator or by adding filtering techniques. This was done successfully at Cerfacs in 2018 as shown in Figure 2.4 for a vortex crossing an interface from a fine grid (left) to a coarse one (right).

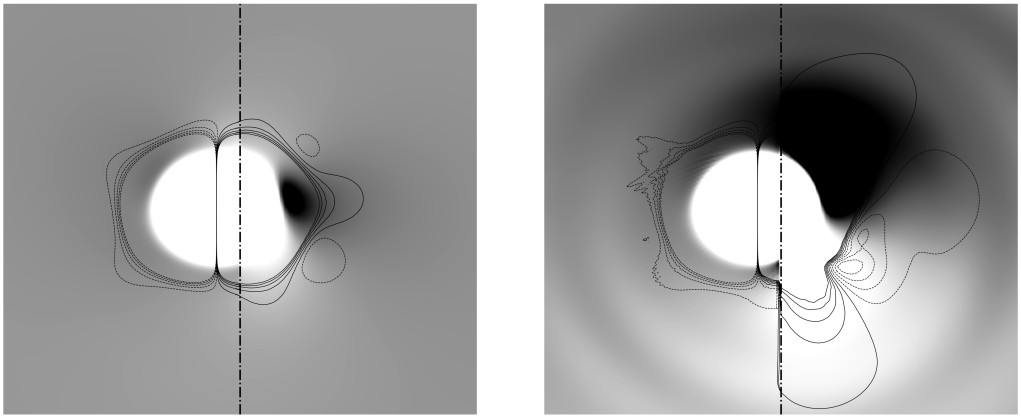

Figure 2.4: Convected vortex crossing a grid refinement interface. Pressure field (color field) and Isocontour of Uy (isolevels). Left: improved formulation. Right: initial formulation.

2.4.3 Stability analysis

The standard LBM is known to suffer from instability issues when increasing the Reynolds and/or the Mach number of the fluid flow. This difficulty is illustrated on Fig. 2.5 where a vortex is convected at $\mathrm{Ma} = 0.3$ with the standard BGK-LBM on the D2Q9 lattice. Before reaching one rotation, high frequency instabilities arise and are responsible for a divergence of the computation.
To understand these instabilities, a generic stability analysis tool called ALIEN (Analysing the spectraL propertIes of the latticE boltzmanN method) has been developed. Its principle is based on the von Neumann framework proposed by Sterling and Chen [12]: the LBM is linearized about a mean steady flow where perturbations are sought in the form of monochromatic plane waves. The linear problem can then be written as an eigenvalue problem of size Q, where Q is the number of velocities of the lattice. Seeking the Q eigenvalues provides Q complex pulsations associated to the linear modes. A spectral map of the maximal amplification rate can be plotted (Fig. 2.5-b) to predict the instabilities observed on Fig. 2.5-a.
Further investigations on the linear modes help explaining the reasons of the instabilities [17]. Numerical errors in the time and space discretization of the collision operator give birth to modal interactions between physical and numerical waves, which are responsible for the strong instability.

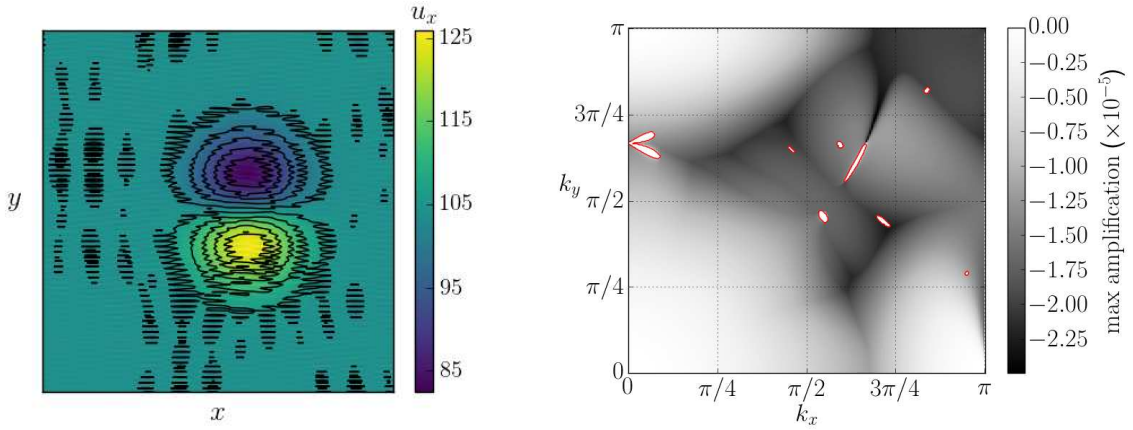

(a) Instability illustration for a Vortex convected at $\mathrm{Ma} = 0.3$.

(b) Maximal amplification rate of the modes observed in the standard D2Q9 BGK-LBM model.

Figure 2.5: Stability analysis for the standard D2Q9 BGK-LBM model.

2.5 Uncertainty Quantification and Sensitivity Analysis Applied to Large Eddy Simulations

2.5.1 Development of a Python Library dedicated to Uncertainty Quantification

UQ work actually started in 2007 at CERFACS under the name JPOD (Jack Proper Orthogonal Decomposition) within the framework of two European projects: SimSAC and ALEF (FP7). The objective was initially to build Surrogate Models in the context of flow simulations. During 5 years, a Python library has been successfully developed, tested and validated on industrial configurations. Then, JPOD has been dormant until 2016 when Uncertainty Quantification capabilities (based on Surrogate Models) were added with the help of EDF, leading to the new name: BATMAN (standing for Bayesian Analysis Tool for Modeling and uncertAinty quaNtification). On November 2017, it was decided to release this library

on GitLab as open-source under the CECILL-B free software license agreement [CFD98]. BATMAN has been used in various collaborative projects involving: Stanford University, Monash University, CSIRO and the BCAM. It allows to build Surrogate Models and to perform Statistical Analysis (Sensitivity Analysis, Uncertainty Propagation, Design of Experiments, Moments..) based on non-intrusive ensemble experiments using any computer solver [CFD99]. It relies principally on two open source packages dedicated to statistics: OpenTURNS (EDF) and scikit-learn.

The main features of BATMAN are:

- Design of Experiment (LHS, low discrepancy sequences, MC..),
- Resampling of the parameter space based on the physic,
- Surrogate Models (Gaussian process, Polynomial Chaos, RBF, scikit-learn's regressors),
- Robust optimization (Expected Improvement),
- Sensitivity Analysis and Uncertainty Propagation,
- Visualization in n-dimensions (HDR, 3d-Kiviat, PDF),
- POD for database optimization or data reduction.

To finish, BATMAN handles automatically the workflow of code computations. It makes the most of HPC resources by managing asynchronous parallel tasks. The internal parallelism of each task does not conflict with the parallel environment of BATMAN.

2.5.2 Geometrical Optimization of a Helically Roughened Heat Exchanger

The objective of this work is to optimize the internal shape of a single-started helically ribbed heat exchanger (see Figure 2.6-a) in order to maximize heat transfer to the wall while keeping pressure losses to reasonable values. LES with AVBP is used for the simulation of the steady state of the flow in a wall-resolved periodic configuration, and a wall heat flux is uniformly imposed on the wall surface. The wall roughness on the inner surface of the heat exchanger consists in a rounded rib. The rib has a rounded shape (Fig. 2.6-b), with a floor width w equal to 3.28 times the rib height e ($w = 3.28 \times e$). The rib cross-section is then fully characterized only by its height e. In addition to e, an important geometrical parameter for the rib shape is the rib pitch p. Both e and p are uncertain geometrical parameters for the optimization process.

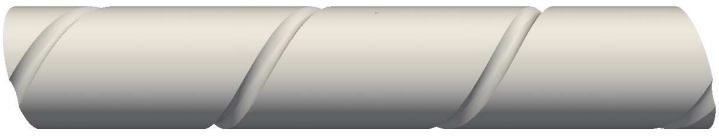

(a) Three pitches are represented.

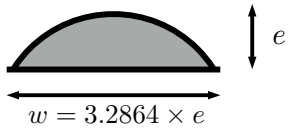

(b) Illustration of the rounded rib cross-section.

Figure 2.6: Geometry of an helical ribbed tube reactor.

Multiple discontinuities of uncertain size are also introduced as input parameters, allowing a wide variety of inner wall roughness. Size and positions of the rib discontinuities are fully characterized by the number

of discontinuities per rib pitch N_D and the length of the discontinuity relative to the length of the remaining rib, called the emptiness ratio E_r. So, N_D and E_r are also uncertain geometrical parameters to optimize, making the total number of input geometrical parameters to optimize equal to 4. Using the cost function proposed by Webb and Eckert, the optimization procedure is based on a surrogate model constructed from *Gaussian Process Regression* and a limited number of numerical simulations is performed (see Figure 2.7 as an example) thanks to an adaptive resampling done with the *Efficient Global Optimization* (EGO) method (BATMAN, see previous section). Results show that a swirling motion in the near wall region significantly decreases the heat transfer efficiency : the optimal roughness shape (see Figure 2.8) includes large and multiple discontinuities which prevent the swirling motion to develop.

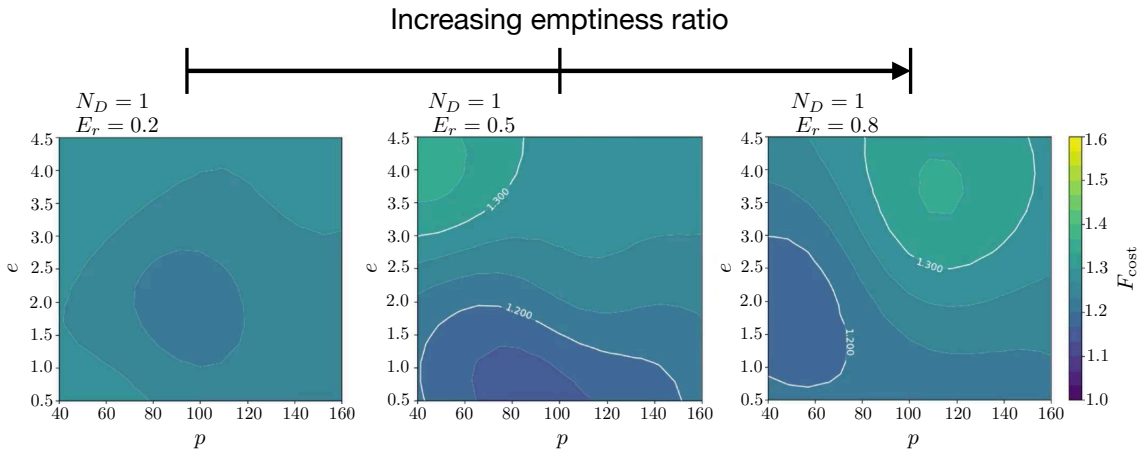

Figure 2.7: Examples of response surfaces for a rib with 1 discontinuity per pitch ($N_D = 1$). $E_r = 0.2$ (left), $E_r = 0.5$ (middle), $E_r = 0.8$ (right).

Figure 2.8: Optimal predicted ribbed tube geometry for heat exchanger applications. Three pitches are represented. (a) Cut in the normal plane showing the inner surface and (b) view of the wall surface from the outside of the tube.

2.5.3 UQ-Driven Robust Design - Assessment of a Swirler Geometry

The heart of a turbomachine is the combustion chamber, fed with fuel by injectors. In order to stabilize the flame, swirled injectors are commonly used today. By impelling a movement of rotation to the flow, a recirculation zone is created directly at the outlet of the injector and ensures sufficient residence time for the fuel to be consumed. The design of swirled injectors is of prime importance when seeking to reduce fuel consumption and pollutant emissions. From expert knowledge, the design of a swirler proceeds

in three steps: (*i*) an exploratory phase is first performed using Reynolds-averaged Navier-Stokes (RANS) computations; (*ii*) the resulting possible geometries installed in the combustion chamber are simulated using LES [CFD69] of turbulent combustion; (*iii*) prototypes are manufactured and tests are performed. For the last step, Additive Manufacturing (AM) is now in use. AM has gained attention as it does not impose any constraint from the design point of view without sacrificing mechanical properties. However, AM induces uncertainties regarding the structural composition of the produced metallic systems, making this an active topic of research. In particular, geometrical uncertainties may result from the deposition method, the scanning method or even the powder size. Especially, some discrepancies in the size of the channels have been experimentally observed. This may leave defects which sizes would depend on the quality of the whole process.

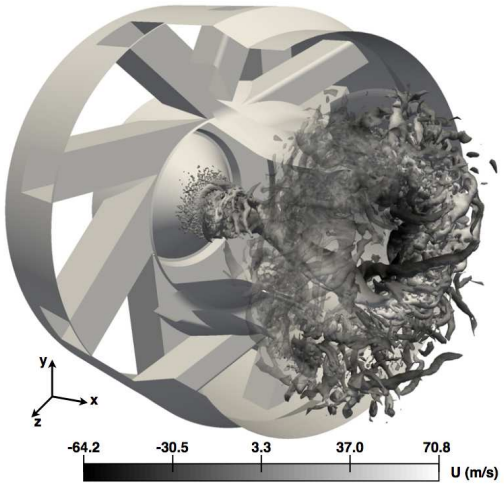

Figure 2.9: LES with AVBP solver of a swirler with 16 channels - Q-criterion colored by axial velocity.

To quantify the impact of AM on the fluid flow, an Uncertainty Quantification study based on LES (BATMAN coupled with AVBP solver) is realized with varying geometries concerning the channels. In our case, the uncertain parameters are the dimensions of 16 channels (see Figure 2.9) which are not totally independent. In fact, AM is a layer-by-layer process which precision relies on the ability of the machine to build up and polish these layers and luckily, it can lead to a correlated set of parameters. Using this correlation, it is then possible to drastically reduce the parameter space dimensions to 6 random variables using the Highest Density Region (HDR) method. From the Principal Component Analysis (PCA), a set of 30 points was sampled from the low discrepancy sequence of Sobol. Results indicate that the response of the system to these geometrical modifications is rather uniform: the geometrical uncertainties are transmitted through the system without amplification. The UQ method used in this work with BATMAN, combining data reduction and high-fidelity LES with AVBP, paves the way for systematic uncertainty studies in the design phase of industrial systems to take into account manufacturing defects. This may lead to the determination of optimized manufacturing tolerances, and finally to significant cost saving.

2.6 Coupling

The optimization of future aeronautical engines will be based on highly detailed CFD simulations for compressor, combustion chamber and turbine. This requires coupling these simulations, something which is almost impossible on existing machines today: running simultaneous LES codes for compressor, combustor and turbine on a parallel architecture up to 500 000 cores is the ultimate challenge of 2020 for HPC in

laboratories but also for industry where such coupled simulations will provide keys to produce competitive engines. To optimize engines, the precise operational margin of each element must be known and this is impossible if all elements are not coupled. For example the temperature of the first stages of the turbine depends directly on the unsteady hot flow of burnt gases leaving the combustor. Predicting the lifetime of the turbine within 50 % accuracy requires to predict the temperature of the blades within a range of the order of 25 K. This is impossible if the inlet temperatures for the turbine computation are not obtained by a simultaneous coupled computation of the combustor and the turbine. Even though the ultimate objective is to compute the full turbine, several validation steps are essential such as:

- accurate predictions of flow fields and wall heat transfer,
- coupling strategies for conjugate heat transfer and for multi-components simulations,
- validation of LES methodologies for turbomachinery stage simulations including near-wall turbulence models for flow and heat transfer,
- post-processing of complex turbulent flows in turbomachinery to extract relevant physical informations from the huge amount of data produced by LES.

Among these issues, two main actions were studied during the period 2017/2018: (1) multi-component Large Eddy Simulations of gas turbine and (2) interaction simulations between engines and plane.

2.6.1 Multi-component Large Eddy Simulations of gas turbine

Computing the interaction between components of a gas turbine requires a solver able to simulate each component. To do so, the AVBP solver dedicated to the simulation of combustion chambers has been extended to simulate rotor/stator configurations since 2011 via the overset gird MISCOG approach [16]. In 2017/2018, a high-order interpolation method has been introduced and validated in MISCOG. This interpolation relies on 1-D Hermite interpolators and has been implemented for various types of 2-D and 3-D elements. It provides third-order accuracy even in the most detrimental case: non-matching cells at the interface, coarsened cells in all directions and moving interface. Then LES of integrated combustion chamber and turbine have been proved to be feasible on both academic configurations [CFD73] and industrial ones. These simulations have shown the importance of inlet conditions for the aerothermal behavior of turbine stages. With this in mind, new inlet boundary conditions have been integrated in the AVBP solver. The following subsections provide more details about these 3 axes: (1) high order interpolation, (2) inlet conditions for turbine computation and (3) new inlet boundary conditions implementation in AVBP.

Third-order interpolation to treat rotor/stator interface

Prior to the application of the proposed solution to rotor/stator problems, many validation cases have been conducted focusing on acoustic wave propagation, convection of inviscid and viscous vortices and rotating boundaries. These test cases were performed by post-doctoral fellows (Gaofeng Wang and Jérôme de Laborderie) funded by RTRA in Toulouse and a national program supported by Safran called CN2020[1]. They have lead to two publications in Journal of Computational Physics [16, CFD70]. The primary objectives were to qualify and quantify errors introduced by the coupling approach with respect to known solutions or solutions obtained with a unique computational domain. The main outputs of these various tests are the following:

[1] In the CN2020 program, AVBP was compared to many other high-order codes (including spectral differences and Discontinuous Galerkin methods) and confirmed the high performances obtained with AVBP and MISCOG.

- Accurate transfer of flow variables across the interfaces is essential to limit dissipative and dispersive errors on the vortical, acoustic and entropic waves typically found in LES. That is the reason why a third-order interpolation method has been introduced in TurboAVBP. This interpolation relies on 1D Hermite interpolators and has been implemented for various types of 2D and 3D elements. The high-order interpolation keeps the global accuracy of the AVBP schemes, even in the most detrimental case: non-matching cells at the interface, coarsened cells in all directions and moving interface.
- The computations of wave propagation through moving overlapping regions raise interesting fundamental questions similar to the treatment of boundary conditions studied by Vichnevetsky and Bowles [15] or Sengupta [11]. Analytical studies and tests performed with MISCOG showed that three types of spurious waves can be generated at the interface, representing a numerical discontinuity for the flow. They consist of physical waves, *i.e.* acoustic waves, numerical waves, *i.e.* Nyquist frequency waves, and waves only present with a moving interface since they are caused by the temporally evolving spatial interpolation error. The high-order interpolation has been shown to drastically reduce these waves respectively to the second-order accurate interpolation method available in OpenPALM.
- When viscous flows are simulated, the study of velocity derivatives through the interface has shown that a high-order interpolation is required to properly transfer diffusive fluxes, whatever the convective scheme. Indeed a second-order interpolation method systematically yields discontinuities of velocity derivatives at the interface.
- The overset grid method is known to be not globally conservative by nature. This represents a limitation for its application to turbomachinery flows, for which mass flow conservation is expected. To guarantee minimal losses on conservation, homogeneous sizes of donor and receptor cells are recommended to be used along with third-order interpolation. For all cases (including real compressor and turbine cases), the relative difference in mass flow observed in TurboAVBP is negligible (less than 0.01%).

Integrated combustion chamber and turbine LES

A Large Eddy Simulation of an integrated combustion chamber simulator and its turbine stage (European project FACTOR) was performed as reference to investigate the sensitivity of inlet conditions on aerodynamic and thermal fields of the turbine stage (Fig. 2.10) [CFD73]. Comparisons between the integrated computation (case A) and the simulation of a stage alone (case B) without turbulence injection provide similarities as well as important differences. Both simulations give similar predictions in the global aerodynamics of both stator vanes and rotor passages in terms of flow expansion and secondary flows. The main differences are due to the unsteady flow features such as deterministic eddies and turbulence coming from the chamber that is not injected in the isolated stage simulation. They concern first the turbulent activities mainly in the stator. The aerodynamic fluctuations in the rotor passages are mainly driven by secondary flows and few differences are observed. On the other hand, important differences are seen in the range of temperatures in both stator vanes and rotor passages: with turbulent fluctuations at the inlet of the turbine stage, case A shows more mixing and thus less segregation of temperature. Contrarily, since the inlet condition is steady in case B, more coherent patterns are predicted with higher range of temperatures (both lower and higher).
Comparisons with experimental data on the FACTOR turbine are ongoing [14]. Moreover, the definition of inlet boundary conditions for standalone turbine stage simulations, based on the analysis of the combustion chamber / turbine flow field interface has been investigated and is presented in the following section.

Realistic inlet conditions for turbine stage computations

In 2018, a methodology to implement non-reflecting boundary conditions for turbomachinery applications, based on characteristic analysis was proposed and the paper describing this extension of NSCBC is in

press [10]. For these simulations, inlet conditions usually correspond to imposed total pressure, total temperature, flow angles and species composition. While directly imposing these quantities on the inlet boundary condition works correctly for steady RANS simulations, this approach is not adapted for compressible unsteady Large Eddy Simulations because it is fully reflecting in terms of acoustics. Deriving non-reflecting conditions in this situation requires to construct characteristic relations for the incoming wave amplitudes. These relations must impose total pressure, total temperature, flow angle and species composition, and simultaneously identify acoustic waves reaching the inlet to let them propagate without reflection. This treatment must also be compatible with the injection of turbulence at the inlet. The proposed approach shows how characteristic equations can be derived to satisfy all these criteria. It has been tested on several cases, ranging from a simple inviscid 2D duct to a rotor/stator stage with turbulence injection.
Then, the definition of inlet boundary conditions for standalone high fidelity turbine stage simulations is crucial to obtain meaningful LES predictions and 1D time averaged profiles are most likely inappropriate. The integrated simulation of a combustion chamber and its high pressure turbine presented in the previous section serves as a reference for standalone stator vane simulations performed afterwards using inlet boundary conditions retrieved from the integrated simulation [CFD54]. Using instantaneous flow fields from the reference simulation allows to a large extent to recover the correct flow field, which is a huge improvement over simulations using usual 2D constant boundary conditions, with or without injection of synthetic turbulence. Differences between the fully integrated simulation and that using constant boundary conditions are principally due to the lack of mixing and strong persistent vortex structures in the standalone high pressure turbine simulation using usual constant boundary conditions. Changes of secondary flow patterns also impact the temperature distribution on the nozzle guide vane walls.

2.6.2 elsA coupling

Due to Intellectual Property Rights (IPR) issues, airframe and engine Manufacturers do not want to share their geometries. However, in order to obtain the true performances of an aircraft, it is necessary to simulate the global model (aircraft with engines installed). Since September 2017, Cerfacs is involved in the development of a platform to perform high-fidelity coupled simulations distributed on remote machines. The coupling process is managed with the Cerfacs/Onera open source software OpenPalm. Simulations are performed with the Onera software elsA. The aim is to run the numerical simulation of the external flow on a supercomputer from Airbus and the simulation of the internal flow on supercomputers made available by Airbus partners. As a result, both geometrical configurations remain only known from their owners. Up to now, the platform has been tested on academic configurations on Cerfacs in-house supercomputers and on several Airbus supercomputers. Before testing the target configuration, physical results obtained with the semi-industrial configuration shown in Fig 2.11 are currently being analyzed.

2.7 CFD Data Processing

Cerfacs develops a generic data-processing library called Antares since 2012. The project is managed with the web application Redmine (issue tracking, documentation, etc.), the source code with Git, and the documentation and tutorials are disseminated thanks to a website (www.cerfacs.fr/antares) and face-to-face trainings. The library helps designers processing CFD data at large. It can be used all along the CFD process from the set up phase of a CFD computation (initialization) to the postprocessing of data generated during simulations. If the CFD steering process is managed by the python software, this library can also be used to co-process data (in situ) during massively parallel simulations to reduce the amount of generated data. This library provides a python application programming interface. The large choice of features available within the Python/NumPy framework enables to write complex data analysis procedures. Thus, CFD users can develop their own numerical tools on top of Antares data structures. Finally it is free for research purposes so that users have a clear view of the library contents, and can modify them if necessary. This

library is currently provided to many research labs and industries (www.cerfacs.fr/antares/partners.html). In particular, Safran Aircraft Engines has built its own data processing software based on the Antares library, which is in production mode since 2018. Similar in-house tools from Safran Helicopter Engines and Airbus are still in progress in methods and tools departments, and will soon be available to designers as well.

Developments

During the past two years, a close collaboration with Safran took place to help them using the library to develop their application scenarios. Many turbomachinery configurations were tested as axial compressor, centrifugal turbine, dual stream gas turbine, with various numerical treatments as surface cuts, isosurfaces, parametrisation of section, extraction of surfaces, thermodynamic averages, chorochronic reconstruction, etc. Some other generic features have been developed such as the management of boundary condition data and a generic computing system to compute physical quantities.

Examples of Application

Among all applications treated with Antares, the SCONE project (Clean sky program) is illustrated here with the simulation of a counter-rotating open rotor with a Large Eddy Simulation using a chorochronic approach to reduce CPU time.

References

[1] C. Bogey, N. de Cacqueray, and C. Bailly, (2009), A shock-capturing methodology based on adaptative spatial filtering for high-order non-linear computations, *J. Comput. Phys.*, **228**, 1447–1465.

[2] H. Chen, O. Filippova, J. Hoch, K. Molvig, R. Shock, C. Teixeira, and R. Zhang, (2006), Grid refinement in lattice Boltzmann methods based on volumetric formulation, *Physica A: Statistical Mechanics and its Applications*, **362**, 158–167.

[3] J. Crank and P. Nicolson, (1996), A practical method for numerical evaluation of solutions of partial differential equations of the heat conduction type, *Advances in Computational Mathematics*, **6**, 207–226.

[4] C. Dapogny, C. Dobrzynski, and P. Frey, (2014), Three-dimensional adaptive domain remeshing, implicit domain meshing, and applications to free and moving boundary problems, *J. Comp. Physics*, **262**, 358–378.

[5] A. Dupuis and B. Chopard, (2003), Theory and applications of an alternative lattice Boltzmann grid refinement algorithm., *Physical review. E, Statistical, nonlinear, and soft matter physics*, **67**, 066707.

[6] K. Heun, (1900), Neue Methoden zur approximativen Integration der Differentialgleichungen eincr unablaingigen Ver'anderliehen, *Zeitschrift für angewandte Mathematik und Physik*, **45**, 23–38.

[7] J. Jacob, O. Malaspinas, and P. Sagaut, (2018), A new hybrid recursive regularised Bhatnagar–Gross–Krook collision model for Lattice Boltzmann method-based large eddy simulation, *Journal of Turbulence*, 1–26.

[8] G. Jiang and C. Shu, (1996), Efficient implementation of Weighted ENO schemes, *J. Comp. Physics*, **126**, 202–228.

[9] Y. Li, E. Perlman, M. Wan, Y. Yang, C. Meneveau, R. Burns, S. Chen, A. Szalay, and G. Eyink, (2008), A public turbulence database cluster and applications to study lagrangian evolution of velocity increments in turbulence, *J. Turb.*, **9**, N31.

[10] N. Odier, M. Sanjose, L. Gicquel, T. Poinsot, S. Moreau, and F. Duchaine, (2018), A characteristic inlet boundary condition for compressible, turbulent, multispecies turbomachinery flows, *Computers and Fluids*, In press.

[11] T. K. Sengupta, (2004), *Fundamentals of Computational Fluid Dynamics*, Universities Press, Hyderabad (India).

[12] J. D. Sterling and S. Chen, (1996), Stability Analysis of Lattice Boltzmann Methods, *Journal of Computational Physics*, **123**, 196–206.

[13] M. Thomas, J. Dombard, F. Duchaine, L. Gicquel, and C. Koupper, (2018), Impact of realistic inlet condition on LES predictions of isolated high pressure vanes, In *12th International Symposium on Engineering Turbulence Modelling and Measurements (ETMM12)*, Montpellier, France.

[14] M. Thomas, J. Dombard, F. Duchaine, L. Gicquel, and C. Koupper, (2019), Large eddy simulation of combustor and complete single-stage high-pressure turbine of the factor test rig, In *ASME Turbo Expo 2019: Turbine Technical Conference and Exposition*, no. GT2019-91206, Phenix, USA.

[15] R. Vichnevetsky, (1982), Invariance theorems concerning reflection at numerical boundaries, Tech. Rep. 08544, Princeton University, Dept of Mech. and Aerospace Eng.

[16] G. Wang, F. Duchaine, D. Papadogiannis, I. Duran, S. Moreau, and L. Y. M. Gicquel, (2014), An overset grid method for large eddy simulation of turbomachinery stages, *Journal of Computational Physics*, **274**, 333–355.

[17] G. Wissocq, P. Sagaut, and J.-F. Boussuge, (2018), An extended spectral analysis of the lattice Boltzmann method: modal interactions and stability issues, *Journal of Computational Physics, under review*.

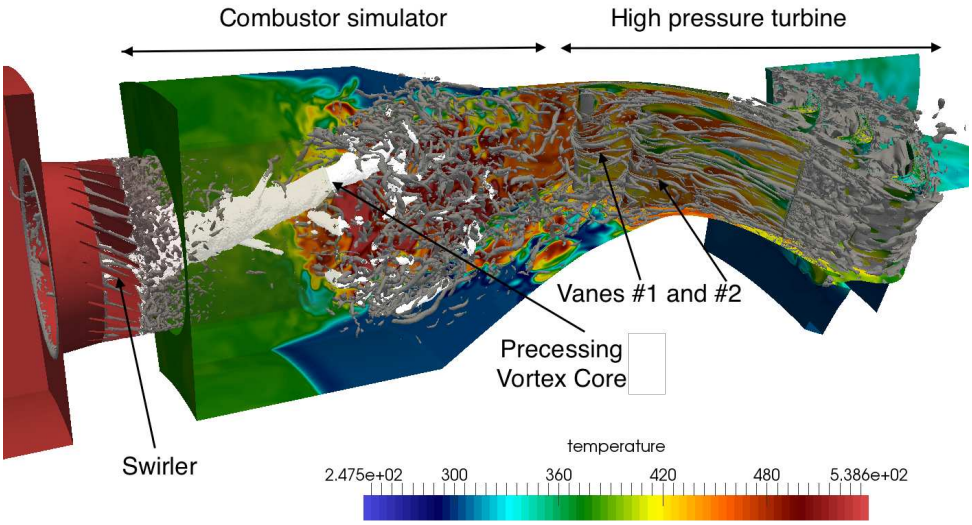

Figure 2.10: Instantaneous view of the turbulent activity in the integrated combustion chamber and turbine LES of the FACTOR configuration: precessing vortex core in white (iso-surface of low pressure), turbulent eddies in grey (iso-surface of Q-criterion) and temperature field on walls and periodicity.

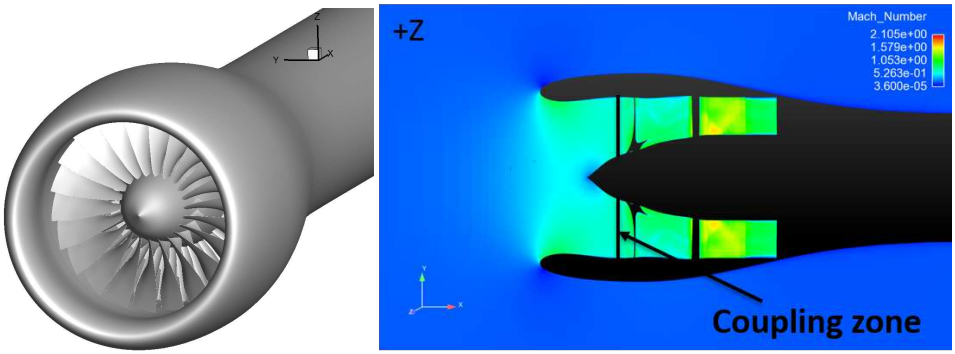

Figure 2.11: Fan-Nacelle configuration (left) and meridional view (right) of the configuration showing the location of the coupling interface between the two numerical simulations distributed on two different supercomputers.

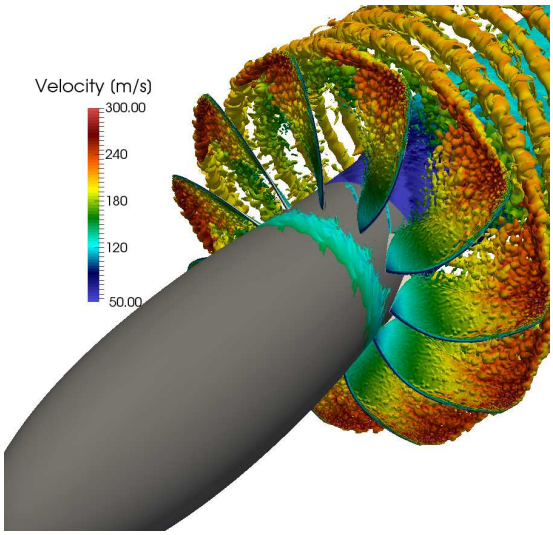

Figure 2.12: Isosurface of entropy colored by velocity magnitude. Numerical results from Cror LES simulation processed by with the Antares library.

Physical Models

3.1 Introduction

Phyiscal models are constantly improved in all codes of the CFD team and in 2017/2018, a specific effort was devoted to four main areas:

- Turbulent combustion and multiphase reacting flows
- Cold magnetized plasma
- Wall modelling
- Cooling (by effusion) of combustion chamber liner and high pressure turbine

These fields have very different levels of maturity in terms of understanding of the physics and their modelling. Turbulent combustion is now able to handle complex phenomena including accurate turbulence, chemistry and sprays. Plasma models are in the stage of validation of the fluid equations in generic configurations. Wall modeling and effusion cooling are recurrent, hard-to-solve problems for LES of aerospace flows.

3.2 Turbulent combustion

Today's challenge of turbulent combustion modelling and simulation is to provide reliable predictions of system operability and performance, in the context of low-emission burners and reduction of fossil fuel consumption. This requires an accurate description of fuel oxidation chemistry, including the formation of gaseous pollutant and soot. It allows also to investigate in more details ignition phenomena and the impact of liquid injection of fuel blends.

3.2.1 Combustion chemistry and pollutant emissions

The optimization of existing industrial systems and the design of new ones must comply with more and more stringent regulations on pollutant emissions and fuel consumption. To correctly predict them, both turbulent flow and combustion chemistry must be properly reproduced, as well as their strong interaction. Today, including an accurate but computationally affordable chemistry in 3D flow computations remains a challenge. Two methods have been used for long: tabulated methods which consist in using 1D laminar flame solutions and two chemical variables (progress variable and mixture fraction) on the one hand, and globally fitted chemical mechanisms that are based on 1 to 4 global reactions on the other hand. Although computationally cheap, none of them allows to accurately reproduce the detailed flame structure, the flow-combustion interactions in complex turbulent flames, and consequently the pollutant emissions. An alternative is to use Analytically Reduced Chemistry (ARC) [31, 27], a knowledge-based reduction approach, which accurately describes combustion phenomena by retaining the most important species and reactions, and remains computationally affordable due to the introduction of quasi steady state (QSS) species [24]. Combined to the Dynamic Thickened Flame (DTFLES) turbulent combustion model, benefits

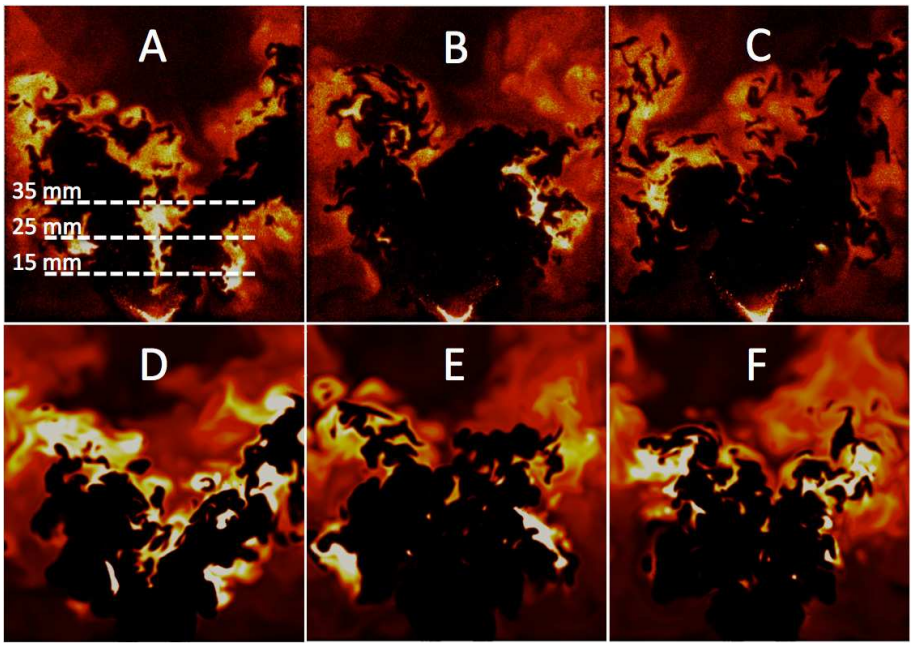

Figure 3.1: N-heptane/air spray flame in the KIAI-Spray configuration. Instantaneous fields of experimental OH-PLIF (A-B-C) and numerical fields of OH mass fraction (D-E-F). From [CFD65].

of ARC in terms of flame structure (velocity, temperature, combustion regimes, CO and OH species) have been shown in a variety of lab-scale configurations, from methane/air turbulent diffusion flames [CFD82] to ethylene/air turbulent swirled flames [CFD76] and n-heptane/air turbulent spray flames [CFD65] (Fig. 3.1).

For aeronautical engines, one key point is the modelling of commercial kerosenes which are typically composed of paraffins, naphthens and aromatics, with an average chemical formula which ranges from $C_{10.9}H_{20.9}$ to $C_{12}H_{23}$. They are generally represented by a surrogate fuel with a limited number of hydrocarbons, that are chosen to suitably reproduce their physical properties (surface tension, boiling temperature) and chemical properties (flame speed). Surrogates are typically composed of long hydrocarbon chains, from n-octane to n-hexadecane, along with cyclic hydrocarbons such as methylcyclohexane. If detailed chemical kinetic schemes for such surrogates are available [28, 33], the application of the ARC methodology to these complex fuels is very recent. One possibility is to use a single-component surrogate (typically n-decane or n-dodecane) [22]. A second one called HyChem has been very recently proposed by Pr H. Wang (Stanford University) and co-authors [32, 34]. HyChem relies on the assumption that any fuel, no matter how complex it is, is not directly oxidized but first decomposes into smaller molecules in a pyrolysis process. These pyrolysis products then start the oxidation process, and the associated radical buildup and heat release. This decomposition into a pyrolysis step and an oxidation process of smaller molecules directly reflects in the detailed kinetic models for real fuels which can thus be obtained by merging a pyrolysis mechanism and a detailed foundational oxidation kinetic mechanism for lighter hydrocarbons. In collaboration with Pr H. Wang, Felden *et al.* [CFD75] have for the first time been able to account for a multi-component surrogate in a LES of a kerosene-air combustor, showing the capacity of the HyChem approach coupled to ARC to accurately reproduce both the flame structure and the pollutant emissions such as CO and NOx by comparison with measurements (Fig. 3.2). This research work on kinetic models for complex multi-component fuels continues within the European projet JETSCREEN, started in

June 2017, which aims at evaluating the impact of biofuels (addition of alternative fuels to classical jet-A fuel) on the operability of an aeronautical combustor.

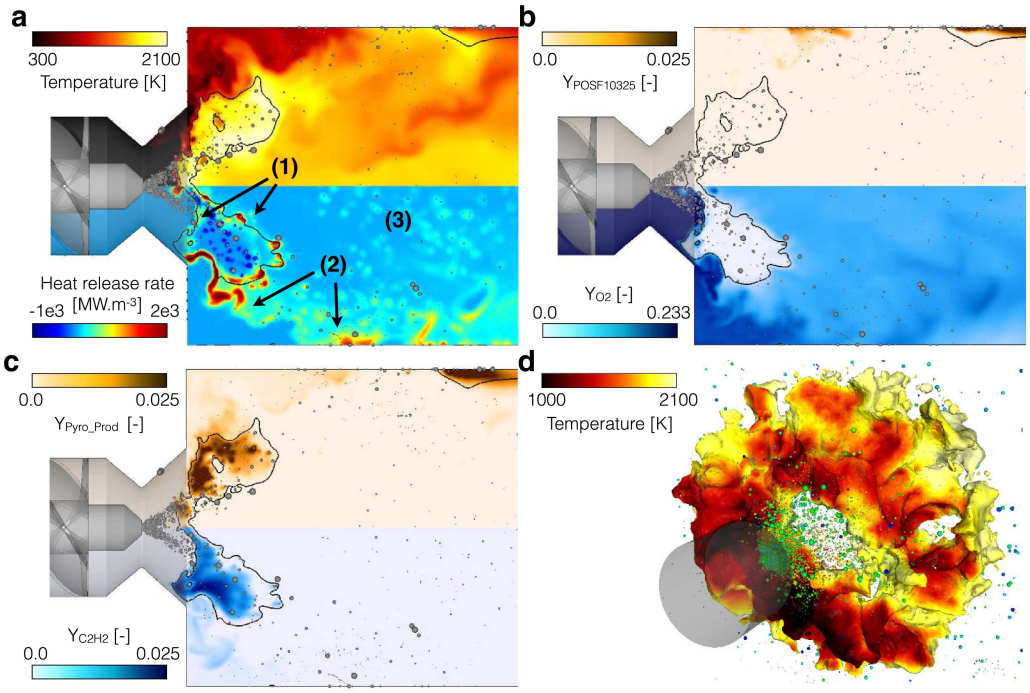

Figure 3.2: Instantaneous fields in a central z-normal cut plane of the LDI jetA/air combustor [CFD75]. (a) Temperature (top) and heat release rate (bottom), (b) fuel mass fraction (top) and $O2$ mass fraction (bottom), (c) pyrolysis products mass fraction (top) and $C2H2$ mass fractions (bottom) and (d) 3D-view of the rich torus using an iso-surface of mixture fraction $Z = 0.8$. The black iso-line indicates stoichiometry.

Thanks to the accurate prediction of soot precursors, ARC is also a promising method for soot prediction in industrial systems because it provides correct levels for soot precursors. Within the European project SOPRANO, the gaseous ARC chemistry was coupled to a semi-deterministic Lagrangian approach for the solid particles and a two-equation empirical soot model, and assessed against experiments in an experimental ethylene-air burner studied at DLR at 3 and 5 bars in the context of the International Sooting Flame (ISF) workshop (www.adelaide.edu.au/cet/isfworkshop/) [CFD77]. The research work on soot prediction will be continued within the ANR ASTORIA project, started in October 2018, which will allow a better description of heterogeneous chemistry at the particle surface by accounting for the soot aggregate morphology.

3.2.2 Ignition

Ignition is a critical phase for furnaces, torch flames or engines. The objective is to ensure fast and reliable ignition in all operating conditions of the system, at a minimum cost in terms of manufacturing and energy consumption. The challenge depends on the burner type and use: furnaces and large flames raise mostly safety questions, whereas the concern for aeronautical engines is more about altitude relight in non-favorable conditions and rocket engines require smooth ignitions with limited over-pressure.
Ignition is always triggered by an energy deposit, achieved via an igniter which can be either a spark plug, a Laser, a torch or more recently a plasma discharge system. The interaction of the igniter with the flow and

the details of the combustion onset are not yet fully understood and the subject of many research projects to develop more efficient igniting systems, such as for example Nanosecond Repetitively Pulsed (NRP) discharge or microwave-assisted ignition. After the first phase during which the igniter creates a small burning kernel, a critical phase starts where the kernel must grow and become a turbulent propagating flame that attaches to the injector. In aeronautical engines with multiple injectors a final phase is the light-round, where the flame propagates in the annular burner, igniting successively the injectors until full ignition. In turbulent burners, the flame kernel generated by the igniter may be subjected to strong shear and vorticity, which deform and split the kernel into small volumes until extinction. This makes ignition a stochastic phenomenon, linked to the local flow structure and turbulence, and is re-enforced in the case of non-premixed or spray burners by a fuel vapor heterogeneous field. All these aspects are studied in the team, namely from the spark and first kernel generation, to the flame development and full burner ignition. Some illustrations are given below.
Figure 3.3 shows the heat release generated by a plasma discharge in a pin-pin configuration (Fig. 3.3 left). Two simulations have been run, one with combustion chemistry only and one with combustion and plasma chemistry (Fig. 3.3 right). Results show that dissociations are important at the very early moments of ignition, but that recombinations occur too rapidly to significantly impact flame ignition [CFD66].

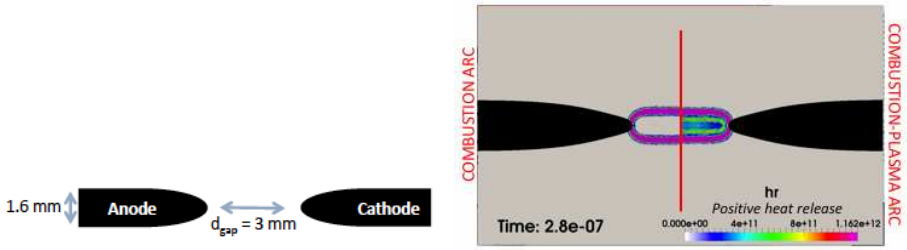

Figure 3.3: Positive heat release in a pin-pin plasma discharge in a propane-air mixture.

Following the work of Esclapez [20], ignition has been studied in the case of liquid fuel injection in a single burner configuration (KIAI [25] and in a full multi-injector annular burner (MICCA-spray [23]. The driving mechanisms for ignition failure or success have been identified, and found to be mainly the local mixture flammability and turbulence which can destroy the flame kernel if sufficiently intense [CFD65]. Figure 3.4 shows a flame kernel developing in a turbulent spray, colored by the gaseous equivalence ratio (left) and the hear release (right): it is clear how the presence of droplets in zone C induces a sufficiently high equivalence ratio and heat release to sustain combustion, whereas the absence of droplets in zones A and B prevents the flame to propagate in these regions. Light-round ignition was found very similar to the purely gaseous case, with a predominant role of hot gas expansion in flame propagation. Figure 3.5 illustrates the very good agreement between the obtained propagating flame and the observed experimental flame.

3.2.3 Spray combustion

Current industrial issues related to engine efficiency, reliability and pollutant emissions require an accurate prediction tool to deal with complex multi-physics interactions ranging from gas-liquid interface and liquid atomization to spray combustion including droplet evaporation. The numerical resolution of these different phenomena is out of reach in non-academic configurations and requires accurate modeling.

3.2.3.1 Liquid-gas interface and atomization

The current methodology to simulate atomizers, named FIM-UR, is to inject a parameterized spray with droplet size distribution obtained from correlations [29, 30]. This technique has been successfully applied

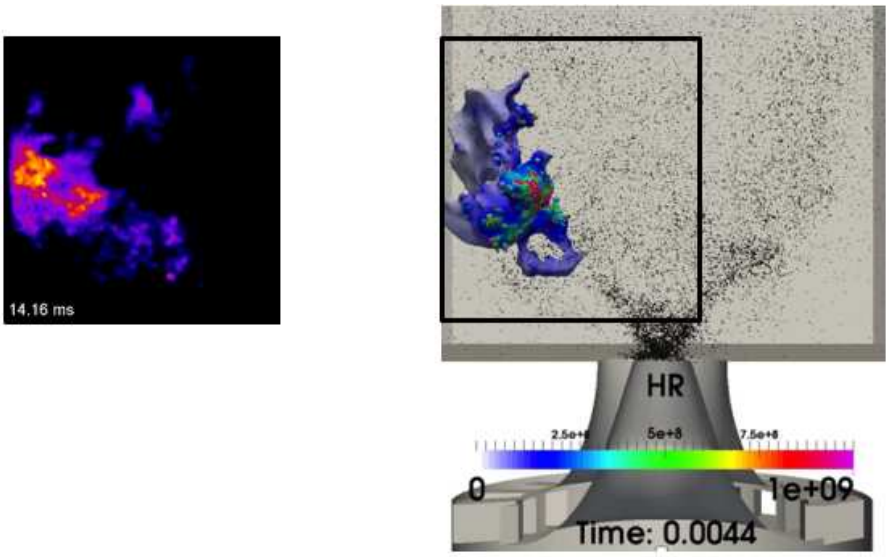

Figure 3.4: Ignition of n-heptane liquid swirl injector. Left: experimental image [25]. Right: LES result.

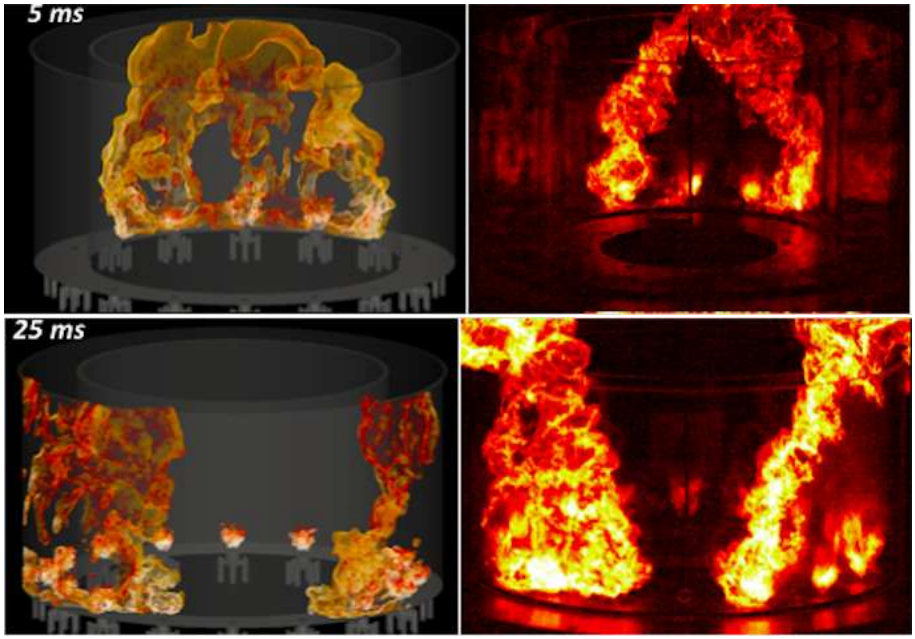

Figure 3.5: Ignition of a full annular burner with heptane liquid swirl injectors at two instants. For each instant, left: simulation and right: experiment [23].

to pressure swirl atomizers in various combustion chambers. However, it is not sufficient for airblast atomizers where the initial spray impacts a wall to create a thin film which eventually atomizes downstream the prefilmer lip. Phenomenological models were proposed in [18] and [21] to describe the spray/wall interaction and to evaluate the particle size distribution downstream the prefilmer. They chose a Lagrangian formulation at it gives naturally access to the polydisperse behavior of the spray. To continue and improve these models, two PhD theses have started in 2018. The film model has already been improved by solving the momentum equation instead of assuming equilibrium between shear and gradient forces at the liquid/gas interface. This allowed to reproduce an impinging spray on a flat plate and the generated secondary spray. A good agreement with measurements was obtained for both the film formation and the secondary spray penetration as shown in Fig 3.6. The whole methodology including the FIM-UR initial spray, spray/wall

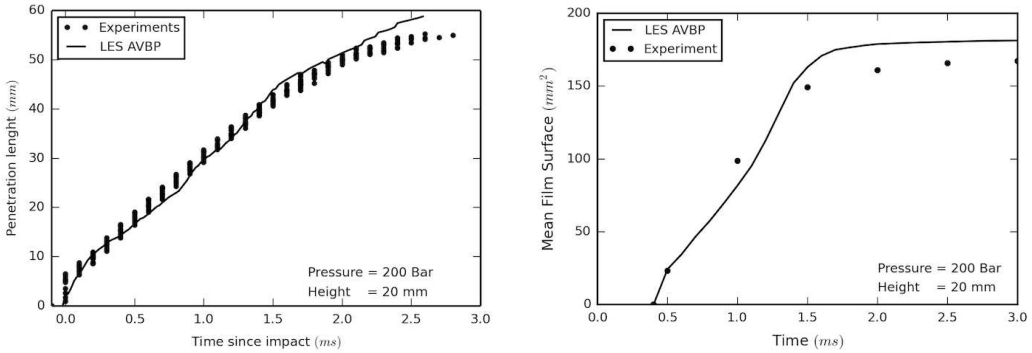

Figure 3.6: Comparison of the secondary spray penetration length (left) and liquid film surface (right) between experiment and simulation of an impacting spray.

interaction and film atomization, named PAMELA, was applied to an aeronautical airblast injector. Results are shown in Fig 3.7. The comparison of the particle size distribution between simulation and experiment

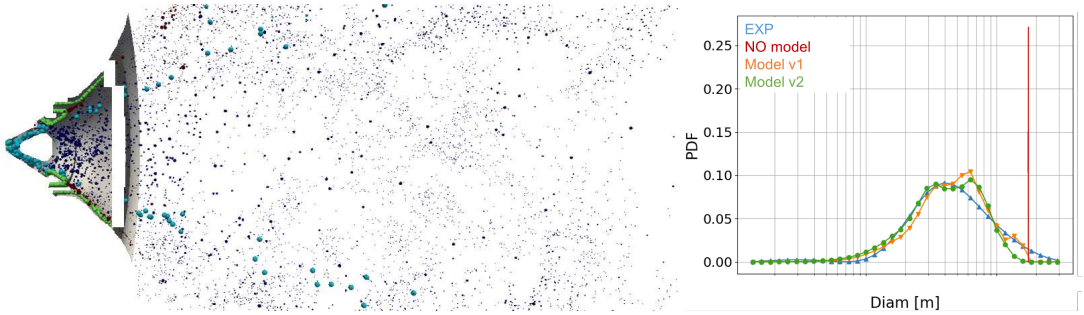

Figure 3.7: Simulation of an airblast injector: view of the Lagrangian phase (left) and PDF of particle sizes downstream the injector (right), compared with experiment. The vertical line corresponds to the "No model" approach.

in a transverse plane located 2 cm downstream the injector in Fig. 3.7 (left) shows the good results obtained in this configuration. Further work is however still required to make the PAMELA model more generic.
A drawback of the phenomenological models FIM-UR and PAMELA is that they are insensitive to what happens in the combustion chamber, in particular pressure fluctuations which may modify the spray and

consequently alter the response of the burner to hydrodynamic or thermo-acoustic instabilities. With the objective of describing these phenomena, various methodologies aiming to predict atomization and the liquid/gas interface are currently evaluated in collaboration with the EM2C laboratory (CentraleSupelec). Based on the work of [26] the interface is artificially thickened and solved on the computational grid. One issue is to include advanced thermodynamics for two-phase flows and liquid-gas equilibrium in the AVBP solver, and is the topic of current work in the team.

3.2.3.2 Two-phase combustion

Large Eddy Simulation of turbulent combustion may be combined with either an Eulerian or a Lagrangian description of the liquid fuel, taking into account dispersion and evaporation of the droplets, which have a significant impact on the combustion. The approaches and models used to model both phenomena have been recently extensively studied and validated in the CFD team, allowing to focus on understanding and modelling turbulent spray flames.

Compared to gaseous flames, spray flame structures have been shown to vary significantly depending on the gas and spray characteristics (initial droplet diameter, overall equivalence ratio, liquid loading and relative velocity between gaseous and liquid phases). Figure 3.8 shows the impact of the relative velocity between air and droplets on the evaporation and reaction rates in 1D laminar n-heptane/air heterogeneous flames. Spray flames can be either similar to gaseous flames or be mainly controlled by evaporation, leading to very different flame thicknesses. Furthermore, the laminar speed of a 1D spray flame varies and depends on the two-phase flow characteristics. An analytical expression for laminar spray flame speed was proposed by [CFD97] for the various spray flame structures that have been identified. On top of allowing a better understanding of spray flame phenomena, such analysis and results are critical for the extension of the thickened flame model to turbulent spray flames.

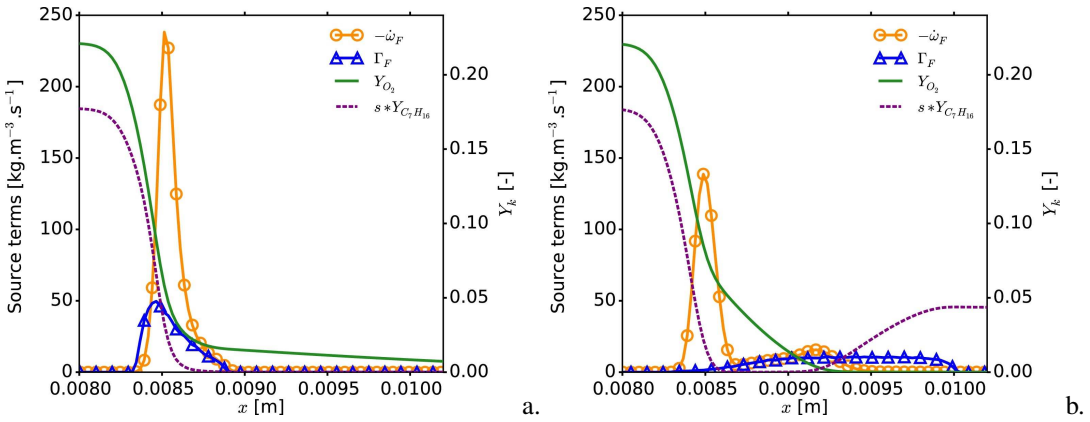

Figure 3.8: Impact of relative velocity on source terms and mass fraction profiles in a 1D n-heptane/air flame. a. U_gas/U_liq=1 ; b. U_gas/U_liq=30.

A second important step was to validate the numerical approach and the various physical models in turbulent spray flames. This was achieved with the KIAI-Spray configuration, two-phase version of the lab-scale KIAI configuration experimentally studied by [19] at CORIA, that was computed with a resolved flame approach [CFD101, CFD184]. A detailed comparison between measurements and LES results for both the gas and the liquid phases highlighted the capacity of two-phase LES to accurately predict complex turbulent

spray flames. One critical aspect, very challenging to capture, is the lift-off height of the flame, which was well reproduced numerically (see Fig. 3.9).

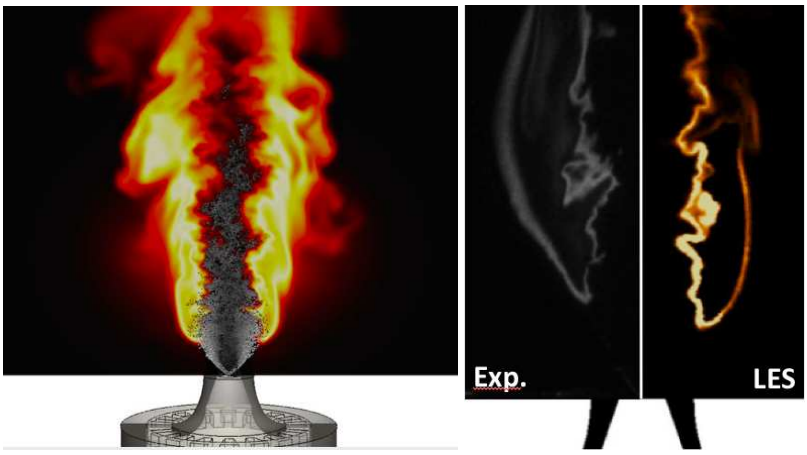

Figure 3.9: Two-phase flame in the KIAI burner [19]. Left : visualization of the flame obtained with AVBP; Right: comparison of the OH-PLIF image with the numerical heat release [CFD101, CFD184].

3.3 Plasma propulsion

In an increasingly competitive satellite market, electric propulsion has recently regained attention. Indeed, electric propulsion can reach higher exhaust velocities compared to chemical systems and thus result in lower propellant mass requirements. Hall thrusters are very efficient and competitive electric propulsion devices are currently in use in a number of telecommunications and government spacecraft. The physics of Hall thrusters is very intricate and non-linear because of the complex electron transport across the magnetic field and its coupling with the electric field. Even though this type of thruster is known since the 1960s, complex physical phenomena such as erosion or electron anomalous transport are not yet fully understood and directly impact the thruster performance and lifetime. Today, the design and development of Hall thrusters is still semi empirical with long and expensive qualifications in vacuum test facilities: there is still no predictive numerical tool capable of simulating real thrusters and helping to design them. With the support of Safran, CERFACS is engaged since 2014 in the development of such a numerical tool. This tool, called AVIP, is a massively parallel and unstructured 3D solver for low pressure plasmas. Its objective is to understand the complex plasma processes occurring in electric thrusters, to improve the efficiency of existing systems and eventually to provide the foundation for breakthroughs in the design of new thrusters. AVIP proposes two opposite and complementary modeling approaches: the Lagrangian approach (Particle-In-Cell (PIC) simulations) and the Eulerian approach (fluid simulations). In PIC simulations, different kinds of particles or macroparticles (electrons, ions and neutrals) are individually tracked. They can interact with each other (collisions) and with the electromagnetic field that remains defined on a Eulerian mesh. In fluid simulations, the particles dynamics is described with macroscopic averaged variables. The set of equations to solve is very similar to the one solved in CFD for two-phase flows. PIC simulations are often considered as much more accurate than fluid simulations but are very expensive since they require tracking a very large number of particles (typically $10^9 - 10^{10}$).
The PIC solver of AVIP was initiated during the Post-Doc of F. Pechereau (funded by Safran, 2014-2017). Its development is currently continuing in W. Villafana PhD thesis started in March 2017 and funded by

Safran. It allows to perform reference simulations used to develop and test modeling options for the fluid solver. The development of the fluid solver in AVIP started in January 2016 with the PhD of V. Joncquières (funded by Safran). Both solvers rely heavily on the strong expertise of CERFACS acquired during the development of the LES solver AVBP. In particular, the massively parallel architecture of AVBP has been copied and many algorithms and numerical methods originally developed for two-phase flows have been directly used in AVIP. Many new developments have however been needed. From an algorithmic point of view, the main developments carried out since 2014 concerned the collision module (implementation of a Monte-Carlo method), the merging algorithms for limiting the number of computational particles and the Poisson solver used to compute the electric field. This last subject is the object of a fruitful collaboration with the HiePACS team of INRIA on the development of the MaPHys library (Massively Parallel Hybrid Solver for large linear systems) now available in the code. New numerical schemes (HLLC (Harten-Lax-van Leer-Contact) Riemann schemes) and boundary conditions have also been developed for the specific needs of the fluid plasma model. From a physical modeling point of view, the main scientific advances concern the development of a 10-moment fluid model [CFD31]. This approach is much more accurate than standard drift-diffusion models classically used to model low-pressure plasma. A major question remains, however, as to the ability of this fluid model to reproduce the plasma instabilities typically encountered in Hall thrusters (Fig. 3.10). On this subject, AVIP benefits from the internationally

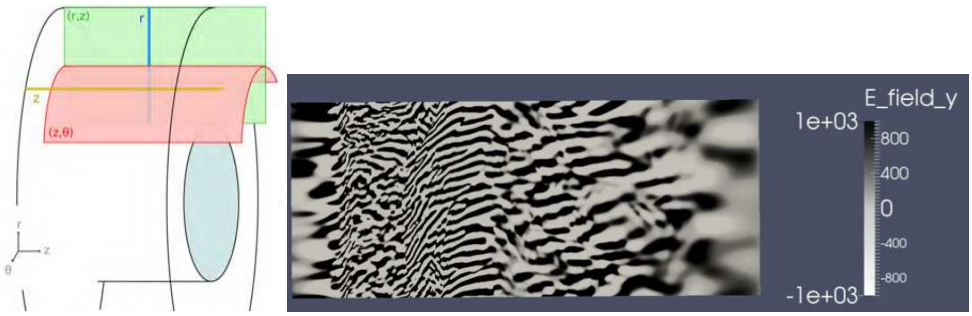

Figure 3.10: Azimuthal instability in a simplified 2D z-θ configuration.

recognized expertise of the Laboratoire de Physique des Plasmas (LPP Ecole Polytechnique), which collaborates closely to the project. CERFACS is also associated to LPP in the frame of the ANR "Chaire industrielle" POSEIDON, coordinated by A. Bourdon and partly funded by Safran.

Before going to realistic 3D thruster computations, both the fluid and PIC approaches have been thoroughly tested and validated on many test cases. CERFACS participates in different benchmarks within the framework of the RTRA project IMPULSE. This project involves physicists, engineers and applied mathematicians from several Toulouse laboratories (LAPLACE, IMT, ONERA, CNES), that work together to improve the models and methods used to describe the magnetized plasmas of electric thrusters. In parallel with these benchmarks, first 3D computations of an anode layer Hall thruster (a compact version of a real Hall thruster) have been recently performed thanks to a PRACE allocation of 18 million core-hours (Fig. 3.11). Although this new solver is dedicated to the simulation of plasma flows in Hall thrusters, this work may also be seen as a stepping stone for future other applications such as nanosecond pulsed discharges for plasma assisted combustion or flow control.

3.4 Wall Modelling

Accurate predictions of high Reynolds boundary layer flows are essential, especially in aeronautical applications. The boundary layer flow state directly impacts airfoil or turbomachinery's performance.

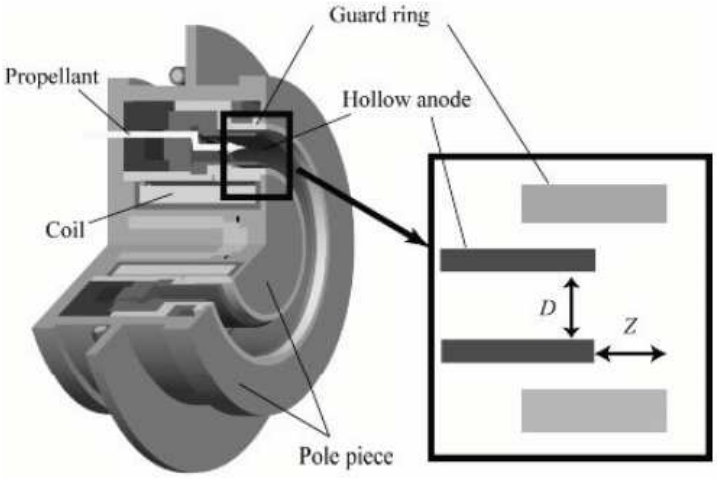

Figure 3.11: Cross-section view of an anode layer Hall thruster.

Boundary layers are controlled by many complex phenomena such as pressure gradients, compressibility effects and/or temperature gradients. By solving the large energetic scales of the flow and modeling only the small scales, LES can address this challenge. However, near-wall turbulence contains very small scales and it is well known that simulating them would require prohibitively fine meshes for high Reynolds number flows. This problem remains the main bottleneck for LES of high Reynolds wall-bounded flows.
Wall-Modeled LES (WMLES) is a way to tackle this limitation by solving only the outer layer of a boundary layer and modeling the inner layer's influence from a RANS perspective. However, WMLES does not yet have a sufficient level of maturity to be applied to industrial geometries. Standard wall models are either analytical or numerical. Analytical wall models are restricted to simple flows, while numerical wall models have a high computational cost and usually require a secondary grid, making them difficult to industrialize. To fill this gap and accurately predict the turbulent boundary layers flows in complex geometries, a hybrid wall model has been developed: the iWMLES (*integral WMLES*) [CFD64]. This model is based on the resolution of the integral boundary layer equations from parametrized velocity and temperature profiles, which allows it to be low in computing resources and easy to use. The ability of the iWMLES to take into account the effects characterizing the boundary layers present in aeronautical flows has been demonstrated first on academic flows and then applied successfully to an axial compressor stage, demonstrating its robustness.

3.5 Cooling of combustion chamber liner and high pressure turbine

One key element of reliable and efficient combustors is the engineer's capacity of anticipating the thermal environment of future engines. Indeed, current trends result in higher and higher end combustion temperatures with the absence of dilution systems to cool down the hot stream prior to its entree in the turbine stage or its impact on the combustor walls. The temperature reached being significantly increased, more sophisticated cooling strategies need to be introduced. This specific and new context is at the origin of actions at CERFACS through several PhD's.

On the combustor side, the introduction of multiperforated plates as effusion systems has been very early on addressed by S. Mendez [42] to ease LES of real designs. In this pioneering work, homogeneization

was a key assumption of the model introduced at the time. With the increase in computing power, current mesh resolutions allow for partial resolution of the effusion hole and improvement of the modeling could be expected as underlined by the work of R. Bizzari [CFD170, CFD59]. With this new model, the geometrical heterogeneity induced by the discrete spatial distribution of holes on the wall is retained and partly represented by the grid, missing information being modeled. The main outcome of this improved modeling is a clear improvement of the mixing process between the hot stream coming from the chamber and the cooler fluid coming from the effusion system [CFD60]. As a result, wall temperature estimates are more precise as evidenced in the comparison of measurements and predictions for a real engine in Fig. 3.12.

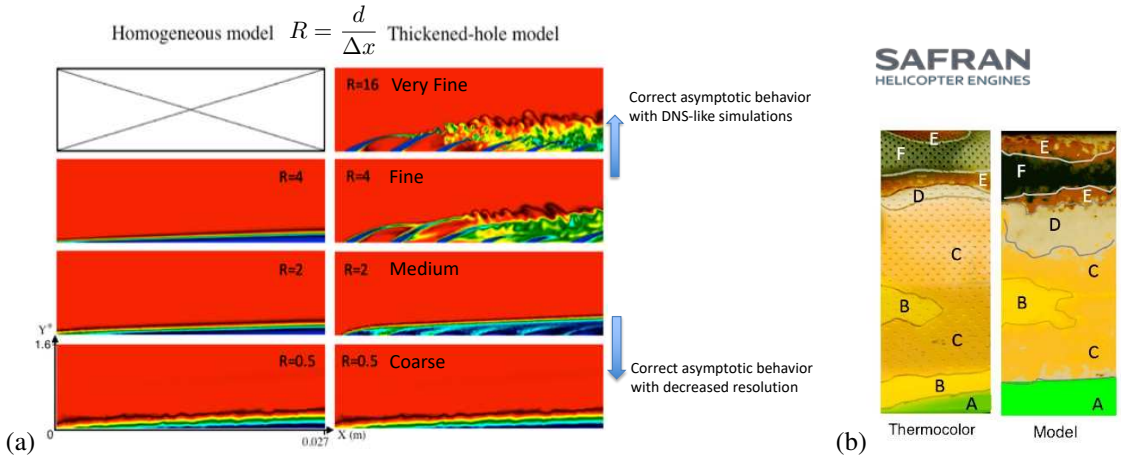

Figure 3.12: LES prediction of near wall flow with the new heterogeneous multiperforated model: (a) instantaneous view of the flow temperature field as a function of the modeling approach (homogeneous vs heterogeneous models) as well as grid resolution; (b) is a qualitative comparison of the combustor wall temperature issued by thermocolor and a LES simulation based on the heterogeneous model.

The aerothermal issue also appears in the turbine stages [CFD60], the first blade subject to the most extreme temperature spots being the Nozzle Guiding Vane (NGV) located directly after the combustor. In this case, the previously derived model can be also applied despite the changes of operating conditions of the effusive jet: the number of jets in this component is much smaller and their diameter is larger resulting in an operating condition different from the multiperforated plates present in the combustor. This last subject will be studied in the PhD thesis of A. Perrot (CIFRE SAFRAN SHE). Despite the difficulties, preliminary tests confirm the potential of the model as illustrated by M. Harnieh [CFD30] and in Fig. 3.13.

To finish on aerothermal flow predictions, the most critical part of next generation of engines will remain the first row of rotating blades which in addition to the aerothermal context, also need to sustain strong mechanical constraints induced by their high speed rotation. For this component, LES is used as a fundamental tool to understand of the sub-components present to cool these blades. Among others, internal cooling systems can be addressed by wall resolved LES to confront the thermal response of an impinging jet on a flat or curved plate as studied by P. Aillaud [CFD167, CFD57, 36] for example, Fig. 3.14(a)&(b). Likewise Trailing edge cooling can be analyzed with the same tool 3.14(c). Finally, internal cooling channel systems can be analyzed in the same fashion to understand the complex effects induced by the coupling of heat transfer and rotation. This direction of work has been specifically investigated by T. Grosnickel (CIFRE SAFRAN SHE) and is illustrated on Fig. 3.15.

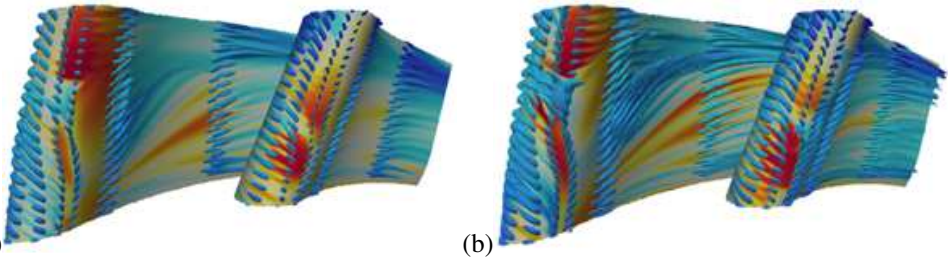

(a) (b)

Figure 3.13: Comparisons of the film cooling technology effect on the wall temperature of a NGV LES (a) obtained simulating and resolving the jet injection holes and (b) obtained using the heterogeneous model developed for combustor liners.

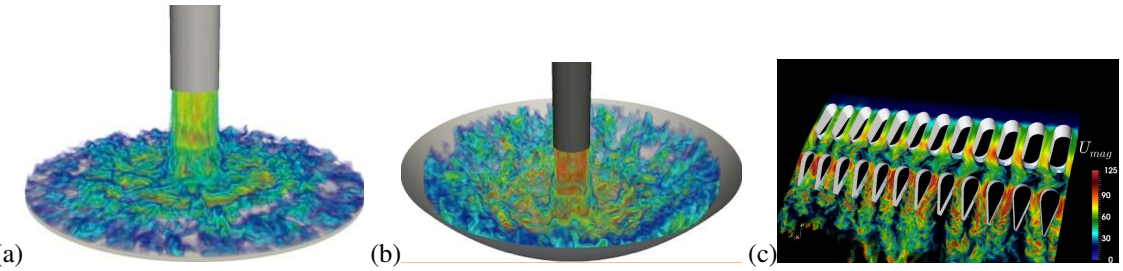

(a) (b) (c)

Figure 3.14: Wall resolved LES applied to (a) a jet impacting on a flat plate and (b) the same jet impacting on a curved plate accompanied by an instantaneous view of (c) the mixing induced in a trailing edge cooling slot.

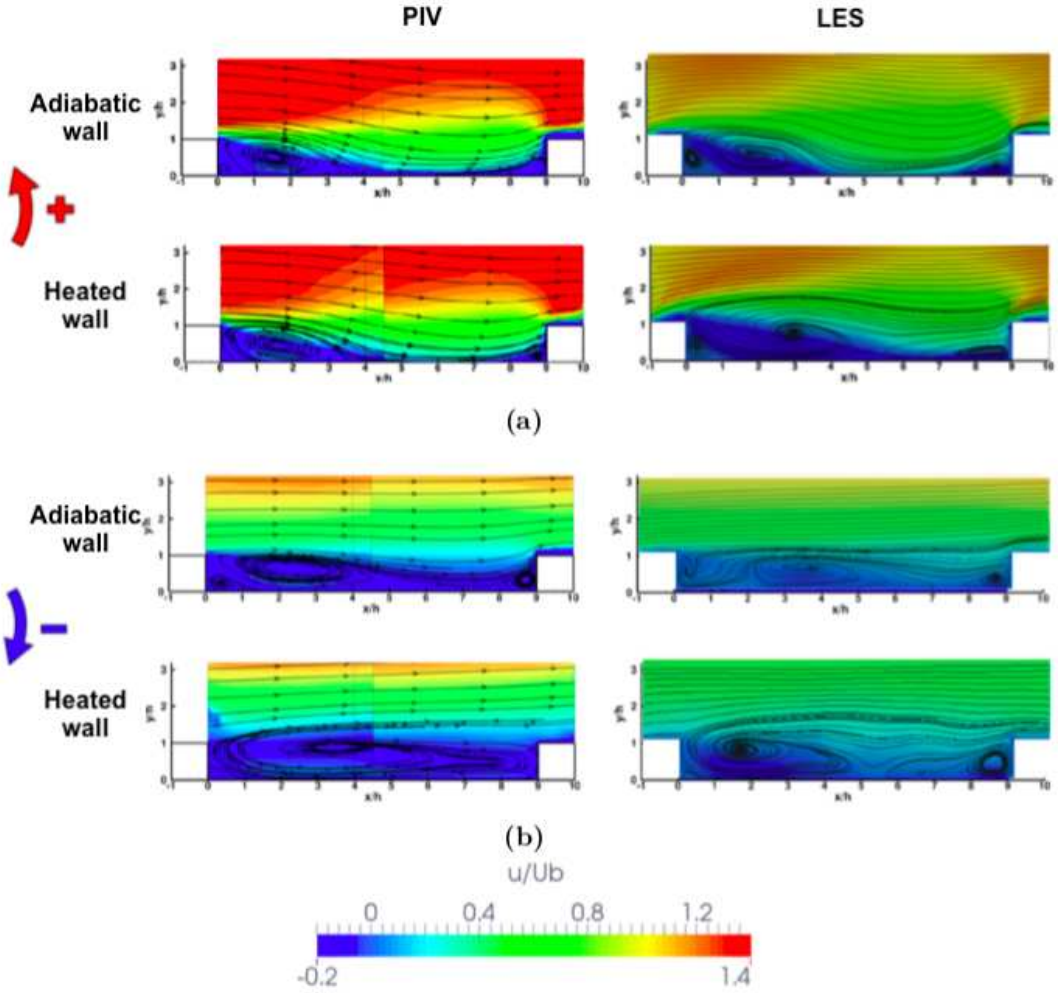

Figure 3.15: Flow prediction (axial velocity field) in a ribbed channel under (a) positive and (b) negative rotations with and without a heated wall. This configuration is typical of rotating cooling channels found in turbines for which experimental data was obtained by VKI.

References

[18] G. Chaussonnet, (2014), *Modeling of liquid film and breakup phenomena in large-eddy simulations of aeroengines fueled by airblast atomizers - th/cfd/14/15*, PhD thesis, Université de Toulouse - MeGeP - Dyphasique.

[19] M. Cordier, A. Vandel, G. Cabot, B. Renou, and A. Boukhalfa, (2013), Laser-induced spark ignition of premixed confined swirled flames, *Combustion Science and Technology*, **185**, 379–407.

[20] L. Esclapez, E. Riber, and B. Cuenot, (2015), Ignition probability of a partially premixed burner using LES, *Proceedings of the Combustion Institute*, **35**, 3133–3141.

[21] N. Iafrate, (2016), *Simulation aux grandes échelles diphasique dans les moteurs downsizes à allumage commandé*, phd thesis.

[22] T. Jaravel, (2016), *Prediction of pollutants in gas turbines using Large Eddy Simulation*, phd thesis, CERFACS.

[23] P. K., D. D., V. G., S. T., and C. S., (2018), Flame and Spray Dynamics During the Light-Round Process in an Annular System Equipped With Multiple Swirl Spray Injectors, In *ASME. Turbo Expo: Power for Land, Sea, and Air*.

[24] T. Lovas, P. Amnéus, F. Mauss, and E. Mastorakos, (2002), Comparison of automatic reduction procedures for ignition chemistry, *Proceedings of the Combustion Institute*, **29**, 1387–1393.

[25] J. Marrero Santiago, A. Verdier, G. Godard, A. Vandel, G. Cabot, M. Boukhalfa, and B. Renou, (2016), Experimental study of laser ignition probability, kernel propagation and air and fuel droplet properties in a confined swirled jet-spray burner, In *18th International Symposium on the Application of Laser and Imaging Techniques to Fluid Mechanics*, 84.

[26] J. Matheis and S. Hickel, (2018), Multi-component vapor-liquid equilibrium model for LES of high-pressure fuel injection and application to ECN SprayA, *International Journal of Multiphase Flow*, **99**, 294 – 311.

[27] P. Pepiot, (2008), *Automatic Strategies to Model Transportation Fuel Surrogates*, phd thesis, Stanford University.

[28] E. Ranzi, A. Frassoldati, R. Grana, A. Cuoci, T. Faravelli, A. Kelley, and C. Law, (2012), Hierarchical and comparative kinetic modeling of laminar flame speeds of hydrocarbon and oxygenated fuels, *Progress in Energy and Combustion Science*, **38**, 468–501.

[29] M. Sanjosé, J.-M. Senoner, F. Jaegle, B. Cuenot, S. Moreau, and T. Poinsot, (2011), Fuel injection model for Euler-Euler and Euler-Lagrange Large-Eddy Simulations of an evaporating spray inside an aeronautical combustor, *International Journal of Multiphase Flow*, **37**, 514 – 529.

[30] M. Sanjosé, (2009), *Evaluation de la méthode Euler-Euler pour la simulation aux grandes échelles des chambres à carburant liquide - th/cfd/09/108*, PhD thesis, Institut National Polytechnique de Toulouse.

[31] T. Turányi, K. Hughes, M. Pilling, and A. Tomlin, (2009), KINALC website, *http://respecth.hu/*.

[32] H. Wang, R. Xu, K. Wang, C. Bowman, R. Hanson, D. Davidson, K. Brezinsky, and F. Egolfopoulos, (2018), A physics-based approach to modeling real-fuel combustion chemistry - I. Evidence from experiments, and thermodynamic, chemical kinetic and statistical considerations, *Combustion and Flame*.

[33] H. Wang, X. You, A. V. Joshi, and S. G. Davis, (2007), USC Mech Version II. High-temperature combustion reaction model of H2/CO/C1-C4 Compounds.

[34] R. Xu, K. Wang, S. Banerjee, J. Shao, T. Parise, Y. Zhu, S. Wang, A. Movaghar, D. J. Lee, R. Zhao, X. Han, Y. Gao, T. Lu, K. Brezinsky, F. Egolfopoulos, D. Davidson, R. Hanson, C. Bowman, and H. Wang, (2018), A physics-based approach to modeling real-fuel combustion chemistry – II. Reaction kinetic models of jet and rocket fuels, *Combustion and Flame*.

Applications

4.1 Introduction

Applications of CERFACS tools to real combustors and more generally indutrial applications is a primary driver of CERFACS CFD activity and past successes. Thanks to the link with CERFACS' partners as well as to external collaborations, many applications of industrial interests have been dealt with in the 2017-2018 years. Among others, the following fields of applications are detailed in this document:

- Space related applications,
- Aeronautical engine issues and demonstrations,
- Turbomachinery,
- Safety,
- Chemical processes,
- Large-size systems,
- Aeroacoustics and combustion instabilities.

4.2 Space propulsion

Space propulsion is a subject of research for which most of the effort within the team has focused on liquid combustion and heat transfer complemented by investigations on flow stability.

4.2.1 Liquid rocket engines

Liquid rocket engines require complex cooling systems to endure the extremely high heat fluxes at the chamber walls. This issue is currently becoming even more critical in the context of low-cost engines and re-usability where an accurate prediction of wall heat flux is critical and has led to the derivation of a new formulation for the coupled dynamic / thermal wall law [40]. This wall law has been validated in two cases. The first case is the CONFORTH configuration, tested on the MASCOTTE test bench at ONERA [45] in rocket engine representative sub-critical conditions, i.e., with liquid oxygen. The second case is a gaseous methane / oxygen combustor studied at TU München [35]. In both cases, the heat flux was correctly predicted for the CONFORTH case (Fig. 4.1). In this particular configuration, it was shown that the liquid spray controls the flame length and therefore the wall heat flux [CFD182, CFD178].

The validated methodology to predict wall heat fluxes in liquid rocket engines was then applied to a ribbed configuration to test the efficiency of longitudinal ribs as heat flux enhancers to reduce the heat load [43].

To meet the new market low-cost requirements, hydrogen will be replaced by methane in the next generation of liquid rocket engines. This raises a number of questions regarding the flame structure and stability:

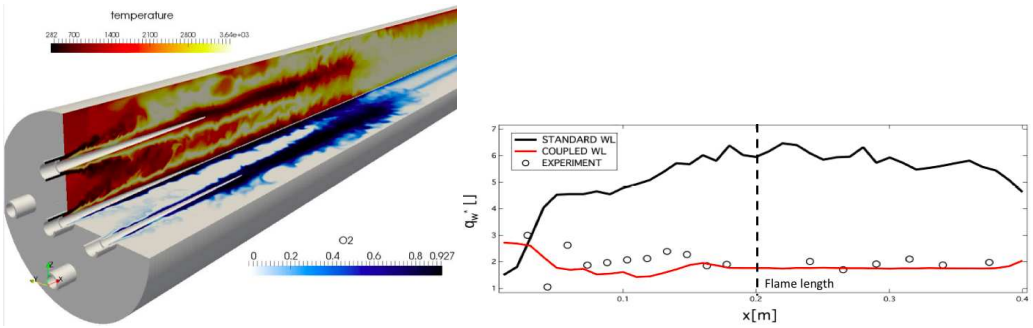

Figure 4.1: CONFORTH configuration (left) and comparison between the measured and computed wall heat flux (right)[CFD182].

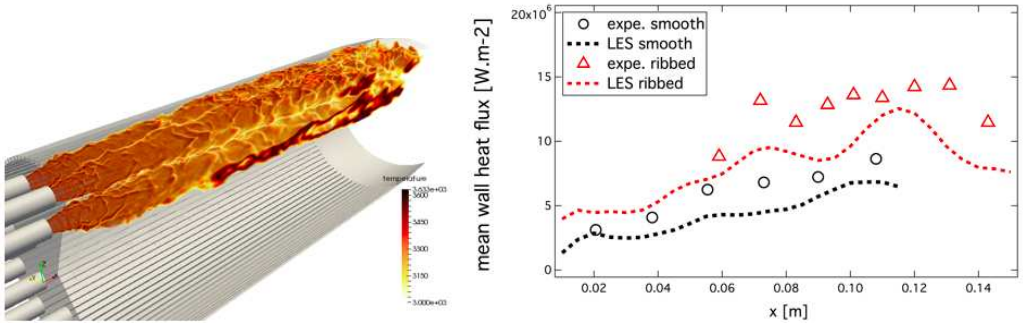

Figure 4.2: Prediction of wall heat flux in a ribbed configuration. Comparison with a smooth combustion chamber and validated vs experiments [CFD178].

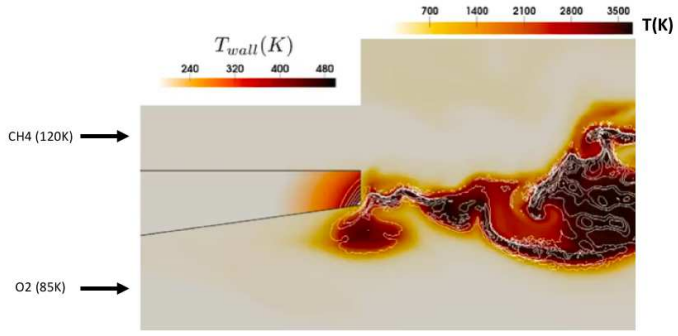

Figure 4.3: Coupled flow / heat conduction simulation of a doubly transcritical CH_4, LOX flame [CFD86].

methane properties lead to doubly transcritical injection in some operating conditions. in addition, the much slower chemistry may introduce a non-negligible chemical time in the flame response to hydrodynamics and acoustics. To answer these questions, the methane - oxygen flame structure and stabilization in doubly transcritical conditions was studied using AVBP with a real gas equation of state [CFD86]. The focus was on the injector lip, using Direct Numerical Simulation and coupled flow dynamics / solid heat conduction to understand the flame stabilization processes. Figure 4.3 shows an instantaneous view of the temperature field in both fluid and solid domains. Strong self-sustained oscillations of the flame root and of the temperature field were found, both being bimodal and oscillating at similar frequencies, evidencing a strong influence of heat transfer in the lip on the flame root stabilization.

4.2.2 Turbopumps

Turbo-pumps are also a crucial element of liquid propulsion and are investigated in the PhD of M. Queguineur (CIFRE from ARIANEGROUP and CNES). Indeed, flow stability must be ensured throughout this highly critical machine. Throughout the course of developments of this component, observations and experience have underlined the potential triggering of damaging oscillatory motions of the flow in the cavities located between the fixed and rotating parts of turbo-pumps. To avoid such fluctuations, leading to miss-tuned operating conditions, drastic loss of performance or life-span of the device, measures need to be taken. To investigate this specific problem, LES was originally applied to an enclosed rotor-stator (RS) configuration in the PhD work of T. Bridel-Bertomeu (CIFRE from ARIANEGROUP and CNES), leading to several interesting conclusions [CFD63, 39].

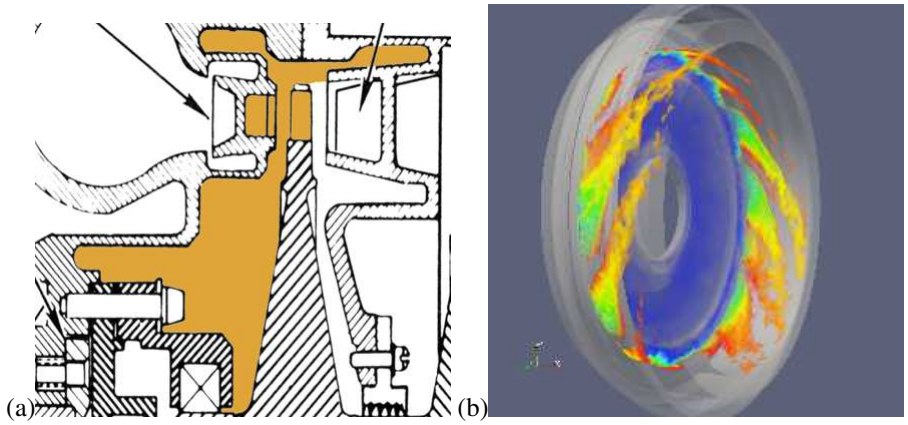
(a) (b)

Figure 4.4: Turbopump flow prediction: (a) view of a typical turbopump cavity to be addressed by LES and (b) corresponding instantaneous view of the flow organization as simulated by LES: volume rendering of the cavity local cold flow concentration.

Complemented by advanced post processing analyses like Dynamic Mode Decomposition (DMD) [37, CFD62], these preliminary works have allowed to identify the so-called pressure band which is found to originate from the flow cavity stability. Ongoing research on the subject with applications to real cavity configurations by M. Queguineur, Fig. 4.4 (a)& (b), confirms the simple geometry analyses and predictions for a real space engine turbo-pump turbine cavity, in spite of the complexity of the geometry and the much higher rotation Reynolds numbers.

Following these simulation results, theory and more specifically Linear Stability Analysis (LSA) was used to establish a predictive strategy for academic RS-cavity flows, given the underlying mean flow field. The AVLP code (local $1D$ parallel flow stability solver) and more recently the GIFIE code ($2D$

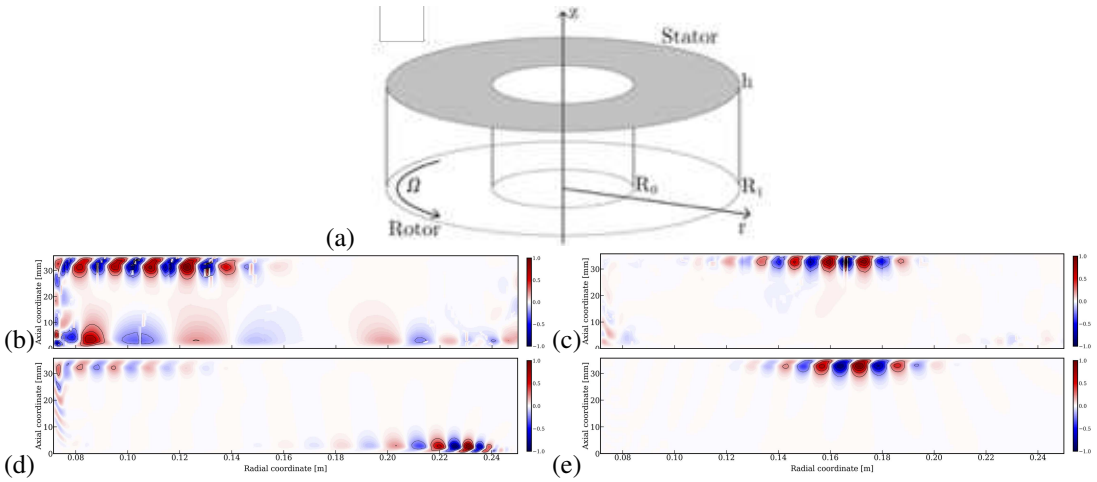

Figure 4.5: Rotor / stator cavity flow analysis: (a) geometrical view of the LES domain (cavity with aspect ratio H/R=1.18 at radial Reynolds number 10^5) and axial velocity fluctuation fields extracted by DMD, (b) & (c), and predicted by GIFIE, (d) & (e). Two azimuthal spiral modes of oscillation of order m are considered since present in the LES prediction: (b) & (d), $m = 12$ and (c) & (e), $m = 29$.

gloabal stability solver), a Linearized Navier-Stokes Equations solver dedicated to axisymmetric $2D$ mean flows were completed and thoroughly tested against test-cases from the literature. Confrontations of the GIFIE predicitions against DMD extractions of unsteadiness from LES for a simple RS-cavity confirm the adequacy of such formalisms for improved understanding, Fig. 4.5. More interestingly, GIFIE opens perspectives for flow sensitivity analyses and in the long run flow control or geometry optimization.

4.3 Aeronautical engines

Aeronautical engine and more specifically gas turbine engine applications have been at the core of the success of the CFD team with multiple major contributions involving CERFACS'partners as well as scientific publications. Recent advances on the matter have focused on the transfer of the tools to industrial partners complemented by the integration of these solutions in the design chain of combustors at SAFRAN for example. As a follow up of these actions, new applications now deal with thermal cooling within the combustor or the turbine, the latter context emerging with the development of LES for turbomachinery applications as detailed thereafter.

4.3.1 Real burner predictions

Multiple combustor computations have been based on the basis of the fundamental developments described previously. These demonstrations usually remain confidential since obtained on industrial geometries. The objectives were the validation of the new multi-phase flow reacting LES solver based on the Euler-Lagrange formalism or the capability of turbulent combustion models coupled to complex chemistry to capture pollutant emissions. A typical example is provided on Fig. 4.6 where the LEMCOTEC burner was simulated using ABVP to evaluate pollutant levels issued by operating the combustor at different thermal conditions [CFD81].

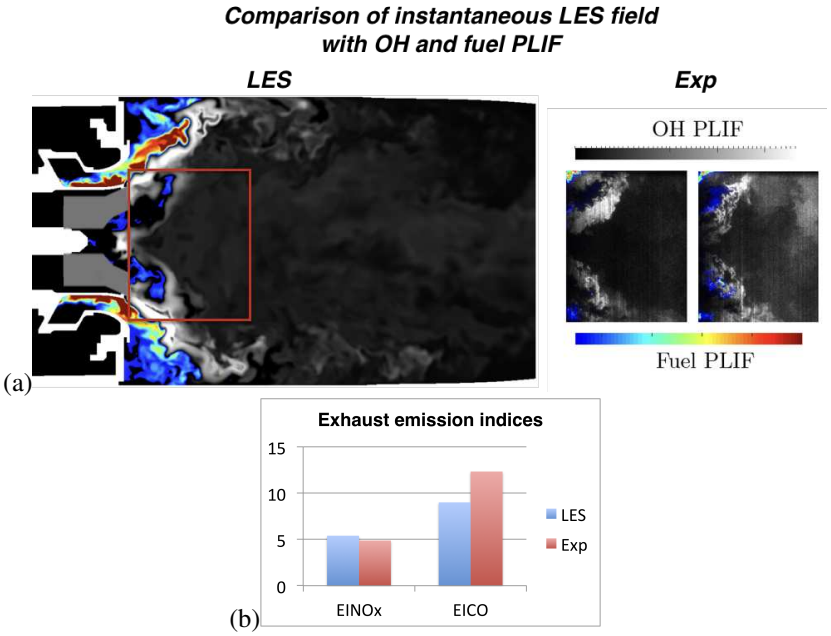

Figure 4.6: LES prediction of NOx and NO levels for the LEMCOTEC burner: (a) instantaneous view of the combustion field and (b) resulting pollutant indices.

4.3.2 Turbomachinery

Turbomachinery is an essential component of aeronautical applications. Compressors or turbines indeed determine the overall power and operative limits of engines. With the different tools present in the CFD team, several industrial turbomachinery components of practical interest have been addressed in a recent past as vehicles to demonstrate the capacity of LES to deal with such complex applications. Following these efforts and the interest from CERFACS' partners, recent LES have focused on these flows to produce better quality predictions. In that respect, fundamentals dedicated to the accuracy as well as efficiency of parallel LES coupled solutions allow today the use of TurboAVBP along with mesh adaptation strategies for faster and more accurate flow predictions in these devices. More specifically, the tool can now deal with industry relevant problems such as combustor / turbine interactions [CFD53] (PhD of M. Thomas, CIFRE SAFRAN Helicopter Engines) or near-stall operation of axial and radial compressors as detailed below:

- The DGEN demonstrator (COFFECCI RTRA project), Fig. 4.7 (a) & (b): a fan from a real engine demonstrator equipped with multiple diagnostics and studied by ISAE-Supaero Toulouse.
- An engine radial compressor, Fig. 4.7 (c) studied in relation with SAFRAN Helicopter Engines [CFD20].
- The FACTOR demonstrator (FACTOR EU project), Fig. 4.7 (d): a non-reacting combustor turbine component rig experimentally studied at Florence University (UNIFI) in its three-sector version or at DLR (Germany) in its full annular version to understand next engine generations combustor turbine interactions [CFD54, CFD73, CFD53].

Although still under validation against experimental data, these turbomachinery LES predictions constitute today world premieres. Such capabilities are now being transferred towards industry on proprietary

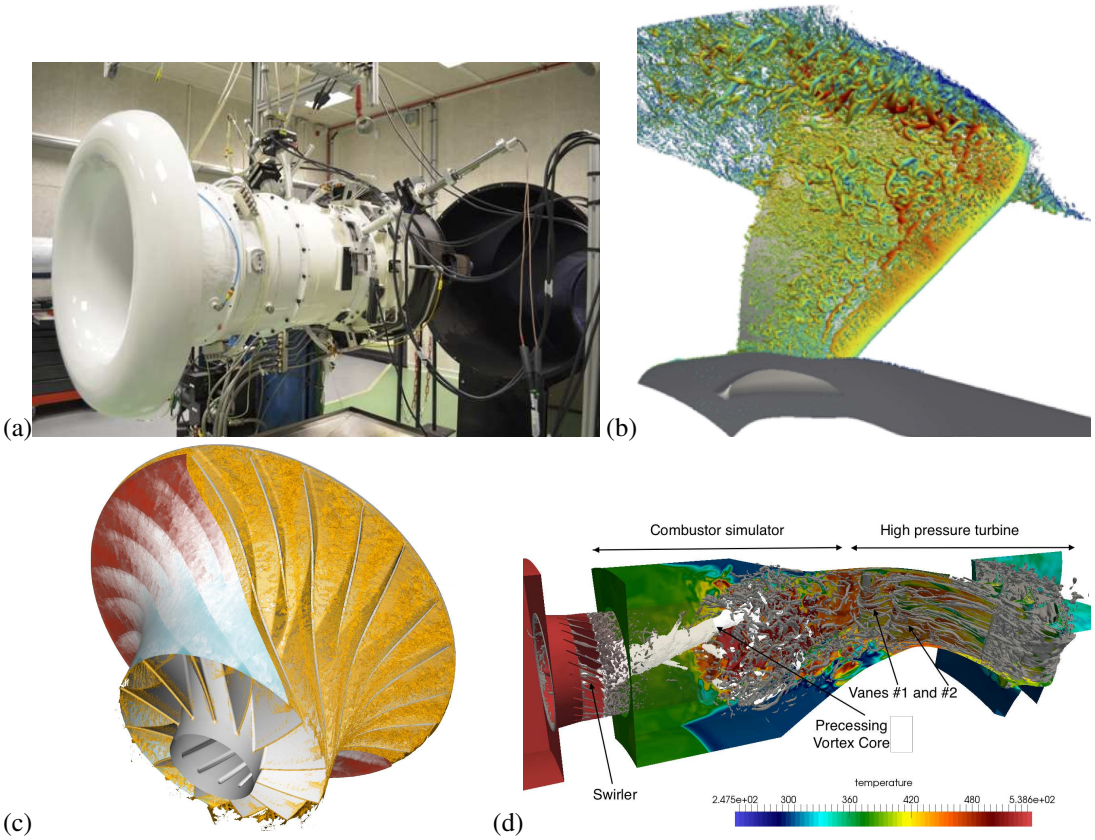

Figure 4.7: LES of turbomachinery components computed at CERFACS using the Turbo AVBP LES solver: DGEN engine (Price Induction), (a) experiment (ISAE Toulouse); (b) LES instantaneous flow field [CFD37]; (c) real engine radial compressor and (d) fully integrated LES simulation of the FACTOR combustor / turbine interaction demonstrator [CFD52, CFD73].

geometries as well as through the implication of the offices of methods from SAFRAN that invest in the tool [CFD70] so it can be recast for future use by industry or research partners. The objectives are for partners to contribute to CERFACS' efforts in evaluating turbomachinery LES in its wall-resolved formalism as well as in its wall-modeled context (PhD of M. Harnieh conducted in the context of the AITEB project). Complementarily to the tools improvement, the fundamentals of wall flow models and of associated techniques are still being pursued within the CFD team (PhD dissertation of A. Perrot, CIFRE SAFRAN Helicopter Engines). A typical example is the development of automated CFD solvers and mesh adaptation: originally constructed for combustor non-reacting swirled flows, the strategy has been recast for fully compressible and anisothermal flows (PhD of M. Harnieh). Applied to the DGEN configuration (COFECCI support to the post-doc position of N. Odier), Fig. 4.8, it has lead to improved flows predictions and overall gain in CPU cost.

TurboAVBP is also used by research partners for turbomachinery noise predictions, Fig. 4.9(a), by Prof. S. Moureau (LMFA and Sherbrooke University) around the NASA SDT fan databasis. Similar work is supported by Airbus through the PhD work of S. Esnault on fan liner treatment (OPTIMA DGA project).

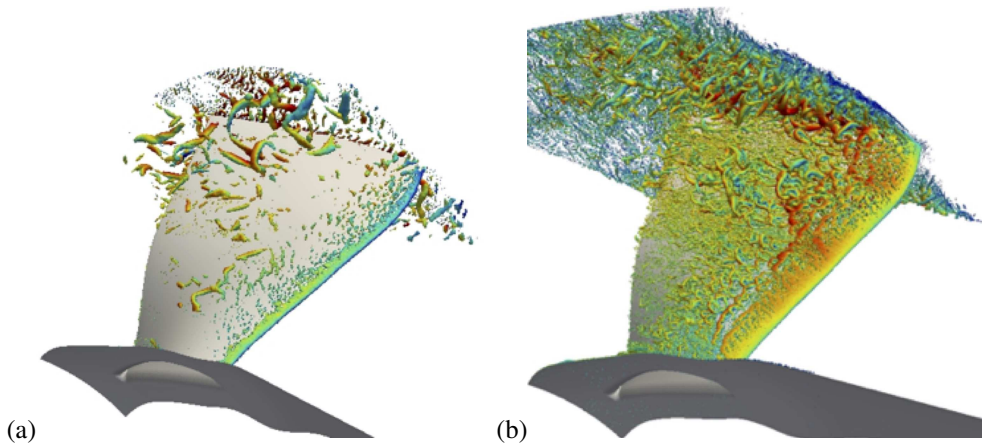

(a) (b)

Figure 4.8: Mesh adaptation to the DGEN fan LES simulations: (a) flow structures issued by the initial LES prediction relying on a first user-defined mesh and (b) same flow organization issued after automatic mesh adaptation based on the initial flow prediction of (a). For both predictions, turbulent features are visualized through and iso-surface of Q criterion colored by the local velocity magnitude.

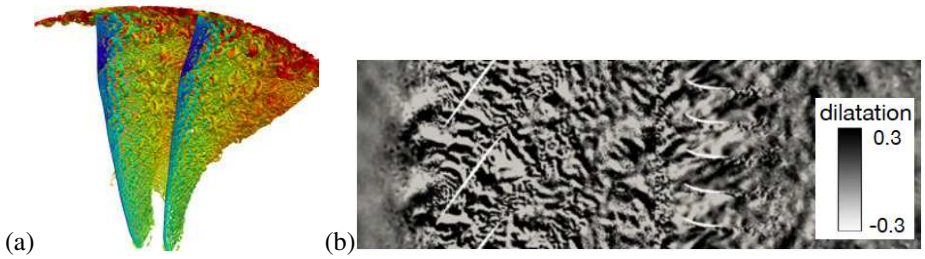

(a) (b)

Figure 4.9: NASA SDT LES predictions: (a) Q criterion iso-surface to evidence the flow structures around the SDT fan configuration accompanied by (b) a view of the velocity dilatation field illustrative of the acoustic field generated within the machine in a radial plane at 97% height.

All these applications are continuously being fed with fundamental researches around various areas of aerodynamics and CFD thanks to the support of National and European projects like:

- ATOM: Collaborative project involving multiple French agencies (SAFRAN, ONERA, CERFACS...) around high performance tools and environments to ease full engine integration and simulations on high-end computing facilities.

- FLORA: European project involving SAFRAN Helicopter Engines, LMFA and CERFACS to improve the next generation of radial compressors at nominal condition and near surge.

4.4 Large size systems

In the industrial sector of energy production and refinery, very large size flames are encountered for example in torch flames or in furnaces. Like the propulsion industry, this sector now faces environmental constraints which are difficult to satisfy at the design stage without predictive numerical simulation approaches such as Large Eddy Simulation. The challenge then is to keep the computational cost at a reasonable level. Thanks to a specific methodology based on desynchronized multi-block approach, two cases of very large size flames and plumes, up to 10 meters long, have been computed by CERFACS in 2018. The first case is a burner containing a series of 12 torch flames typically used on oil rigs. The aim was to investigate the flame behavior in view of optimization. The second test case is a refinery furnace, with the objective of predicting the impact of CO2 addition on the pollutant emissions. This last case is a refinery furnace of very large size, studied in the framework of the IMPROOF project (Fig. 4.10).

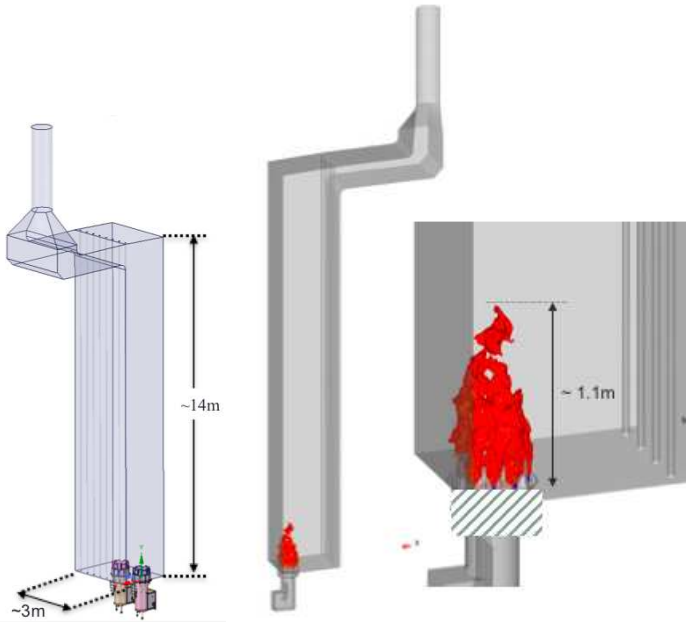

Figure 4.10: Flame in a refinery furnace (IMPROOF European project). Geometry (left) and heat release iso-surface colored by temperature (right).

4.5 Safety

The consequences of gas explosions can be devastating, causing numerous fatalities and the destruction of large parts of industrial facilities. In the explosion of a gas cloud, the main issue is the pressure increase (the so-called over-pressure), which controls the severity of the explosion and is determined by a complex unsteady interaction between combustion, turbulence and geometry. Controlling and reducing this over-pressure in industrial accidents is thus the key point in any safety related procedure. In this context, the main objective of the safety project at CERFACS is to further develop and improve the numerical tools to simulate gas explosion phenomena in realistic conditions. The pioneer work (for CERFACS) of P. Quillatre (PhD defended in 2014) showed that LES in general, and AVBP in particular, were the proper tools to tackle this challenge. As for any LES of turbulent combustion, the quality of numerical predictions relies largely on the turbulent combustion model. This is especially true when the computational domain sizes become large and the flame resolution low, as in realistic explosion configurations [CFD105]. CERFACS has been actively working on this topic since 2014, in collaboration with EM2C Paris (Dr. D. Veynante) to develop and validate new types of combustion models based on a dynamic procedure to automatically determine flame wrinkling factors [CFD106].

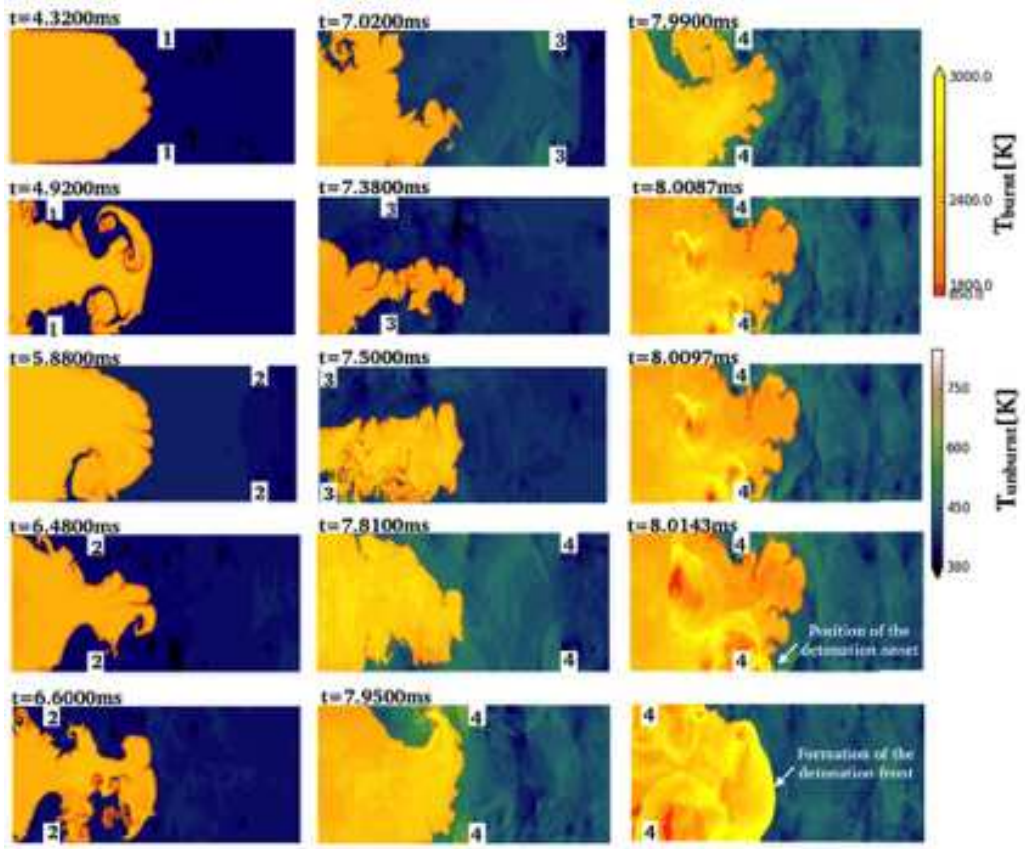

Figure 4.11: DNS of the GraVent explosion channel, flame/obstacle interactions prior to DDT. The temperature field is displayed using two different color palettes: one for the unburnt material and one for the burnt material. The numbers on each frame corresponds to the obstacle number.

This work, which focused on deflagration scenarios only, was continued with the PhD of O. Dounia (funded by Total, 2014-2018) and extended to the scenarios of detonation. The transition to detonation (DDT) is a complex and feared problem in the context of industrial safety due to the high levels of over pressure (and therefore destruction) generated by this mode of propagation. Despite years of theoretical and numerical efforts, a clear description of the different mechanisms that can trigger DDT remains incomplete. $2D$ DNS and $3D$ LES of flame propagation in a closed configuration equipped with obstacles (GraVent explosion channel, TU Munich) have shown the capacity of AVBP to correctly predict the different regimes of propagation, i.e. deflagration or detonation (Fig. 4.11), depending on the operating conditions considered (variation of the mixture equivalence ratio). A controversial issue on this field is the influence of chemistry modeling (simple single-step or detailed kinetic schemes) on DDT. Whatever the chemistry modeling used, shock reflection was found to be the common ingredient for DDT. However, results highlighted radically different transition mechanisms: with simplified chemistry, the detonation wave emerges from a region of unreacted material, which corresponds to the commonly observed scenario in the literature whereas the transition to detonation is triggered inside the flame brush when it is computed with detailed chemistry (Fig. 4.12) [CFD173].

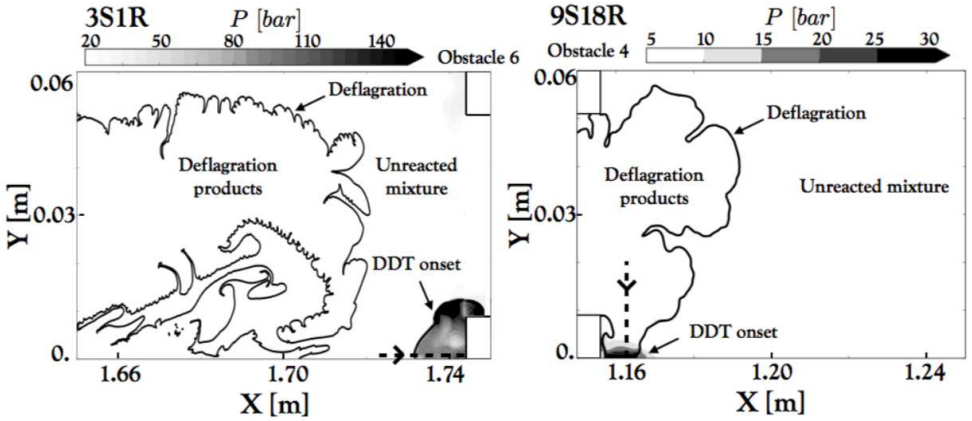

Figure 4.12: Zoom on the onset of detonation: pressure field and isocontour of progress variable c = 0.5 are displayed. Left: single-step mechanism. Right: detailed mechanism. This picture shows that the detonation emerges from the unburnt material from a hot spot with no direct involvement of the flame front, whereas the flame seems to be an active participant in the DDT scenario in the multi-step chemistry case.

More recently, the mitigation of explosions using chemical inhibitors has also been studied: a LES methodology was developed to simulate the inhibition of premixed hydrocarbon/air flames by sodium bicarbonate ($NaHCO_3$) particles (Fig. 4.13). This methodology used analytically reduced chemical schemes, derived using the chemistry reduction tool YARC (collaboration with Dr P. Pepiot, Cornell University). For various fuels and a wide range of equivalence ratios, particles with a strong potential for flame inhibition were identified and a criterion for efficient inhibition, based on the maximum particle size, was proposed [CFD72]. This work is currently being extended to other fuels (hydrogen) and other inhibitors (potassium bicarbonate) as part of O. Dounia's post-doc started in September 2018.

Safety research at CERFACS has grown fast since 2015 and CERFACS has become a member of the french Groupe de Travail Explosion project, led by INERIS. This collaboration with many other industrial and research partners (ENGIE, Air Liquide, Apsys, Fluidyn, CEA, IRSN) aims at testing and comparing various CFD solvers for the prediction of gas explosion phenomena. This consortium is a great opportunity

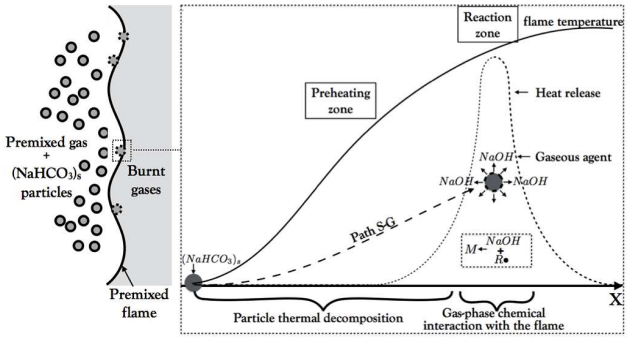

Figure 4.13: Schematic of the flame inhibition mechanism by sodium bicarbonate. Path S-G refers to the path from the Solid bicarbonate particle to the gaseous agent NaOH. $R\bullet$ stands for a radical species and M denotes a group of stable species

to compare AVBP to different RANS and LES codes well established in the field of safety, such as FLACS (GexCon) of Fluidyn-MP (Fluidyn).

4.6 Chemical processes

Thermal steam cracking is an industrial process which transforms heavy, less valuable fractions of crude oil into lighter and commercially more important products such as olefins. A critical factor to steam cracking is heat transfer, as the chemical conversion is most efficient in narrow temperature ranges. Artificially increasing the roughness of the inner surface of the reactor is a passive and efficient method for heat transfer enhancement, which is why ribbed reactors are commonly used for cracking applications. However, this method induces an increase in pressure loss, which is detrimental to the chemical selectivity of olefins and must be limited. To evaluate the overall impact of surface roughness on the process is difficult due to expensive measurements, and numerical simulation appears as an attractive tool to optimize the reactor design as demonstrated in the framework of the PhD of R. Campet et CERFACS.

Numerical simulations of steam cracking process are challenging because of the size of the computational domain (cracking reactors), the complex flow dynamics and the stiffness of the chemical mechanism. To make such simulations possible, a specific methodology was developed in the framework of the PhD of M. Zhu [46] to allow LES of such flows within a reasonable computational time. This strategy uses a periodic configuration of only one rib pitch length. The correct flow dynamics and thermochemistry are imposed by specific source terms added to the conservation equations. The validation in a ribbed tube configuration has confirmed the suitability of the approach in AVBP if compared against detailed experimental measurements performed at the Von Karman Institute. For practical applications, simulations including chemical mechanism for butane cracking were performed inside both a ribbed reactor and a smooth reactor designed in order to investigate the impact of artificial roughness on olefin selectivity. As expected, the heat transfer efficiency and the pressure loss were found higher in the ribbed reactor, leading to a more homogeneous temperature field. Ethylene production was also higher in the smooth reactor, which is both an effect of the lower operating pressure, which is known to favor light olefin production, and of the more stratified temperature distribution. On the contrary, propene production was found to be more important in the ribbed reactor due to more homogeneous temperature.

Thanks to previous findings and capabilities, an optimization of the internal reactor coil geometry has been initiated based on Gaussian processes and series of LES with the objective to maximize olefin

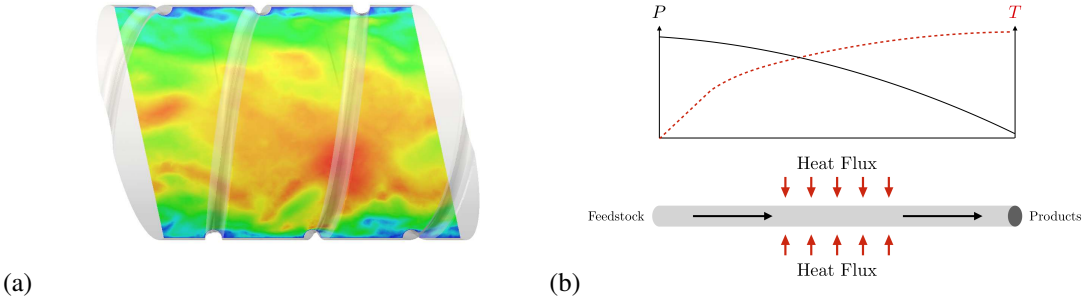

(a) (b)

Figure 4.14: (a) Instantaneous flow velocity in a ribbed tube for the cracking process in (b).

production. The optimization software BATMAN developed at CERFACS [CFD98, 44, CFD99] is used in a completely automatic procedure, including statistical prediction of the response surface and addition of new simulations to improve the response surface accuracy.

4.7 Aeroacoustics and combustion instabilities

4.7.1 Jet noise

Over the last decades, aircraft noise has been an increasing annoying phenomena that affects our health and environment. For an airplane, jet noise represents one the most noisy sources during take-off (for the population living in the vicinity of airport), but also during the flight (for the airplane passengers). CERFACS has been involved in numerical studies of jet noise source mechanism for ten years. During the AeroTraNet2 Project, a Marie Curie Action of the European Commission's 7th Framework Programme (FP7), research was done on the shock-cell noise, which is a distinctive noise that appears in industrial turbofans at off-cruise design flight conditions. In this context, the work of C. Pérez Arroyo (PhD defended in 2016) focuses on the identification of temporal and spatial signatures of broadband shock-associated noise for single stream isolated jets [CFD94]. Thanks to advanced numerical simulations, Fig. 4.15(a), the instantaneous view of the train of shock-cells interacting with turbulence can be observed using numerical Schlieren and vorticity magnitude maps. Following this work, the noise radiated by a realistic isolated under-expanded dual stream jet has been investigated to characterize the changes due to the presence of a central plug and a hot primary stream, Fig. 4.15(b). More recently, the noise of an installed subsonic configuration, Fig. 4.16, was also simulated to obtain more realistic descriptions of both flow physics and acoustic field. Ultimately, the final objective of this specific action is to realize full aircraft configuration with the aim to improve the design and reduce sound pollution.

4.7.2 Combustion instabilities

Most combustion systems are designed to operate in stable regimes. However, all experimentalists working on steady combustion chambers know that 'sometimes', a chamber starts exhibiting unexpected oscillations. These instabilities (often called thermoacoustic) lead to noise and vibration, which can be ignored or tolerated if the level of oscillations remains small (less than a few mbars). In other cases, however, pressure oscillations can reach values of the order of a large fraction of the mean pressure and lead to serious consequences: flame quenching, flashback, loss of control or destruction of the combustor.

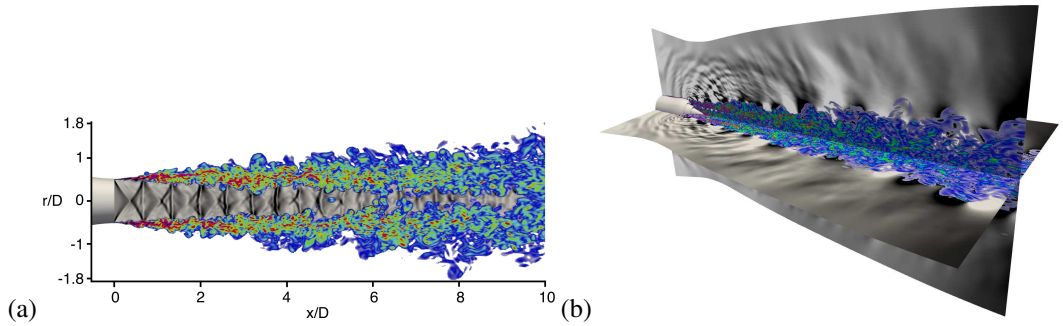

Figure 4.15: LES of under-expanded jets: (a) under-expanded jet' and (b) dual-stream jets. Both views show an instantaneous flow field of the vorticity modulus (in color) and (a) the magnitude of the density gradient (numerical Schlieren, in gray) while (b) shows the acoustic radiated pressure fluctuation (in gray).

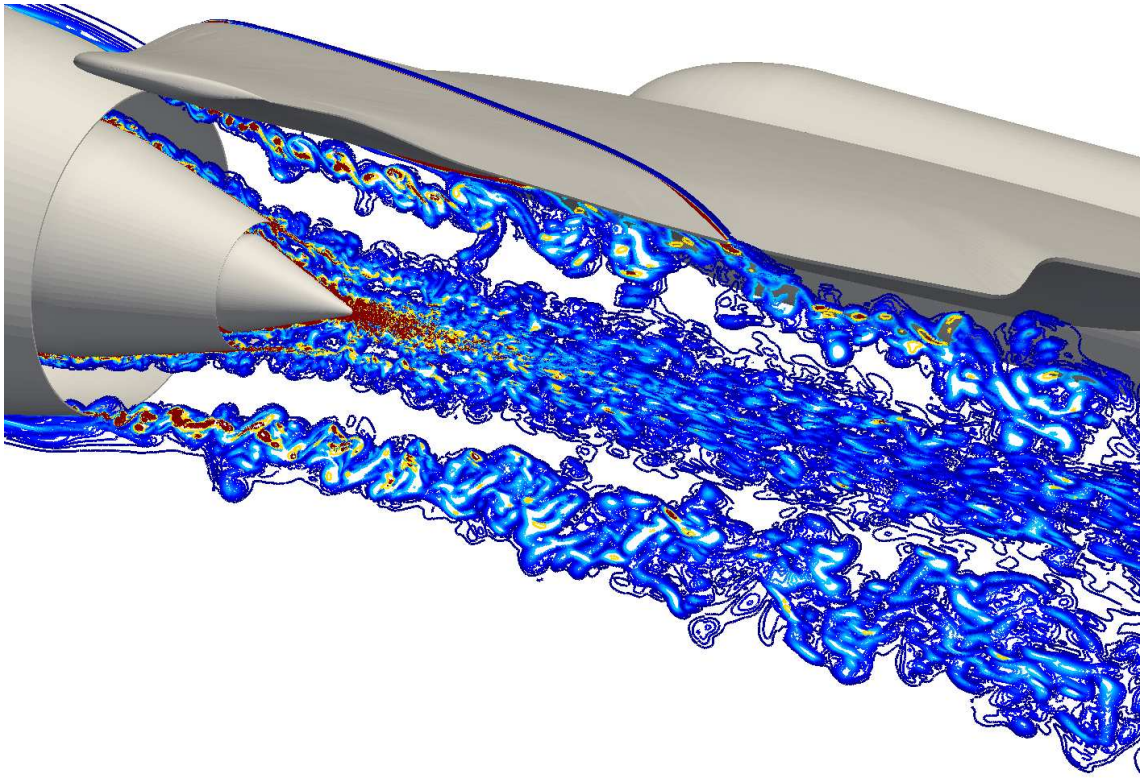

Figure 4.16: LES of an installed Ultra High By-Pass Ratio engine jet: instantaneous flow field of the vorticity modulus.

Thermoacoustic instabilities (CIs), also called flame dynamics, are the main reason why LES methods were introduced more than 10 years ago: no other method can capture these resonant mechanisms where combustion and acoustics couple. CERFACS was and remains leader in the simulations of combustion instabilities. The CERFACS tools incorporate methods as expensive as LES of full unsteady combustion in complex chambers but also acoustic solvers where only the acoustic field is searched for and Reduced Order Models (ROM) can be developed to complement numerical solvers and provide guidelines for control or UQ studies. The ERC advanced grant INTECOCIS (intecocis.inp-toulouse.fr) has supported many of the fundamental research efforts over the last 5 years. It has stopped in February 2018 but is now replaced by bilateral contracts and two ITN Marie Curie projects on instabilities in annular chambers (ANNULIGHT and MAGISTER) which started in october 2017.

An interesting aspect of CIs investigated in 2017 is their coupling with the wall temperature of the chambers where flames are stabilized. Experimentalists are aware that the wall temperatures of a combustion chamber affect the thermoacoustic combustion instabilities which can develop in the combustor: a chamber does not exhibit the same noise and unstable modes when it starts with cold walls or when it has run for a few minutes and walls have reached a higher steady temperature. Investigating this phenomenon requires to couple a flow/flame solver which can capture the flame dynamics with a heat conduction code which can predict the wall temperature field. This was done at CERFACS and IMFT using AVBP for the flow and AVTP for heat conduction, coupled with OPENPALM.

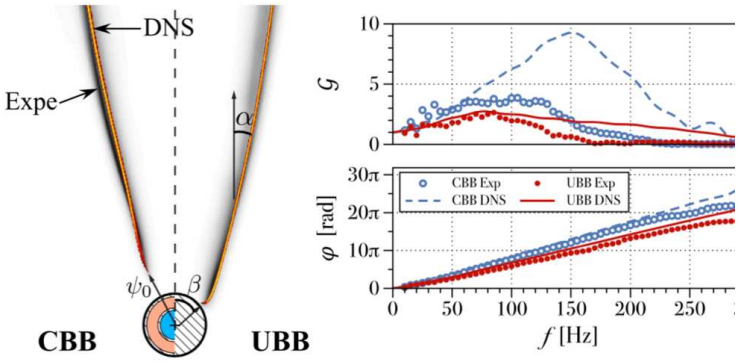

Figure 4.17: Measuring and simulating the effects of flame holder temperature on the dynamics of a laminar premixed flame [CFD89]. Left: configuration; CBB: Cooled Bluff Body where the flame holder temperature is fixed to 400 K by a water cooling system; UBB: Uncooled Bluff Body case where the flameholder temperature is 650 K. The two sides of the left image compare the flame positions. Right: Flame Transfer Functions of UBB and CBB cases, showing the drastic effects of cooling. Coupled DNS (AVBP/AVTP coupled with OPENPALM) are compared to measurements performed at IMFT.

This methodology was applied for laminar and turbulent flames by CERFACS together with IMFT in 2017. For a laminar premixed flame, the comparison between experiments and DNS (Fig. 4.17) revealed the strong effect of temperature of the solid (here a cylinder) used to stabilize the flame on both the flame position and on its response to acoustic waves (measured by the transfer function between velocity oscillations and total heat release fluctuations).

This result, obtained for a low-power, laminar flame was generalized to a swirled, turbulent flame [CFD84]. Here LES was used to account for the much higher Reynolds number: Kraus et al used AVBP coupled to AVTP (to compute the heat conduction in the chamber walls) to show that the turbulent flame of Karlsruhe Institute of Technology (KIT) was strongly influenced by the wall temperature (Fig. 4.18). Heat propagates

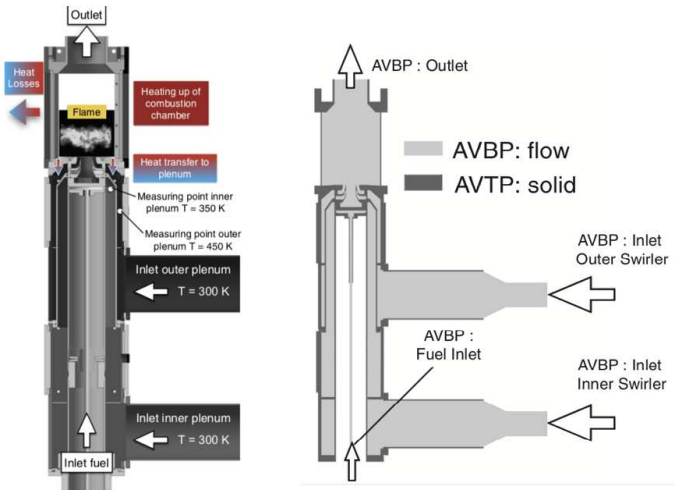

Figure 4.18: The experimental installation of Karlsruhe (left image) and the numerical setup (right image) used by Kraus et al [CFD84] to perform a coupled computation involving an LES of the reacting flow (on the gray domain) and heat conduction through the combustor walls (on the black domain).

not only to the chamber walls : it also diffuses upstream of the chamber through the walls and heats up the reacting gases even before they enter the chamber (Fig. 4.19). Computations and experiments (at KIT) were also shown to match much better especially for thermoacoustic activity when the temperature of the solid is computed and not arbitrarily imposed as done in most LES. More generally these results indicate that, as the precision offered by DNS and LES codes increases, the quality of the boundary conditions must also increase: it does not make much sense to perform a high-fidelity simulation of an engine in which arbitrary conditions are used for wall temperatures. These temperatures must be determined with a precision which is compatible with the flow solver itself and conjugate heat transfer LES are needed.

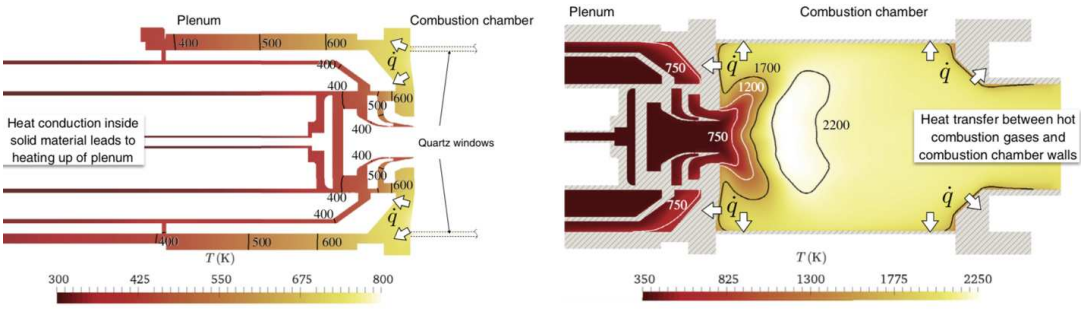

Figure 4.19: Coupled LES/heat conduction in the swirled turbulent combustor of Fig. 4.18 [CFD84]. Left: temperature in the walls showing how the plenum gets heated by heat diffusion through the walls. Right: mean temperature field in the chamber.

Combustion instabilities continue to remain a major issue for rocket engines and CERFACS is collaborating with CNES and ARIANEGROUP to simulate them both for existing hydrogen / oxygen engines [CFD103] and for the future methane / oxygen engines. For these future engines, the numerical challenge is considerable: both reactants will be introduced in a cryogenic state and therefore with large densities

(corresponding to liquid fuels). As soon as combustion will proceed, the combustion products will be gaseous and therefore will have a low density. Density gradients will be enormous: instead of a ratio 8 to 1 in most gaseous flames, these methane oxygen flames will reach density ratios of 300 to 1, a daunting proposition for most CFD codes which was addressed for the first time in 2018 in collaboration with the EM2C laboratory [CFD86].

A second difficulty to simulate instabilities in rocket engines is the importance of boundary conditions which have to be represented by impedances. The outlet nozzle of an engine for example, plays a crucial role on instabilities. When these impedances are not real, their treatment in an LES solver requires the introduction of so-called TDIBC (Time Domain Impedance Boundary Conditions), a largely untouched research topic today. In 2017 and 2018, CERFACS collaborated with Pr C. Scalo (Purdue) to develop TDIBC methods in AVBP. Another capability of TDIBC is to replace a long chimney by its equivalent impedance thereby diminishing greatly the mesh requirements [CFD71].

Theory still takes an important place in thermoacoustics at CERFACS with the development of analytical approaches dedicated to the prediction of unstable modes. LES is too expensive to be used for design and faster tools are needed. One of them is based on a network approach of acoustic waves propagating in the chamber. The resolution of the network equations is a problem in itself and a state space approach is being developed since 2018 in the PhDs of C. Laurent (ENS Cachan) and F. Dupuy (SAFRAN). This method should allow to use both time and frequency descriptions of combustion instabilities at a fraction of the LES cost.

Turbulent combustion models remain essential elements of any LES for turbulent combustion. The CERFACS team continues to study these models and their link with other elements of the modeling effort (chemistry description, accuracy of numerical scheme, boundary conditions). CERFACS participated to the US workshop on LES of turbulent combustion in 2017 by computing the Volvo experiment [CFD96] where a premixed flame is stabilized on a triangular wedge (Fig. 4.20).

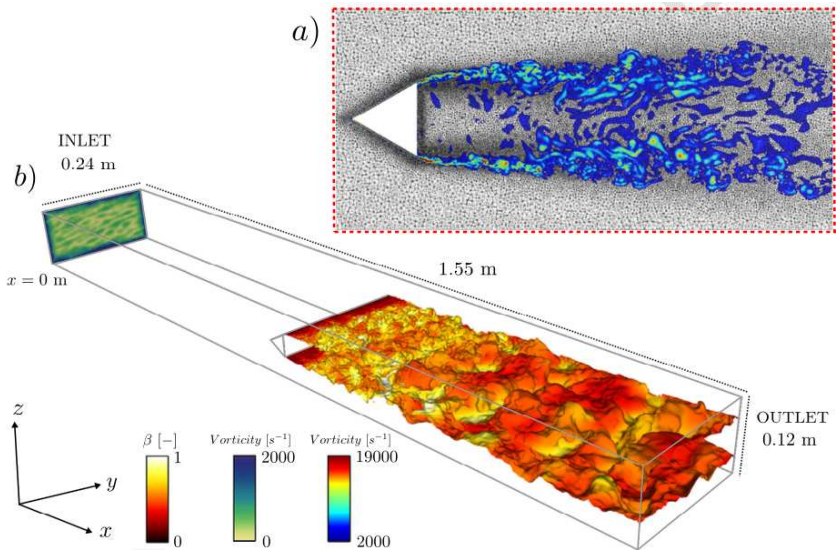

Figure 4.20: LES of the Volvo flame [CFD96]: (a) two-dimensional cut of the vorticity field and (b) isosurface of temperature and inlet turbulence.

Rochette et al proved that dynamic subgrid scale models for turbulent combustion rate but also order of precision of the numerical method and chemistry description played similar roles and that none of them could be forgotten if a precise solution was sought for both the mean flow and for instabilities.

References

[35] O. AIDN, O. KNAB, S. CELANO, M.and SILVESTRI, C. KIRCHBERGER, and G. SCHLIEBEN, (2015), Transregio SFB/TRR 40 - Test Case 1. 6th Technical Report, tech. rep.

[36] P. Aillaud, F. Duchaine, L. Gicquel, and S. Didorally, (2016), Secondary peak in the Nusselt number distribution of impinging jet flows: A phenomenological analysis, *Physics of Fluids*, **28**, 095110–1– 095110–22.

[37] T. Bridel-Bertomeu, L. Gicquel, and G. Staffelbach, (2016), Wall modeled LES and its impact on rotor/stator cavity unsteady features, In *ASME Turbo-Expo 2016 - Turbomachinery Technical Conference and Exposition*, Seoul, South Korea, GT2016–57244.

[38] T. Bridel-Bertomeu, L. Gicquel, and G. Staffelbach, (2017), Unsteady Macro-Structures from Large-Eddy Simulation of Industrial Turbopump Turbine Cavity, *AIAA Journal*, **55**, 2198–2214.

[39] T. Bridel-Bertomeu, (2016), *Investigation of unsteady phenomena in rotor/stator cavities using Large Eddy Simulation*, phd thesis, Ecole Doctorale : Mécanique, Energétique, Génie Civil, Procédés (MEGeP).

[40] O. Cabrit and F. Nicoud, (2009), Direct simulations for wall modeling of multicomponent reacting compressible turbulent flows, *Physics of Fluids*, **21**, 055108.

[41] F. Duchaine, J. Dombard, L. Gicquel, and C. Koupper, (2017), On the importance of inlet boundary conditions for aerothermal predictions of turbine stages with Large Eddy Simulation, *Computers and Fluids*, **154**, 60–73.

[42] S. Mendez and F. Nicoud, (2008), Large Eddy Simulation of a bi-periodic turbulent flow with effusion, *Journal of Fluid Mechanics*, **598**, 27 – 65.

[43] H. Negishi, A. Kumakawa, S. Moriya, N. Yamanishi, and H. Sunakawa, (2009), Thrust Chamber with Hot Gas Side Wall Ribs, In *AIAA*, no. January, 1–14.

[44] P. Roy, N. Elmocayd, S. Ricci, J.-C. Jouhaud, N. Goutal, M. De Lozzo, and M. Rochoux, (2018), Comparison of Polynomial Chaos and Gaussian Process surrogates for uncertainty quantification and correlation estimation of spatially distributed open-channel steady flows, *Stochastic Environmental Research and Risk Assessment*, **32**, 1723–1741.

[45] P. S., (2014), Heat transfer and GOX&LOX/GH2 flame imaging analysis in a high pressure and high mixture ratio rocket combustor, In *Space Propulsion*.

[46] M. Zhu, (2015), *Large Eddy Simulation of thermal cracking in petroleum industry*, PhD thesis, Université de Toulouse - Ecole doctorale MEGeP Dynamique des Fluides.

Publications

5.1 Books

[CFD1] C. Perez-Arroyo, G. Daviller, G. Puigt, and C. Airiau, (2018), *Hydrodynamic - Acoustic Filtering of a Supersonic Under-Expanded Jet*, vol. ERCOFACT Series, Springer International Publishing, ercofact series ed.

[CFD2] T. Poinsot and D. Veynante, (2018), *Combustion*, John Wiley & Sons.

5.2 Conferences Proceedings

[CFD3] P. Aillaud, F. Duchaine, L. Gicquel, and S. Didorally, (2017), Characterization of the surface curvature effect using LES for a single round impinging jet, In *Proceedings of ASME Turbo Expo 2017: Turbine Technical Conference and Exposition*, Charlotte, NC, USA, GT2017–64159.

[CFD4] P. Aillaud, F. Duchaine, O. Gicquel, C. Koupper, and G. Staffelbach, (2017), Large Eddy Simulation of trailing edge cutback film cooling: Impact of internal stiffening ribs on the adiabatic effectiveness, In *7th European Conference for Aeronautics and Aerospace Sciences (EUCASS 2017)*, vol. CD, Milan, Italy.

[CFD5] R. Bizzari, A. Dauptain, and F. Nicoud, (2018), A short overview of the models developed during my PhD for Safran Helicopter Engine - Invited speaker, In *INCA*, Bordes, France, SAFRAN HE.

[CFD6] R. Bizzari, A. Dauptain, L. Gicquel, and F. Nicoud, (2017), A thickened-hole model for LES over multiperforated liners, In *4e Colloque du réseau d'INitiative en Combustion Avancée (INCA)*, Palaiseau, France, SAFRAN TECH.

[CFD7] R. Bizzari, M. Férand, A. Dauptain, G. Staffelbach, S. Richard, J.-D. Mueller, T. Ogier, G. Exilard, and F. Nicoud, (2018), Mesh local refinement to enhance effusion cooling models; Invited conference, In *12th International Symposium on Engineering Turbulence Modelling and Measurements (ETMM12)*, Montpellier (France).

[CFD8] R. Bizzari, D. Lahbib, A. Dauptain, F. Duchaine, S. Richard, and F. Nicoud, (2018), A model able to assess multiperforated liners temperature from an unresolved adiabatic simulation, In *Journée SFT - Groupes "Convection" et "Modélisation et Simulation Numérique"*, S. F. de Thermique, ed., Paris, France.

[CFD9] F. Collin-Bastiani, J. Marrero-Santiago, A. Verdier, A. Vandel, G. Cabot, E. Riber, S. Richard, A. Cayre, B. Renou, and B. Cuenot, (2017), On the extinction and ignition mechanisms along the ignition events in the KIAI spray burner. A joint experimental and numerical approach, In *4e Colloque du réseau d'INitiative en Combustion Avancée (INCA)*, Paliseau, France, SAFRAN TECH.

[CFD10] F. Collin-Bastiani, O. Vermorel, C. Lacour, S. Richard, A. Cayre, and B. Cuenot, (2017), DNS of plasma to combustion transition in spark ignition using analytically reduced chemistry, In *4e Colloque du réseau d'INitiative en Combustion Avancée (INCA)*, Paliseau, France, SAFRAN TECH.

[CFD11] C. Coreixas, G. Wissocq, G. Puigt, J.-F. Boussuge, and P. Sagaut, (2017), General regularization step for standard and high-order lattice Boltzmann methods, In *14th International Conference for Mesoscopic Methods in Engineering and Science*, France, Ecole Centrale de Nantes.

[CFD12] B. Cuenot, (2017), Advanced Numerical Simulation for turbulent combustion : methods & selected applications - Invited conference, In *FORUM AE Final Conference*, Paris, France - 15 june 2017.

[CFD13] B. Cuenot, (2017), Large Eddy Simulation of turbulent reacting flows and coupled multi-physics: methods and selected applications - Invited seminar, Australia - August 2017, University of Melbourne.

[CFD14] B. Cuenot, (2017), Large Eddy Simulation of turbulent spray flames - Invited conference, In *Sixth International Workshop on the Turbulent Combustion of Sprays (TCS-6)*, September 17, 2017, Napoli, Italy.

[CFD15] B. Cuenot, (2017), Use of Large Eddy Simulation to predict pollutant emissions by industrial system - Invited conference, In *13th International Conference on Energy for a Clean Environment (CLEAN AIR CONFERENCE)*, 2-6 july 2017, Sao Miguel, Azores, Portugal.

[CFD16] M. Daroukh, N. Gourdain, S. Moreau, J.-F. Boussuge, and C. Sensiau, (2017), Impact of Inlet Distortion on Fan Tonal Noise, In *Proceedings of 12th European Conference on Turbomachinery Fluid dynamics & Thermodynamics*, STOCKHOLM SUEDE, KTH, Paper ID: ETC2017–201.

[CFD17] M. Daroukh, S. Moreau, N. Gourdain, J.-F. Boussuge, and C. Sensiau, (2017), Tonal Noise Prediction of a Modern Turbofan Engine with Large Upstream and Downstream Distortion, In *International Symposium on Transport Phenomena and Dynamics of Rotating Machinery (ISROMAC 2017)*, Maui, Hawaii.

[CFD18] J. de Laborderie, F. Duchaine, and L. Gicquel, (2017), Analysis of a high-pressure multistage axial compressor at off-design conditions with coarse Large Eddy Simulations, In *12th European Conference on Turbomachinery Fluid Dynamics & Thermodynamics*, EUROTURBO, ed., Stockholm, Sweden, Paper ID: ETC2017–125.

[CFD19] M. Djokic, K. Van Geem, G. Heynderickx, S. Dekeukeleire, S. Vangaever, F. Battin-Leclerc, G. Bellos, W. Buysschaert, B. Cuenot, T. Faravelli, M. Henneke, D. Jakobi, P. Lenain, A. Munoz, J. Olver, M. Van Goethem, and P. Oud, (2017), IMPROOF: Integrated Model Guided Process Optimization of Steam Cracking Furnaces, In *International Conference on Sustainable Design and Manufacturing - SDM 2017*, vol. 68, Springer, Cham, 589–600.

[CFD20] J. Dombard, F. Duchaine, L. Gicquel, G. Staffelbach, N. Buffaz, and I. Trebinjac, (2018), Large Eddy Simulations in a transonic centrifugal compressor, In *Proceedings of ASME Turbo Expo 2018: Turbine Technical Conference and Exposition*, vol. Volume 2B, Oslo, Norway, International Gas Turbine Institute, V02BT44A030 – 10 pages.

[CFD21] A. Felden, L. Esclapez, A. Misdariis, E. Riber, B. Cuenot, and H. Wang, (2017), Including real fuel chemistry in Large-Eddy Simulations, In *7 TH European Conference for Aeronautics and Aerosp Sciences (EUCASS)*, vol. CD, Milan, Italy.

[CFD22] A. Felden, E. Riber, B. Cuenot, and P. Pepiot, (2017), A library of Analytically Reduced Chemical schemes for a large range of CFD applications: from methane to aviation kerosene, In *4e Colloque du réseau d'INitiative en Combustion Avancée (INCA)*, Palaiseau, France, SAFRAN TECH.

[CFD23] M. Férand, G. Daviller, S. Moreau, C. Sensiau, and T. Poinsot, (2018), Using LES for combustion noise propagation to the far-field by considering the jet flow of a dual-stream nozzle, In *24th AIAA/CEAS Aeroacoustics Conference*, Atlanta, Georgia (USA), 1–18.

[CFD24] L. Gallen, A. Felden, E. Riber, and B. Cuenot, (2017), Prediction of soot in a gaseous non-premixed burner using a Lagrangian approach, In *4e Colloque du réseau d'INitiative en Combustion Avancée (INCA)*, Paliseau, France, SAFRAN TECH.

[CFD25] L. Gicquel, (2017), Engine Scale Stability prediction using Large Eddy Simulations - invited conference, In *The first International Workshop on Near Limit Flames*, Boston, USA, July 29-30 2017, Princeton University.

[CFD26] L. Gicquel, (2017), Recent Applications of Massively Parallel Large Eddy Simulations to address Industrial Problems - invited conference, In *HPC Combustion Spanish Workshop*, Barcelona, Spain June 2nd 2017, Barcelona Supercomputing Center.

[CFD27] T. Grosnickel, F. Duchaine, L. Gicquel, and C. Koupper, (2017), Large Eddy Simulations of static and rotating ribbed channels in adiabatic and isothermal conditions, In *Proceedings of ASME Turbo Expo 2017: Turbine Technical Conference and Exposition*, no. GT2017-64241, 12 pp.

[CFD28] M. Harnieh, L. Gicquel, and F. Duchaine, (2017), Sensitivity of Large Eddy Simulations to inflow condition and modeling if applied to a transonic high-pressure cascade vane, In *Proceedings of ASME Turbo Expo 2017: Turbine Technical Conference and Exposition*, Charlotte, NC, USA, paper GT2017–64686.

[CFD29] M. Harnieh, L. Gicquel, and F. Duchaine, (2018), Large eddy simulations of a highly loaded transonic blade with separated flow - Invited conference, In *Turbomachinery Technical Conference & Exposition 2018*, Oslo, Norway, ASME International Gas Turbine Institute, GT2018–75730.

[CFD30] M. Harnieh, M. Thomas, R. Bizzari, L. Gicquel, and F. Duchaine, (2018), Assessment of a coolant injection model on cooled high-pressure vanes in Large Eddy Simulation - Invited conference, In *12th International Symposium on Engineering Turbulence Modelling and Measurements (ETMM12)*, ERCOFTAC, ed., Montpellier, France.

[CFD31] V. Joncquières, F. Pechereau, A. Alvarez Laguna, A. Bourdon, O. Vermorel, and B. Cuenot, (2018), A 10-moment fluid numerical solver of plasma with sheaths in a Hall Effect Thruster, In *AIAA Joint Propulsion Conference*, Cincinatti, USA, AIAA.

[CFD32] J. Lamouroux, S. Richard, Q. Malé, G. Staffelbach, A. Dauptain, and A. Misdariis, (2017), On the Combination of Large Eddy Simulation and Phenomenological Soot Modelling to Calculate the Smoke Index From Aero-Engines Over a Large Range of Operating Conditions, In *ASME Turbo Expo 2017: Turbomachinery Technical Conference and Exposition*, vol. 4B, Charlotte, USA - June 26–30, 2017, International Gas Turbine Institute, GT2017–64262.

[CFD33] D. Maestro, F. Di Sabatino, D. Lacoste, and B. Cuenot, (2017), Large Eddy Simulation of Nanosecond Repetitively Pulsed Discharges for the Control of Thermoacoustic Instabilities, In *4e Colloque du réseau d'INitiative en Combustion Avancée (INCA)*, Palaiseau, France, SAFRAN TECH.

[CFD34] M. Marino, N. Gourdain, G. Legras, and D. Alfano, (2017), Aerodynamic simulation strategies assessment for a Fenestron® in hover flight, In *EUCASS 2015 Book Series – Advances in AeroSpace Sciences - Progress in Flight Physics*, Array, ed., vol. 9, Kraków, Poland, 81–106.

[CFD35] F. Ni, M. Brebion, F. Nicoud, and T. Poinsot, (2017), Accounting for acoustic damping in a 3D Helmholtz solver, In *24TH INTERNATIONAL CONGRESS ON SOUND AND VIBRATION*, London, UK.

[CFD36] N. Odier, F. Duchaine, L. Gicquel, G. Dufour, and N. Garcia-Rosa, (2017), Comparison of LES and RANS predictions with experimental results of the fan of a turbofan, In *Proceedings of 12th European Conference on Turbomachinery Fluid dynamics & Thermodynamics*, no. Paper ID: ETC2017-126, Stockholm, Sweden.

[CFD37] N. Odier, F. Duchaine, L. Gicquel, G. Staffelbach, A. Thacker, N. Garcia-Rosa, G. Dufour, and J.-D. Mueller, (2018), Evaluation of Integral Turbulence Scale Through the Fan Stage of a Turbofan Using Hot Wire Anemometry and Large Eddy Simulation, In *ASME Turbo Expo 2018: Turbomachinery Technical Conference & Exposition*, vol. Volume 2C, Oslo, Norwa, ASME, pp. V02CT42A021.

[CFD38] M. Queguineur, T. Bridel-Bertomeu, L. Gicquel, and G. Staffelbach, (2018), Local and global stability analysis of an academic rotor/stator cavity, In *ASME. Turbo Expo: Power for Land, Sea, and Air*, vol. 2A of GT2018-75008, Oslo, Norway, V02AT45A001; 11 pages.

[CFD39] B. Rochette, B. Cuenot, A. Cayre, and S. Richard, (2017), Influence of relative velocity on two-phase flow laminar flame structure and propagation properties, In *4e Colloque du réseau d'INitiative en Combustion Avancée (INCA)*, Palaiseau, France, SAFRAN TECH.

[CFD40] B. Rochette, O. Vermorel, L. Gicquel, T. Poinsot, and D. Veynante, (2018), ARC versus two-step chemistry and third-order versus second-order numeric scheme for Large Eddy Simulation of the Volvo burner, In *2018 AIAA Aerospace Sciences Meeting*, vol. january 8-11, 2018, Kissimmee, Florida, AIAA, AIAA 2018–0442.

[CFD41] A. Rona, E. Hall, G. Puigt, R. Camussi, C. Schram, C. Airiau, C. Felli, and C.-H. Lai, (2017), European doctoral training in aeroacoustics by a Marie Curie integrated training network, In *24th International Congress on Sound and Vibration - ICSV24 PROCEEDINGS*.

[CFD42] P. Roy, G. Daviller, J.-C. Jouhaud, and B. Cuenot, (2017), Uncertainty Quantification-Driven Robust Design Assessment of a Swirler's Geometry, In *4e Colloque du réseau d'INitiative en Combustion Avancée (INCA)*, Palaiseau, France, SAFRAN TECH.

[CFD43] P. Roy, (2017), Improving Surrogate Model-based Uncertainty Quantification Application to LES - POSTER, In *MASCOT-NUM 2017*, GDR-MASCOT-NUM, ed., Paris, France, Institut Henri Poincaré et AgroParisTech.

[CFD44] T. Schmitt, G. Staffelbach, S. Ducruix, S. Gröning, J. Hardi, and M. Oschwald, (2017), Large-Eddy Simulations of a lab-scale liquid rocket engine: influence of fuel injection temperature on thermo-acoustic stability, In *7th European Conference for Aeronautics and Space Sciences (eucass 2017)*, Italy, Politecnico Milano.

[CFD45] L. Segui-Troth, L. Gicquel, F. Duchaine, and J. de Laborderie, (2017), LES of the LS89 cascade: influence of inflow turbulence on the flow predictions, In *12th European Conference on Turbomachinery Fluid Dynamics & Thermodynamics*, EUROTURBO, ed., Stockholm, Sweden, Paper ID: ETC2017–159.

[CFD46] G. Staffelbach and T. Schmitt, (2017), Prédiction des instabilités de combustion haute fréquence dans les moteurs fusée cryotechniques - invited conference, In *Journée Retours Grand challenge OCCIGEN2*, Montpellier, France.

[CFD47] G. Staffelbach, S. Ducruix, S. Gröning, J. Hardi, and M. Oschwald, (2017), Large - Eddy Simulations of a lab - scale liquid rocket engine: influence of fuel injection temperature on thermo - acoustic stability, In *7th European Conference for Aeronautics and Aerospace Sciences (EUCASS 2017)*, vol. CD, Italy, Politecnico Milano.

[CFD48] G. Staffelbach, (2017), Combustion applications - Extreme Scale Demonstrators Workshop for industrial users - invited conference, In *32nd conference in the ISC High Performance*, Francfort, Allemagne, ETP4HPC.

[CFD49] G. Staffelbach, (2017), Highlights of mesh adaptation and LES - invited conference, In *1st "PaMPA day" workshop*, Bordeaux, France, INRIA.

[CFD50] G. Staffelbach, (2017), Legacy codes an modern architectures - invited conference, In *Research day - Informatik 10 System Simulation*, Germany, University of Erlangen.

[CFD51] G. Staffelbach, (2018), Mesh adaptation for Large Eddy Simulation for compressible combustion - Invited conference, In *3rd MMG day 2018*, Jussieu Paris, France, Mmg PLATFORM.

[CFD52] M. Thomas, A. Dauptain, F. Duchaine, L. Gicquel, C. Koupper, and F. Nicoud, (2017), Comparison of Heterogeneous and Homogeneous Coolant Injection Models for Large Eddy Simulation of Multiperforated Liners Present in a Combustion Simulator, In *ASME Turbo Expo 2017 Proceedings : Design Methods and CFD Modeling for Turbomachinery*, vol. 2B: Turbomachinery, Charlotte, North Carolina, USA,, International Gas Turbine Institute, GT2017–64622 (12pp.).

[CFD53] M. Thomas, F. Duchaine, L. Gicquel, and C. Koupper, (2017), Advanced Statistical Analysis Estimating the Heat Load Issued by Hot Streaks and Turbulence on a High-Pressure Vane in the Context of Adiabatic Large Eddy Simulations, In *ASME Turbo Expo 2017 Proceedings : Design Methods and CFD Modeling for Turbomachinery*, vol. 2B: Turbomachinery, Charlotte, North Carolina, USA,, International Gas Turbine Institute, GT2017–64648 (12 pages).

[CFD54] M. Thomas, F. Duchaine, L. Gicquel, and C. Koupper, (2018), Impact of realistic inlet condition on les predictions of isolated high pressure vanes, In *12th International ERCOFTAC Symposium on Engineering Turbulence Modelling and Measurements (ETMM12)*, Montpellier, France.

[CFD55] J. Vanharen, G. Puigt, J.-F. Boussuge, and A. Balan, (2017), Optimised Runge-Kutta time integration for the Spectral Difference method, In *23rd AIAA CFD Conference*, Denver, Colorado USA.

[CFD56] G. Wissocq, J.-F. Boussuge, and P. Sagaut, (2018), Investigating the stability of the LBM-BGK through an extended von Neumann analysis, In *27th International Conference on Discrete Simulation of Fluid Dynamics*, Massachusetts (USA), Worcester Polytechnic Institute.

5.3 Journal Publications

[CFD57] P. Aillaud, L. Gicquel, and F. Duchaine, (2017), Investigation of the concave curvature effect for an impinging jet flow, *Physical Review Fluids*, **2**, 114608 – 34 pages.

[CFD58] S. Berger, F. Duchaine, and L. Gicquel, (2018), Bluff-body Thermal Property and Initial State Effects on a Laminar Premixed Flame Anchoring Pattern, *Flow Turbulence and Combustion*, **100**, 561–591.

[CFD59] R. Bizzari, D. Lahbib, A. Dauptain, F. Duchaine, L. Gicquel, and F. Nicoud, (2018), A Thickened-Hole Model for Large Eddy Simulations over Multiperforated Liners, *Flow Turbulence and Combustion*, **101**, 705–717.

[CFD60] R. Bizzari, D. Lahbib, A. Dauptain, F. Duchaine, S. Richard, and F. Nicoud, (2018), Low order modeling method for assessing the temperature of multi-perforated plates, *International Journal of Heat and Mass Transfer*, **127**, 727–742.

[CFD61] L. Boulet, P. Bénard, G. Lartigue, V. Moureau, S. Didorally, N. Chauvet, and F. Duchaine, (2018), Modeling of Conjugate Heat Transfer in a Kerosene/Air Spray Flame used for Aeronautical Fire Resistance Tests, *Flow Turbulence and Combustion*.

[CFD62] T. Bridel-Bertomeu, L. Gicquel, and G. Staffelbach, (2017), Large scale motions of multiple limit-cycle high reynolds number annular and toroidal rotor/stator cavitieslarge scale motions of multiple limit-cycle high reynolds number annular and toroidal rotor/stator cavities, *Physics of Fluids*, **29**.

[CFD63] T. Bridel-Bertomeu, L. Gicquel, and G. Staffelbach, (2017), Unsteady Macro-Structures from Large-Eddy Simulation of Industrial Turbopump Turbine Cavity, *AIAA Journal*, **55**, 2198–2214.

[CFD64] M. Catchirayer, J.-F. Boussuge, P. Sagaut, M. Montagnac, D. Papadogiannis, and X. Garnaud, (2018), Extended integral wall-model for large-eddy simulations of compressible wall-bounded turbulent flows, *Physics of Fluids*, **30**.

[CFD65] F. Collin-Bastiani, J. Marrero-Santiago, E. Riber, G. Cabot, B. Renou, and B. Cuenot, (2018), A joint experimental and numerical study of ignition in a spray burner, *Proceedings of the Combustion Institute*, **Available online 28 June 2018**.

[CFD66] F. Collin-Bastiani, O. Vermorel, C. Lacour, B. Lecordier, and B. Cuenot, (2018), DNS of spark ignition using Analytically Reduced Chemistry including plasma kinetics, *Proceedings of the Combustion Institute*, **Available online 19 July 2018**.

[CFD67] C. Coreixas, G. Wissocq, G. Puigt, J.-F. Boussuge, and P. Sagaut, (2017), Recursive regularization step for high-order lattice Boltzmann methods, *Physical Review E*, **96**, 033306 (1–22).

[CFD68] M. Daroukh, S. Moreau, N. Gourdain, J.-F. Boussuge, and C. Sensiau, (2017), Effect of Distortion on Turbofan Tonal Noise at Cutback with Hybrid Methods, *International Journal of Turbomachinery, Propulsion and Power*, **2**, 16.

[CFD69] G. Daviller, M. Brebion, P. Xavier, G. Staffelbach, J.-D. Mueller, and T. Poinsot, (2017), A mesh adaptation strategy to predict pressure losses in LES of swirled flows, *Flow Turbulence and Combustion*, **99**, 93–118.

[CFD70] J. de Laborderie, F. Duchaine, L. Gicquel, O. Vermorel, G. Wang, and S. Moreau, (2018), Numerical analysis of a high-order unstructured overset grid method for compressible LES of turbomachinery, *Journal of Computational Physics*, **363**, 371–398.

[CFD71] Q. Douasbin, C. Scalo, L. Selle, and T. Poinsot, (2018), Delayed-time domain impedance boundary conditions (D-TDIBC), *Journal of Computational Physics*, **371**, 50–66.

[CFD72] O. Dounia, O. Vermorel, and T. Poinsot, (2018), Theoretical analysis and simulation of methane/air flame inhibition by sodium bicarbonate particles, *Combustion and Flame*, **193**, 313–326.

[CFD73] F. Duchaine, J. Dombard, L. Gicquel, and C. Koupper, (2017), On the importance of inlet boundary conditions for aerothermal predictions of turbine stages with Large Eddy Simulation, *Computers and Fluids*, **154**, 60–73.

[CFD74] R. Dupuis, J.-C. Jouhaud, and P. Sagaut, (2018), Surrogate Modeling of Aerodynamic Simulations for Multiple Operating Conditions Using Machine Learning, *AIAA Journal*, **56**, 3622–3635.

[CFD75] A. Felden, L. Esclapez, E. Riber, B. Cuenot, and H. Wang, (2018), Including real fuel chemistry in LES of turbulent spray combustion, *Combustion and Flame*, **193**, 397–416.

[CFD76] A. Felden, E. Riber, and B. Cuenot, (2018), Impact of direct integration of Analytically Reduced Chemistry in LES of a sooting swirled non-premixed combustor, *Combustion and Flame*, **191**, 270–286.

[CFD77] L. Gallen, A. Felden, E. Riber, and B. Cuenot, (2018), Lagrangian tracking of soot particles in LES of gas turbines, *Proceedings of the Combustion Institute*.

[CFD78] A. Ghani and T. Poinsot, (2017), Flame Quenching at Walls: A Source of Sound Generation, *Flow Turbulence and Combustion*, **99**, 173–184.

[CFD79] F.-J. Granados-Ortiz, C. Perez-Arroyo, G. Puigt, C.-H. Lai, and C. Airiau, (2018), On the Influence of Uncertainty in Computational Simulations of a High-Speed Jet Flow from an Aircraft Exhaust, *Computers and Fluids*, **Available online 14 December 2018**.

[CFD80] L. Hero, J.-M. Senoner, A. Blancherin, and B. Cuenot, (2018), Large-Eddy Simulation of Kerosene Spray Ignition in a Simplified Aeronautic Combustor, *Flow Turbulence and Combustion*, **101**, 603–625.

[CFD81] T. Jaravel, E. Riber, B. Cuenot, and G. Bulat, (2017), Large Eddy Simulation of a model gas turbine burner using reduced chemistry with accurate pollutant prediction, *Proceedings of the Combustion Institute*, **36**, 3817–3825.

[CFD82] T. Jaravel, E. Riber, B. Cuenot, and P. Pepiot, (2018), Prediction of flame structure and pollutant formation of Sandia flame D using Large Eddy Simulation with direct integration of chemical kinetics, *Combustion and Flame*, **188**, 180–198.

[CFD83] E. Kaiser, M. Morzynski, G. Daviller, J. Kutz, B. Brunton, and S. Brunton, (2018), Sparsity enabled cluster reduced-order models for control, *Journal of Computational Physics*, **352**, 388 – 409.

[CFD84] C. Kraus, L. Selle, T. Poinsot, C. Arndt, and H. Bockhorn, (2017), Influence of Heat Transfer and Material Temperature on Combustion Instabilities in a Swirl Burner, *Journal of Engineering for Gas Turbines and Power-Transactions of the ASME*, **139**, Paper No: GTP–16–1303 pp. 10.

[CFD85] C. Lapeyre, M. Mazur, P. Scouflaire, F. Richecoeur, S. Ducruix, and T. Poinsot, (2017), Acoustically Induced Flashback in a Staged Swirl-Stabilized Combustor, *Flow Turbulence and Combustion*, **98**, 265–282.

[CFD86] C. Laurent, L. Esclapez, D. Maestro, G. Staffelbach, B. Cuenot, L. Selle, T. Schmitt, F. Duchaine, and T. Poinsot, (2018), Flame-wall interaction effects on the flame root stabilization mechanisms of a doubly-transcritical LO2/LCH4 cryogenic flame, *Proceedings of the Combustion Institute*.

[CFD87] S. Le Bras, H. Deniau, C. Bogey, and G. Daviller, (2017), Development of compressible large-eddy simulations combining high-order schemes and wall modeling, *AIAA Journal*, **55**, 1152–1163.

[CFD88] I. Mayo, T. Arts, and L. Gicquel, (2018), The three-dimensional flow field and heat transfer in a rib-roughened channel at large rotation numbers, *International Journal of Heat and Mass Transfer*, **123**, 848–866.

[CFD89] D. Mejia, M. Brebion, A. Ghani, E. Kaiser, F. Duchaine, L. Selle, and T. Poinsot, (2018), Influence of flame-holder temperature on the acoustic flame transfer functions of a laminar flame, *Combustion and Flame*, **188**, 5–12.

[CFD90] S. Moreau, C. Becerril, and L. Gicquel, (2017), Large-Eddy-Simulation prediction of indirect combustion noise in the Entropy Wave Generator experiment, *International Journal of Spray and Combustion Dynamics*.

[CFD91] F. Ni, M. Brebion, F. Nicoud, and T. Poinsot, (2017), Accounting for acoustic damping in a Helmholtz Solver, *AIAA Journal*, **55**, 1205–1220.

[CFD92] N. Odier, G. Balarac, and C. Corre, (2018), Numerical analysis of the flapping mechanism for a two-phase coaxial jet, *International Journal of Multiphase Flow*, **106**, 164–178.

[CFD93] N. Odier, M. Sanjosé, L. Gicquel, T. Poinsot, S. Moreau, and F. Duchaine, (2018), A characteristic inlet boundary condition for compressible, turbulent, multispecies turbomachinery flows, *Computers and Fluids*.

[CFD94] C. Perez-Arroyo, G. Daviller, G. Puigt, C. Airiau, and S. Moreau, (2018), Identification of temporal and spatial signatures of broadband shock-associated noise, *Shock Waves*, pp. 18.

[CFD95] T. Poinsot, (2017), Prediction and control of combustion instabilities in real engines, *Proceedings of the Combustion Institute*, **36**, 1–28.

[CFD96] B. Rochette, F. Collin-Bastiani, L. Gicquel, O. Vermorel, D. Veynante, and T. Poinsot, (2018), Influence of chemical schemes, numerical method and dynamic turbulent combustion modeling on LES of premixed turbulent flames., *Combustion and Flame*, **191**, 417–430.

[CFD97] B. Rochette, E. Riber, and B. Cuenot, (2018), Effect of non-zero relative velocity on the flame speed of two-phase laminar flames, *Proceedings of the Combustion Institute*.

[CFD98] P. Roy, S. Ricci, R. Dupuis, R. Campet, J.-C. Jouhaud, and C. Fournier, (2018), BATMAN: Statistical analysis for expensive computer codes made easy, *Journal of Open Source Software*, **3**, 00493.

[CFD99] P. Roy, L. Segui-Troth, J.-C. Jouhaud, and L. Gicquel, (2018), Resampling Strategies to Improve Surrogate Model-based Uncertainty Quantification - Application to LES of LS89., *International Journal for Numerical Methods in Fluids*, **online**.

[CFD100] O. Schulz, T. Jaravel, T. Poinsot, B. Cuenot, and N. Noiray, (2017), A criterion to distinguish autoignition and propagation applied to a lifted methane-air jet flame, *Proceedings of the Combustion Institute*, **36**, 1637–1644.

[CFD101] F. Shum Kivan, J. Marrero-Santiago, A. Verdier, E. Riber, B. Renou, G. Cabot, and B. Cuenot, (2017), Experimental and numerical analysis of a turbulent spray flame structure, *Proceedings of the Combustion Institute*, **36**, 2567–2575.

[CFD102] F. Thiesset, F. Halter, C. Bariki, C. Lapeyre, C. Chauveau, I. Gökalp, L. Selle, and T. Poinsot, (2017), Isolating strain and curvature effects in premixed flame/vortex interactions, *Journal of Fluid Mechanics*, **831**, 618–654.

[CFD103] A. Urbano, Q. Douasbin, L. Selle, G. Staffelbach, B. Cuenot, T. Schmitt, S. Ducruix, and S. Candel, (2017), Study of flame response from the Large-Eddy Simulation of a 42-injector rocket engine, *Proceedings of the Combustion Institute*, **36**, 2633–2639.

[CFD104] J. Vanharen, G. Puigt, X. Vasseur, J.-F. Boussuge, and P. Sagaut, (2017), Revisiting the spectral analysis for high-order spectral discontinuous methods, *Journal of Computational Physics*, **337**, 379–402.

[CFD105] O. Vermorel, P. Quillatre, and T. Poinsot, (2017), LES of explosions in venting chamber: a test case for premixed turbulent combustion models, *Combustion and Flame*, **183**, 207–223.

[CFD106] P. Volpiani, T. Schmitt, O. Vermorel, P. Quillatre, and D. Veynante, (2017), Large eddy simulation of explosion deflagrating flames using a dynamic wrinkling formulation, *Combustion and Flame*, **186**, 17–31.

[CFD107] G. Wissocq, N. Gourdain, O. Malaspinas, and A. Eyssartier, (2017), Regularized characteristic boundary conditions for the Lattice-Boltzmann methods at high Reynolds number flows, *Journal of Computational Physics*, **331**, 1–18.

[CFD108] P. Xavier, A. Ghani, D. Mejia, M. Brebion, M. Bauerheim, L. Selle, and T. Poinsot, (2017), Experimental and numerical investigation of flames stabilised behind rotating cylinders: interaction of flames with a moving wall, *Journal of Fluid Mechanics*, **813**, 127–151.

5.4 Technical Reports

[CFD109] S. Agarwal, (2018), Rapport de Stage - CERFACS SAFT, working note, Cerfacs, Toulouse, France.

[CFD110] P. Aillaud, (2017), Large Eddy Simulation of gas turbines vanes cooling systems - Rapport avancement de thèse 2A, contract report, Cerfacs, Toulouse.

[CFD111] A. Balan, G. Puigt, and J.-F. Boussuge, (2017), Definition and validation of sensors for hp-adaptation, contract report, CERFACS, Toulouse, France.

[CFD112] A. Balan, G. Puigt, and J.-F. Boussuge, (2017), Validation of the non-conformal hp-adaptation, contract report, CERFACS, Toulouse, France.

[CFD113] N. Barleon, (2018), Etude des plasmas atmosphériques pour la combustion assistée par plasma et simulations numériques de plasma basse pression., working note, ENSEEIHT - CERFACS, Toulouse, France.

[CFD114] V. Baudoui, M. Montagnac, L. Gicquel, and C. Koupper, (2018), Rapport Projet Cascade SP4: Tâche 4.2.2 - Analyse de sensibilité sur le DHP, contract report, CERFACS, Toulouse, France.

[CFD115] V. Bouillin, (2017), Méthodes d'injection de turbulence et d'ondes acoustiques dans un code LES, working note, ISAE SUPAERO - CERFACS, Toulouse, France.

[CFD116] C. Bregman, (2018), Rapport de Stage Interaction Fluide-Structure, working note, CERFACS, Toulouse, France.

[CFD117] T. Bridel-Bertomeu and M. Montagnac, (2017), Conversion de connectivité par faces de maillage non-structuré en connectivité par élément avec Antares - Rapport de synthèse, contract report, CERFACS, Toulouse, France.

[CFD118] T. Bridel-Bertomeu, (2017), Développement de méthodologie de calcul h_H, contract report, Cerfacs, Toulouse, France.

[CFD119] T. Bridel-Bertomeu, (2017), Mise à niveau de la librairie Antares pour le post-traitement d'un cas de turbine centripète, contract report, Cerfacs, Toulouse, France.

[CFD120] R. Campet, (2017), Simulating and Optimizing Steam Cracking Processes - 1st year report: LES of smooth and ribbed tubes, technical report, CERFACS.

[CFD121] J. Carmona, (2018), Rapport d'avancement fin CDD - 06 Novembre 2017 — 14 Janvier 2018, contract report, SAFRAN AE - CERFACS.

[CFD122] N. Cazard, (2018), Exploration de la capacité du Deep Learning á assister des simulations de mécanique des fluides, working note, CERFACS, Toulouse, France.

[CFD123] P. Champeix, (2017), From the spark to the flame study of the plasma chemical kinetic effect on ignition by making a direct numerical simulation on a pin-pin configuration, working note, IMT Mines Albi-Carmaux, Cerfacs Toulouse.

[CFD124] S. Cherkaoui, (2018), Rapport de Stage Adaptation de maillage en mécanique des fluides (Collaboration avec EDF), tech. rep., CERFACS.

[CFD125] A. Colombié, (2018), Simulation LBM-LES d'écoulements turbulents internes, working note, CERFACS, Toulouse ,France.

[CFD126] M. Daroukh and J.-F. Boussuge, (2017), Simulations multi-chorochroniques d'un compresseur axial, contract report, CERFACS - Safran HE.

[CFD127] M. Daroukh, A. Misdariis, and J.-F. Boussuge, (2017), Simulations instationnaires avec raccords glissants d'un compresseur axial avec effets technologiques, contract report, CERFACS - Safran AE.

[CFD128] G. Daviller and S. Le Bras, (2017), Report on LES simulations of UHBR nozzle for Jet Installation noise: link with single-stream jet phenomenology, contract report, CERFACS, TOULOUSE FRANCE.

[CFD129] F. Duchaine, (2017), Rapport final SIMACO3FI, contract report, FONDATION STAE ET CERFACS, Toulouse, France.

[CFD130] L. Esclapez and B. Cuenot, (2017), Simulation of an oil burner - WP2 - Raptor F Burner, contract report, CERFACS Toulouse.

[CFD131] L. Esclapez and B. Cuenot, (2018), Simulation of an oil burner - WP3 - Parametric study on the SRK injector, contract report, CERFACS Toulouse.

[CFD132] L. Esclapez, B. Cuenot, and T. Pringuey, (2017), Simulation of an oil burner - WP1 Evergreen burner, contract report, Schlumberger - CERFACS, Toulouse.

[CFD133] L. Esclapez, D. Maestro, C. Laurent, G. Staffelbach, B. Cuenot, T. Poinsot, C. Cruz, and D. Saucereau, (2017), LES of the Mascotte test bench in doubly transcritical conditions, contract report, CERFACS Toulouse.

[CFD134] M. Fiore, (2017), Influence of cavity purge flow on turbine aerodynamics - Rapport 1A thèse, working note, Cerfacs et Ecole Doctorale MEGeP, Toulouse.

[CFD135] C. Fournier, M. Daroukh, and R. Biolchini, (2018), Post-traitement avancé d'une configuration instationnaire multi-étage de turbomachine avec Antares., contract report, CERFACS, Toulouse.

[CFD136] N. Gindrier, (2018), Développement d'une méthode de suivi lagrangien de particules dans un code CFD d'ordre élevé pour la LES, working note, CERFACS, Toulouse, France.

[CFD137] C. Gout, (2018), Méthodes numériques pour la simulation monocanal d'un étage de turbomachine, working note, ISAE SUPAERO - CERFACS, Toulouse, France.

[CFD138] T. Grosnickel, (2017), Simulation des Grandes Echelles pour la prédiction des écoulements de refroidissement des pales de turbines - travaux thèse 2ème année, contract report, CERFACS, Toulouse, France.

[CFD139] A. Guilbaud and M. Montagnac, (2017), Amélioration des performances CPU pour les raccords non coïncidents dans le logiciel elsA pour les simulations instationnaires. Minimisation du nombre d'échanges de données entre processeurs - rapport final, contract report, CERFACS, Toulouse.

[CFD140] A. Guilbaud and M. Montagnac, (2018), Amélioration des performances CPU pour les raccords non coïncidents dans le logiciel elsA pour les simulations instationnaires. Traitement pour les calculs de flux sur les interfaces des raccords non coïncidents., contract report, CERFACS, Toulouse.

[CFD141] A. Guilbaud, T. Morel, P. Laporte, G. Dejean, M. Montagnac, and J.-F. Boussuge, (2018), Aero-acoustic co-distributed simulation with elsA, contract report, CERFACS, Toulouse, France.

[CFD142] M. Harnieh and F. Jaegle, (2017), AVBP V7.X Tutorial :1D Flame, tutorial, CERFACS, Toulouse, France.

[CFD143] M. Harnieh, L. Gicquel, F. Duchaine, and C. Koupper, (2018), Livrable Final CASCADE, contract report, CERFACS, Toulouse, France.

[CFD144] M. Harnieh, (2017), Définition des pertes en LES et bilans 1D appliqués aux écoulements compressibles dans les turbines, contract report, CERFACS, Toulouse, France.

[CFD145] F. Hermet, (2017), Rapport de stage de fin d'études d'ingénieur - Solveur de nouvelle génération : Extension à la combustion, working note, ENSEEIHT et CERFACS Toulouse.

[CFD146] V. Joncquières, (2018), Rapport d'activités : Calculs CFD de l'injection des neutres dans le PPS-5000, Lot 1, contract report, CERFACS, Toulouse, France.

[CFD147] V. Joncquières, (2018), Rapport d'avancement seconde année de thèse, technical report, CERFACS & SAFRAN.

[CFD148] T. Laroche, (2017), Simulation aux Grandes Échelles de l'injection liquide en moteurs aéronautiques, working note, INPT ENSEEIHT - CERFACS, Toulouse, France.

[CFD149] S. Le Bras, G. Daviller, and H. Deniau, (2017), Large-Eddy Simulation of EXEJET nozzle: operating point OP5, contract report, CERFACS, TOULOUSE FRANCE.

[CFD150] N. Lombard, (2017), Extension de la librairie de post-traitement ANTARES aux solutions très précises obtenues avec le solveur JAGUAR, working note, INP Grenoble (ENSE3) et Cerfacs Toulouse.

[CFD151] R. Macadré, Automatic learning methods for the capture of aerodynamic bifurcations Intership report for 2nd year - Code BATMAN, working note, ENSEEIHT et CERFACS, Toulouse, France.

[CFD152] Q. Malé, (2017), Simulations numériques avancées en aérothermochimie pour la conception d'une technologie d'allumage par jet de gaz chaud dans les moteurs á allumage commandé, working note, INSA Rouen et CERFACS Toulouse.

[CFD153] T. Marchal, (2018), Study and implementation of implicit time integration methods in a high-order CFD code, working note, Institut National Polytechnique de Toulouse - ENSEEIHT , Cerfacs, Toulouse France.

[CFD154] A. Martin, (2017), Création d'un outil de conversion de fichiers CANTERA en CHEMKIN sous Python - Mise á jour du tutoriel AVBP configuration Preccinsta - Stage de 4éme année Ingénieur, working note, Polytech Orleans et CERFACS Toulouse, France.

[CFD155] B. Martin, (2018), Simulation LES de l'ingestion de particules de sable par une turbomachine, working note, Institut Supérieur de l'Aéronautique et de l'Espace SUPAERO, CERFACS, Toulouse France.

[CFD156] M. Montagnac, C. Fournier, and M. Daroukh, (2017), Rapport de synthèse: Post-traitement des écoulements instationnaires en étage de compresseur centrifuge avec Antares., contract report, CERFACS, Toulouse France.

[CFD157] M. Montagnac, (2018), Stockage de données dans la structure de condition aux limites d'Antares., contract report, CERFACS, TOULOUSE.

[CFD158] M. Perini, (2017), Études des interactions stator-rotor dans un étage de turbine, working note, Ecole Centrale de Marseille et CERFACS Toulouse, France.

[CFD159] A. Pestre, (2018), Rapport de Stage PFE: - Développement et Validation du code de Recherche NTMIX3D, working note, ENSEEIHT - CERFACS, Toulouse, France.

[CFD160] G. Staffelbach, (2017), Prototype chaînes d'adaptation de maillage statique disponibles dans MMG3D et intégrés dans AVBP - Livrable ELCI L.2.4.4, contract report, CERFACS, Toulouse, France.

[CFD161] A. Sylla, (2017), Développement de schémas cinétiques chimiques pour hydrocarbures, working note, POLYTECH ORLÉANS - CERFACS TOULOUSE.

[CFD162] M. Tarot, (2017), Simulation numérique directe de flammes diphasiques, working note, Université Pierre et Marie Curie Paris & CERFACS Toulouse - Master SPI - Énergétique et Environnement.

[CFD163] J.-B. Tô, (2017), Aerodynamic study of an iced airfoil using the Lattice Boltzmann Method, working note, INP-ENSEEIHT et CERFACS, Toulouse.

[CFD164] N. Urien, (2018), Évaluation du solveur ProLB sur maillage mobile, working note, ENSEEIHT - CERFACS, Toulouse, France.

[CFD165] J. Wirtz, (2018), Analytically Reduced Chemistries applied to Large-Eddy Simulations of turbulent reacting flows, working note, ISAE SUPAERO - CERFACS, Toulouse, France.

[CFD166] V. Xing, (2018), Exploration of the ability of Deep Learning to learn the characteristics of turbulent flows, working note, Institut Supérieur de l´Aéronautique et de l´Espace-Supaero, CERFACS, Toulouse, France.

5.5 Thesis

[CFD167] P. Aillaud, (2017), *Simulation aux Grandes Echelles pour le refroidissement d'aubage de turbine haute-pression*, phd thesis, Université de Toulouse, INP Toulouse - Ecole doctorale MEGeP.

[CFD168] C. Becerril, (2017), *Simulation of noise emitted by a reactive flow*, phd thesis, INPT Institut National Polytechnique de Toulouse Ecole Doctorale MEGEP.

[CFD169] R. Biolchini, (2017), *Study of temperature effects on subsonic jet noise by Large Eddy Simulation*, phd thesis, Ecole Centrale Lyon.

[CFD170] R. Bizzari, (2018), *Modélisation aérodynamique et thermique des plaques multiperforées en LES*, phd thesis, Université Fédérale de Toulouse, INPT - Ecole doctorale MEGeP.

[CFD171] C. Coreixas, (2018), *High-order extension of the recursive regularized lattice Boltzmann method*, phd thesis, Université de Toulouse, INP Toulouse - Ecole doctorale MEGeP.

[CFD172] M. Daroukh, (2017), *Effects of distortion on modern turbofan tonal noise*, phd thesis, Ecole Doctorale MEGeP - INPT TOULOUSE.

[CFD173] O. Dounia, (2018), *Numerical investigation of gas explosion phenomena in confined and obstructed channels*, phd thesis, Université Fédérale de Toulouse, INPT - Ecole doctorale MEGeP.

[CFD174] F. Duchaine, (2017), *Habilitation Defense "High Performance Code Coupling for Multiphysics and Multicomponent Simulations In Fluid Dynamics"*, hdr, Institut National Polytechnique de Toulouse.

[CFD175] A. Felden, (2017), *Development of analytically reduced chemistries and applications in Large Eddy Simulations of turbulent combustion*, phd thesis, Ecole Doctorale MEGeP - INPT TOULOUSE.

[CFD176] M. Férand, (2018), *Numerical modeling of far-field turbofan-engine combustion noise*, PhD thesis, Université de Toulouse, INP Toulouse - Ecole doctorale MEGeP.

[CFD177] L. Lacassagne, (2017), *Numerical simulations and linear stability analysis of corner vortex shedding in solid rocket motors*, phd thesis, INPT Institut National Polytechnique de Toulouse Ecole Doctorale MEGEP.

[CFD178] D. Maestro, (2018), *Large Eddy Simulations of the interactions between flames and thermal phenomena: application to wall heat transfer and combustion control*, phd thesis, Université Fédérale de Toulouse, INPT - Ecole doctorale MEGeP.

[CFD179] M. Marino, (2017), *Comprehensive analysis of the Fenestron® aerodynamics using advanced numerical simulations*, phd thesis, Ecole Doctorale MEGeP - INPT TOULOUSE.

[CFD180] A. Ndiaye, (2017), *Uncertainty Quantification for the prediction of thermo-acoustic instabilities in gas turbine combustors*, phd thesis, Université de Montpellier II.

[CFD181] F. Ni, (2017), *Accounting for complex flow-acoustic interactions in a 3D thermo-acoustic Helmholtz solver*, phd thesis, INPT Institut National Polytechnique de Toulouse Ecole Doctorale MEGEP.

[CFD182] L. Potier, (2018), *Large Eddy Simulation of the combustion and heat transfer in sub-critical rocket engines*, phd thesis, INP Toulouse.

[CFD183] L. Segui-Troth, (2017), *Multi-physics coupled simulations of gas turbines*, phd thesis, Université de Toulouse, INP Toulouse - Ecole doctorale MEGeP.

[CFD184] F. Shum Kivan, (2017), *Large Eddy Simulation of spray flames and modelling of non-premixed combustion*, phd thesis, Université de Toulouse.

[CFD185] J. Vanharen, (2017), *Méthodes numériques d'ordre élevé pour des écoulements instationnaires autour de géométries complexes.*, phd thesis, INPT Institut National Polytechnique de Toulouse, Ecole Doctorale MEGEP.

4

Scientific Software Operational Performance

COOP activities

1.1 Introduction

COOP is a part of Computer Support Group, focusing on the software engineering needed by Cerfacs research teams. The manpower is evenly distributed on a mainstream part, **Computer Science and Engineering COOP/CSE**, the Exascale related part, **High Performance Computing COOP/HPC** and the Data driven modeling part, **Learning for physical modeling COOP/ML**. Their respective goals for the structure are "reduce the spurious work dedicated to software development", "keep up with the future HPC architecture", and "find practical application of machine learning techniques". Each of these parts are transverse resources shared by research teams. The broad objective is depicted in Fig.1.1.

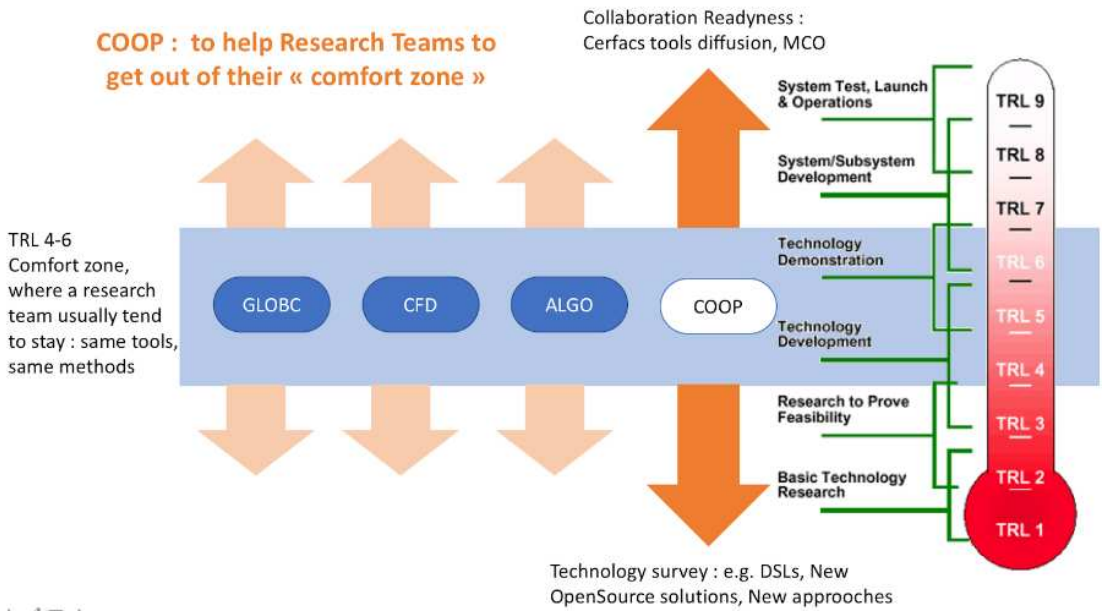

Figure 1.1: Technology Readiness Level is a scale defining the maturity level of techniques. CSG/COOP broad objective is to widen the TRLs range of research teams.

Finally, the COOP activity is transverse, and most, if not all, of the research conducted there is associated to one of the research teams of Cerfacs.

1.2 Computer Science and Engineering

Computational science and engineering (CSE) is a multi-disciplinary field lying at the intersection of mathematics and statistics, computer science, and core disciplines of science and engineering. Within the

COOP activity, COOP/CSE main objective is to reduce the work waste due to use of poorly implemented techniques within the CERFACS teams. To achieve this objective, the COOP/CSE staff performs technology survey, tries new approaches on real cases, then build training material.

1.2.1 Sustainable programming

A sustainable programming approach means, in the present context, to take into account the constraints of support, extensibility, portability and the most disregarded one , learn-ability. Tackling these constraints is at the same time more time-consuming in the short term and extremely energy-saving in the long run.
A specific training workshop "Code programming standards", was designed by COOP/CSE for first year CERFACS PHD : four Fridays in a row, 14 trainees were working as a development team on a tiny project. The group is therefore forced into the usual hurdles of team developments : interface harmonization, versioning conflicts, syntax standardization, inline documentation. The workshop is scheduled to happen twice a year.
In 2018, according to our experience on the situations treated by COOP/CSE, the main missing element in the implementation of most of our softwares is the concept of an Application Programming Interface. This element is the key to automatic non-regression and to inter-operability of softwares. After exploring several related topics : RESTfull standard [1], OpenAPI standard[2], JSON-Schema[3] and Cerberus validation structures[4], we are converging on a tailored API approach suited to the unusual constraints of a research HPC software. The application is done on the combustion code AVBP, but could be adapted or inspire other codes.

1.2.2 Solving middle-sized problems : best practices

Alongside the CERFACS softwares meant for raw supercomputing, a constellation of "middle-sized" problems co-exists dedicated to either pre-processing / post processing or stand-alone low-detail modelisations. "Middle sized problems" means in this context that a laptop or desktop computer computational power is enough, as long as the implementation is efficient.
COOP/CSE focused on two PDEs problems in 2018 : a 2-D heat conduction solver with transverse forcing, and a 2-D radiative solver using the P1 approximation. The idea was to identify a sustainable programming strategy for middle sized problems. After several tests on existing libraries, the most promising compromise is to start with a Python3 implementation, with efficient use of numerical modules (Numpy, Scipy, for starters). An example, still work in progress, is available on gitlab.com[5]. The positive aspects of such a strategy are :

1. The amount of training material online is almost un-rivaled.
2. Working efficiently with Numpy and Scipy objects is an excellent first training for HPC-proof coding.
3. Performances are fair : a homogeneous Laplacian on 10^6 d.o.f. is solved on a laptop in seconds. The Bi-coonjugate gradient stabilized, and compressed sparse row storage are taken from SciPy.
4. Portability is ensured by one of the largest development communities.

Concerning Point 2, the developer must avoid at all costs "for/do" and "if" blocks, unnecessary copies, space matrix storage and premature optimization. This work is extremely close to a Domain Specific Language porting.

[1] https://restapitutorial.com/
[2] https://www.openapis.org/
[3] http://json-schema.org/
[4] http://docs.python-cerberus.org/en/stable/
[5] https://gitlab.com/cerfacs/arnica

A strong negative aspect is however the need for experimented developers from the C/C++/FORTRAN culture to move to this higher level language.
Today, most of the classical applied mathematics methods are implemented in a Python Module. Besides, Cerfacs applicants CVs show more often experience in Python than in Fortran or C. As a conclusion, the Python3 with Numerical modules is a reliable alternative to the usual C/FORTRAN executables relying on BLAS and LAPACK libraries, with lower additional costs of training, support and distribution in the long run.

1.3 High Performance Computing (HPC)

HPC as always is one of the core activities of CERFACS. In COOP we focus on extreme performance and new technologies watch. This activity is supported via the participation to multiple projects reviewed on HPC and scientific excellence (PRACE) as well as early bird access to new systems (VSRs) to test the applications and perform challenge simulations out of reach with the standard accesses. In this period we instigated 4 PRACE awards and collaborated to 1 PRACE award with EMC2. Additionally we were invited to participate to the VSR's the Joliot-Curie system with two projects (partnering with RENAuLT and CORIA respectively), the OCCIGEN2 system at CINES/GENCI and the TERA1000 system at CEA DAM. In parallel we were granted access to the TACC (Austin TEXAS) and the THETA (ARNL) systems in the US for preparatory access and technology watch on new architectures. These projects allowed to gain experience and optimise the code for Skylake and KNightLanding architectures (Fig. 1.2).

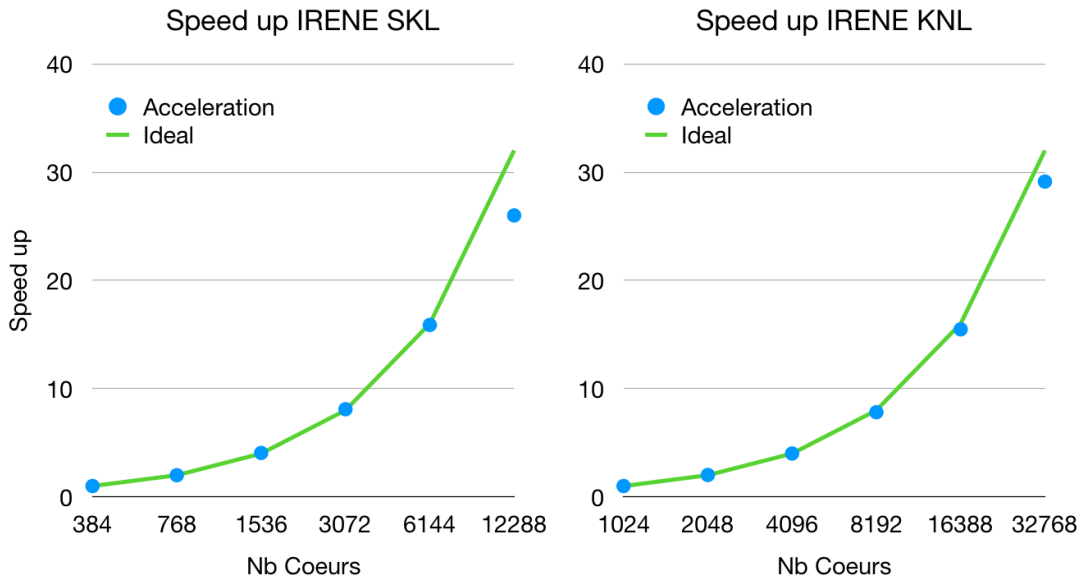

Figure 1.2: Strong scaling acceleration on the IRENE Joliot CURIE system for AVBP for an LES of an explosion.

In 2017, we were invited as guests to the GENCI Cellule de veille technologique to share and exchange with the participants on new technologies and approches towards performances on up-coming architectures. This allowed the first experience on ARM processors and the first GPU implementation of the CFD solver AVBP.

Additionnaly, CERFACS has invested subtantial effort into exploring emmerging fringe technologies, in this case mostly Quantum computing.

1.3.1 First experience with AVBP-GPU

For the past ten years, graphical processing units (GPUs) have had an increansingly important role on the HPC market. Mainly developped for Scientific computing by NVIDIA, they are today a viable alternative to standard architectures (based on CPUs). CERFACS has been exploring GPUs for almost a decade in one form or the other however early efforts were hindered by the lack of a simple and stable programing model and languague. The introduction and merging of OpenACC with OpenMP has resolved this major hurdle. Since 2017, with the support of the Cellule de veille technologique de GENCI, IBM and NVIDIA, an effort to port and test the AVBP code from the CFD group on GPUs architectures was undertaken by a postdoc (Joeffrey LEGAUX). Initially focused on the early access system OUESSANT from IDRIS (Power 8 architecture + P100 Nvidia GPUS) it was later continued on the Kraken machine at CERFACS (SKYLAKE processor + V100 Nvidia GPUS). This work was performed in collaboration with NVIDIA and IBM first and lately with CALMIP who has granted CERFACS access to its GPU platform.

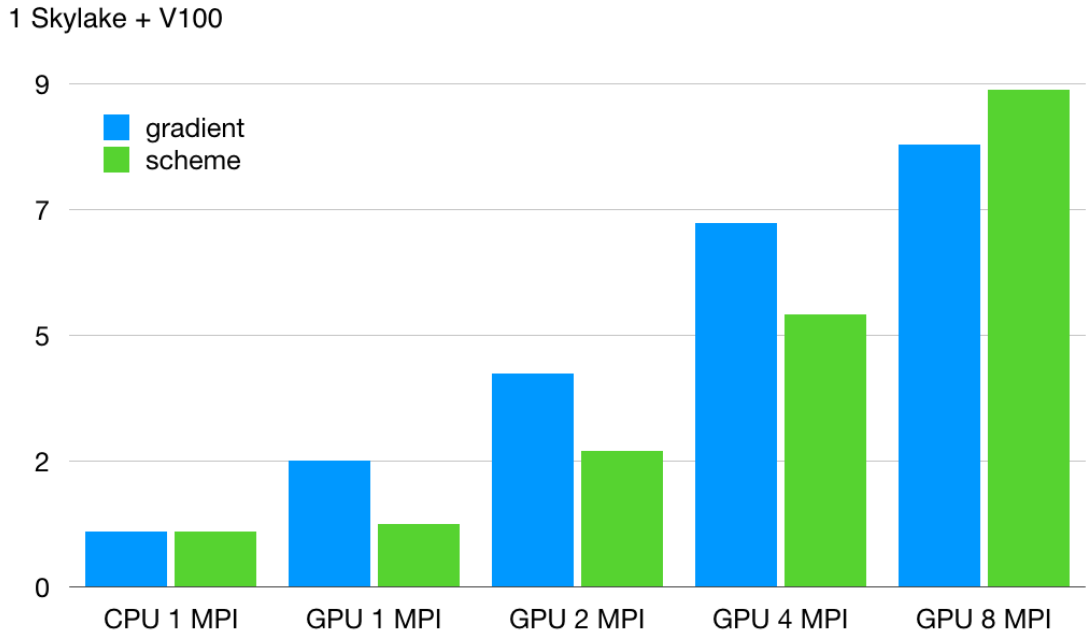

Figure 1.3: Acceleration of the scheme and gradient kernel using multiple process on a single V100 GPU compare to a Skylake processor. Simulation of an explosition using AVBP 7.3 with OpenACC enabled.

1.3.2 Quantum computing

With the advent of the first quantum computer commercial offers (DWAVE and IBM at the moment) and new technological advancements from Google, Rigetti and intel on quantum architectures, there is a new interest for research in this technologies. Large investment plans exist in the USA, China and Europe to catalyse the developement and accelerate the adoption of this new trend to benefit of the technology economically as soon as possible. Even though it is not currently clear when or which technology will be

the most mature in time (current timeframe is between 3 to 10 years at the earliest, 30 years at the latest) and the applications that will be possible it is a clear topic for technology watch. With this in mind several key parteners of CERFACS expressed their interest on having the laboratory explore this new technology. CERFACS has started investing on the subject since early 2018 with an intership (Adrien SUAU) to evaluate the state of the art of the domain. Also a worskhop was co-organised with IBM on the subject in June 2018. Adrien SUAU continued with CERFACS as an engineer working towards the implementation of quantum algorithms that may be applicable to CFD

Building a "state of the art"

One of the major goal of the internship was to build the most extensive state of the art possible around the field of quantum computing. The state of the art can be divided in 2 parts: a bibliography and a list of existing technologies. The bibliography contains research papers about:

- **The basics of quantum computing**. These research papers have been selected to help beginners in the field, to reduce the time they spend searching for good references and directly provide them a list of approved books and research papers.
- **Quantum algorithms**. This part contains research papers about quantum algorithms that may have an application in scientific computing.

Along with the construction of a bibliography, a list of the "technologies" related to quantum computing has been built. The "technologies" studied are:

1. Quantum chips (hardware).
2. Quantum simulators (software running on classical supercomputers).
3. Programming languages for quantum computing.

Implementing quantum algorithms

During the construction of the state of the art, several algorithms were flagged as interesting from a scientific computing point of view. The most interesting one for the CERFACS is probably the HHL algorithm that solves a sparse linear system of equations logarithmically in the size of the system but several other algorithms may be really promising:

1. **Grover algorithm** because it is applicable on a huge variety of problems.
2. **Variational Quantum Eigensolver** that is probably the most interesting quantum algorithm for near-term quantum computations as it does not require large coherence times.

The two algorithms presented above have already been implemented in several programming languages, which is not the case for the HHL algorithm. This is why it has been decided to hire a research engineer for a fixed-term contract of one year to implement a first version of the HHL algorithm. The implementation will be performed with the resources shared between the partners of the TQCI consortium: namely the QLM and Atos' quantum library.

1.3.3 Optimization of industrial computation codes

Thanks to different collaborations with shareholders, CERFACS has been involved in projects aiming to improve the performance of some computation codes. Particularly, the subsequent activities were performed during the internship followed by a fixed-term contract of Raphaël TAPIA.

Actions on ProLB

Through a collaboration with Airbus and CS (*Communication & Systèmes*), the first work consisted in helping to improve parallel performances of ProLB in a portable way. This software is a CFD solution based on the Lattice Boltzmann method (LBM).

First of all it was necessary to do a porting work of the code on different architectures, and those which have been tested are : Intel Haswell, Intel Skylake, Intel KNL and ARM. Then many analysis were carried out in order to provide an expertise on performances, and among the various observed criteria were the scalability, the cache interactions, the load balancing, the communication aspects, ... These analysis led to make betterment suggestions to the main developers, some of which have been included to the project's master branch.
Afterward, optimizations were achieved at the *incore* level on a few computation-intensive kernels, which mainly consist in assisting the compile-time automatic vectorization, optimizing data movements or achieving instruction reductions. As a result of these modifications a twofold gain has been obtained on the concerned kernels.

In a near future, i.e. in 2019, this work will be pursued through a collaborative project called Albatros. But this time, the main focus will be the amelioration of the scalability to large amounts of computation nodes (over 2000).

Actions on GINS

A collaboration with the CNES led to work on GINS, an old scientific software (used for over 50 years) written in Fortran, the primarily function of which is orbit determination applied to geodesy. This time, because the existing code is essentially sequential a fair objective has been estimated, that is to obtain a tenfold acceleration.

A preliminary task was to redesign the whole build-system in order to migrate to a more modern and robust usage. The validation of the new system has been validated through porting tests on 3 different Intel processors : Skylake, Haswell and Nehalem.
Subsequently, analysis were carried out so the improvable points could be determined. Indeed, a 3-levels optimization plan has been established :

1. in-core acceleration
2. multithread parallelization with OpenMP
3. multinodes parallelization with MPI

Work is currently focused on the first level, then the focus will be put on level 2 while a new recruit might arrive in 2019 to undertake actions at the third level.

1.4 Learning for physical modeling

In 2018, the transverse multi-team project "Helios" (High pErformance LearnIng for cOmputational phySics) was born at CERFACS, matching the recruitement of C. Lapeyre. In it, recent developments in the field of Machine Learning are investigated for their potential to revolutionize computational physics, as they have e.g. the field of image processing. Peta-scale databases produced by modern physics simulations have long since outgrown human capacity to analyse them thoroughly, and offer unique opportunities to go beyond historical hand-designed approaches and extend them through systematic data collection

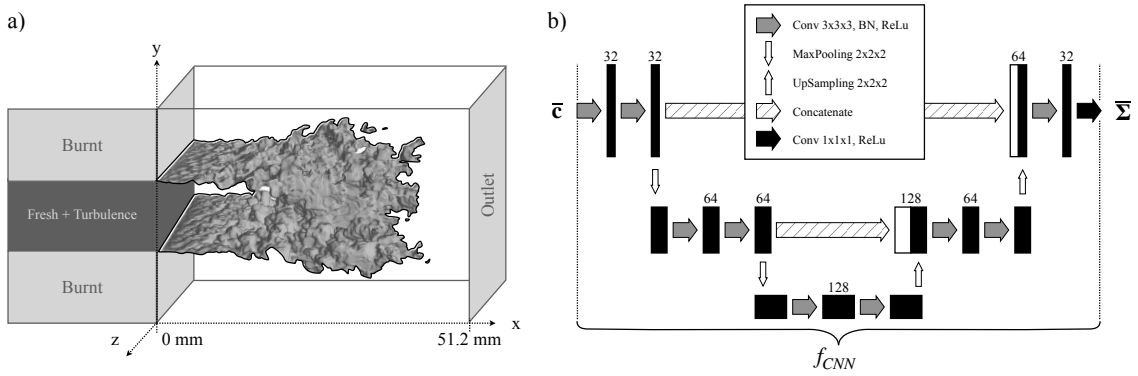

Figure 1.4: a) Numerical domain and view of a typical flame from the TRAIN1 simulation. b) Architecture of the U-net neural network used in this study. Numbers above convolutional layers show the amount of filters used in the layer.

and learning. Specifically, Deep Learning, with the training of Artificial Neural Networks, is a very promising technique which is actively investigated for several reasons: its capacity to systematically extract information from previously underexploited databases; its ability to integrate complex multiscale patterns in physical models, to a level of complexity never reached in traditional hand-designed approaches; and for compression, generation and parametrization issues regarding high-dimensional data.

In 2018, the main focus of Helios has been to explore the crossover possibilities between deep learning algorithms and many physical modeling topics at CERFACS. Two main activities have already emerged, and the matching results are described below.

1.4.1 A CNN as a turbulent combustion model

In the combustion community, the determination of the subgrid-scale (SGS) contribution to the filtered reaction rate in reacting flows LES is an example of closure problem that has been daunting for a long time. Indeed, SGS interactions between the flame and turbulent scales largely determine the flame behavior, and modeling them is an important factor to obtain overall flame dynamics. Many turbulent modeling approaches are based on a reconstruction of the subgrid-scale wrinkling of the flame surface and the so-called *flamelet* assumption, whereby the mean turbulent reaction rate can be expressed in terms of *flame surface area*. The evaluation of the amount of flame surface area due to unresolved flame wrinkling is the core of all LES models based on flame surface areas in the last 50 years. This task is akin to an image processing one, a field that convolutional neural networks (CNNs) have been shown to excel at.

This observation led to two main studies in 2018: the first was an *a priori* study comparing models from the literature with a CNN; in the second, a version of AVBP was coupled with a CNN to perform the LES, and an *a posteriori* comparison with a state of the art dynamic model was performed. The target configuration for both studies was a premixed stoichiometric methane-air slot-burner. All DNS were performed using AVBP on a $512 \times 256 \times 256$ mesh, with a well resolved flame front. Figure 1.4(a) shows a view of the domain and typical flame. The same domain is also used for LES, with coarsened versions of the mesh. The quantity to model is the filtered *flame surface density* $\overline{\Sigma}$, and it is predicted using the filtered progress variable $\bar{c}$. Instead of algebraically predicting $\overline{\Sigma}$ from $\bar{c}$ at one node, the CNN reads the vector $\overline{\mathbf{c}}$ of values over an entire subdomain Ω, and produces a prediction for the matching field of $\overline{\mathbf{\Sigma}}$ over Ω. The function

f_{CNN} therefore performs

$$\overline{\mathbf{\Sigma}} = f_{CNN}(\overline{\mathbf{c}}) \tag{1.1}$$
$$f_{CNN} : \mathbb{R}^{\Omega} \mapsto \mathbb{R}^{\Omega}.$$

The CNN in these studies is inspired from the convolutional U-Net segmentation architecture, adapted for the regression task of predicting $\overline{\mathbf{\Sigma}}$ from $\overline{\mathbf{c}}$. The neural network architecture is shown in Fig. 1.4(b). It is trained on two established DNS of the slot burner, and then tested on a configuration with a pulsed inlet. Figure 1.5 shows the flame surface area in the DNS, and predicted by various models including the CNN on the same setup, showing that the CNN is largely the most accurate. This work has led to a submission in

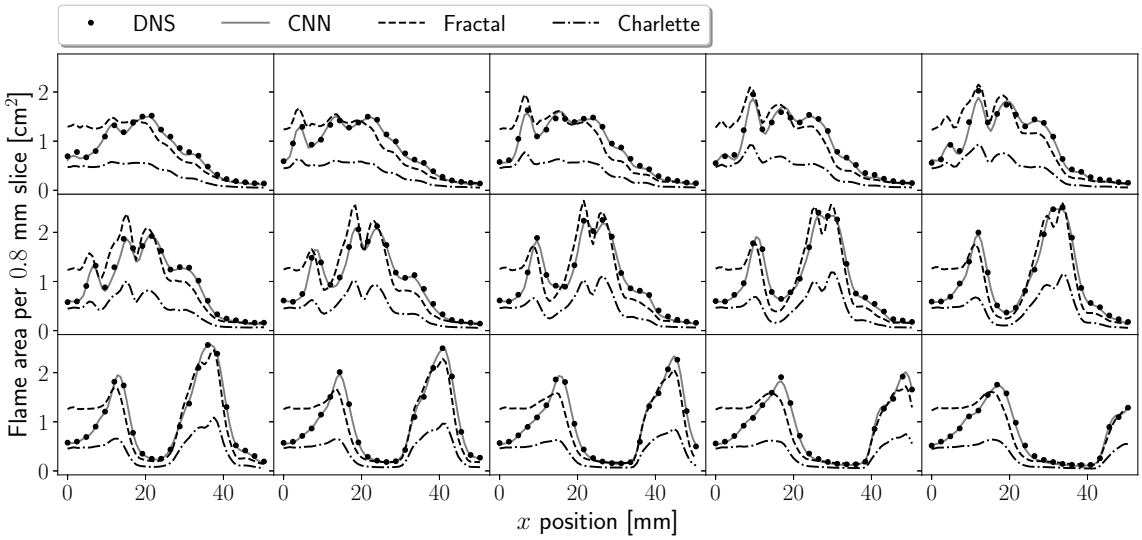

Figure 1.5: *A priori* comparison. Flame surface areas at each location x is shown for 15 snapshots as an inlet pulse is convected downstream.

Combustion and Flame at the end of 2018.
After of the good results of the *a priori* approach, an *a posteriori* study was then performed. The same slot burner was pulsated harmonically, both in a DNS and LES setup, ensuring the same large scale dynamics in all simulations. Three simulations were performed: a DNS (PULSE_DNS); an LES with the dynamic formulation as a model for $\overline{\Sigma}$ (PULSE_DYN); and an LES coupled with the CNN (PULSE_CNN); Fig. 1.6 shows the radial profiles of $\overline{c}$ for the three simulations, demonstrating that the CNN enabled to recover the flame length more accurately than the state-of-the-are dynamic model.
This work was performed during the internship of Nicolas Cazard [COOP7]. Following this work, a Ph.D. student has been recruited: Victor Xing will start in January 2019, after completing an internship on a relevant topic [COOP9].

1.4.2 Geologically plausible generations using GANs

A focus group on the physics of geological reservoirs was created at CERFACS in 2018, through three main topics of expertise: (1) data assimilation, (2) data science and (3) uncertainty quantification. In 2018, topic (2) has started to be investigated through the internship of Camille Besombes [COOP6], followed by a Ph.D. starting in October.
The starting point of this work was to reproduce some recent results from the literature on specific data given by Total. The data is a set of $10,000$ binary images of 100×100 pixels representing either channels

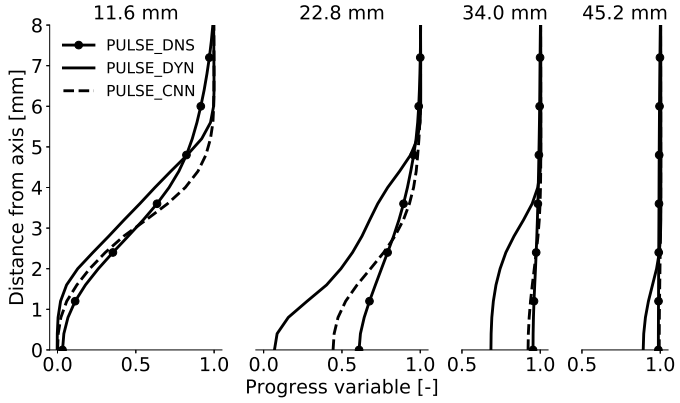

Figure 1.6: *A posteriori* comparisons. Mean profiles of progress variable for PULSE simulations at four downstream locations.

(1) or background (0) (Fig. 1.7 top). These images are the result of empirical iteration and validation by geologists, and are considered to be a sample from the distribution of "plausible images". In the context of

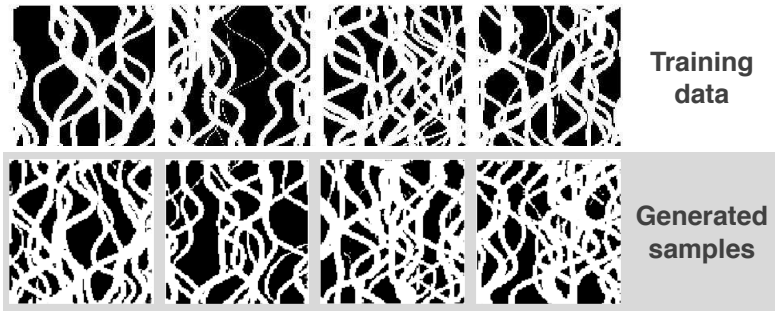

Figure 1.7: Images from the dataset (top) and samples produced by the trained GAN (bottom).

reservoir modeling, one challenge is to assimilate various forms of engineering knowledge into the reservoir topology. Current generators do not enable to continually morph the plausible images, and can only produce uncorrelated images. To do this, one emerging method is to train a generative neural network to produce images similar to the training set. Such a network is continuous relative to its inputs, and enables such morphing.
The approach followed in this study was to train a Generative Adversarial Network (GAN) to produce channel images. Fig. 1.7 (bottom) shows some sample realizations coming from the trained generator, and demonstrates how high-quality realizations of similar overall characteristics compared to the samples (top) are produced. Following work during the Ph.D. will focus on making this generative approach relevant to the data-assimilation process.

1.4.3 Flame front tracking in forest fires

With the increase of available earth observation data, notably using satellite imaging ([COOP8]), the study of large scale natural phenomena such as forest fires is can now be improved through data-driven techniques. However, the detection of the burnt and unburnt areas in a very large number of images (known as image

segmentation) is a tedious task for humans. In order to accelerate this task, a study led by Ronan Paugam and Nicolas Cazard ([COOP7]) was performed, where "u-net" architectures of convolutional neural networks (CNN) were trained to perform the image segmentation.
The test case considered was a dataset produced by airborne observations, as part of a fieldwork campaign organized by Prof. Martin Wooster (Dept of Geog. University College London) in Kruger National Park, 2014 South Africa. This high-resolution (in time and space) test case is less challenging than satellite observation data, but is considered as a first step for the method. The input image retained is that of radiance (Fig. 1.8 (a)). In order to obtain training labels, several images were annotated by hand, producing a mask of burnt / unburnt pixels (Fig. 1.8 (b)). The CNN is then trained to perform the segmentation, and reaches a good description of the flame front (Fig. 1.8 (c)).

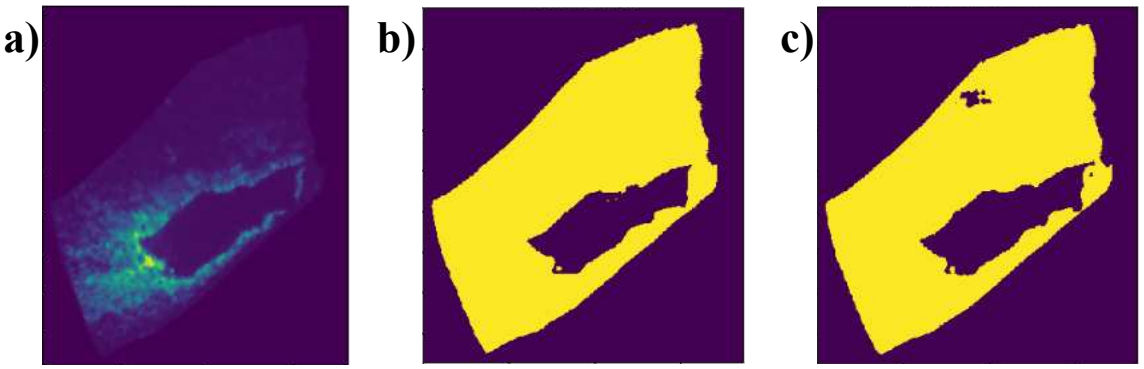

Figure 1.8: Example image from Kruger fire experiment. a) radiance observed from airborne camera. b) hand-made mask of burnt (yellow) and unburnt (purple) pixels. c) mask automatically produced by the trained CNN.

Publications

2.1 Conferences Proceedings

[COOP1] R. Bizzari, A. Dauptain, L. Gicquel, and F. Nicoud, (2017), A thickened-hole model for LES over multiperforated liners, In *4e Colloque du réseau d'INitiative en Combustion Avancée (INCA)*, Palaiseau, France, SAFRAN TECH.

[COOP2] R. Bizzari, M. Férand, A. Dauptain, G. Staffelbach, S. Richard, J.-D. Mueller, T. Ogier, G. Exilard, and F. Nicoud, (2018), Mesh local refinement to enhance effusion cooling models; Invited conference, In *12th International Symposium on Engineering Turbulence Modelling and Measurements (ETMM12)*, Montpellier (France).

[COOP3] R. Bizzari, D. Lahbib, A. Dauptain, F. Duchaine, S. Richard, and F. Nicoud, (2018), A model able to assess multiperforated liner's temperature from an unresolved adiabatic simulation, In *Journée SFT Numérique et couplage thermique*, Paris, France.

[COOP4] J. Lamouroux, S. Richard, Q. Malé, G. Staffelbach, A. Dauptain, and A. Misdariis, (2017), On the Combination of Large Eddy Simulation and Phenomenological Soot Modelling to Calculate the Smoke Index From Aero-Engines Over a Large Range of Operating Conditions, In *ASME Turbo Expo 2017: Turbomachinery Technical Conference and Exposition*, vol. 4B, Charlotte, USA - June 26–30, 2017, International Gas Turbine Institute, GT2017–64262.

[COOP5] M. Thomas, A. Dauptain, F. Duchaine, L. Gicquel, C. Koupper, and F. Nicoud, (2017), Comparison of Heterogeneous and Homogeneous Coolant Injection Models for Large Eddy Simulation of Multiperforated Liners Present in a Combustion Simulator, In *ASME Turbo Expo 2017 Proceedings : Design Methods and CFD Modeling for Turbomachinery*, vol. 2B: Turbomachinery, Charlotte, North Carolina, USA,, International Gas Turbine Institute, GT2017–64622 (12pp.).

2.2 Technical Reports

[COOP6] C. Besombes, (2018), Modélisation de Réservoir Géologique par Réseau Générateur Antagoniste, working note, ENSEEIHT et CERFACS, Toulouse, France.

[COOP7] N. Cazard, (2018), Exploration de la capacité du Deep Learning à assister des simulations de mécanique des fluides, working note, CERFACS, Toulouse, France.

[COOP8] M. Ronzié, (2018), Etude et mise en place du Deep Learning sur des données satellites du CNES, working note, Bordeaux INP ENSEIRB MATMECA - CERFACS Toulouse.

[COOP9] V. Xing, (2018), Exploration of the ability of Deep Learning to learn the characteristics of turbulent flows, working note, Institut Supérieur de l'Aéronautique et de l'Espace-Supaero, CERFACS, Toulouse, France.